
Electronic Thesis and Dissertation Repository

8-22-2016 12:00 AM

Time-dependent behaviour of micro-tunneling construction in Queenston shale

Hayder Mohammed Salim Al-Maamori
The University of Western Ontario

Supervisor

Dr. Hesham El Naggar
The University of Western Ontario

Graduate Program in Civil and Environmental Engineering

A thesis submitted in partial fulfillment of the requirements for the degree in Doctor of Philosophy

© Hayder Mohammed Salim Al-Maamori 2016

Follow this and additional works at: <https://ir.lib.uwo.ca/etd>



Part of the [Geotechnical Engineering Commons](#)

Recommended Citation

Al-Maamori, Hayder Mohammed Salim, "Time-dependent behaviour of micro-tunneling construction in Queenston shale" (2016). *Electronic Thesis and Dissertation Repository*. 4064.

<https://ir.lib.uwo.ca/etd/4064>

This Dissertation/Thesis is brought to you for free and open access by Scholarship@Western. It has been accepted for inclusion in Electronic Thesis and Dissertation Repository by an authorized administrator of Scholarship@Western. For more information, please contact wlsadmin@uwo.ca.

Abstract

The Queenston shale among other shales from southern Ontario exhibits time-dependent deformation behaviour. This behaviour is manifested in the form of volume increase which can cause damage to the hosted underground structures. The time-dependent deformation of rocks can cause cracks in the springline of tunnels, wall inward movement, roof spalling and floor heave, which requires costly remedial measures. The expansion of the existing infrastructure in southern Ontario requires construction techniques, such as micro-tunneling to build new tunnels and pipelines under existing structures with minimal impact to these structures and to the environment. However, adopting this technique in swelling rocks, such as the Queenston shale requires an evaluation of its feasibility and functionality prior to its application. Accordingly, a comprehensive study that included experimental and numerical investigations was conducted to evaluate the impact of lubricant fluids used in micro-tunneling applications on their time dependent behaviour. The experimental program evaluated the impact of water, bentonite and polymer solutions on the Queenston shale through: i) investigating the influence of lubricant fluids on the time-dependent deformation behaviour of the Queenston shale through performing free swell, semi-confined, and null swell tests on Queenston shale in these fluids, ii) investigating the impact of lubricant fluids on the strength of the Queenston shale utilizing Brazilian, direct tension, unconfined compression, and triaxial compression tests, before and after soaking in lubricant fluids, and iii) investigating the depth of penetration of lubricant fluids and water into the Queenston shale. It was revealed that the impact of polymer solution was significant in reducing the time-dependent deformation of the Queenston shale compared to bentonite solution and water. The strength of the Queenston shale was remarkably decreased after their continuous exposure to water and lubricant fluids with minimal impact caused by polymer solution. The penetration of lubricant fluids was found to be smaller than for water, and a relation was derived to compute the penetration depth of each fluid in Queenston shale with time. The numerical investigation comprised finite element parametric analyses using the derived tests results along with time-dependent deformation model employing the computer program PLAXIS 2D. Different pipe diameter, pipe depth, in-situ stress ratio, and waiting time before final grouting were used in the analyses.

Accordingly, micro-tunneling was found to be workable and suitable technique to construct tunnels and pipelines in the Queenston shale of southern Ontario. Recommendations to use the appropriate strength of the concrete, waiting time and the most suitable depth for micro-tunneling applications are given. The results are envisioned to aid in determining whether or not micro-tunneling technique is a feasible construction technique for pipelines / tunnels in Queenston shale of southern Ontario.

Keywords

Queenston shale, lubricant fluids, bentonite solution, polymer solution, time-dependent deformation, swelling, strength, multistage triaxial, penetration, hydraulic conductivity, finite element, modelling, tunnels, pipelines, micro-tunneling

Co-Authorship Statement

This thesis has been prepared according to the regulations of integrated article format thesis specified by the Faculty of Graduate Studies at the University of Western Ontario and it has been co-authored as:

CHAPTER 2: A COMPILATION OF THE GEO-MECHANICAL PROPERTIES OF ROCKS IN SOUTHERN ONTARIO AND THE NEIGHBOURING REGIONS

By: Hayder Mohammed Salim Al-Maamori; Mohamed Hesham El Naggar and Silvana Micic

Published in the Open Journal of Geology, 2014, **4**, 210-227.

Contributions:

Hayder Al-Maamori: compiled the geo-mechanical test measurements data, categorized and presented them in tables, interpreted the data and wrote the draft of the paper.

Hesham El Naggar: Initiated the idea of the paper; reviewed the data interpretations and assisted in writing the paper.

Silvana Micic: reviewed the data interpretations and assisted in writing the paper.

CHAPTER 3: INFLUENCE OF LUBRICANT FLUIDS ON SWELLING BEHAVIOUR OF QUEENSTON SHALE IN SOUTHERN ONTARIO

By: Hayder Mohammed Salim Al-Maamori; Mohamed Hesham El Naggar; Silvana Micic and K.Y. Lo

Published in the Canadian Geotechnical Journal, 2016, **53** (7), 1059-1080.

Contributions:

Hayder Al-Maamori: collect rock samples; performed the testing program; interpreted the results and wrote the draft of the paper.

Hesham El Naggar: guided throughout the testing program; reviewed the results interpretations and assisted in writing the paper.

Silvana Micic: reviewed the results interpretations and assisted in writing the paper.

K.Y. Lo: reviewed the results interpretations and assisted in writing the paper.

CHAPTER 4: THE INFLUENCE OF WATER AND LUBRICANT FLUIDS ON THE PEAK STRENGTH OF QUEENSTON SHALE FROM SOUTHERN ONTARIO

By: Hayder Mohammed Salim Al-Maamori; Mohamed Hesham El Naggar; Silvana Micic and K.Y. Lo

Submitted for publication in the Canadian Geotechnical Journal, April, 2016.

Contributions:

Hayder Al-Maamori: collect rock samples; modified the triaxial cell; performed the testing program; interpreted the results and wrote the draft of the paper.

Hesham El Naggar: guided throughout the testing program; reviewed the results interpretations and assisted in writing the paper.

Silvana Micic: reviewed the results interpretations and assisted in writing the paper.

K.Y. Lo: reviewed the results interpretations and assisted in writing the paper.

CHAPTER 5: STRENGTH ENVELOPES OF NIAGARA QUEENSTON SHALE UNDER DIFFERENT WETTING CONDITIONS UTILIZING MULTISTAGE TRIAXIAL COMPRESSION TEST

By: Hayder Mohammed Salim Al-Maamori; Mohamed Hesham El Naggar; Silvana Micic
and K.Y. Lo

Submitted for publication in the Canadian Geotechnical Journal, March, 2016.

Contributions:

Hayder Al-Maamori: collect rock samples; modified the triaxial cell; performed the testing program; interpreted the results and wrote the draft of the paper.

Hesham El Naggar: guided throughout the testing program; reviewed the results interpretations and assisted in writing the paper.

Silvana Micic: reviewed the results interpretations and assisted in writing the paper.

K.Y. Lo: reviewed the results interpretations and assisted in writing the paper.

**CHAPTER 6: DEPTH OF PENETRATION OF LUBRICANT FLUIDS AND WATER
INTO THE QUEENSTON SHALE OF SOUTHERN ONTARIO**

By: Hayder Mohammed Salim Al-Maamori; Mohamed Hesham El Naggar and Silvana

Submitted for publication in the Canadian Geotechnical Journal, April, 2016.

Contributions:

Hayder Al-Maamori: collect rock samples; design the test apparatus; performed the testing program; interpreted the results; suggested an approach to calculate the hydraulic conductivity of the Queenston shale and wrote the draft of the paper.

Hesham El Naggar: reviewed the design of the test apparatus; guided throughout the testing program; reviewed the results interpretations and assisted in writing the paper.

Silvana Micic: reviewed the results interpretations and assisted in writing the paper.

CHAPTER 7: FINITE ELEMENT ANALYSES OF TIME-DEPENDENT DEFORMATION AND INDUCED STRESSES IN CONCRETE PIPES CONSTRUCTED IN QUEENSTON SHALE USING MICRO-TUNNELING TECHNIQUE

By: Hayder Mohammed Salim Al-Maamori; Mohamed Hesham El Naggar and Silvana Micic

Submitted for publication in the Canadian Geotechnical Journal, July, 2016.

Contributions:

Hayder Al-Maamori: developed the finite element model; verified the model with laboratory tests and documented in-situ measurements; performed the analyses; interpreted the results and wrote the draft of the paper.

Hesham El Naggar: guided throughout the modelling process; reviewed the results interpretations and assisted in writing the paper.

Silvana Micic: reviewed the results interpretations and assisted in writing the paper.

Dedication

To my parents with gratitude

and

To my family with love

Acknowledgments

I would like to extend my sincere thanks and appreciations to my supervisor Dr. Hesham El Naggar for his valuable advices, guidance and fully dedication to review my work throughout the research period. I would like to thank my co-supervisor Dr. Silvana Micic for being available at any time to give help and advice; for training me to perform rock swelling tests and for her valuable guidance. I am very grateful to Dr. Lo, K.Y. for his valuable guidance and wise tips throughout my research.

I am thankful to the faculty; staff and fellow graduate students at the Geotechnical Research Centre for their support. I am very grateful to Wilbert Logan for his unlimited support. I am also grateful to Caitlin Marshal, Tim Stephens and Melody Richards for their assistance during my research. I appreciate Gary Lusk for visiting the university labs and giving advice on the triaxial cell used in this research. I appreciate Dr. Clement Yuen and Dr. Evert Hoek for giving valuable advice in this research.

I would like to thank Clayton Cooke; Dan Sweiger; Ian Vinkenvleugel; Cody Ruthman; Paul Sheller; Stephen Mallison and Katherine Manweiler from the machine shop and engineering stores at the University of Western Ontario for their assistance and support.

I would also like to thank deeply Kim Law and Stephen Wood from the department of earth sciences and Karen Nygard and Dr. Richard Gardiner from the Biotron Research Centre at the University of Western Ontario for giving me training and assistance during my research.

I would like to extend my deep appreciation and thanks to Ward and Burke Micro-tunneling Ltd., especially Mr. Robert Ward and Mr. John Grennan for the generous financial support and technical support throughout this research.

Finally, I am very grateful and thankful to my wife Tahreer; my son Mustafa; my daughter Shahd and my son Abdullah for their patience; support; inspiration and love through this long research journey.

Table of Contents

Abstract.....	i
Co-Authorship Statement.....	iii
Dedication	vii
Acknowledgments	viii
Table of Contents.....	ix
List of Tables	xviii
List of Figures.....	xxxii
List of Appendices.....	xxxix
List of abbreviations; symbols and nomenclature	xxxix
Chapter 1	1
INTRODUCTION	1
1.1 GEOLOGICAL BACKGROUND.....	1
1.2 OVERVIEW.....	2
1.3 MICRO-TUNNELLING CONSTRUCTION TECHNIQUE.....	4
1.4 RESEARCH OBJECTIVE.....	7
1.5 THESIS OUTLINE.....	8
1.6 ORIGINAL CONTRIBUTIONS.....	10
1.5 REFERENCES.....	11
Chapter 2	14
A COMPILATION OF THE GEO-MECHANICAL PROPERTIES OF ROCKS IN SOUTHERN ONTARIO AND THE NEIGHBOURING REGIONS	14
2.1 INTRODUCTION.....	14

2.2 SUMMARY OF COMPILED MEASUREMENTS.....	15
2.2.1 In-Situ Horizontal Stresses.....	15
2.2.2 Strength and Stiffness Properties of Rocks.....	19
2.2.3 Time-Dependent Deformation Properties of Rocks.....	22
2.2.4 Dynamic Properties of Rocks.....	23
2.3 SUMMARY AND CONCLUSIONS.....	24
2.4 REFERENCES.....	25
Chapter 3.....	74
INFLUENCE OF LUBRICANT FLUIDS ON THE SWELLING BEHAVIOUR OF QUEENSTON SHALE IN SOUTHERN ONTARIO.....	757
4	
3.1 INTRODUCTION.....	74
3.2 OBJECTIVE AND SCOPE OF WORK.....	76
3.3 SOURCE OF ROCK SAMPLES.....	76
3.3.1 Preserving Recovered Rocks.....	77
3.3.2 Sample Cutting.....	77
3.4 TESTING METHODOLOGY.....	78
3.4.1 Lubricant Fluids.....	78
3.4.2 Tests for Swelling Behaviour.....	79
3.5 COMPLEMENTARY TESTS.....	80
3.5.1 Mineralogical Tests.....	80

3.5.1.1 X-Ray Diffraction.....	80
3.5.1.2 Scanning Electron Microscopy.....	84
3.5.1.3 Cation Exchange Capacity Test.....	91
3.5.2 Ancillary Tests.....	92
3.5.2.1 Determination of Calcite and Dolomite Contents.....	92
3.5.2.2 Moisture Content Determination.....	93
3.5.2.3 Rock Pore Water Salinity Determination.....	94
3.5.2.4 Rate of Absorption of Water.....	96
3.6 RESULTS AND DISCUSSION.....	98
3.6.1 Free Swell Test.....	98
3.6.2 Semi-Confined Swell Test.....	104
3.6.3 Null Swell Test.....	108
3.7 CONSTRUCTION OF SWELLING ENVELOPES.....	111
3.8 SUMMARY AND CONCLUSIONS.....	114
3.9 REFERENCES.....	116
Chapter 4.....	135
THE INFLUENCE OF WATER AND LUBRICANT FLUIDS ON THE PEAK STRENGTH OF QUEENSTON SHALE FROM SOUTHERN ONTARIO.....	135
4.1 INTRODUCTION.....	135

4.1.1 Work Objective and Scope.....	136
4.2 BOREHOLE.....	137
4.3 MINERALOGICAL COMPOSITION OF MQS.....	139
4.4 TEST METHODOLOGY.....	140
4.4.1 Maintaining Specimens During Soaking Period.....	142
4.4.2 Modified High Capacity Triaxial Cell.....	144
4.4.3 Electronic Strain Gauges.....	146
4.4.4 Triaxial Compression Test Procedure.....	147
4.5 RESULTS AND DISCUSSION.....	148
4.5.1 Brazilian Split Test.....	148
4.5.1.1 Discussion.....	150
4.5.2 Direct Tension Test.....	158
4.5.3 Unconfined Compression Test.....	159
4.5.3.1 Discussion.....	160
4.5.3.2 Poisson’s Ratio; Elastic Modulus and Shear Modulus.....	167
4.5.4 Triaxial Compression Test.....	168
4.5.4.1 Discussion.....	169
4.6 CONSTRUCTING STRENGTH ENVELOPES OF MILTON QUEENSTON SHALE.....	177
4.7 SUMMARY AND CONCLUSIONS.....	179

4.8 REFERENCES.....	180
Chapter 5	184
STRENGTH ENVELOPES OF NIAGARA QUEENSTON SHALE UNDER DIFFERENT WETTING CONDITIONS UTILIZING MULTISTAGE TRIAXIAL COMPRESSION TEST	184
5.1 INTRODUCTION.....	184
5.1.1 Objective and Scope of Work.....	186
5.2 TEST PROGRAM AND PROCEDURE.....	186
5.3 RESULTS AND DISCUSSION.....	191
5.3.1 X-Ray Diffraction Analyses.....	191
5.3.2 Brazilian Split Strength.....	195
5.3.3 Unconfined Compression Strength.....	197
5.3.4 Multistage Triaxial Compression Strength.....	200
5.3.5 Poisson’s Ratio.....	203
5.3.6 Elastic Modulus and Shear Modulus.....	211
5.4 DEVELOPING STRENGTH ENVELOPES OF NIAGARA QUEENSTON SHALE.....	212
5.5 COMPARISON OF STRENGTH MEASURED IN MULTISTAGE AND SINGLE- STAGE TRIAXIAL COMPRESSION TESTS.....	216
5.6 COMPARISON OF STRENGTH ENVELOPS OF NIAGARA AND MILTON QUEENSTON SHALE.....	220

5.6 SUMMARY AND CONCLUSIONS.....	222
REFERENCES.....	223
Chapter 6.....	227
DEPTH OF PENETRATION OF LUBRICANT FLUIDS AND WATER IN QUEENSTON SHALE OF SOUTHERN ONTARIO.....	227
6.1 INTRODUCTION.....	227
6.2 RESEARCH OBJECTIVE.....	229
6.3 MATERIALS.....	230
6.3.1 Rock Cores.....	230
6.3.2 Lubricant Fluids.....	230
6.4 TEST METHODOLOGY.....	231
6.4.1 Fluid Penetration Test Setup.....	231
6.4.2 Supplementary Tests.....	233
6.4.2.1 Moisture Content Determination.....	233
6.4.2.2 Rock Pore Fluid Salinity.....	234
6.4.2.3 Calcite Content.....	235
6.4.3 A Suggested Approach of Calculating Hydraulic Conductivity of the Queenston Shale.....	235
6.5 RESULTS AND DISCUSSION.....	239
6.5.1 Moisture Content.....	240

6.5.2 Rock Pore Fluid Salinity.....	243
6.5.3 Calcite Content.....	246
6.5.4 Fluid Penetration.....	246
6.5.5 Hydraulic Conductivity	249
6.6 SUMMARY AND CONCLUSIONS.....	253
6.7 REFERENCES.....	254
Chapter 7.....	258
FINITE ELEMENT ANALYSES OF TIME-DEPENDENT DEFORMATION AND INDUCED STRESSES IN CONCRETE PIPES CONSTRUCTED IN QUEENSTON SHALES USING MICRO-TUNNELING TECHNIQUE.....	258
7.1 INTRODUCTION.....	258
7.2 RESEARCH OBJECTIVE.....	259
7.3 GEOLOGICAL BACKGROUND.....	260
7.3.1 Locations of Investigated Queenston Shale.....	260
7.4 FINITE ELEMENT (FE) PLAXIS 2D ROCK SWELLING MODEL.....	262
7.5 DEVELOPMENT OF MATHEMATICAL TIME-DEPENDENT DEFORMATION MODEL OF ROCKS IN SOUTHERN ONTARIO.....	265
7.6 VERIFICATION OF FE PLAXIS 2D ROCK SWELLING MODEL.....	266
7.6.1 FE Model of Free Swell Test.....	269
7.6.2 FE Model of Semi-Confined Swell Test.....	273

7.6.3	FE Model of the Null Swell Test.....	276
7.6.4	Modelling Excavations In Rocks.....	279
7.6.4.1	The Niagara Wheel Pit Excavation.....	279
7.6.4.2	The Scotia Plaza Foundation Excavation.....	284
7.6.5	Modelling Circular Tunnel in Rock and Comparison with Closed Form Solutions.....	288
7.7	TWO-DIMENSIONAL FINITE ELEMENT MODELLING OF TIME DEPENDENT DEFORMATION BEHAVIOUR AND INDUCED STRESSES IN TUNNELS CONSTRUCTED USING MICRO-TUNNELING IN QUEENSTON SHALE.....	293
7.7.1	SENSITIVITY ANALYSIS.....	298
7.7.2	Influence of Stress Ratio (K_0).....	299
7.7.3	Influence of Pipe Diameter.....	301
7.7.4	Influence of Pipe Depth.....	303
7.7.5	Influence of Construction Period.....	306
7.7.6	Variation of Bending Moment At Springline And Crown.....	308
7.7.7	Pipe Inward Convergence At The Springline.....	311
7.8	SUMMARY, CONCLUSIONS AND RECOMMENDATIONS.....	314
7.9	REFERENCES.....	315

Chapter 8	321
SUMMARY, CONCLUSIONS AND RECOMMENDATIONS	321
8.1 SUMMARY.....	321
8.2 CONCLUSIONS.....	324
8.3 8.3 RECOMMENDATIONS AND FUTURE RESEARCH.....	327
Appendix A	328
STANDARD DEVIATION OF TIME-DEPENDENT DEFORMATION AND STRENGTH MEASUREMENTS	328

List of Tables

TABLE	DESCRIPTION	PAGE
CHAPTER 2: A COMPILATION OF THE GEO-MECHANICAL PROPERTIES OF ROCKS IN SOUTHERN ONTARIO AND THE NEIGHBOURING REGIONS		
Table 2.1	In-situ stress measurements in rocks of southern Ontario and neighboring regions.....	31
Table 2.2	Strength and time-dependent deformation properties of rocks in southern Ontario and neighbouring regions	47
Table 2.3	Dynamic properties of rocks in southern Ontario and neighbouring regions.....	72
CHAPTER 3: INFLUENCE OF LUBRICANT FLUIDS ON THE SWELLING BEHAVIOUR OF QUEENSTON SHALE IN SOUTHERN ONTARIO		
Table 3.1	Percentage minerals of Milton and Niagara Queenston shales from x-ray diffraction analyses	120
Table 3.2	Cation exchange capacity of Milton and Niagara Queenston shales and bentonite solution.....	121
Table 3.3	Free swell test and complementary tests results of Milton Queenston shale.....	122
Table 3.4	Free swell test and complementary tests results of Niagara Queenston shale....	124
Table 3.5	Semi-confined swell test in vertical direction, and complementary tests results of Milton Queenston shale.....	126
Table 3.6	Semi-confined swell test in horizontal direction, and complementary tests results of Milton Queenston shale.....	128
Table 3.7	Semi-confined swell test in vertical and horizontal directions and complementary tests results of Niagara Queenston shale.....	130
Table 3.8	Null- swell test in vertical and horizontal directions, and complementary tests results of Milton Queenston shale.....	131

TABLE	DESCRIPTION	PAGE
	Table 3.9 Null- swell test in vertical and horizontal directions, and complementary tests results of Niagara Queenston shale.....	132
	Table 3.10 Rate of absorption of water of Niagara and Milton Queenston shales in ambient fluids.....	133
	Table 3.11 Summary results of free swell tests, semi-confined swell tests, and null swell tests performed on Milton and Niagara Queenston shale.....	134
 CHAPTER 4: THE INFLUENCE OF WATER AND LUBRICANT FLUIDS ON THE PEAK STRENGTH OF QUEENSTON SHALE FROM SOUTHERN ONTARIO 		
	Table 4.1 Brazilian splitting strength of Milton Queenston shale in vertical direction and supplementary test results.....	152
	Table 4.2 Brazilian splitting strength of Milton Queenston shale in horizontal direction and supplementary test results.....	154
	Table 4.3 Unconfined compression strength and strength parameters of Milton Queenston shale in vertical direction and supplementary test results.....	162
	Table 4.4 Unconfined compression strength and strength parameters of Milton Queenston shale in horizontal direction and supplementary test results.....	163
	Table 4.5 Triaxial compression strength and strength parameters of Milton Queenston shale in vertical direction and supplementary test results.....	171
	Table 4.6 Triaxial compression strength and strength parameters of Milton Queenston shale in horizontal direction and supplementary test results.....	172
 CHAPTER 5: STRENGTH ENVELOPES OF NIAGARA QUEENSTON SHALE UNDER DIFFERENT WETTING CONDITIONS UTILIZING MULTISTAGE TRIAXIAL COMPRESSION TEST 		
	Table 5.1 Mineralogical composition of Niagara Queenston shale.....	192

TABLE	DESCRIPTION	PAGE
	Table 5.2 Brazilian split strength test results of Niagara Queenston shale.....	198
	Table 5.3 Unconfined compression strength test results and strength parameters of Niagara Queenston shale.....	201
	Table 5.4 Test results multistage triaxial compression strength and strength parameters of Niagara Queenston shale.....	205
 CHAPTER 6: DEPTH OF PENETRATION OF LUBRICANT FLUIDS AND WATER IN QUEENSTON SHALE OF SOUTHERN ONTARIO 		
	Table 6.1 Fluids penetration results and properties of the Queenston shale after terminating fluids penetration tests.....	241
	Table 6.2 Properties of Queenston shale specimens and applied fluids.....	250
	Table 6.3 Calculated hydraulic conductivity of the Queenston Shale.....	252
 CHAPTER 7: FINITE ELEMENT ANALYSES OF TIME-DEPENDENT DEFORMATION AND INDUCED STRESSES IN CONCRETE PIPES CONSTRUCTED IN QUEENSTON SHALE USING MICRO-TUNNELING TECHNIQUE 		
	Table 7.1 Time-dependent deformation parameters for (Lo and Hefny 1996 swelling model) from (Al-Maamori et al., 2016).....	267
	Table 7.2 Parameters used in the analysis of the Niagara Wheel Pit (Lee and Lo, 1976)..	280
	Table 7.3 Parameters used in the analysis of the Scotia plaza excavation (Trow and Lo, 1989).....	285
	Table 7.4 Parameters used in the analyses of the Lo and Hefny 1996 model, (Lo and Hefny, 1996).....	289

TABLE	DESCRIPTION	PAGE
	Table 7.5 Properties of concrete pies used in micro-tunnelling applications (Ward and Burke microtunnelling Ltd.).....	294
	Table 7.6 Time-dependent deformation and strength parameters of the Queenston shale used in finite element analyses.....	295

APPENDIX A: STANDARD DEVIATION OF TIME-DEPENDENT DEFORMATION AND STRENGTH MEASUREMENTS

	Table A.1. Standard deviation of free swell test of Milton Queenston shale.....	328
	Table A.2. Standard deviation of free swell test of Niagara Queenston shale.....	329
	Table A.3. Standard deviation of vertical semi-confined swell test of Milton Queenston shale.....	330
	Table A.4. Standard deviation of horizontal semi-confined swell test of Milton Queenston shale.....	331
	Table A.5. Standard deviation of null swell pressure of Milton Queenston shale in vertical and horizontal direction.....	332
	Table A.6. Standard deviation of the Brazilian Split test of Milton Queenston shale in vertical direction.....	333
	Table A.7. Standard deviation of the Brazilian split strength of Milton Queenston shale in horizontal direction.....	334
	Table A.8. Standard deviation of unconfined compression strength of Milton Queenston shale in vertical direction.....	335
	Table A.9. Standard deviation of unconfined compression strength of Milton Queenston shale in horizontal direction.....	336

List of Figures

FIGURE	DESCRIPTION	PAGE
CHAPTER 1: INTRODUCTIO		
Figure 1.1.	Queenston shale and other rocks forming bedrock of southern Ontario: a) sectional view of rock strata, b) geological map of bedrock.....	3
Figure 1.2.	Stages of development of time-dependent deformation of the rock and its influence on a pipe / tunnel constructed using micro-tunneling construction technique (assuming inadequate design of the pipe).....	5
CHAPTER 2: A COMPILATION OF THE GEO-MECHANICAL PROPERTIES OF ROCKS IN SOUTHERN ONTARIO AND THE NEIGHBOURING REGIONS		
Figure 2.1.	Locations of the geo-mechanical data measurements (from Google Maps web site).....	16
CHAPTER 3: INFLUENCE OF LUBRICANT FLUIDS ON THE SWELLING BEHAVIOUR OF QUEENSTON SHALE IN SOUTHERN ONTARIO		
Figure 3.1	X-ray diffraction traces of Milton Queenston shale and Niagara Queenston shale: (a, c) bulk specimens; (b, d) separated clay-size fractions.....	83
Figure 3.2	Preparations of specimens and locations of scanning electron microscopy imaging.....	86
Figure 3.3	Scanning electron microscopy images at surfaces of Milton Queenston shale specimens: (a, b) vertical and horizontal sections of specimen soaked in polymer solution; (c, d) vertical and horizontal sections of specimen soaked in bentonite solution.....	88
Figure 3.4	Scanning electron microscopy images on vertical sections of Milton Queenston shale: (a, b, c) intact near outer surface, at 15 mm , and at centre; (d, e, f) after 100 days of soaking in polymer solution; (g, h, i) after 100 days of soaking in bentonite solution; (j, k, l) after 100 days of soaking in water.....	89

FIGURE	DESCRIPTION	PAGE
Figure 3.5	Scanning electron microscopy images on horizontal sections of Milton Queenston shale: (a, b, c) intact near outer surface, at 15 mm, and at centre; (d, e, f) after 100 days of soaking in polymer solution; (g, h, i) after 100 days of soaking in bentonite solution; (j, k, l) after 100 days of soaking in water.....	90
Figure 3.6	Free swell test on Milton Queenston shale (MQS) in water, polymer and bentonite solutions (from M-FST22 TO M-FST30): (a, c, e) vertical swelling strains, (b, d, f) horizontal swelling strains.	100
Figure 3.7	Free swell test on Niagara Queenston shale (NQS) in water, polymer and bentonite solutions (from N-FST10 TO M-FST18): (a, c, e) vertical swelling strains; (b, d, f) horizontal swelling strains.	101
Figure 3.8	Semi-confined swell tests on Milton Queenston shale (MQS) in water, polymer and bentonite solutions: (a, c, e), vertical swelling strains under stress of 0.01, 0.1 & 1.0 MPa; (b, d, f) horizontal swelling strains under stress of 0.01, 0.1 and 0.7 MPa.....	106
Figure 3.9	Semi-confined swell tests on Niagara Queenston shale (NQS) in water, polymer and bentonite solutions: (a, c) vertical swelling strains under stress of 0.01 & 0.1 MPa; (b, d) horizontal swelling strains under stress of 0.01, & 0.3 MPa.....	107
Figure 3.10	Null-swell tests on Milton Queenston shale (MQS) in water, polymer and bentonite solutions: (a, c) null-swell stress in the vertical direction; (b, d) null-swell stress in the horizontal direction.....	109
Figure 3.11	Null-swell tests on Niagara Queenston shale (NQS) in water, polymer and bentonite solutions: (a) null-swell stress in the vertical direction; (b) null-swell stress in the horizontal direction.....	110
Figure 3.12	Swelling envelopes of Milton Queenston shale (MQS): (a) in the vertical direction; (b) in the horizontal direction.....	112
Figure 3.13	Swelling envelopes of Niagara Queenston shale (NQS): (a) in the vertical direction; (b) in the horizontal direction.....	113

FIGURE	DESCRIPTION	PAGE
CHAPTER 4: THE INFLUENCE OF WATER AND LUBRICANT FLUIDS ON THE PEAK STRENGTH OF QUEENSTON SHALE FROM SOUTHERN ONTARIO		
Figure 4.1	Borehole logging of the recovered samples of Queenston shale from Milton, Ontario.....	138
Figure 4.2	Steps followed to protect specimens during soaking period: (a) Intact specimen; (b, c, d) steps of preserving the specimen; (e, f) preserved specimen after soaking period.....	143
Figure 4.3	Sectional view of the modified triaxial compression cell: 1) cell body, 2) cell base, 3) central pedestal, 4) piston, 5) ventilation valve, 6) inlet/outlet junction, 7) one-way inlet valve, 8) outlet adjusting valve, 9) outlet needle valve, 10) assembly cap, 11) adjusting seat, 12) adjusting cap, 13) specimen's platen, 14) pressure transducer, 15) sealing gland, 16) electronic foil strain gauge, 17) strain gauge wires, 18) cell chamber, 19) rubber washer and stopper, 20) rubber casket: and 21) rock specimen.....	145
Figure 4.4	Schematic drawing of the orientation of specimens in the Brazilian split test.	149
Figure 4.5	Scanning electron microscopy images of Milton Queenston shale (MQS): (a) vertical surface of intact specimen; (b) horizontal surface of intact specimen, c) polymer coating on MQS and (d) bentonite coating on MQS.....	155
Figure 4.6	Brazilian splitting test performed on: (a) intact specimens and specimens soaked for hundred days in (b) water; (c) polymer solution and (d) bentonite solution; (1) vertical specimens; (2) horizontal specimen.....	157
Figure 4.7	Results of unconfined compressive strength performed on vertically cored Milton Queenston shale specimens: (a) intact specimen; specimens soaked for hundred days in: (b) water, (c) polymer solution and (d) bentonite solution, respectively.....	164

FIGURE	DESCRIPTION	PAGE
Figure 4.8	Results of unconfined compressive strength performed on horizontally cored Milton Queenston shale specimens: (a) intact specimen; specimens soaked for hundred days in: (b) water, (c) polymer solution and (d) bentonite solution, respectively.....	165
Figure 4.9	Unconfined compressive strength test performed on: (a) intact specimens and specimens soaked for hundred days in: (b) water; (c) polymer solution and (d) bentonite solution; 1) vertical specimens, 2) horizontal specimen.....	166
Figure 4.10	Triaxial compressive strength test performed on: (a) intact specimens and specimens soaked for hundred days in: (b) water; (c) polymer solution and (d) bentonite solution; (1) vertical specimens, (2) horizontal specimen.....	174
Figure 4.11	Results of triaxial compression strength performed on vertically cored Milton Queenston shale specimens at $\sigma_3=5.0$ MPa: (a) intact specimen; specimens soaked for hundred days in: (b) water, (c) polymer solution and (d) bentonite solution, respectively.....	175
Figure 4.12	Results of triaxial compression strength performed on horizontally cored Milton Queenston shale specimens at $\sigma_3=5.0$ MPa: (a) intact specimen; specimens soaked for hundred days in: (b) water, (c) polymer solution and (d) bentonite solution, respectively.....	176
Figure 4.13	Strength envelopes of Milton Queenston shale (Intact and after soaking in water; polymer solution and bentonite solution): (a, b) principal stresses; (c, d) normal and shear stresses.....	178

CHAPTER 5: STRENGTH ENVELOPES OF NIAGARA QUEENSTON SHALE UNDER DIFFERENT WETTING CONDITIONS UTILIZING MULTISTAGE TRIAXIAL COMPRESSION TEST

Figure 5.1 Longitudinal section in the modified triaxial cell: (1) cell body; (2) cell base; (3) central pedestal; (4) piston; (5) ventilation valve; (6) inlet/outlet junction; (7) one-way inlet valve; (8) main adjustment valve; (9) needle adjustment valve; (10) specimen's cap; (11)

FIGURE	DESCRIPTION	PAGE
	adjusting seat; (12) specimen's platen; (13) pressure transducer; (14) sealing gland; (15) electronic foil strain gauge; (16) strain gauge wires; (17) cell chamber; (18) rubber washer and stopper; (19) rubber casket and (20) rock specimen.....	190
Figure 5.2	X-ray diffraction traces of Niagara Queenston shale powder: (a) Bulk powder specimens; (b) Separated clay-size portions specimens.....	193
Figure 5.3.	Scanning electron microscopy images on horizontal sections of Queenston shale before and after soaking for 100 days in water, polymer solution and bentonite solution.	196
Figure 5.4	Typical results of unconfined compression strength test of Niagara Queenston shale: (a) intact specimen; (b) soaked in water; (c) soaked in polymer solution and (d) soaked in bentonite solution, for 100 days.....	202
Figure 5.5	Multistage triaxial compression strength test performed on intact Niagara Queenston shale.....	207
Figure 5.6	Multistage triaxial compression strength test performed on Niagara Queenston shale soaked for 100 days in water.....	208
Figure 5.7	Multistage triaxial compression strength test performed on Niagara Queenston shale soaked for 100 days in polymer solution.....	209
Figure 5.8	Multistage triaxial compression strength test performed on Niagara Queenston shale soaked for 100 days in bentonite solution.....	210
Figure 5.9	Strength Envelopes of Niagara Queenston shale: (a) Principal stresses and (b) Normal and shear stresses.....	213
Figure 5.10	Mohr-Coulomb parameters of Niagara Queenston shale: (a) change in cohesion with minor principal stress and (b) change in internal frictional angle with minor principal stress.....	215
Figure 5.11	Comparative display of the strength of intact Milton Queenston shale measured from multistage triaxial and single-stage triaxial tests.....	218

FIGURE	DESCRIPTION	PAGE
5.12	Strength envelope of Milton Queenston shale based on multistage triaxial compression test and single-stage triaxial compression test results.....	219
5.13	Comaparision of strength envelopes of Niagara and Milton Queenston shales: (a) principal stresses and (b) normal and shear stresses.....	221

CHAPTER 6: DEPTH OF PENETRATION OF LUBRICANT FLUIDS AND WATER IN QUEENSTON SHALE OF SOUTHERN ONTARIO

Figure 6.1	Test setup to investigate depth of penetration of lubricant fluids into shale.....	232
Figure 6.2	Schematic drawing for calculating the hydraulic conductivity of the Queenston shale	237
Figure 6.3	Fluid penetration in the Queenston shale: (a) water; (b) polymer solution and (c) bentonite solution.....	242
Figure 6.4	Change in moisture content of the Queenston shale with distance from source of fluid application.....	244
Figure 6.5	Change in pore fluid salinity of the Queenston shale with distance from source of fluid application.....	245
Figure 6.6	Penetration depth of fluids into the Queenston shale with time.....	248

CHAPTER 7: FINITE ELEMENT ANALYSES OF TIME-DEPENDENT DEFORMATION AND INDUCED STRESSES IN CONCRETE PIPES CONSTRUCTED IN QUEENSTON SHALE USING MICRO-TUNNELING TECHNIQUE

Figure 7.1	Geological map of southern Ontario.....	261
Figure 7.2	Rock swelling models: (a) Grob’s swelling law; (b) Lo and Hefny swelling model.....	263

FIGURE	DESCRIPTION	PAGE
Figure 7.3	Rock swelling tests apparatus developed earlier at the University of Western Ontario and their finite element models.....	268
Figure 7.4	Graphical results of finite element models of swelling tests: (a, b) free swell test in water; (c, d) semi-confined swell tests in polymer solution in vertical and horizontal directions, respectively, (e, f) null swell test in bentonite solution in vertical and horizontal direction, respectively.....	271
Figure 7.5	Computed finite element results and measured laboratory free swell tests results of Milton Queenston shale in water, polymer and bentonite solutions in vertical and horizontal directions.....	272
Figure 7.6	Computed finite element results and measured laboratory semi-confined swell tests results of Milton Queenston shale in water, polymer and bentonite solutions in vertical and horizontal directions.....	275
Figure 7.7	Computed finite element results and measured laboratory null swell tests of Milton Queenston shale in water, polymer and bentonite solutions in vertical and horizontal directions.....	278
Figure 7.8	Finite element model of the Niagara wheel pit excavation.....	281
Figure 7.9	Time-dependent deformation of the Niagara wheel pit excavation at Rochester shale level.....	283
Figure 7.10	Scotia plaza excavation: (a) finite element model and (b) measured and calculated deformation of excavation face.....	287
Figure 7.11	Calculated and computed axial thrust and bending moment in concrete lining with full slip interface: (a, b) Lo and Hefny (1996) closed form solution results; (c, d) Finite Element analyses results.....	291

FIGURE	DESCRIPTION	PAGE
Figure 7.12	Calculated and computed axial thrust and bending moment in concrete lining with no slip at interface: (a, b) Lo and Hefny (1996) closed form solution results; (c, d) Finite Element analyses results.....	292
Figure 7.13	Finite element mesh used to model the Queenston shale and a pipeline / tunnel constructed using micro-tunneling technique.....	297
Figure 7.14	Variation of pipe convergence at springline with time for different sizes of FE mesh.....	300
Figure 7.15	Variation of maximum tangential tensile stress at springline of concrete pipes constructed in Milton Queenston shale at different construction periods; different in-situ stress ratios (K_s) and different diameters: (a) at 1.7 m depth; (b) at 10 m depth and (c) at 20 m depth below top of the Queenston shale layer.....	302
Figure 7.16	Maximum tangential stresses at springline and crown of a concrete pipe constructed in Milton Queenston shale with in-situ stress ratio = 5: (a, c) using polymer solution and (b, d) using bentonite solution.....	304
Figure 7.17	Maximum tangential stresses at springline and crown of a concrete pipe constructed in Niagara Queenston shale with in-situ stress ratio = 5: (a, c) using polymer solution and (b, d) using bentonite solution.....	305
Figure 7.18	Variation of tangential tensile stress developed at the springline of 1.8 m diameter concrete pipe constructed at 1.7 m depth below top of the Queenston shale layer with different construction period.....	307
Figure 7.19	Bending moment at springline and crown of a concrete pipe after 30 years of construction in Milton Queenston shale with in-situ stress ratio = 5: (a, c) using polymer solution and (b, d) using bentonite solution.....	309
Figure 7.20	Bending moment at springline and crown of a concrete pipe after 30 years of construction in Niagara Queenston shale with in-situ stress ratio = 5: (a, c) using polymer solution and (b, d) using bentonite solution.....	310

FIGURE	DESCRIPTION	PAGE
Figure 7.21	Contours of the horizontal deformation occurred after 30 years of the construction.....	312
Figure 7.22	Predicted inward convergence of 1.8 m diameter concrete pipe at the springline.....	313

LIST OF APPENDICES

PPENDIX A.....	328
-----------------------	------------

LIST OF ABBREVIATIONS AND SYMBOLS

A	Cross-sectional area (m ²)
ASTM	American Society of Testing and Materials
BGL	Below ground level
Ca(HCO ₃) ₂	Calcium hydrogen carbonate (Calcium bicarbonate)
CEC	Cation Exchange Capacity
C _{fl}	Fluid constant (m/day ^{0.588})
d	Tunnel / pipe diameter
<i>d</i>	Depth of fluid penetration
D _f	Final Diameter (fluid penetration test)
D _i	Initial Diameter (fluid penetration test)
E	East
E _h	Elastic modulus I horizontal direction (GPa)
E _v	Elastic modulus in vertical direction (GPa)
G	Shear modulus (GPa)
HSP	Horizontal swelling potential (% strain/ log cycle of time)
<i>i</i>	Hydraulic gradient (m/m)
K	Hydraulic conductivity (m/s)
k _{qi}	Axial swelling parameter (Grob's law)
K _o	In-situ stress ratio (in-situ horizontal stress / vertical overburden stress)
L _f	Final length (m)
L _i	Initial length (m)
MQS	Milton Queenston shale
N	North
NQS	Niagara Queenston shale
SEM	Scanning electron microscopy

S_i	Initial rate of water absorption ($\text{mm/s}^{0.5}$)
S_s	Secondary rate of water absorption ($\text{mm/s}^{0.5}$)
t	Time (days)
USBM	United States Bureau of Mines Probe
UTM	Universal Transvers Mercator Coordinates
VSP	Vertical swelling potential (% strain/ log cycle of time)
w	Moisture content (%)
XRD	X-Ray diffraction
σ_i	Applied Stress (MPa)
σ_c	In Grob's law: minimum stress to limit excessive swelling (MPa); In Lo and Hefny, 1996 swelling model: minimum stress required to stop swelling (MPa)
σ_{th}	Minimum stress to start suppression of swelling (MPa)
σ_{qoi}	Maximum axial swelling stress (MPa)
ν	Poisson's ratio
ν_h	Poisson's ratio for the effect of horizontal stress on horizontal strain
ν_v	Poisson's ratio for the effect of vertical stress on horizontal strain

Chapter 1

INTRODUCTION

1.1 GEOLOGICAL BACKGROUND

The region of southern Ontario lies between the Appalachian Basin and the Michigan Basin with the majority of southern Ontario is covered by the Appalachian sedimentary basin. The Appalachian basin consists of Precambrian metamorphic rocks overlain by Paleozoic deposits. It is bounded by Precambrian basement highs and Findley arches in the West, the Frontenac arch in the North and the Taconic Mountain Range in the East and South, where sediments were eroded during the Taconic and Appalachian origins. The arches are Precambrian granitic rock highs (Perras, 2009). The topographic nature of southern Ontario is relatively flat with the exception of the Niagara Escarpment and a hilly ground from Lake Huron to Rochester in New York (Perras et al., 2015). The Appalachian basin has coarse-grained sedimentary rocks with high stresses (Stearn et al., 1979). In this basin, the sedimentary rocks of southern Ontario composed of rock formations of different ages from Cambrian to Devonian with the younger formations outcrop at the south-western part of Ontario. One of these rock formations is the Queenston shale, which was formed in the upper Ordovician age following the formation of the Georgian Bay shale.

Figure 1.1 shows a geological map of southern Ontario and a sectional view made through the rock strata. It can be noted that the Queenston shale layer outcrops at the south west shores of Lake Ontario and extends up to the North. The thickness of the Queenston shale gradually decreases towards the south-west, as indicated in Figure 1.1 (a) and it becomes overlain by other rocks. According to its location and depth, the Queenston shale layer forms the hosting ground of engineering projects in major cities in south-west shores of Lake Ontario. The region of southern Ontario has high in-situ horizontal stress in some of its parts. These parts form a belt of high in-situ horizontal

stresses stretches from Rochester in New York State westward through Niagara Falls, turning northeast around Lake Ontario following the lake shore line and extending at least as far east as Wesleyville, Ontario (Lo, 1978). This indicates that the Queenston shale layer has considerably high in-situ stresses, which found to be ranging between 9-24 MPa (Lo and Yuen, 1981). The other important characteristic of this shale is the high rock pore water salinity compared to other rocks (Lee and Lo, 1993). It is also well established that the Queenston shale has time-dependent deformation behaviour (Lo and Lee, 1990; Lee and Lo, 1993; Hefny et al., 1996; Lo and Hefny, 1996 and Hawlader et al., 2003).

The time-dependent behavior may cause damage to the underground structures, such as invert heave and cracks in the springline of tunnels (Bowen et al., 1976, Einstein and Bischoff, 1975). The time-dependent deformation behavior of the Queenston shale of southern Ontario was found to be caused by fulfillment of the following three conditions: i) the relief of the initial stresses which serves as initiating mechanism, ii) the accessibility of water and iii) an outward salt concentration gradient from the pore fluid of the rock to the ambient fluid (Lee and Lo, 1993). When all these conditions are met, the time-dependent deformation occurs. If none of these conditions are satisfied, the time-dependent deformation is not expected. If one or more of these conditions are satisfied, the time-dependent deformation may or may not occur (Lee and Lo, 1993). It is obvious that these conditions are satisfied in most of the construction techniques of underground structures and the time-dependent deformation of the Queenston shale is expected to occur.

1.2 OVERVIEW

The increasing demand to extend existing infrastructure and the need for new tunnels and pipelines in major cities of southern Ontario has promoted the use of construction techniques that have minimal impact on people, existing structures and the

environment. In this regard, one of the efficient methods to construct pipelines and tunnels is the micro-tunnelling construction technique and its applications in different

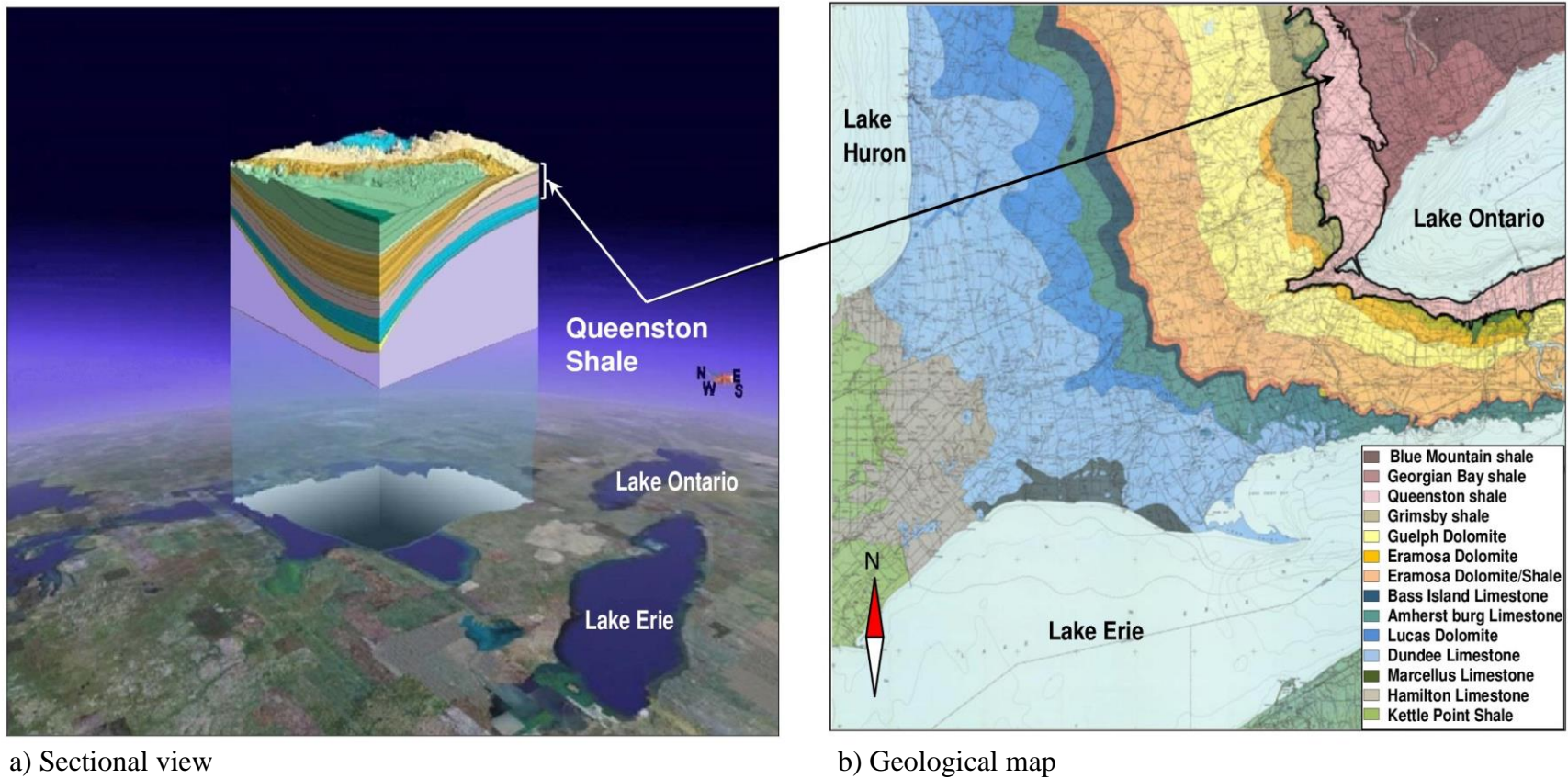


Figure 1.1. Queenston shale and other rocks forming the bedrock of southern Ontario: a) sectional view of rock strata, b) geological map of the bedrock.

types of ground. It offers many advantages over the traditional cut and cover procedure to install pipelines and conventional tunneling applications. It minimizes impact on the environment and reduces disturbance to people and existing facilities. It eliminates obstructions to existing structures, such as road interchanges; highways; railways and other essential structures that must have uninterrupted operation during construction.

In micro-tunneling applications, lubricant fluids, such as bentonite solution and polymer solution are used to facilitate the installation of the pipe / tunnel segments during the machine advance. These lubricant fluids are kept around the pipe / tunnel during the construction period, and they are replaced with permanent cement grout at end of construction. The construction period may last for several weeks depending on the ground situation. During this period, lubricant fluids contact the excavated ground and may percolate deep into it. The Queenston shale forms the host rock for potential micro-tunneling projects to construct pipeline / tunnel in many sites in southern Ontario. This shale has time-dependent deformation behavior in the form of volume increase, which may affect the micro-tunneling machine during the construction period or may cause damage to constructed pipeline / tunnel. Therefore, the time-dependent deformation behavior associated with micro-tunneling technique has to be evaluated prior to using this technique in Queenston shale of southern Ontario.

1.3. MICRO-TUNNELING CONSTRUCTION TECHNIQUE

Micro-tunneling is a construction technique used to construct pipelines and tunnels in different types of ground. It consists mainly of the boring machine that drills through the rock, the hydraulic jacking system that pushes the machine forward while it cuts, the slurry system to transport the rock cuttings to the ground surface, vertical shafts (i.e. starting shaft and receiving shaft) at different intervals to handle the machine and the jacking system and lubricant fluids to facilitate the movement of the pipe through the ground and to give relative support to the excavation.

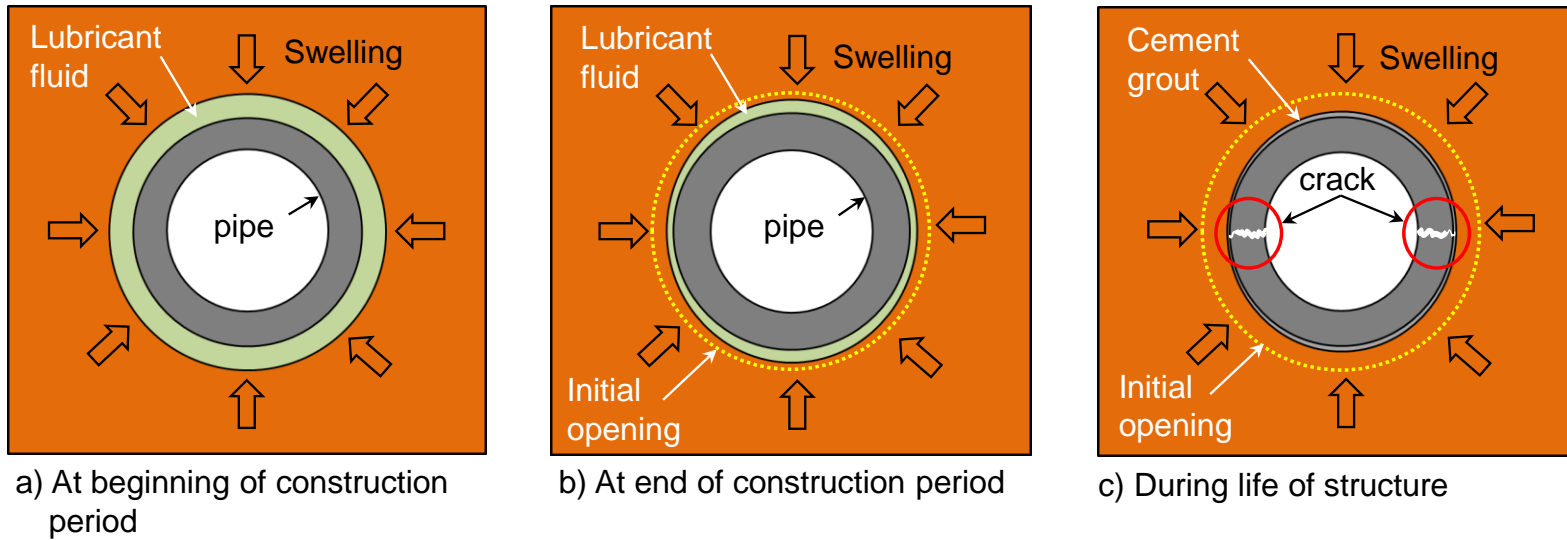


Figure 1.2. Stages of development of time-dependent deformation of the rock and its influence on a pipe / tunnel constructed using micro-tunneling construction technique (assuming inadequate design of the pipe).

First, the vertical shafts are constructed and the hydraulic jacking system is placed in position at the bottom of the starting shaft. Second, the boring machine is lowered into the starting shaft and placed in its track rail and starts drilling and advances through the rock with the aid of the jacking system. While the boring machine advances, pipe segments are placed behind it in a continuous manner. This process continues until the machine reaches the receiving shaft where it removed to the ground surface. The boring machine drills through the rock with slightly bigger diameter than the diameter of the constructed pipe. During the construction period, the gap between the excavation and the pipe is filled with lubricant fluid (i.e. bentonite solution or polymer solution) under a pressure of 200 kPa. The main function of lubricant fluids is to reduce the frictional forces between the ground and the pipe while it moves forward.

Figure 1.2 is a schematic drawing showing the stages of micro-tunneling construction technique in Queenston shale and its time-dependent deformation effects on the constructed pipe. Figure 1.2 (a), shows the constructed pipe surrounded by lubricant fluid filling the gap between the excavated rock and the pipe to facilitate its advance. Immediately after excavation, the Queenston shale starts its time-dependent deformation causing inward deformation of the excavated tunnel. At this stage, the pipe is safe and it does not expose to loads from the Queenston shale. After several weeks, the size of the excavated tunnel decreased due to the time-dependent deformation of the Queenston shale, as indicated in Figure 1.2 (b). The inward deformation can be uneven due to the difference in the vertical and horizontal in-situ stresses and the anisotropic behavior in the time-dependent deformation of the Queenston shale. At this stage, the pipe does not expose to loads from the ground due to the existing gap.

In current practice of constructing tunnels in swelling rocks, to mitigate effects of the time-dependent deformation of swelling rock, such as the Queenston shale, installing the final support is delayed for few month allowing for majority of swelling to occur. To apply this mitigation in micro-tunnelling applications, the gap between the installed pipe and the excavated tunnel may be kept full with the lubricant fluid for longer than the

construction period before replacing the lubricant fluid with the permanent cement grout. After several weeks from the completion of construction process, more time-dependent deformation has occurred causing more decrease of the size of excavated tunnel, as it can be seen in Figure 1.2 (c) where dotted circle represents the original excavated tunnel. At this moment, the pipe becomes in contact with the swelling ground through the cement grout. If the pipe was not designed adequately and the swelling of the ground is high, cracks may appear in the pipe, as it is shown in Figure 1.2 (c).

1.4 RESEARCH OBJECTIVES

The main objectives of this research are twofold: to investigate the effects of lubricant fluids utilized in micro-tunneling construction on the time-dependent deformation and mechanical properties of Queenston shale of southern Ontario and to evaluate the impact of these changes on stresses induced in the infrastructure constructed employing the micro-tunneling technique in Queenston shale. To achieve these objectives, the research was sub-divided into the following four research areas:

- i. Study of the influence of bentonite and polymer solutions used in micro-tunneling applications on the time-dependent deformation behavior of Queenston shale.
- ii. Study of the impact of bentonite and polymer solutions on the strength properties of Queenston shale.
- iii. Investigation of the depth of percolation of bentonite and polymer solutions and water into Queenston shale.
- iv. Development of a finite element model to investigate time-dependent deformation and induced stresses on a pipeline / tunnel constructed in the Queenston shale using micro-tunneling technique.

1.5 THESIS OUTLINE

This thesis has been prepared in the integrated article format specified by the School of Graduate and Postgraduate Studies at the University of Western Ontario. Each chapter in this thesis was written as an individual article, with the exception of chapter 1 “Introduction”, and chapter 8 “Summary, Conclusions and Recommendations”. In Chapters two through seven, the literature review for the subject dealt with is included together with its relevant list of references.

Chapter 2 presents a compilation of the geo-mechanical properties of rocks in southern Ontario and the neighboring regions. The presented geo-mechanical properties includes: i) the measured in-situ horizontal stresses, ii) the strength and time-dependent deformation properties and iii) the dynamic properties. The compiled measurements presented in this chapter can be used as a source for preliminary evaluation of rock properties in southern Ontario and the neighboring regions. The chapter contains a discussion section that focuses on the geo-mechanical properties of the Queenston shale which is the rock formation considered in this research.

Chapter 3 deals with the time-dependent deformation behavior of Queenston shale in lubricant fluids (i.e. bentonite solution and polymer solution) used in micro-tunneling applications. The influence of these fluids on the time-dependent deformation behavior of Queenston shale is investigated. Lubricant fluids were used instead of water in the time-dependent deformation tests (i.e. Lo et al., 1978; and Lo and Hefny, 1999). The results of free swell test, semi-confined swell test, and null swell test performed on two Queenston shale samples from Milton and Niagara Falls regions are presented. These tests were performed on vertical and horizontal samples with respect to the rock bedding, using lubricant fluids as ambient fluids. This chapter also presents results of x-ray diffraction; scanning electron microscopy; rock pore fluid salinity; calcite content; rate of absorption; and cation exchange capacity tests. The chapter discusses the behavior of the Queenston shale in lubricant fluids and a mechanism for this behavior is suggested.

Chapter 4 investigates the strength degradation of Milton Queenston shale after its exposure to lubricant fluids and water. It presents results of four main tests performed on this shale: i) Brazilian split test; ii) unconfined compression test; iii) single stage triaxial compression test and iv) direct tension test, performed on vertically and horizontally cored samples from Milton, Ontario. The modifications required to accommodate size variation of the rock samples that were made to the triaxial compression cell are presented. Results of complimentary tests, such as rock pore fluid salinity and the calcite content of the Queenston shale samples are also presented. The chapter discusses the strength behavior of the Queenston shale in lubricant fluids and water, and suggests a mechanism for this behavior. The developed strength envelopes of Milton Queenston shale in its intact condition (i.e. as recovered from in-situ) and after soaking in lubricant fluids and water for 100 days are presented. The calculated elastic properties in vertical and horizontal direction with respect to rock bedding of Milton Queenston shale are evaluated and their variation is discussed.

Chapter 5 focusses on the multistage triaxial compression test performed on Queenston shale samples from Niagara, Ontario using the modified triaxial cell. This chapter demonstrates application of the multistage triaxial compression test to measure the Queenston shale strength in multiple confining pressures using the same sample. Results of strength tests performed on the Queenston shale are presented, which demonstrate the decrease in their strength upon continuous exposure to lubricant fluids and water. In addition, the results of i) unconfined compression test; ii) Brazilian split test and ii) direct tension test performed on intact and soaked samples in lubricant fluids and water are presented. The calcite content; rock pore fluid salinity and the elastic properties of the Niagara Queenston shale samples are provided. Furthermore, the strength tests are summarized in the form of strength envelopes. Finally, the loss in strength of Queenston shale upon soaking in lubricant fluids and water is discussed and an explanation of its causes is provided.

In Chapter 6, a test apparatus and a procedure are developed to measure the percolation depth of lubricant fluids used in micro-tunneling applications and water into the Queenston shale of southern Ontario. Based on the testing observations, an empirical correlation was proposed, which can be used to calculate the percolation depth of these fluids into the Queenston shale with time. The procedure followed to calculate the primary permeability of the Queenston shale is also explained.

A finite element model was developed in Chapter 7, which can be used for the analysis of micro-tunneling projects in Queenston shale of southern Ontario. The chapter provides the details of the finite element model and its mathematical basis. Extensive verification of the numerical model was conducted through comparisons with: i) laboratory time-dependent deformation tests; ii) two reported excavations in swelling rocks with in-situ measurements and iii) the closed form solutions of circular tunnel in swelling rock suggested by Lo and Hefny (1996). The verified numerical model was then utilized to conduct a comprehensive parametric study considering important micro-tunnels parameters including: tunnel diameter and depth; shale in-situ stress ratio and construction duration. Finally, conclusions are drawn and recommendations are made for micro-tunneling applications in Queenston shale of southern Ontario.

Chapter 8 provides the summary of research; drawn conclusions and recommendations for micro-tunneling applications in the Queenston shale of southern Ontario and for future research work.

1.6 ORIGINAL CONTRIBUTIONS

The original research contributions in this thesis are:

- The study of the influence of lubricant fluids used in micro-tunneling applications on the time-dependent deformation behavior of Queenston shale of southern Ontario.

- The modifications made to the triaxial cell to perform triaxial compression (both single stage and multistage) tests on Queenston shale of variable size and high confining pressure.
- The study of strength degradation of Queenston shale caused by water and lubricant fluids used in micro-tunneling applications.
- The development of test apparatus and test procedure to measure the percolation depth of water and lubricant fluids into the Queenston shale.
- Development of a finite element model to predict time-dependent deformations and induced stresses in a pipeline / tunnel constructed in the Queenston shale using micro-tunneling technique.

1.7 REFERENCES

- Bowen, C.F.P., Hewson, F.I., MacDonald, D.H., and Tanner, R.G. 1976. Rock squeeze at Thorold Tunnel. *Canadian Geotechnical Journal*, **13**(2): 111-126.
- Einstein, H.H., and Bischoff, N. 1975. Design of tunnels in swelling rocks. In *Proceedings of the 16th Symposium on Rock Mechanics*, University of Minnesota, Minneapolis, Minn. pp. 185-197.
- Hawlader, B.C., Lee, Y.N., and Lo, K.Y. 2003. Three-dimensional stress effects on time-dependent swelling behaviour of shaly rocks. *Canadian Geotechnical Journal*, **40** (3): 501-511.
- Hefny, A., Lo, K.Y., and Huang, J.A. 1996. Modelling of long-term time-dependent deformation and stress-dependency of Queenston shale. In *Proceedings of Canadian Tunnelling 1996*. The Tunnelling Association of Canada. pp. 115-146.

- Lee, Y.N., and Lo, K.Y. 1993. The swelling mechanism of Queenston shale. In Proceedings of Canadian Tunnelling 1993. The Tunnelling Association of Canada. pp. 75-97.
- Lo, K.Y. 1978. Regional distribution of in situ horizontal stresses in rocks of Southern Ontario. Canadian Geotechnical Journal, **15**(3): 371-381.
- Lo, K.Y. and Hefny, A.M. 1999. Measurements of Residual Expansion Rates Resulting from Alkali-Aggregate Reaction in Existing Concrete Dams. ACI Materials Journal, **96** (3): 339-345.
- Lo, K.Y. and Hefny, A. 1996. Design of tunnels in rock with long-term time-dependent and nonlinearly stress-dependent deformation. Canadian Tunnelling 1996, The Tunnelling Association of Canada, Toronto, Ontario, pp. 179-214.
- Lo, K.Y., and Lee, Y.N. 1990. Time-dependent deformation behaviour of Queenston shale. Canadian Geotechnical Journal, **27** (4): 461-471.
- Lo, K.Y., Wai, R.S.C., Palmer, J.H.L. and Quigley, R.M., 1978. Time-dependent deformation of shaly rocks in Southern Ontario. Canadian Geotechnical Journal, **15** (4): 537-547.
- Lo, K.Y., and Yuen, C.M.K. 1981. Design of tunnel lining in rock for long term time effects. Canadian Geotechnical Journal, **18** (1): 24-39.
- Perras, M. A., 2009. Tunnelling in horizontally laminated ground: The influence of lamination thickness on anisotropic behaviour and practical observations from the Niagara tunnel project. MSE Thesis. Queen's University, Kingston, Ontario, Canada, 2009. 335 pages.
- Perras, M.A., Wannenmacher, H, and Diederichs, M.S., 2015. Underground Excavation Behaviour of the Queenston Formation: Tunnel Back Analysis for Application to

Shaft Damage Dimension Prediction. *Rock Mechanics and Rock Engineering*,
48:1647-1671.

Stearn, C.W., Carroll, R.L., and Clark, T.H. (eds) 1979. *Geological Evolution of North America*. John Wiley and Sons, Toronto.

Chapter 2

A COMPILATION OF THE GEO-MECHANICAL PROPERTIES OF ROCKS IN SOUTHERN ONTARIO AND THE NEIGHBOURING REGIONS¹

2.1 INTRODUCTION

The strength and deformation parameters of the rock are required in the design process of underground structures, in addition to the initial in-situ stresses that exist at a specific depth in the hosting rock. During the past few decades, extensive investigations of the initial in-situ stresses in rocks of southern Ontario and the neighboring regions (i.e. New York; Ohio; Michigan; Indiana; Illinois; Wisconsin and Minnesota) and their strength and deformation properties including time-dependent deformation properties were carried out. The investigations revealed that the rocks of these regions are subjected to high initial horizontal in-situ stresses that are of great influence on the deformation behavior of these rocks with time.

The deformation of rocks with time is defined as the time-dependent deformation behavior, which can be manifested as different types of distress on the existing underground structures in southern Ontario (Lo, 1978). These distresses were observed in the form of cracks in the tunnels lining at the springline, invert heave, buckling of lining concrete of canal floors, bottom heaves in quarries and long-term movement of walls of unsupported excavations. In many cases, the resulting defects can cause severe damage to underground structures that require costly remedial and maintenance works (Lo, 1978).

¹ A version of this chapter has been published in the Open Journal of Geology, 2014, **4**: 210-227.

The time-dependent deformation behavior of rocks in southern Ontario was extensively investigated during the past decades (Hefny et al., 1996; Lee and Lo, 1993; Lo and Lee, 1990; Lo, 1989; Lo et al., 1987 and 1981; Lo and Hori, 1979 and Lo et al., 1978). Considering osmosis and diffusion as a mechanism of swelling, these investigations were based on measuring the swell deformation of intact rock specimens submerged in water with variable confining pressures and variable salinity of the ambient water. However, present-day tunnel drilling technologies such as micro-tunneling and horizontal direction drilling involve fluids such as bentonite slurry and synthetic polymers solutions during the drilling process, which may influence the strength and the time-dependent deformation behavior of rock in the vicinity of the tunnel annulus. Bearing this in mind, it is quite important to investigate the influence of these drilling fluids on the strength and time-dependent deformation behavior of rocks in this region, as will be presented in the next chapters.

This chapter presents a compilation of in-situ stress measurements, strength and stiffness measurements, time-dependent deformation measurements, and some dynamic properties measurements of different rock formations in southern Ontario and the neighboring regions. The compiled data serve as initial source of information for the research studies presented in this thesis and for any prospective study of the geo-mechanical properties of the rocks in these specified regions. Figure 2.1 displays the locations of the sites from which the measurements were compiled.

2.2 SUMMARY OF COMPILED MEASUREMENTS

2.2.1 In-Situ Horizontal Stresses

The measured values and directions of the in-situ horizontal stresses at different locations in southern Ontario and the neighboring regions were summarized and presented in Table 2.1. The presented data were compiled from sites where different measuring techniques were used to evaluate the in-situ stresses at variable depths and diversity of rock formations specifically in southern Ontario and the surrounding regions

(i.e. New York; Ohio; Michigan; Indiana; Illinois; Wisconsin and Minnesota). In general, one of the earliest attempts to measure the in-situ stresses in rocks was made by Hast in the 1950's in Scandinavia as described in (Terzaghi, 1962). This attempt was followed by numerous studies that resulted in developing several methods to measure the in-situ stresses in different locations all over the world, many of which were in southern Ontario. The most common methods to measure the initial horizontal in-situ stresses in rocks are: i) the hydraulic fracturing (hydro-fracturing test); ii) the over-coring technique with U.S. Bureau Mines probe (USBM); and iii) the under-coring technique with electrical strain gauges affixed in the borehole under consideration.

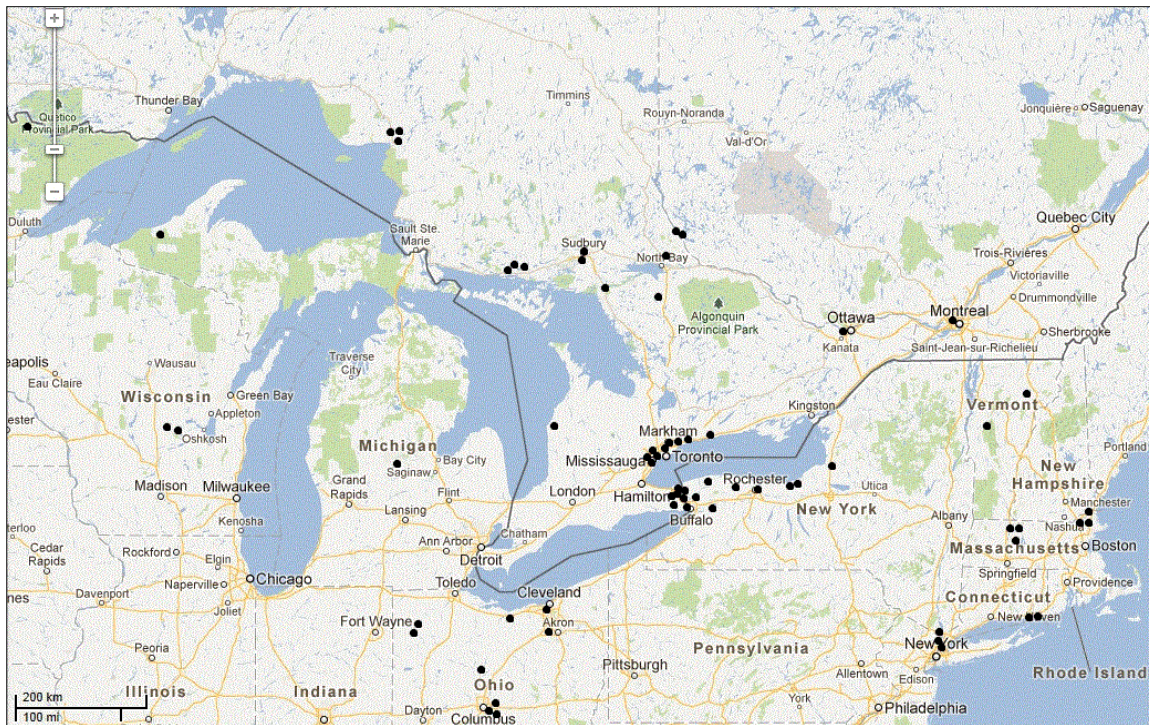


Figure 2.1. Locations of the geo-mechanical data measurements (from Google Maps web site)

The hydraulic fracturing test consists essentially of sealing off a section of a borehole and injecting a fluid into the interval to induce a fracture in the surrounding rock. The orientation of the resulting fracture and the pressures required to maintain the fracture are incorporated in an analysis to determine the in-situ stresses (Von Schonfeldt and Fairhurst, 1972, and Lindner and Halpern, 1978). The over-coring technique with

USBM probe consists of drilling a hole to the required depth and then, from the bottom of this hole, a pilot hole of 38 mm diameter is drilled and the USBM probe is fixed in that hole. Then, the pilot hole is over-cored by employing a large diameter core bit to separate the rock core cylinder containing the probe from in-situ. Later, the rock core cylinder is removed from the ground and tested in a hydraulic chamber to determine the modulus of elasticity and to calculate the in-situ horizontal stress from elastic theory relationships (Lindner and Halpern, 1978). The under-coring technique employs a package of electrical strain gauges, which is affixed to the base of the borehole. The waterproof electrical package and connections are sealed in a cylindrical form of plastic, and are affixed with quick setting epoxy at the bottom of the borehole. The deformation measurements of the borehole are taken before and after extending the core bit beyond the base of the borehole which under-cores the electrical strain gauges (Lindner and Halpern, 1978).

From the summarized data presented in Table 2.1, the value of the initial in-situ horizontal stress in rock formations of southern Ontario and the neighboring regions varies from a relatively small amount (<1 MPa) for sandstone in Ohio (Lindner and Halpern, 1978 and Rough and Lambert, 1971) to a much higher amount (>80 MPa) for sandstone in Michigan (Haimson, 1976). The high variation of the measured in-situ stress in rocks depends on the rock formation, rock type, depth of measurement and interbedded layers in the rock mass where stress measurements were taken. For example, the Georgian Bay shales in Toronto, Ontario possess an initial in-situ horizontal stress of a considerably high value of 1.25 - 9.5 MPa in the major horizontal stress direction and 0.86 - 6.32 MPa in the minor horizontal stress direction at depth of 6.0 - 18.2 m (Lo and Yuen, 1981 and Lo, 1989). The Queenston shale from the Niagara Falls area, Ontario, exhibits an initial in-situ horizontal stresses of 14.3 - 17.1 MPa in the major horizontal stress direction and 8.6 - 11.3 MPa in the minor horizontal stress direction at depth of 93.9 - 123.8 m (Lo and Hefney, 1993). In addition, shale in Ohio, at 10.3 - 18.6 m depth, possesses comparatively high in-situ horizontal stresses of 5.56 - 38.13 MPa and 4.69 - 32.41 MPa in the major and minor in-situ horizontal stress directions, respectively (Lindner and Halpern, 1978). In the presented data, the highest measured in-situ horizontal stresses in shale of North America were recorded in Michigan, where the stress

measurements were taken at overwhelming depths that exceeded 5100 m. The measured in-situ horizontal stresses in shale of Michigan at that depth were 135.0 MPa and 95.0 MPa in the major and minor in-situ horizontal stress directions, respectively (Haimson and Fairhurst, 1970).

On the other hand, sandstone of Elliot Lake, Ontario, at 427.0 m depth, exhibits an in-situ horizontal stress of 35.37 MPa and 24.13 MPa in the major and minor in-situ horizontal stress direction, respectively (Van Heerden and Grant, 1967), while for similar depths in New York State the in-situ horizontal stresses in the sandstone were varying from 10.17 MPa in the minor in-situ horizontal stress direction to 15.69 MPa in the major in-situ horizontal stress direction (Haimson and Stahl, 1969). In Michigan, the in-situ horizontal stresses were measured at 3660 m depth in the sandstone layer and were found as high as 90.0 MPa and 67.0 MPa in the major and minor in-situ horizontal stress directions, respectively (Haimson, 1976).

The limestone in Kincardine, Ontario and the limestone in Barberton, Ohio exhibits considerably high in-situ horizontal stresses of 44.7 MPa and 23.0 MPa in the major and in the minor in-situ horizontal stress directions, respectively, at depths of around 700 m (Lam et al., 2011 and Obert, 1962). Similarly, the measured in-situ horizontal stresses at 341m to 420 m depth in the granite layer in Wawa, Ontario and in Manitoba were as high as 60.0 MPa in the major in-situ horizontal stress direction and 40.0 MPa in the minor in-situ horizontal stress direction (Fairhurst, 2004, Lindner and Halpern, 1978 and Buchbinder et al., 1965). Although the in-situ vertical stresses from the overburden are not presented here in the compiled data, it could be perceived that in general, the rock formations in Ontario and neighbouring regions are subjected to high in-situ horizontal stresses.

Lo (1978) analyzed natural geological features, such as: faulting; folding and buckling or pop-up of surface rock strata; distress in shallow and deep excavation such as heaves in the Dufferin quarry in Milton; jamming of Niagara generation station wheel pit; bending and buckling of steel beams structures of hydro-electric power plants; crushing and spalling of arch and floor heave of the hydro tunnels in the Niagara area and Chippawa Canal in Ontario. Based on these analyses, it was suggested by Lo (1978) that

these observations were evidence of high in-situ horizontal stresses that resulted from the current movement of continental drift according to tectonic theory, and not due to the past overburden load during glaciation ages (Lo, 1978). From the recorded in-situ stress measurements and the observation of natural phenomena, it was proposed that the belt of high in-situ horizontal stresses stretches from Rochester in New York State westward through Niagara Falls, turning northeast around Lake Ontario following the lake shore line and extending at least as far east as Wesleyville, Ontario (Lo, 1978).

High in-situ horizontal stress in rocks is a general phenomenon that exists in many regions in North America and the world. However, the rock formations in southern Ontario and the neighboring states, in specific, exhibit very high in-situ horizontal stresses. These high in-situ horizontal stresses, after their relief, might be of significant influence on the time-dependent deformation characteristics of these rocks, which in turn might cause serious damage to the constructed underground structures.

2.2.2 Strength and Stiffness Properties of Rock

The measured tensile strength; compressive strength; elastic (Young's) modulus and Poisson's ratio of different rock formations in southern Ontario and the neighboring regions are summarized and presented in Table 2.2. The presented data were compiled from available relevant literature.

The tensile strength of intact rock is measured in a laboratory either directly with the direct tension test or indirectly with the indirect tension test, which is commonly known as the Brazilian split test. In the direct tension test, a cylindrical rock specimen is subjected to a direct uniaxial tensile stress along its longitudinal axis until failure. In the Brazilian split test, the indirect tensile strength of the rock is measured on disc specimens by applying a compressive stress across the disc perimeter until failure. The failure occurs along the diameter of the disc specimen in a biaxial state of stress where one principal stress is highly compressive. In general, the indirect tensile strength of rock measured from the Brazilian split test is higher than the tensile strength of the same rock measured from the direct tension test.

The compressive strength; elastic (Young's) modulus and Poisson's ratio of intact rocks are all measured in a laboratory either through a uniaxial compression test or a triaxial compression test. In the uniaxial compression test, a cylindrical rock specimen is subjected to a compressive stress along its longitudinal axis until failure occurs, while in the triaxial compression test, failure is similarly induced when the rock specimen is subjected to a specific value of confining pressure. In both tests, electronic strain gauges can be fixed onto the specimen, parallel and perpendicular to the longitudinal axis of the specimen, to measure the axial and diametric deformations during the tests. Elastic theory is then used to calculate the elastic modulus and Poisson's ratio.

The strength and stiffness characteristics of intact rock specimens extracted from different rock formations in southern Ontario and the neighboring regions were extensively investigated over the past decades (Hefny and Lo, 1995; Lo et al., 1987; Van Heerden and Grant, 1967 and Palmer and Lo, 1976). However, the in-situ medium (i.e. the rock mass) comprises of intact rock blocks that are separated by discontinuities such as joints, fissures and faults (Hoek, 2001). These discontinuities have a great influence on the overall strength characteristics of the rock mass, and therefore they have to be prudently considered in evaluating the overall strength of the rock mass. The rock mass modulus can be measured in-situ by recording the deformation in the diameter of a pre-drilled monitoring hole through the rock mass while extending the tunnel excavations. The deformation is recorded using an extensometer probe that is affixed at the bottom of the monitoring hole. Another field test method was developed in 1987 by Lo et al. to measure the rock mass modulus at the surface of the excavated rock. In principle, the developed method consisted of measuring the variation in the diametric distance between each opposite pair of pre-glued props into pre-drilled holes from the surface of the rock layer, in a rosette pattern, while extending a central hole into the rock layer from the surface. The elastic theory was then used to calculate the rock mass modulus (Lo et al., 1987). The developed method was used to measure the rock mass modulus of the limestone layer at the intake and discharge tunnels of Darlington Generating Station, east of Toronto. The values of the measure rock modulus from this method were consistent with those evaluated from extensometer measurements in the tunnel.

As mentioned earlier, the strength data presented in Table 2.2 were assembled from laboratory tests performed on intact rock specimens of samples extracted from variable depths and diversity of rock formations in the concerned area. In general, the dolomitic limestone of the Lockport formation possesses the highest uniaxial compression strength of 199 - 246 MPa among all other rocks in southern Ontario (Lo and Hori, 1979). The sandstone of Whirlpool formation and the dolostone of Lockport formation exhibit uniaxial compression strength of 190 MPa and 200 MPa, respectively (Lo, 1989). The black shale of Collingwood formation and the Rochester shale exhibit a high uniaxial compression strength of 80 - 85 MPa in contrast to other shales in southern Ontario, such as Georgian Bay; Grimsby; Power Glen; Blue Mountain and Queenston in which the uniaxial compression strength ranges between 20 - 30 MPa (Lo, 1989). Moreover, most of the sedimentary rocks of southern Ontario possess anisotropy in their uniaxial compression strength, with respect to the rock bedding.

As it can be seen from Table 2.2, the available measurements of the tensile strength of rocks in the specified area are very limited. However, it is reported that the tensile strength of Queenston shale from different sites in southern Ontario varies between 1MPa to 15 MPa in contrast to Sherman Fall shale where the tensile strength is 0.1 - 3 MPa. It is also reported that the dolostone and mudstone of De Cew formation possess a tensile strength of 5 MPa (Lam et al., 2011).

The elastic modulus of siderite and tuff in Wawa, Ontario was reported as 67.6 - 118.0 GPa and 68.3 - 115.8 GPa (Herget, 1973), respectively. The quartzite and sandstone of Elliot Lake, Ontario possess an elastic modulus of 80.0 GPa and 76.0 GPa respectively (Eisbacher and Bielenstein, 1971 and Van Heerden and Grant, 1967), while the shales, in general, possess an average elastic modulus of 10.0 GPa (Lam et al., 2011; Lee and Lo, 1993; Lo, 1989; Lo et al., 1987; Lo and Yuen, 1981 and Lo et al., 1978,). On the other hand, the Poisson's ratio of rocks in southern Ontario is ranging from 0.13 for Georgian Bay shale (Lo and Hori, 1979) to 0.6 for argillaceous limestone of Cobourg formation (Lam et al., 2011). Moreover, most of the sedimentary rocks of Southern Ontario possess anisotropy in their strength and stiffness properties, with respect to the bedding planes.

As stated earlier, the presented measurements in Table 2.2 are based on laboratory tests performed on freshly recovered intact rocks from the ground. In practice, the rocks at the surfaces of the tunnel excavations are actually exposed either to water or other drilling fluids, such as bentonite slurry or synthetic polymers solutions as part of the construction process. These drilling fluids are used either as lubricant fluids to facilitate the pipe installation through the rock mass or as a mean to convey the excavated material. As indicated earlier, there is lack of information with regard to the influence of the exposure of rocks to the drilling fluids and lubricant fluids near the surfaces of excavation on the strength characteristics of these rocks. Therefore, the influence of lubricant fluids on the strength and stiffness characteristics of the Queenston shale from southern Ontario is dealt with in part this thesis.

2.2.3 Time-Dependent Deformation Properties of Rocks

The swelling potential of rocks is an important factor in designing underground structures and has a significant influence on the stability of these structures. As proposed by Lo et al., (1978), the swelling potential in the swelling rocks can be defined as the swelling strain per log cycle of time and it can be calculated through the free swell test. In the free swell test, the intact rock specimen is submerged in water and allowed to expand freely in all directions while the swelling strain is measured in three orthogonal directions (Lo et al., 1978). The horizontal swell strain is measured in the direction parallel to the bedding planes of the rock sample, while the vertical swell strain is measured in the direction perpendicular to the rock bedding planes. The measured swelling potential in the vertical and horizontal directions with respect to the rock bedding for different rock formations in southern Ontario and the neighboring regions are presented in Table 2.2.

As it can be seen in Table 2.2, most of the shaly rock formations exhibit anisotropy in their swelling behavior in the direction parallel and perpendicular to the rock bedding planes (Lee and Lo, 1993; Lo and Lee, 1990 and Lo et al., 1978). For example; the Queenston shale from Niagara Falls exhibits swelling potential of 0.37% - 0.54% in the vertical direction and 0.22% - 0.34% in the horizontal direction (Lo and Lee, 1990). The Georgian Bay shale from different sites in southern Ontario indicates swelling

potential of 0.2% - 0.22% in the vertical direction and 0.03% - 0.14% in the horizontal direction (Lo et al., 1978). The Rochester shale exhibits relatively small swelling potential averaging 0.16% and 0.07% in the vertical and horizontal directions, respectively. In general, the limestone displays small swelling potential due to their high calcite content however, some shaly limestone such as Gasport shaly limestone exhibits swelling potential of 0.08% in both horizontal and vertical directions (Lo et al., 1978).

Lee and Lo (1993) investigated the swelling mechanism of shales in Southern Ontario by submerging the shale specimens in water with varying salt concentrations. Based on the results of their investigations, they suggested that the swelling mechanism of shales in this region was based on the process of osmosis and diffusion which occurred between the rock pore water and the ambient fluid. It was concluded that swelling occurs if three conditions are met: i) relief of initial stress; ii) accessibility of water and iii) an outward salt concentration gradient from the rock pore fluid to the ambient fluid. They assumed that swelling may or may not occur if only one or two of these conditions are met. Although the swelling behavior of shales in southern Ontario was extensively investigated in water (Lo, 1993; Lo and Lee, 1990 and Lee and Lo, 1989), there is a lack of information with respect to the swelling behavior of these shales in drilling and lubricant fluids, such as bentonite solution and synthetic polymers solutions.

2.2.4 Dynamic Properties of Rocks

The compressional wave velocity, shear wave velocity, dynamic Poisson's ratio and dynamic modulus of different rock formations in southern Ontario were compiled and presented in Table 2.3. The compressional wave and the shear wave velocities were measured on intact rock specimens and the dynamic Poisson's ratio and the dynamic modulus were calculated using the fundamental equations for torsional vibration (Lo and Lee, 1990; Lo et al., 1987 and Lo and Hori, 1979).

In general, the presented data revealed anisotropy in the dynamic behavior of the sedimentary rocks in southern Ontario. For the same rock formation, the value of the dynamic modulus in the direction parallel to the bedding planes is higher than that in the direction perpendicular to the bedding planes. It should be noted that the presented

dynamic properties are obtained for intact rock specimens. However, the effect of saturation in drilling and lubricant fluids such as bentonite solution and synthetic polymers solution on the dynamic properties of rocks needs to be investigated.

2.3 SUMMARY AND CONCLUSIONS

A comprehensive literature review of the geo-mechanical properties of rock formations in southern Ontario and the neighboring regions (New York, Pennsylvania, Ohio, Michigan, Indiana, Illinois, Wisconsin, and Minnesota) was performed. The available data on the measured in-situ stresses and the direction of major principal stress; strength and stiffness properties; time-dependent deformation properties and dynamic properties of different rocks were compiled. The presented data can serve as a preliminary source of information for the research performed in this thesis and for prospective studies of the geo-mechanical properties of the rocks in southern Ontario and the neighboring regions.

From this compiled data, the following conclusions can be drawn:

- 1) The initial in-situ horizontal stress in rock formations of southern Ontario and the neighboring regions varies from a relatively small amount, <1 MPa, to a much higher amount, >100 MPa, depending on the rock formation; depth and inter-bedded layers in the rock mass. For depths up to 30 m where most of the engineering projects are located, the in-situ horizontal stresses in rocks of southern Ontario and the neighboring regions can be up to 38.13 MPa. While for depths greater than 30 m and up to 1000 m where mining projects are located, the in-situ horizontal stresses range between 1.59 MPa to 85.7 MPa. Moreover, the in-situ horizontal stresses are high for depths greater than 1000 m, where hydrocarbons projects are located, ranging from 42.0 MPa to as high as 135.0 MPa.
- 2) Among shales of southern Ontario and the neighboring regions, the Queenston shale of Niagara Falls region exhibits a high swelling potential of 0.37% - 0.54% in the vertical

direction and 0.22% - 0.34% in the horizontal direction, with respect to the bedding planes.

- 3) The sedimentary rocks and shales in particular, possess apparent anisotropy in their strength, time-dependent deformation and dynamic properties, with respect to the rock bedding.
- 4) Although the time-dependent deformation behavior of rocks in southern Ontario and the neighboring regions was extensively investigated using water as an ambient solution, there is lack of information with respect to the behavior of these rocks in fluids such as bentonite solution and synthetic polymers solution. For most of the tunnel drilling process through the rock mass, other than blasting, fluids such as bentonite slurry and synthetic polymers solutions are used either to convey the excavated materials or to lubricate the annulus of the excavated tunnel. Therefore, it is quite indispensable to investigate the influence of these fluids on the strength, time-dependent deformation and dynamic characteristics of these rocks, which is covered through the research work performed in this thesis.

2.4 REFERENCES

- Benson, R.P., Kierans, T.W. and Sigvaldason, O.T. 1970. In-Situ and Induced Stresses at the Churchill Falls Underground Powerhouse, Labrador. Proceedings of the 2nd Congress of the International Society for Rock Mechanics, **4**, 821-832.
- Bonnechere, F. 1969. A Comparative Field Study of Rock Stress Determination Techniques. Missouri River Division, Report No. 68101, Corps of Engineers, Omaha.
- Buchbinder, G.G.R., Nyland, E. and Blanchard, J.E. 1965. Measurement of Stress in Bore-Holes, in Drilling for Scientific Purposes. Proceedings of the International Upper Mantle Symposium, Ottawa, 2-3 September 1965, pp. 85-93.

- Coates, D.F., Grant, F. and Heerden, W.L. 1968. Stress Measurements at Elliot Lake. Canada Mines Branch Reprint Series, Canada Mines Branch, R. Duhamel, pp. 603-613.
- Dames and Moore Consultants 1974. Geological Report. Report No. 4852-002-18, Limerick Generating Station.
- Dames and Moore Consultants 1973. In-Situ Stress Measurement. Report of Investigation, North Anna Power Project.
- Eisbacher, G.H. and Bielenstein, H.U. 1971. Elastic Strain Recovery in Proterozoic Rocks Near Elliot Lake, Ontario. *Journal of Geophysical Research*, **76**: 2012-2021.
- Fairhurst, C. 2004. Nuclear Waste Disposal and Rock Mechanics: Contributions of the Underground Research Laboratory (URL), Pinawa, Manitoba, Canada. *International Journal of Rock Mechanics and Mining Sciences*, **41**: 1221-1227.
- Fairhurst, C. 2003. Stress Estimation in Rock: A Brief History and Review. *International Journal of Rock Mechanics and Mining Sciences*, **40**: 957-973.
- Foundation Sciences Incorporation 1971. Bear Swamp Project-Rock Mechanics Studies. New England Power Service Company, Westborough.
- Franklin, J.A. and Hungr, O. 1978. Rock Stresses in Canada: Their Relevance to Engineering Projects. *Rock Mechanics*, **6**: 25-46.
- Goldberg, Z. and Dunicliff and Associates 1976. Report on in-Situ Stress Measurements, Genessee River Interceptor, Southwest Rochester, New York, File No. 1661, Firelands Sewer and Water Construction Company, New York.

- Haimson, B.C. 1976. The Hydrofracturing Stress Measuring Technique-Method and Recent Field Results in the US. The Proceedings of the International Society of Rock Mechanics Symposium, Sydney, pp. 23-30.
- Haimson, B. and Fairhurst, C. 1970. In-Situ Stress Determination at Great Depth by Means of Hydraulic Fracturing. Rock Mechanics-Theory and Practice. The Proceedings of the 11th Symposium on Rock Mechanics, 16-19 June 1969, Berkeley, pp. 559-584.
- Haimson, B. and Stahl, E.J. 1969. Hydraulic Fracturing and the Extraction of Minerals through Wells. The Proceedings of the 3rd Symposium on Salt, Northern Ohio Geological Society, Cleveland, pp. 421-432.
- Hefney, A. and Lo, K.Y. 1995. Interpretation of Initial Stresses from Hydraulic Fracturing Tests at AECL's Underground Research Laboratory, Manitoba. Tunnelling Association of Canada Annual Publication, 123-134.
- Hefney, A. and Lo, K.Y. 1992. The Interpretation of Horizontal and Mixed-Mode Fractures in Hydraulic Fracturing Test in Rocks. Canadian Geotechnical Journal, **29**: 902-917.
- Hefney, A., Lo, K.Y. and Huang, J.A. 1996. Modelling of Long-Term Time-Dependent Deformation and Stress Dependency of Queenston Shales. Tunnelling Association of Canada Annual Publication, 115-146.
- Herget, G. 1973. Variation of Rock Stresses with Depth at a Canadian Iron Mine. International Journal of Rock Mechanics and Mining Sciences & Geomechanics Abstracts, **10**: 37-51.
- Hoek, E. 2001. Big Tunnels in Bad Rocks-2000 Terzaghi Lecture. American Society of Civil Engineers Journal of Geotechnical and Geoenvironmental Engineering, **127**: 726-740.

- Hooker, V.E. and Johnson, C.F. 1977. In-Situ Stresses along the Appalachian Piedmont. Proceedings of the 4th Canadian Symposium on Rock Mechanics, Ottawa, 29-30 March 1967, pp. 137-155.
- Lam, T., Engelder, T., Leech, R.E.J. and Jensen, M. 2011. Regional Geomechanics–Southern Ontario. Nuclear Waste Management Organization and AECOM Canada Ltd., Technical Report No. NWMO DGR-TR-2011-13.
- Lee, Y.N. and Lo, K.Y. 1993. The Swelling Mechanism of Queenston Shale. Canadian Tunnelling 1993, The Tunnelling Association of Canada, pp.75-97.
- Lindner, E.N. and Halpern, J.A. 1978. In-Situ Stress in North America: A Compilation. International Journal of Rock Mechanics and Mining Sciences and Geomechanics Abstracts, **15**: 183-203.
- Lo, K.Y. 1989. Recent Advances in Design and Evaluation of Performance of Underground Structures in Rocks. Tunnelling and Underground Space Technology, **4**: 171-183.
- Lo, K.Y. 1978. Regional Distribution of in Situ Horizontal Stresses in Rocks of Southern Ontario. Canadian Geotechnical Journal, **15**: 371-381.
- Lo, K.Y. and Hefney, A. 1993. The Evaluation of In-Situ Stresses by Hydraulic Fracturing Tests in Anisotropic Rocks with Mixed-Mode Fractures. Canadian Tunnelling 1993, The Tunnelling Association of Canada, pp. 59-73.
- Lo, K.Y. and Hori, M. 1979. Deformation and Strength Properties of Some Rocks in Southern Ontario. Canadian Geotechnical Journal, **16**: 108-120.
- Lo, K. Y., and Yuen, C.M.K. 1981 Design of Tunnel Lining in Rock for Long Term Time Effects. Canada Geotechnical Journal, **18**: 24-39.

- Lo, K.Y. and Lee, Y.N. 1990. Time-Dependent Deformation Behaviour of Queenston Shales. *Canadian Geotechnical Journal*, **27**: 461-471.
- Lo, K.Y. and Lukajic, B. 1984. Predicted and Measured Stresses and Displacements around the Darlington Intake Tunnel. *Canadian Geotechnical Journal*, **21**: 147-165.
- Lo, K.Y., Cooke, B.H. and Dunbar, D.D. 1987. Design of Buried Structures in Squeezing Rock in Toronto, Canada. *Canadian Geotechnical Journal*, **24**: 232-241.
- Lo, K.Y., Lukajic, B., Yuen, C.M.K. and Hori, M. 1982. In-Situ Stresses in a Rock Overhang at the Ontario Power Generating Station, Niagara Falls. *Proceedings of the 23rd Symposium on Rock Mechanics, Berkeley, 25-27 August 1982*, pp. 343-352.
- Lo, K.Y., Palmer, J. H. L. and Quigly, R.M. 1978. Time-Dependent Deformation of Shaly Rocks in Southern Ontario. *Canadian Geotechnical Journal*, **15**: 537-547.
- Lo, K.Y., Yung, C.B. and Lukajic, B. 1987a. A Field Method for the Determination of Rock-Mass Modulus. *Canadian Geotechnical Journal*, **24**: 406-413.
- Map of Southern Ontario and Neighbouring Regions, Google Maps.
- Metaltech Inspection Ltd. 1970. Rapport D'Investigation, Mesure Des Contraintes En Place. Contract No. 1009-61, Commission Hydro-Electrique du Quebec.
- Moruzi, G.A. 1968. Application of Rock Mechanics in Mine Planning and Ground Control. *Current Rock Mechanics, Chap. 3, Studies at Falconbridge. Canadian Mining Journal*, **89**: 12-15.
- Obert, L.A. 1962. In-situ Determination of Stress in Rock. *Mining Engineering*, **14**: 51-58.

- Palmer, H.L. and Lo, K.Y. 1976. In Situ Measurements in Some Near Surface Rock Formation-Thorold, Ontario. *Canadian Geotechnical Journal*, **13**: 1-7.
- Rough, R.L. and Lambert, W.G. 1971. In-Situ Strain Orientations: A Comparison of Three Measuring Techniques. Report of Investigation, 7575, US Department of Interior, Bureau of Mines, USA.
- Sbar, M.L. and Sykes, L.R. 1973. Contemporary Compressive Stress and Seismicity in Eastern North America: An Example of Intra-Plate Tectonics. *Geological Society of America Bulletin*, **84**: 1861-1882.
- Sellers, J.B. 1969. Strain Relief Overcoring to Measure in-Situ Stresses. Niagara Falls Project, Corps of Engineers, Buffalo District.
- Terzaghi, K. 196). Measurement of Stresses in Rock. *Géotechnique*, **12**: 105-124.
- Thompson, P.M. and Chandler, N.A. 2004. In-Situ Rock Stress Determinations in Deep Boreholes at the Underground Research Laboratory. *International Journal of Rock Mechanics and Mining Sciences*, **41**: 1305-1316.
- Van Heerden, W.L. and Grant, F. 1967. A Comparison of Two Methods for Measuring Stress in Rock. *International Journal of Rock Mechanics and Mining Sciences & Geomechanics Abstracts*, **4**: 367-382.
- Von Schonfeldt, H. and Fairhurst, C. 1972. Field Experiments on Hydraulic Fracturing. *American Institute of Mining Engineers*, **253**: 69-77.

Table 2.1. In-situ stress measurements in rocks of southern Ontario and neighboring regions

Province/State/ City	Project	Rock Formation	Rock Type	Depth (m)	Horizontal minor stress (MPa)	Horizontal major stress (MPa)	Direction of Major Horizontal Stress	Method used	Source of data
Ontario/ Dufferin Creek	Outcrop in Dufferin Creek, Ontario	_	Shale	9.1 - 15.2	6.9	_	_	USBM	Lo, (1978)
Ontario/ Elliot Lake	Mine in Elliot Lake, Ontario	_	Quartzite Diabase	390.0 - 415.0 256	21.4 - 44.1 15.2-	44.1 41.4	_	_	Coates et al., (1968)
Ontario/ Elliot Lake	Mine in Elliot Lake, Ontario	_	Sandstone/ Quartzite	204.8 - 701.0	17.24 - 22.06	20.69 - 36.54	East	OC	Eisbacher and Bielenstein, (1971)
Ontario/ Elliot Lake	Mine in Elliot Lake	_	Sandstone/ Quartzite	427	24.13	35.37	_	USBM	Van Heerden and Grant ((1967)

Note: D: door stopper with South African CSIR strain cell; HF: hydro-fracturing technique; MSP: modified stress path method (Loand Hefny, 1993); OC: over coring technique; USBM: the US bureau of mines deformation meter.

Province/State/ City	Project	Rock Formation	Rock Type	Depth (m)	Horizontal minor stress (MPa)	Horizontal major stress (MPa)	Direction of Major Horizontal Stress	Method used	Source of data
Ontario/ Kincardine	Bruce Nuclear Repository Site in Kincardine, Ontario	Cobourg	limestone	670	23	44.7	N 75°E	HF	Lam et al., (2011)
Ontario/ Mississauga	Heart Lake Tunnel in	Georgian Bay	Shale	6.0 - 18.2	0.86 - 6.32	1.25 - 9.5	N10°-48 °E, N2° - 86°W	USBM	Lo and Yuen, (1981)
Ontario/ Mississauga	Mississauga, Ontario Outcrop in Mississauga, Ontario	—	Shale	9.1 - 15.2	7.6	—	—	—	Lo, (1978)

Note: D: door stopper with South African CSIR strain cell; HF: hydro-fracturing technique; MSP: modified stress path method (Loand Hefny, 1993); OC: over coring technique; USBM: the US bureau of mines deformation meter.

Province/State/ City	Project	Rock Formation	Rock Type	Depth (m)	Horizontal minor stress (MPa)	Horizontal major stress (MPa)	Direction of Major Horizontal Stress	Method used	Source of data
Ontario/ Niagara Falls	SABNGS No3 in Niagara Falls	Queenston Shale		93.9 - 123.8	8.6 - 11.3	14.3 - 17.1	—	MSP	Lo and Hefny, (1993)
Ontario/ Ottawa	Outcrop in Ottawa	—	—	13.7	2.6	—	—	USBM	Franklin and Hungr (1978)
Ontario/ Port Hope	Wesleyville Generating Station, Port Hope	Trenton	Limestone	36.6	9.7	8.0 - 13.0	N 15°w	—	Lo, (1978)
Ontario/ Scarborough	Tunnel in Scarborough	—	Shale	70.1	1.59	1.69	N 90°E	USBM	Franklin and Hungr (1978)

Note: D: door stopper with South African CSIR strain cell; HF: hydro-fracturing technique; MSP: modified stress path method (Loand Hefny, 1993); OC: over coring technique; USBM: the US bureau of mines deformation meter.

Province/State/ City	Project	Rock Formation	Rock Type	Depth (m)	Horizontal minor stress (MPa)	Horizontal major stress (MPa)	Direction of Major Horizontal Stress	Method used	Source of data
Ontario/ Thorold	Tunnel In Thorold	Gasport	Shaly limestone	18.3	6.63- 12.7	8.14- 14.69	N 60°E	USBM	Lo, (1978), Lo et al., (1982 and 1978)
Ontario/ Thorold	Thorold Tunnel	Gasport	Dolomite	12.7 - 16.19	5.23 - 12.104	6.633 - 13.0	N27° - 88°W, N62°E	USBM	
		Gasport	Dolomitic limestone	17.26	6.682 - 6.861	6.861 - 8.99	N60° - 76°E		
		Gasport	Fossiliferous limestone	19.82	6.647	13.833	N56°E		

Note: D: door stopper with South African CSIR strain cell; HF: hydro-fracturing technique; MSP: modified stress path method (Loand Hefny, 1993); OC: over coring technique; USBM: the US bureau of mines deformation meter.

Province/State/ City	Project	Rock Formation	Rock Type	Depth (m)	Horizontal minor stress (MPa)	Horizontal major stress (MPa)	Direction of Major Horizontal Stress	Method used	Source of data
Ontario/ Thorold	Thorold Tunnel	Gasport	Argillaceous limestone	24.7	6.848	10.513	N60°E	USBM	Lo, (1978), Lo et al., (1982 and 1978)
		Gasport	Limestone with shaly interbeds	74.7 - 299.5	5.23 - 12.104	6.633 - 13.0	N27° - 88°W, N62°E		
Ontario/ Thorold	Thorold Tunnel	Gasport member of Lockport and Decew formations	Dolomite	41.7 - 53.1	5.2 - 12.7	6.6 - 13	N27° - 88°W, N62°E	USBM	Palmer and Lo, (1976)

Note: D: door stopper with South African CSIR strain cell; HF: hydro-fracturing technique; MSP: modified stress path method (Loand Hefny, 1993); OC: over coring technique; USBM: the US bureau of mines deformation meter.

Province/State/ City	Project	Rock Formation	Rock Type	Depth (m)	Horizontal minor stress (MPa)	Horizontal major stress (MPa)	Direction of Major Horizontal Stress	Method used	Source of data
Ontario/ Thorold	Thorold Tunnel	Gasport member of Lockport and Decew formation	Dolomitic limestone Shaly limestone Fossiliferous limestone Argillaceous limestone	56.6 60.0 - 61.0 65 81	5.2-6.6 11.0 - 6.63 6.83	6.8-9.03 11.2 14.69 13.8 10.5	N76°E N58° - 60°E N56°E N60°E	USBM	Palmer and Lo, (1976)
Ontario/ Thorold	Outcrop in Thorold	-	Dolomite Dolomitic limestone	12.7 - 15.5 16.2 - 17.3	5.21- 12.07 6.59 - 6.66	9.03 - 12.07 8.14 - 8.96	N 27°- W, N 88°W N 62° E, N 76° E	OC	Lindner and Halpern, (1978)

Note: D: door stopper with South African CSIR strain cell; HF: hydro-fracturing technique; MSP: modified stress path method (Loand Hefny, 1993); OC: over coring technique; USBM: the US bureau of mines deformation meter.

Province/State/ City	Project	Rock Formation	Rock Type	Depth (m)	Horizontal minor stress (MPa)	Horizontal major stress (MPa)	Direction of Major Horizontal Stress	Method used	Source of data
Ontario/ Thorold	Outcrop in Thorold	—	Shaly limestone	18.3 - 18.6	11.03 - 11.17	14.69	N 60°E, N 58°E	OC	Lindner and Halpern, (1978)
Ontario/ Wawa	Mine in Wawa	—	Limestone	19.8 - 24.7	6.63-6.83	10.48 - 13.79	N 56°E, N 60°E	—	Buchbinder et al., (1965)
Ontario/Wawa	Mine in Wawa, Ontario	—	Granite	341.4	40	60	—		
			Siderite	365.8	20.06 - 34.27	21.44 - 42.47	S 47° - 63°E	D	Herget, (1973)
			Tuff	478.5	27.65 - 34.06	30.0 - 47.16	S 42° - 63°W		
			Meta - diorite	573.0	21.51	31.58	S 18° - E		
			Chert	573.0	16.62 - 21.37	19.93 - 38.27	S 44° W, N 4° W		

Note: D: door stopper with South African CSIR strain cell; HF: hydro-fracturing technique; MSP: modified stress path method (Loand Hefny, 1993); OC: over coring technique; USBM: the US bureau of mines deformation meter.

Province/State/ City	Project	Rock Formation	Rock Type	Depth (m)	Horizontal minor stress (MPa)	Horizontal major stress (MPa)	Direction of Major Horizontal Stress	Method used	Source of data
Ontario/ Wawa	Mine	–	–	332	27.9	–	–	D	Franklin and Hungr (1978)
Ontario/ Darlington	Darlington Generation Station, Ontario	–	Ordovician limestone	228.0- 300.0	10.5 - 11.3	17.2 - 19.6	N 70 E ± 7°	HF	Lam et al., (2011)
Ontario/ Toronto	Darlington Intake Tunnel, Toronto	Whitby	Shaly limestone	74.7 - 299.5	5.8	9.3	N 63°E	–	Lo et al., (1987)
Ontario/ Toronto	Heart Lake Tunnel in Toronto	Georgian Bay	Shale	6.57 - 18.20	0.80 - 6.32	1.25 - 9.50	N 10° - 48°E, N 2 - 86°W	–	Lo, (1989)

Note: D: door stopper with South African CSIR strain cell; HF: hydro-fracturing technique; MSP: modified stress path method (Loand Hefny, 1993); OC: over coring technique; USBM: the US bureau of mines deformation meter.

Province/ State/ City	Project	Rock Formation	Rock Type	Depth (m)	Horizontal minor stress (MPa)	Horizontal major stress (MPa)	Direction of Major Horizontal Stress	Method used	Source of data
Ontario/ North Bay	Outcrop in North Bay	–	–	13.7	8.3	–	–	D	Franklin, and Hungr (1978)
Ontario/ Sudbury	Tunnel in Sudbury, Ontario	–	Jasperoid	45.7	44.82	51.71	–	–	Lindner and Halpern, (1978), Moruzi (1968)
Quebec/Lake Beauchene	Tunnel in Lake Beauchene	–	Gneiss W. Mica, Quartz	64.0	7.58	20	N 70° W	–	Lindner and Halpern, (1978), Metaltech Inspection Ltd. (1970)
Quebec/ Churchhill	Cavern adit in Churchhill Falls	–	Gneissic	305.0	11.72	13.79	–	OC	Benson et al., (1978)

Note: D: door stopper with South African CSIR strain cell; HF: hydro-fracturing technique; MSP: modified stress path method (Loand Hefny, 1993); OC: over coring technique; USBM: the US bureau of mines deformation meter.

Province/ State/ City	Project	Rock Formation	Rock Type	Depth (m)	Horizontal minor stress (MPa)	Horizontal major stress (MPa)	Direction of Major Horizontal Stress	Method used	Source of data
Quebec/ James Bay	Mine in James Bay, Quebec	—	Monzonite / Syenite	121.9	5.48 - 11.24	8.14- 20.69	N 0°E	D	Franklin, and Hungr (1978)
Manitoba	Underground Research Laboratory in Manitoba	— —	Granite Granite Granite	336.6 - 515 420 470.1- 471.5	31.0 - 42.0 45.0 54.5 - 62.5	60.0 - 83.4 60.0 61.0 -76.7	— - —	MSP - —	Hefny and Lo (1995 and 1992) Fairhurst, (2004 and 2003) Thompson and Chandler, (2004)
				579.5- 670.8	56.9 -76.0	61.0 -76.7			
				745	46.8 - 51.8	57.9 - 61.5			
				851.3	56.2-78.3	62.6 -85.7			

Note: D: door stopper with South African CSIR strain cell; HF: hydro-fracturing technique; MSP: modified stress path method (Loand Hefny, 1993); OC: over coring technique; USBM: the US bureau of mines deformation meter.

Province/ State/ City	Project	Rock Formation	Rock Type	Depth (m)	Horizontal minor stress (MPa)	Horizontal major stress (MPa)	Direction of Major Horizontal Stress	Method used	Source of data
New York/ Alma Township	Oil Field-Deep Boring in Alma Township	_	Sandstone	502.9	10.17	15.69	N 77°E	HF	Haimson, and Stahl, (1969)
New York/ Briarcliff Manor	Outcrop in Briarcliff Manor	_	Gneiss	5.6 - 13.1	1.48 - 3.62	0.08 - 11.39	N 0°-90°E, N64°-74°W	OC	Lindner and Halpern, (1978)
New York/ Clarendon	Deep Borehole in Clarendon	-	Sandstone/ limestone	_	_	10.24	N 64°E	USBM	Franklin, and Hungr (1978)

Note: D: door stopper with South African CSIR strain cell; HF: hydro-fracturing technique; MSP: modified stress path method (Loand Hefny, 1993); OC: over coring technique; USBM: the US bureau of mines deformation meter.

Province/ State/ City	Project	Rock Formation	Rock Type	Depth (m)	Horizontal minor stress (MPa)	Horizontal major stress (MPa)	Direction of Major Horizontal Stress	Method used	Source of data
New York/ Dale	Deep Boring in Dale	_	Sandstone	_	11.89	18.61	_	HF	Lindner and Halpern, (1978), Sbar, and Sykes (1973)
New York/ Niagara Gorge	Outcrop in Niagara Gorge	_	Dolomite	0.2 - 6.7	0.3-2.28	6.0-6.21	N34°-55°E	OC	Lindner and Halpern, (1978) Sellers, (1969)
New York/ Nyack	Outcrop in Nyack	_	Diabase	0.2 - 0.5	0.47	1.19	N 2°E	OC	Lindner and Halpern, (1978), Hooker, and Johnson, (1977)

Note: D: door stopper with South African CSIR strain cell; HF: hydro-fracturing technique; MSP: modified stress path method (Loand Hefny, 1993); OC: over coring technique; USBM: the US bureau of mines deformation meter.

Province/ State/ City	Project	Rock Formation	Rock Type	Depth (m)	Horizontal minor stress (MPa)	Horizontal major stress (MPa)	Direction of Major Horizontal Stress	Method used	Source of data
New York/ Rochester	Sewer System in Rochester	_	Dolomite	7.5- 15.4	4.87 - 10.43	5.56 - 29.89	N10°-86°E, N80° - 82°W	OC	Goldberg, and Dunnicliff and Associates (1976)
New York/ Somerset	Outcrop in Somerset	_	Sandstone	8.5	3.17	4.41	N 15°W	OC	Lindner and Halpern,(1978),
New York/ Sterling	Outcrop in Sterling	_	Sandstone	10.1 - 32.3	4.59 - 6.55	8.27 - 10.34	N22°- 90°W	OC	Lindner and Halpern, (1978), Dames and Moore Consultants (1973 and 1974)

Note: D: door stopper with South African CSIR strain cell; HF: hydro-fracturing technique; MSP: modified stress path method (Loand Hefny, 1993); OC: over coring technique; USBM: the US bureau of mines deformation meter.

Province/ State/ City	Project	Rock Formation	Rock Type	Depth (m)	Horizontal minor stress (MPa)	Horizontal major stress (MPa)	Direction of Major Horizontal Stress	Method used	Source of data
Illinois	Oil Field- Deep Boring in southern Illinois	_	Carbonate	99.1	2.41	7.76	N 62°E	OC	Haimson, and Fairhurst, (1970)
Michigan	Deep Boring in Gratiot Co.	_	Shale	5108	95	135	_	OC	Haimson, (1976)
			Sandstone	3660	67	90			
			Dolomite	3805	42	56			
Minnesota/ Coldspring	Quarry in Coldspring	_	Granite	15	5.58	16.48	N 40°E	OC	Von Schonfeldt and Fairhurst, (1972)
Minnesota/ Ely	Tunnel in Ely	_	Gabbro	305	10.3	16.5	_	OC	

Note: D: door stopper with South African CSIR strain cell; HF: hydro-fracturing technique; MSP: modified stress path method (Loand Hefny, 1993); OC: over coring technique; USBM: the US bureau of mines deformation meter.

Province/ State/ City	Project	Rock Formation	Rock Type	Depth (m)	Horizontal minor stress (MPa)	Horizontal major stress (MPa)	Direction of Major Horizontal Stress	Method used	Source of data
Minnesota/ St. Cloud	Quarry in St. Cloud	_	Granite	_	10.58	15.1	N 50°E	D	Bonnechere, (1969)
Ohio Ohio/ Barberton	Boring in Ohio Mine in Barberton, Ohio	_	Shale Limestone	10.3 - 18.6 701	4.69 - 32.41 5.58 - 23.44	5.58 - 38.13 44.82	N45°-83°W N54°- 86°E N 90°W	OC HF	Lindner and Halpern, (1978) Obert, (1962)
Ohio/Falls Township	Oil Field- Deep Boring in Falls Township	_	Sandstone	808	11.2	24.13	N 64°E	OC	Haimson and Fairhurst, (1970)

Note: D: door stopper with South African CSIR strain cell; HF: hydro-fracturing technique; MSP: modified stress path method (Loand Hefny, 1993); OC: over coring technique; USBM: the US bureau of mines deformation meter.

Province/ State/ City	Project	Rock Formation	Rock Type	Depth (m)	Horizontal minor stress (MPa)	Horizontal major stress (MPa)	Direction of Major Horizontal Stress	Method used	Source of data
Ohio/ Hocking State Forest	Outcrop in Hocking State Forest	_	Sandstone	0.9 - 1.2	0.37	0.63	N 61°E, N 83°E	OC	Rough and Lambert. (1971)
Wisconsin/ Montello	Deep Boring in Montello, Wisconsin	_	Granite	75.0 - 188.1	6.2 - 8.2	14.0 - 20.0	N 63°E ± 20°	HF	Lindner and Halpern, (1978) , Rough and Lambert. (1971)

Note: D: door stopper with South African CSIR strain cell; HF: hydro-fracturing technique; MSP: modified stress path method (Loand Hefny, 1993); OC: over coring technique; USBM: the US bureau of mines deformation meter.

Table 2.2. Strength and time-dependent deformation properties of rocks in southern Ontario and neighboring regions

Province/ State/ City	Project	Rock Formation	Rock Type	Depth/ Elevation (m)	Tensile Strength (MPa)	Uniaxial Compressive Strength UCS (MPa)	Elastic Modulus E (GPa)	Poisson's Ratio ν	Swelling Potential (%)	Source of Data
Ontario/ Elliot Lake	Mine	–	Quartzite	390	–	31.0 - 44.1	80.0	–	–	Van Heerden, and Grant (1967)
Ontario/ Elliot Lake	Mine	–	Sandstone /Quartzite	204.8 - 701.0	–	–	76.0	–	–	Eisbacher, and Bielenstein, (1971)
Ontario/ Elliot Lake	Mine	–	Quartzite	390 - 415	–	–	80.0	–	–	Coates et al., (1968)[30]
Ontario/ Kincardine	Typical values from different sites in southern Ontario	Lockport Goat Island	Dolostone	–	–	137.0 - 282.0	58.0 - 81.0	0.2 - 0.4	0.0 <i>h</i>	Lam et al., (2011), Lee and Lo, (1993)

Note: d: result from direct tension test; b: results from Brazilian test; v: results from vertically cored samples/or measurements in the vertical direction; h: results from horizontally cored samples/or measurements in the horizontal direction ; i: results from inclined 45° cored samples with respect to the bedding planes.

Province/ State/ City	Project	Rock Formation	Rock Type	Depth/ Elevation (m)	Tensile Strength (MPa)	Uniaxial Compressive Strength UCS (MPa)	Elastic Modulus E (GPa)	Poisson's Ratio ν	Swelling Potential (%)	Source of Data
Ontario/ Kincardine	Typical values from	Lockport Gasport	Shaly limestone	–	–	27.0-255.0	25.0-70.0	0.1-0.5	0.08 <i>h</i>	Lam et al., (2011), Lee and Lo, (1993)
	different sites in	De Cew	Dolostone/ Mudstone	–	5.0	74.0-174.0	43.0-57.0	0.3-0.4	0.04 <i>h</i>	
	southern Ontario for	Irondequoit Reynales	–	–	–	60.0-185.0 53.0- 41.0	50.0-78.0 22.0-49.0	0.1-0.5 0.2-0.5	–	
	Bruce Nuclear site	Cabot Head	–	–	5.0 - 14.0	20.0-127.0	–	–	–	
		Queenston	Shale	–	1.0 – 15.0	12.0 – 118.0	7.0 – 34.0	0.1 – 0.5	0.3 <i>h</i>	

Note: d: result from direct tension test; b: results from Brazilian test; v: results from vertically cored samples/or measurements in the vertical direction; h: results from horizontally cored samples/or measurements in the horizontal direction ; i: results from inclined 45° cored samples with respect to the bedding planes.

Province/ State/ City	Project	Rock Formation	Rock Type	Depth/ Elevation (m)	Tensile Strength (MPa)	Uniaxial Compressive Strength UCS (MPa)	Elastic Modulus E (GPa)	Poisson's Ratio ν	Swelling Potential (%)	Source of Data
Ontario/ Kincardine	Typical values from different Sites for	Georgian Bay	Shale	–	–	3.0-206.0	1.0-58.0	0.1-0.5	0.15 <i>h</i>	Lam et al., (2011), Lee and Lo, (1993)
	Bruce Nuclear site	Cobourg	–	–	–	22.0-140.0	10.0-67.0	0.1-0.6	–	
		Lockport Eramosa	Dolostone	–	–	118.0	63.0	0.4	0.0 <i>h</i>	
		Rochester	Shale	–	–	85.0	23.0	–	0.07 <i>h</i>	
		Grimsby	Sandstone/ Shale	–	–	25.0	8.0	–	0.27 <i>h</i>	
		Power Glen	Sandstone/ Shale	–	–	26.0	9.0	–	0.17 <i>h</i>	
		Blue Mountain	Shale	–	–	27.0	2.0	–	0.15 <i>h</i>	

Note: d: result from direct tension test; b: results from Brazilian test; v: results from vertically cored samples/or measurements in the vertical direction; h: results from horizontally cored samples/or measurements in the horizontal direction ; i: results from inclined 45° cored samples with respect to the bedding planes.

Province/ State/ City	Project	Rock Formation	Rock Type	Depth/ Elevation (m)	Tensile Strength (MPa)	Uniaxial Compressive Strength UCS (MPa)	Elastic Modulus E (GPa)	Poisson's Ratio ν	Swelling Potential (%)	Source of Data
Ontario/ Kincardine	Typical values from different Sites for	Collingwood	Black shale	–	–	80.0	20.0	–	0.0 <i>h</i>	Lam et al., (2011), Lee and Lo, (1993)
			Grey mudstone	–	–	58.0	10.0	–	0.15 <i>h</i>	
	Bruce Nuclear site	Lindsay	Limestone with shaly interbeds	–	–	110.0	46.0	–	0.05 <i>h</i>	
		Verulam	Shaly limestone	–	–	23.0	57.0	–	0.05 <i>h</i>	
		Gull River	Limestone	–	–	143.0	63.0	–	0.0 <i>h</i>	

Note: d: result from direct tension test; b: results from Brazilian test; v: results from vertically cored samples/or measurements in the vertical direction; h: results from horizontally cored samples/or measurements in the horizontal direction ; i: results from inclined 45° cored samples with respect to the bedding planes.

Province/ State/ City	Project	Rock Formation	Rock Type	Depth/ Elevation (m)	Tensile Strength (MPa)	Uniaxial Compressive Strength UCS (MPa)	Elastic Modulus E (GPa)	Poisson's Ratio ν	Swelling Potential (%)	Source of Data
Ontario/ Kincardine	Typical values from different sites for Bruce Nuclear site	Precambrian	Medium grained	–	–	190.0	60.0	–	0.0 <i>h</i>	Lam et al., (2011), Lee and Lo, (1993)
		Granitic Gneiss	Coarse grained	–	–	140	46	–	0.0 <i>h</i>	
		Amherstburg	Dolostone	–	–	33.0-113.0	8.0-40.0	–	–	
			Limestone	–	–	23.0-182.0	12.0-66.0	–	–	
Ontario/ Mississauga	Heart Lake tunnel	Georgian Bay Queenston	Shale	6.0 - 18.2	–	–	12.4	0.15	–	Lo and Yuen (1981)

Note: d: result from direct tension test; b: results from Brazilian test; v: results from vertically cored samples/or measurements in the vertical direction; h: results from horizontally cored samples/or measurements in the horizontal direction ; i: results from inclined 45° cored samples with respect to the bedding planes.

Province/ State/ City	Project	Rock Formation	Rock Type	Depth/ Elevation (m)	Tensile Strength (MPa)	Uniaxial Compressive Strength UCS (MPa)	Elastic Modulus E (GPa)	Poisson's Ratio ν	Swelling Potential (%)	Source of Data
Ontario/ Niagara Falls	Sir Adam Beck Niagara generating station No. 3	Queenston	Shale	95.64 - 114.33	-	-	-	-	0.22- 0.34 <i>h</i> 0.37 - 0.54 <i>v</i>	Lee and Lo, (1993), Lo and Lee, (1990)
Southern Ontario	Different Sites In Southern Ontario	Rochester	Interbedded shale and Dolomite	-	-	20.0-40.0	20.0	-	-	
		Georgian Bay	Interbedded shale/ Siltstone/	-	-	30.0-190.0	20.0-40.0	-	-	Lo, (1978)

Note: d: result from direct tension test; b: results from Brazilian test; v: results from vertically cored samples/or measurements in the vertical direction; h: results from horizontally cored samples/or measurements in the horizontal direction ; i: results from inclined 45° cored samples with respect to the bedding planes.

Province/ State/ City	Project	Rock Formation	Rock Type	Depth/ Elevation (m)	Tensile Strength (MPa)	Uniaxial Compressive Strength UCS (MPa)	Elastic Modulus E (GPa)	Poisson's Ratio ν	Swelling Potential (%)	Source of Data
Southern Ontario	Different Sites In Southern Ontario	Collingwood	Interbedded shale/Mudst one	–	–	20.0-70.0	7.0-20.0 <i>v</i> 14.0-35.0 <i>h</i>	–	–	Lo, (1978)
Ontario/ Sudbury	Tunnel	–	Jasperoid	45.7	–	–	83.0	–	–	Lindner and Halpern, (1978), Moruzi, (1968)
Ontario/ Thorold	Outcrop	–	Dolomite	12.7 - 15.5	–	–	71.0-73.0	–	–	Lindner and Halpern, (1978)
			Dolomitic limestone	16.2 - 17.3	–	–	73.0-74.0	–	–	

Note: d: result from direct tension test; b: results from Brazilian test; v: results from vertically cored samples/or measurements in the vertical direction; h: results from horizontally cored samples/or measurements in the horizontal direction ; i: results from inclined 45° cored samples with respect to the bedding planes.

Province/ State/ City	Project	Rock Formation	Rock Type	Depth/ Elevation (m)	Tensile Strength (MPa)	Uniaxial Compressive Strength UCS (MPa)	Elastic Modulus E (GPa)	Poisson's Ratio ν	Swelling Potential (%)	Source of Data
Ontario/ Thorold	Outcrop	–	Shaly limestone	18.3 - 18.6	–	–	43.0	–	–	Lindner and Halpern, (1978)
			limestone	19.8 - 24.7	–	–	55.0	–	–	
Ontario/ Thorold	Thorold tunnel	Gasport	Dolomite	12.7 - 53.1	–	–	71.0-73.0	0.27-0.3	–	Palmer and Lo, (1976)
		Member of Lockport/ De Cew formation	Dolomitic limestone	56.6	–	–	74.0	0.3	–	
			Shaly limestone	60.0 - 61.0	–	–	43.0	0.25	–	
			Fossili- ferous limestone	65.0	–	–	55.0	0.3	–	
			Argillaceous limestone	81.0	–	–	55.0	0.3	–	

Note: d: result from direct tension test; b: results from Brazilian test; v: results from vertically cored samples/or measurements in the vertical direction; h: results from horizontally cored samples/or measurements in the horizontal direction ; i: results from inclined 45° cored samples with respect to the bedding planes.

Province/ State/ City	Project	Rock Formation	Rock Type	Depth/ Elevation (m)	Tensile Strength (MPa)	Uniaxial Compressive Strength UCS (MPa)	Elastic Modulus E (GPa)	Poisson's Ratio ν	Swelling Potential (%)	Source of Data
Ontario/ Toronto	Darlington intake tunnel	Whitby	Shaly limestone	83.4	–	52.0 - 63.3 <i>h</i>	52.9 - 54.6 <i>h</i>	0.25 - 0.27 <i>h</i>	–	Lo et al., (1984)
				84.4- 84.7	–	87.6 - 88.2 <i>v</i>	39.6 - 43.6 <i>v</i>	0.34 - 0.37 <i>v</i>	–	
Ontario/ Toronto	Domed stadium	Georgian Bay	Shale	19.8 - 26.3	–	11.2 - 17.2	2.2	0.3	–	Lo et al., (1987)
Ontario/ Wawa	Mine	–	Siderite	365.8	–	–	67.6 - 118.0	–	–	Herget, (1973)
			Tuff	478.5	–	–	68.3-115.8	–	–	
			Meta - diorite	573.0	–	–	52.4-70.3	–	–	
			Chert	573.0	–	–	51.7-80.0	–	–	

Note: d: result from direct tension test; b: results from Brazilian test; v: results from vertically cored samples/or measurements in the vertical direction; h: results from horizontally cored samples/or measurements in the horizontal direction ; i: results from inclined 45° cored samples with respect to the bedding planes.

Province/ State/ City	Project	Rock Formation	Rock Type	Depth/ Elevation (m)	Tensile Strength (MPa)	Uniaxial Compressive Strength UCS (MPa)	Elastic Modulus E (GPa)	Poisson's Ratio ν	Swelling Potential (%)	Source of Data
Southern Ontario	Research program for the National Research Council of Canada, different sites in Southern Ontario	Lockport	Dolomitic limestone	157.0 -	—	180.0 <i>h</i>	76.0 <i>h</i>	0.14-0.33	0.02 <i>h</i>	Lo et al., (1978)
				168.0	—	200.0 <i>v</i>	67.0 <i>v</i>	—	0.01 <i>v</i>	
		Gasport shaly limestone	—	—	105.0 <i>h</i>	44.0 <i>h</i>	—	0.08 <i>h</i>		
			—	—	120.0 <i>v</i>	27.0 <i>v</i>	—	0.08 <i>v</i>		
Rochester	Shale	26.2 - 26.52	—	70.0 <i>h</i>	27.0 <i>h</i>	—	0.07 <i>h</i> 0.16 <i>v</i>			
		Georgian Bay	Shale	10.17 - 15.33	—	35.0 <i>h</i>	21.0 <i>h</i>	0.06 - 0.25	0.03-0.14 <i>h</i> 0.2- 0.22 <i>v</i>	

Note: d: result from direct tension test; b: results from Brazilian test; v: results from vertically cored samples/or measurements in the vertical direction; h: results from horizontally cored samples/or measurements in the horizontal direction ; i: results from inclined 45° cored samples with respect to the bedding planes.

Province/ State/ City	Project	Rock Formation	Rock Type	Depth/ Elevation (m)	Tensile Strength (MPa)	Uniaxial Compressive Strength UCS (MPa)	Elastic Modulus E (GPa)	Poisson's Ratio ν	Swelling Potential (%)	Source of Data
Southern Ontario	Research program for the National Research Council of Canada, different sites in Southern Ontario	Collingwo- od	Grey	17.0 -	—	35.0 <i>h</i>	23.0 <i>h</i>	0.2	0.15 <i>h</i>	Lo et al., (1978)
			Mudstone	24.64		60.0 <i>v</i>	10.0 <i>v</i>		0.45 <i>v</i>	
		Trenton- Black River	Black shale	17.0 -	—	70.0 <i>h</i>	37.0 <i>h</i>	0.1-0.25	0.0 <i>h</i> ,	
				24.64		80.0 <i>v</i>	20.0 <i>v</i>		0.0 <i>v</i>	
			Limestone	12.9 -	—	130.0 <i>h</i>	55.0 <i>h</i>	0.19-0.4	0.0 <i>h</i>	
				35.5						
		Shaly limestone	12.9 -	—	100.0 <i>h</i>	57.0 <i>h</i>	—	0.06 <i>h</i> 0.09 <i>v</i>		
		Queenston Shale	—	—	—	—	—	0.04 <i>h</i> 0.14 <i>v</i>		

Note: d: result from direct tension test; b: results from Brazilian test; v: results from vertically cored samples/or measurements in the vertical direction; h: results from horizontally cored samples/or measurements in the horizontal direction ; i: results from inclined 45° cored samples with respect to the bedding planes.

Province/ State/ City	Project	Rock Formation	Rock Type	Depth/ Elevation (m)	Tensile Strength (MPa)	Uniaxial Compressive Strength UCS (MPa)	Elastic Modulus E (GPa)	Poisson's Ratio ν	Swelling Potential (%)	Source of Data
Southern Ontario	different sites	Lockport	Shaly limestone (Gasport)	159.94 -	-	124.0-212.0 ν	25.3-	0.14-0.29 ν	-	Lo and Hori, (1979)
				162.05		27.0-115.0 h	61.2 ν	0.24 h		
	Research program for the National Research Council of Canada, different sites in Southern Ontario	Lockport	Fossiliferous limestone (Gasport)	159.23	-	152.0 ν	59.1 ν	0.24 ν	-	Lo and Hori, (1979)
				157.33		102.0 h	75.9 h	0.33 h		
	Georgian Bay	Shale	15.33	-	35.0 ν	5.5 ν	0.13 ν	-		
			10.17		41.0 h	12.1 h	0.06 - 0.25 h			

Note: d: result from direct tension test; b: results from Brazilian test; ν : results from vertically cored samples/or measurements in the vertical direction; h : results from horizontally cored samples/or measurements in the horizontal direction ; i : results from inclined 45° cored samples with respect to the bedding planes.

Province/ State/ City	Project	Rock Formation	Rock Type	Depth/ Elevation (m)	Tensile Strength (MPa)	Uniaxial Compressive Strength UCS (MPa)	Elastic Modulus E (GPa)	Poisson's Ratio ν	Swelling Potential (%)	Source of Data	
Southern Ontario	Research program for the National Research Council of Canada, different sites in Southern Ontario	Collingwood	Black Shale	22.76	–	80.0 <i>v</i>	20.4 <i>v</i>	0.18 <i>v</i>	–	Lo and Hori, (1979)	
				18.49	–	25.0 - 72.0 <i>h</i>	14.8- 38.0 <i>h</i>	0.10- 0.15 <i>h</i>	–		
				16.99	–	21.0 <i>i</i>	13.4 <i>i</i>	0.09 <i>i</i>	–		
		Collingwood	Grey Shale	23.34	–	58.0 <i>v</i>	9.8 <i>v</i>	0.2 <i>v</i>	–		–
				23.28	–	32.0 - 35.0 <i>h</i>	19.7- 26.0 <i>h</i>	0.09- 0.15 <i>h</i>	–		
				Trenton	Shaly limestone	12.93 -	–	84.0 -	53.4-		0.19-
		26.06	–	129.0 <i>h</i>		60.5 <i>h</i>	0.39 <i>h</i>	–			
		Trenton	Limestone	35.41	–	75.0 <i>v</i>	54.8 <i>v</i>	0.35 <i>v</i>	–		–

Note: d: result from direct tension test; b: results from Brazilian test; v: results from vertically cored samples/or measurements in the vertical direction; h: results from horizontally cored samples/or measurements in the horizontal direction ; i: results from inclined 45° cored samples with respect to the bedding planes.

Province/ State/ City	Project	Rock Formation	Rock Type	Depth/ Elevation (m)	Tensile Strength (MPa)	Uniaxial Compressive Strength UCS (MPa)	Elastic Modulus E (GPa)	Poisson's Ratio ν	Swelling Potential (%)	Source of Data
Southern Ontario	Research program for the National Research Council of Canada, different sites in Southern Ontario	Trenton	Limestone	35.48	—	133.0 <i>h</i>	54.8 <i>h</i>	0.24 -0.4 <i>h</i>	—	Lo and Hori, (1979)
				35.53	—	91.0 <i>i</i>	45.7 <i>i</i>	0.35 <i>i</i>	—	
		Rochester	Shale	26.37	—	85.0 <i>v</i>	22.5 <i>v</i>	0.16 <i>v</i>	—	
				26.24 -	—	61.0 -	21.8 -	0.24 -	—	
				26.52	—	85.0 <i>h</i>	32.3 <i>h</i>	0.26 <i>h</i>	—	
				26.29	—	40.0 <i>i</i>	19.0 <i>i</i>	0.39 <i>i</i>	—	
		Lockport	Dolomite (Goat Island)	168.17	—	246.0 <i>v</i>	64.0 <i>v</i>	0.29 <i>v</i>	—	
				168.1	—	207.0 <i>h</i>	63.3 <i>h</i>	0.31 <i>h</i>	—	

Note: d: result from direct tension test; b: results from Brazilian test; v: results from vertically cored samples/or measurements in the vertical direction; h: results from horizontally cored samples/or measurements in the horizontal direction ; i: results from inclined 45° cored samples with respect to the bedding planes.

Province/ State/ City	Project	Rock Formation	Rock Type	Depth/ Elevation (m)	Tensile Strength (MPa)	Uniaxial Compressive Strength UCS (MPa)	Elastic Modulus E (GPa)	Poisson's Ratio ν	Swelling Potential (%)	Source of Data
Southern Ontario	Research program for the National Research Council of Canada, different sites in Southern Ontario	Lockport	Dolomitic limestone (Gasport)	165.15	–	208.0 <i>v</i>	57.7 <i>v</i>	0.32 <i>v</i>	–	Lo and Hori, (1979)
				165.07	–	46.0 <i>h</i>	–	–	–	
		Lockport	Dolomitic limestone/ Limestone (Gasport)	163.86	–	199.0 <i>v</i>	61.2 <i>v</i>	0.25 <i>v</i>	–	
				163.78	–	191.0 <i>h</i>	63.3 <i>h</i>	0.28 <i>h</i>	–	

Note: d: result from direct tension test; b: results from Brazilian test; v: results from vertically cored samples/or measurements in the vertical direction; h: results from horizontally cored samples/or measurements in the horizontal direction ; i: results from inclined 45° cored samples with respect to the bedding planes.

Province/ State/ City	Project	Rock Formation	Rock Type	Depth/ Elevation (m)	Tensile Strength (MPa)	Uniaxial Compressive Strength UCS (MPa)	Elastic Modulus E (GPa)	Poisson's Ratio ν	Swelling Potential (%)	Source of Data
Southern Ontario	Thorold tunnel, Niagara wheel pit, Toronto power station, heart lake tunnel in Mississauga, Darlington intake tunnel, Scotia plaza and domed stadium in Toronto	Lockport (Eramosa) Lockport (Goat Island) Lockport (Gasport) De Cew Rochester	Dolostone Dolostone Shaly Limestone Dolostone/ Mudstone Shale	--	--	120.0 200.0 120.0 74.0 85.0	63.0 62.0 27.0 57.0 23.0	--	0.0 <i>h</i> 0.0 <i>h</i> 0.08 <i>h</i> 0.04 <i>h</i> 0.07 <i>h</i>	Lo, (1989)

Note: d: result from direct tension test; b: results from Brazilian test; v: results from vertically cored samples/or measurements in the vertical direction; h: results from horizontally cored samples/or measurements in the horizontal direction ; i: results from inclined 45° cored samples with respect to the bedding planes.

Province/ State/ City	Project	Rock Formation	Rock Type	Depth/ Elevation (m)	Tensile Strength (MPa)	Uniaxial Compressive Strength UCS (MPa)	Elastic Modulus E (GPa)	Poisson's Ratio ν	Swelling Potential (%)	Source of Data
Southern Ontario	Thorold tunnel, Niagara wheel pit, Toronto power station, heart lake tunnel in Mississauga, Darlington intake tunnel, Scotia Plaza Dom stadium in Toronto	Irondequoit	Limestone	–	–	90.0	60.0	–	–	Lo, (1989)
		Reynolds	Dolostone	–	–	106.0	40.0	–	–	
		Grimsby	Sandstone	–	–	132.0	42.0	–	–	
			Shale	–	–	25.0	8.0	–	0.27 <i>h</i>	
		Power Glen	Sandstone	–	–	158.0	52.0	–	–	
			Shale	–	–	26.0	9.0	–	0.17 <i>h</i>	
		Whirlpool	Sandstone	–	–	190.0	55.0	–	–	
		Queenston	Shale	–	–	30.0	10.0	–	0.30 <i>h</i>	

Note: d: result from direct tension test; b: results from Brazilian test; v: results from vertically cored samples/or measurements in the vertical direction; h: results from horizontally cored samples/or measurements in the horizontal direction ; i: results from inclined 45° cored samples with respect to the bedding planes.

Province/Project State/ City	Rock Formation	Rock Type	Depth/ Elevation (m)	Tensile Strength (MPa)	Uniaxial Compressive Strength UCS (MPa)	Elastic Modulus E (GPa)	Poisson's Ratio ν	Swelling Potential (%)	Source of Data
Southern Ontario	Thorold Bay	Georgian Shale	–	–	20.0	4.0	–	0.15 <i>h</i>	Lo, (1989)
Niagara wheel pit, Toronto power station, heart lake tunnel in Mississauga,	Blue Mountain	Shale	–	–	27.0	2.0	–	0.15 <i>h</i>	
Darlington intake tunnel, Scotia plaza and domed stadium in Toronto	Collingwood	Black shale	–	–	80.0	20.0	–	0.00 <i>h</i>	
		Grey mudstone	–	–	58.0	10.0	–	0.15 <i>h</i>	
	Lindsay	Shaly limestone	–	–	110.0	46.0	–	0.05 <i>h</i>	
	Verulam	Limestone with shaly interbeds	–	–	23.0	57.0	–	0.05 <i>h</i>	

Note: d: result from direct tension test; b: results from Brazilian test; v: results from vertically cored samples/or measurements in the vertical direction; h: results from horizontally cored samples/or measurements in the horizontal direction ; i: results from inclined 45° cored samples with respect to the bedding planes.

Province/ State/ City	Project	Rock Formation	Rock Type	Depth/ Elevation (m)	Tensile Strength (MPa)	Uniaxial Compressive Strength UCS (MPa)	Elastic Modulus E (GPa)	Poisson's Ratio ν	Swelling Potential (%)	Source of Data
Southern Ontario	Thorold tunnel, Niagara wheel pit, Toronto power station, heart lake tunnel in Mississauga, Darlington intake tunnel, Scotia plaza and domed stadium in Toronto	Bobcaygeon limestone		--	--	78.0	56.0	--	--	Lo, (1989)
		Gull River	Limestone	--	--	143.0	63.0	--	0.00 <i>h</i>	
		hadow Lake	Sandstone	--	--	60.0	21.0	--	--	
		Pre Cambrian	Medium grained	--	--	190.0	60.0	--	0.00 <i>h</i>	
		Granitic	Coarse grained	--	--	140.0	46.0	--	0.00 <i>h</i>	
		Gneiss	Gneiss bands	--	--	90.0	46.0	--	--	

Note: d: result from direct tension test; b: results from Brazilian test; v: results from vertically cored samples/or measurements in the vertical direction; h: results from horizontally cored samples/or measurements in the horizontal direction ; i: results from inclined 45° cored samples with respect to the bedding planes.

Province/ State/ City	Project	Rock Formation	Rock Type	Depth/ Elevation (m)	Tensile Strength (MPa)	Uniaxial Compressive Strength UCS (MPa)	Elastic Modulus E (GPa)	Poisson's Ratio ν	Swelling Potential (%)	Source of Data
Southern Ontario	Mississauga, Pickering, Bowmanville, Wesleyville and Port Hope In Ontario	Cobourg	Limestone	—	0.04-2.0 <i>d</i> 3.0-10.0 <i>b</i>	22.0 -140.0	10.0-67.0	0.1-0.6	—	Lam et al., (2011)
			Collingwood shale	—	—	27.0-132.0	2.0-31.0	0.2-0.3	—	
		Sherman Fall	Shale	—	0.1-3.0 <i>d</i> 1.0-12.0 <i>b</i>	23.0-69.0	1.0-73.0	0.1-0.4	—	
			Limestone	—	0.1-3.0 <i>d</i> 1.0-12.0 <i>b</i>	71.0-161.0	1.0-73.0	0.1-0.4	—	
	Kirkfield	—	—	—	34.0 - 115.0	13.0 - 64.0	—	—		

Note: d: result from direct tension test; b: results from Brazilian test; v: results from vertically cored samples/or measurements in the vertical direction; h: results from horizontally cored samples/or measurements in the horizontal direction ; i: results from inclined 45° cored samples with respect to the bedding planes.

Province/ State/ City	Project	Rock Formation	Rock Type	Depth/ Elevation (m)	Tensile Strength (MPa)	Uniaxial Compressive Strength UCS (MPa)	Elastic Modulus E (GPa)	Poisson's Ratio ν	Swelling Potential (%)	Source of Data
Quebec/ Beauchene	Tunnel In Lake Beauchene, Quebec	–	Gneiss W. Mica/ Quartz	64.0	–	–	34.5	–	–	Lindner and Halpern, (1978), Metaltech Inspection Ltd. (1970)
Quebec/ Churchhill falls	Cavern adit in Churchhill falls	–	Gneissic	305.0	–	–	48.0	–	–	Benson et al., (1970)
Manitoba/ Pinawa	Underground research laboratory (URL)	–	Granite	336.6 - 515.0	–	167.0	–	–	–	Hefny and Lo, (1996 and 1995)

Note: d: result from direct tension test; b: results from Brazilian test; v: results from vertically cored samples/or measurements in the vertical direction; h: results from horizontally cored samples/or measurements in the horizontal direction ; i: results from inclined 45° cored samples with respect to the bedding planes.

Province/ State/ City	Project	Rock Formation	Rock Type	Depth/ Elevation (m)	Tensile Strength (MPa)	Uniaxial Compressive Strength UCS (MPa)	Elastic Modulus E (GPa)	Poisson's Ratio ν	Swelling Potential (%)	Source of Data
Manitoba/ Pinawa	(URL)	–	Granite	470.1 - 851.3	–	–	15.6 - 25.8	–	–	Thompson and Chandler, (2004)
Southern Illinois	Oil field- deep boring	–	Carbonate	99.1	–	–	14.0	–	–	Haimson and Fairhurst, (1970)
Minnesota/ St. Cloud	Quarry	–	Granite	–	–	–	47.0	–	–	Bonnechere, (1969)
New York	Oil field- deep boring	–	Sandstone	502.9	–	–	7.0	–	–	Haimson and Stahl, (1969)
New York/ Briarcliff Manor	Outcrop	–	Gneiss	5.6 - 13.1	–	–	3.0 - 52.0	–	–	Lindner and Halpern, (1978)
New York/ Nyack	Outcrop	–	Diabase	0.2 - 0.5	–	–	19.6	–	–	Hooker and Johnson, (1977)

Note: d: result from direct tension test; b: results from Brazilian test; v: results from vertically cored samples/or measurements in the vertical direction; h: results from horizontally cored samples/or measurements in the horizontal direction ; i: results from inclined 45° cored samples with respect to the bedding planes.

Province/ State/ City	Project	Rock Formation	Rock Type	Depth/ Elevation (m)	Tensile Strength (MPa)	Uniaxial Compressive Strength UCS (MPa)	Elastic Modulus E (GPa)	Poisson's Ratio ν	Swelling Potential (%)	Source of Data
New York/ Niagara gorge	Outcrop	–	Dolomite	0.2-6.7	–	–	24.0	–	–	Lindner and Halpern, (1978), Sellers, (1969)
New York/ Rochester	Sewer system	–	Dolomite	–	–	–	50.7- 91.7	–	–	Goldberg and Dunnicliff and Associates (1976)
New York/ Somerset	Outcrop	–	Sandstone	8.5	–	–	17.0	–	–	Lindner and Halpern, (1978),
New York/ Sterling	Outcrop	–	Sandstone	10.1-32.3	–	–	33.0	–	–	Dames and Moore Consultants, (1974 and 1973)
Ohio	Boring	–	Shale	10.3- 18.6	–	–	13.0-28.0	–	–	Lindner and Halpern, (1978)

Note: d: result from direct tension test; b: results from Brazilian test; v: results from vertically cored samples/or measurements in the vertical direction; h: results from horizontally cored samples/or measurements in the horizontal direction ; i: results from inclined 45° cored samples with respect to the bedding planes.

Province/ State/ City	Project	Rock Formation	Rock Type	Depth/ Elevation (m)	Tensile Strength (MPa)	Uniaxial Compressive Strength UCS (MPa)	Elastic Modulus E (GPa)	Poisson's Ratio ν	Swelling Potential (%)	Source of Data
Ohio/ Barberton	Mine	—	Limestone	701.0	—	—	55.0 - 67.0	—	—	Obert, (1962)
Ohio/ Bellefontaine	Quarry	Gasport	Limestone/ Dolomite	0.2-1.0	—	—	34.8	—	—	Lindner and Halpern, (1978)
Ohio/Falls Township	Oil Field - Deep boring	—	Sandstone	808.0	—	—	10.0	—	—	Haimson, and Fairhurst, (1970)
Ohio/ Hocking State Forest	Outcrop	—	Sandstone	0.9-1.2	—	—	7.8	—	—	Rough and Lambert, (1971)

Note: d: result from direct tension test; b: results from Brazilian test; v: results from vertically cored samples/or measurements in the vertical direction; h: results from horizontally cored samples/or measurements in the horizontal direction ; i: results from inclined 45° cored samples with respect to the bedding planes.

Province/ State/ City	Project	Rock Formation	Rock Type	Depth/ Elevation (m)	Tensile Strength (MPa)	Uniaxial Compressive Strength UCS (MPa)	Elastic Modulus E (GPa)	Poisson's Ratio ν	Swelling Potential (%)	Source of Data
Ohio/ Kenton	Quarry	–	Limestone/ Dolomite	0.2-1.0	–	–	34.8	–	–	Lindner and Halpern, (1978)
Ohio/Lima	Quarry	–	Limestone/ Dolomite	0.2-1.0	–	–	34.8	–	–	
Ohio/ Sydney	Quarry	–	Limestone/ Dolomite	0.2-1.0	–	–	34.8	–	–	Lindner and Halpern, (1978)
Wisconsin/ Montello	Deep Boring	–	Granite	75.0 - 188.1	–	–	52.0 - 56.0	–	–	Foundation Sciences Incorporation (1971)

Note: d: result from direct tension test; b: results from Brazilian test; v: results from vertically cored samples/or measurements in the vertical direction; h: results from horizontally cored samples/or measurements in the horizontal direction ; i: results from inclined 45° cored samples with respect to the bedding planes.

Table 2.3. Dynamic properties of rocks in southern Ontario and neighboring regions

Province/ State/ City	Project	Rock Formation	Rock Type	Depth/ Elevation (m)	Mass Density (Mg/m ³)	Compressive Wave Velocity (km/s)	Shear Wave Velocity (km/s)	Dynamic Poisson's Ratio ν_{dy}	Dynamic Modulus E_{dy} (GPa)	Source of Data		
Southern Ontario	Research Program For The National Research Council of Canada, Different Sites In Southern Ontario	Lockport (Gasport)	Shaly limestone	159.94	2.68-2.69 <i>v</i>	—	—	—	44.3-67.5 <i>v</i>	Lo and Hori, (1979)		
				162.05	2.68-2.76 <i>h</i>	—	—	—	63.3-71.0 <i>h</i>			
		Lockport (Gasport)	Fossiliferous limestone	159.23	2.71 <i>v</i>	—	—	—	66.8 <i>v</i>			
				157.33	2.72 <i>h</i>	—	—	—	73.1 <i>h</i>			
		Georgian Bay	Shale	15.33	2.55 <i>v</i>	—	—	—	19.2 <i>v</i>			
				10.17	2.60 <i>h</i>	—	—	—	38.2 <i>h</i>			
				12.1	2.54 <i>i</i>	—	—	—	19.0 <i>i</i>			
				Collingwood	Black shale	22.76	2.53 <i>v</i>	—	—		—	27.4 <i>v</i>
						18.49	2.53 - 2.56 <i>h</i>	—	—		—	51.3-58.4 <i>h</i>
		Collingwood	Grey shale	16.99	2.58 <i>i</i>	—	—	—	37.3 <i>i</i>			
				23.34	2.6 <i>v</i>	—	—	—	4.9 <i>v</i>			
				23.27	2.61-2.64 <i>h</i>	—	—	—	42.2-49.2 <i>h</i>			
		Collingwood	Grey shale	23.29	2.6 <i>i</i>	—	—	—	—			
		Collingwood	Shaly limestone	12.93-	2.68	26.06	—	—	—		—	
				Trenton		Limestone	35.41	2.68 <i>v</i>	—		—	—
35.53	2.68 <i>h</i>	—	—	—	—							
35.48	2.85 <i>i</i>	—	—	—	—							
Rochester	Shale	26.37	2.77 <i>v</i>	—	—	—	38.7 <i>v</i>					

Province/ State/ City	Project	Rock Formation	Rock Type	Depth/ Elevation (m)	Mass Density (Mg/m ³)	Compressive Wave Velocity (km/s)	Shear Wave Velocity (km/s)	Dynamic Poisson's Ratio ν_{dy}	Dynamic Modulus E_{dy} (GPa)	Source of Data		
Southern Ontario	Research Program For The National Research Council of Canada, Different Sites In Southern Ontario	Rochester	Shale	26.24-	2.68-2.72 <i>h</i>	-	-	-	39.4 <i>h</i>	Lo and Hori, (1979)		
				26.5								
		Lockport (Goat Island)	Dolomite	26.29	2.74 <i>i</i>	-	-	-	21.8 <i>i</i>			
				169.37	2.76	-	-	-	61.9 <i>v</i>			
				168.8	2.76	-	-	-	70.3-80.2 <i>h</i>			
				169.21	2.77	-	-	-	74.5 <i>i</i>			
				Lockport (Gasport)	Dolomitic limestone	165.66	2.72 <i>v</i>	-	-		-	73.8 <i>v</i>
				Lockport (Gasport)	Dolomitic limestone	165.57	2.76 <i>h</i>	-	-		-	70.3-86.5 <i>h</i>
						165.74	2.72 <i>i</i>	-	-		-	69.6 <i>i</i>
				Lockport (Gasport)	Dolomitic limestone/ Limestone	164.06	2.72 <i>v</i>	-	-		-	47.8 <i>v</i>
164.17	2.71- 2.72 <i>h</i>	-	-			-	53.4 -66.1 <i>h</i>					
Ontario/ Toronto	Darlington intake tunnel	Whitby	Shaly limestone	83.4	2.58 - 2.70	5.1- 5.12 <i>v</i>	1.0 - 2.49	0.34- 0.37 <i>v</i>	39.6 - 43.6 <i>v</i>	Lo et al., (1987, 1987a)		
				84.4- 84.7	-	4.92 - 5.13 <i>h</i>	-	0.25-0.27 <i>h</i>	52.9-54.6 <i>h</i>			
Ontario /Niagara Falls	Niagara generating station No. 3	Queenston	Shale	95.64 - 114.33	2.66 - 2.68	3.48 - 4.28	-	-	-	Lo and Lee, (1990)		

Note: v: results from vertically cored samples/or measurements in the vertical direction; h: results from horizontally cored samples/or measurements in the horizontal direction; i: results from inclined 45° cored samples with respect to the bedding planes.

Chapter 3

INFLUENCE OF LUBRICANT FLUIDS ON THE SWELLING BEHAVIOUR OF QUEENSTON SHALE IN SOUTHERN ONTARIO²

3.1 INTRODUCTION

The swelling phenomenon is a common expression of the deformation that occurs in some sedimentary rocks in southern Ontario and elsewhere after excavation in the rock mass. Queenston shale, among other shaly sedimentary rocks in southern Ontario, exhibits considerably high swelling potential and time-dependent deformation. The swelling phenomenon can cause major problems to underground structures, many of which have occurred and been recorded in the form of invert heave and lateral inward deflection in several tunnels around the world (Lo and Yuen, 1981).

The swelling phenomenon of shaly rocks in southern Ontario was recognized early in 1903 when an inward deformation in the wheel pit walls at the Canadian Niagara falls was reported (Morison, 1957). Some of the shaly limestone in southern Ontario, such as that in Thorold, also exhibits considerable time-dependent deformation that has caused severe cracks developed in one of the walls of Thorold tunnel just 1 year after construction (Bowen et al., 1976). Similarly, swelling of sedimentary rocks had caused distress in many tunnels in Europe in the form of invert heaves at a rate of hundreds of millimeters per year (Einstein and Bischoff, 1975).

The amount of swelling deformations and the mechanisms that control the swelling depend on the rock type. The hydration process of the anhydrites upon exposure to water controls the swelling deformation of anhydrites. In this process, the anhydrites exhibit an increase in volume when transformed to gypsum upon hydration. In potash and

² A version of this chapter has been published in the Canadian Geotechnical Journal, 2016, **53** (7): 1059-1080.

rock salts, the mechanism that controls the swelling deformation is mainly the creep process. When potash and rock salts creep, the particles undergo a movement of dislocation that leads to gliding in the intracrystalline structure. These changes are manifested in the form of swelling deformation.

The observed swelling deformation of shales and marl when they are in contact with fresh water is mainly attributed to the osmosis and diffusion processes due to ion concentration differences between the double-layer water within the rock and the external free water (Einstein and Bischoff, 1975). The hypothesis that the osmosis and diffusion processes are the controlling mechanisms of the swelling deformation of Queenston shale from southern Ontario was reinforced through the research performed by Lee and Lo (1993). They performed different swelling tests on Queenston and other shales from southern Ontario in water with variable concentrations of NaCl solutions and other fluids and concluded that three conditions should be met in order for swelling of Queenston shale to occur: i) relief of the initial in-situ stresses upon excavation; ii) accessibility of fresh water; and iii) an outward salts concentration gradient from the rock pore fluid to the ambient fluid. Lo and his co-workers extensively investigated the swelling of shales. Lo et al., (1975, 1978) measured and quantified the time-dependent deformations of shaly rocks in southern Ontario. They developed laboratory test methods to measure the swelling strains of rocks considering the confining pressure, and showed that these methods can produce results consistent with field measurements. These test methods were utilized in subsequent research to investigate the swelling behavior of shaly rocks including Queenston shale (Lo and Lee, 1990; Lee and Lo, 1993; Hefny et al., 1996; Lo and Hefny, 1996 and Hawlader et al., 2003). In these studies, the swelling anisotropy, swelling stress-dependency, swelling mechanism, and stress–strain time-dependency of the Queenston shale and other shales from southern Ontario were investigated extensively. These studies used fresh water as the ambient fluid and the results were employed to identify the swelling mechanism of Queenston shale to develop a rheological model and theoretical solutions to calculate the deformation of these swelling shales and the associated stresses that act on built structures. Al-Maamori et al., (2014) compiled the geo-mechanical properties of rocks in southern Ontario and indicated the

necessity to investigate the swelling behaviour of swelling rocks in drilling fluids and lubricant fluids used in micro-tunneling applications.

3.2 OBJECTIVE AND SCOPE OF WORK

The work presented in this chapter forms part of a comprehensive research to investigate the workability and functionality of a micro-tunnelling technique in the Queenston shale of southern Ontario. In this chapter, the influence of lubricant fluids on the swelling behavior of Queenston shale, in comparison to fresh water, is investigated. The free swell, semi-confined swell, and null swell tests developed at the University of Western Ontario by Lo et al., (1975, 1978), Wai (1977), and Lo and Hefny (1999) were utilized to conduct the extensive testing program. The free swell test, semi-confined swell test, and null swell test were performed on vertically and horizontally cut specimens from Milton and Niagara Queenston shales submerged in water, polymer solution, and bentonite solution. Test results have revealed that using lubricant fluids, such as polymer and bentonite solutions, can significantly influence the swelling behaviour of Milton and Niagara Queenston shales in comparison to their behaviour in water. Additional complementary mineralogical and chemical tests were performed to assist in explaining the swelling behaviour of both shales in lubricant fluids. Average values of the swelling test results are presented in the framework of the Lo and Hefny (1996) swelling model to illustrate the variation in swelling behaviour of Queenston shale in lubricant fluids and in water.

3.3 SOURCE OF ROCK SAMPLES

The test program was performed on Queenston shale samples from Milton and Niagara Falls in southern Ontario. The Milton Queenston shale samples were collected from single borehole drilled at the construction site near the interchange between Regional Road 25 and Louis St. Laurent Avenue in Milton from 16.15 m to 34.52 m depth below the ground surface. The Niagara Queenston shale samples were collected from two boreholes drilled in the Niagara Tunnel, approximately 3.00 m to 12.00 m deep from the tunnel invert at the lowest part of the tunnel (i.e., 125 to 137 m below ground

level). The Milton Queenston shale samples were HQ size (i.e., 63 mm in diameter), while Niagara Queenston shale samples were HQ3 size (i.e., 60.5 mm in diameter) (Das 1998).

3.3.1 Preserving Recovered Rocks

To preserve the rock core in in-situ condition an established procedure developed at the Geotechnical Research Centre of the University of Western Ontario was followed. The recovered rock column was wrapped with plastic film (Saran Wrap) layer, and then with another coating layer of electrical tape to maintain moisture. A third layer of a bubble wrap was then added to jacket the rock column prior to placing it inside a hard polyvinyl chloride (PVC) pipe that was cut to fit each rock piece. The PVC pipes were fitted with end caps and flexible rubber top and bottom discs placed on both ends of each rock column piece, secured by a mechanical clamp. In this procedure, the recovered rock column was preserved safely against losing moisture and against breakage during handling and transporting.

3.3.2 Sample Cutting

To ensure consistency of the orientation of the specimens in measuring swelling deformations in the orthogonal horizontal directions with respect to the rock bedding, rock cores were marked with an indication line along the longitudinal axis immediately after recovered from the ground. Queenston shale specimens were cut using a diamond slab saw (Hillquest, USA) that utilizes mineral oil (Pella type A from Shell Canada) for cooling, to produce vertically cored specimens. The Queenston shale cores were re-cored horizontally in the laboratory using a re-coring machine to produce horizontal Queenston shale specimens. The indication line marked in the rock cores was used as reference to ensure that all horizontally re-cored specimens were from the same direction. Immediately after cutting, specimens were wiped thoroughly with a piece of cloth and trichloroethylene T340-4 solution (from Fisher Scientific, Canada) to remove any adhered spots of oil. The Queenston shale specimens were cut and prepared in accordance with the requirements of ASTM-D4543 (2008) standard. The weight and

dimensions of each Queenston shale specimen were measured immediately after cutting to determine the density. In addition, for each Queenston shale specimen a supplementary piece was cut from the rock core just next to the specimen to be used for the determination of the initial values of moisture content, pore water salinity, and calcite content.

3.4 TESTING METHODOLOGY

The swelling behaviour of Queenston shale from southern Ontario has been investigated extensively (Lo, 1978; Lo et al., 1978, 1984; Lee, 1988; Huang, 1993; Hefny et al., 1996 and Hawlader et al., 2003). However, the behaviour of these shales in lubricant fluids, such as bentonite and polymer solutions, that are utilized in the micro-tunneling technique is still lacking. Installation of a pipeline using the micro-tunnelling technique may last for several weeks before the utilized lubricant fluids are replaced with cement grout. During this period, the excavated ground is in direct contact with these lubricant fluids. To investigate the swelling behaviour of Queenston shale when exposed to lubricant fluids, free swell, semi-confined swell, and null swell tests were employed. These swelling tests were conducted using the polymer solution, bentonite solution, and fresh water as ambient fluids that surround Queenston shale samples during the test period.

3.4.1 Lubricant Fluids

The ambient fluids used in this research are those utilized in the micro-tunneling drilling process in rocks as lubricant fluids, namely the bentonite solution and the polymer solution, in addition to fresh water as the standard ambient fluid for swell tests. Mixing proportions were the same as those used in the field (i.e., 8% of bentonite to tap water by weight, and 0.8% of polymer to tap water by volume). The bentonite used was HYDRAUL-EZ (borehole stabilizer and lubricant, sodium bentonite clay from CETCO, USA), and the polymer used was TK60 (liquid polymer concentrate, anionic polyacrylamide suspension in a water-in-oil emulsion from Morrison Mud, Division of Mudtech Ltd., UK). The bentonite and polymer solutions were prepared by gradually

adding the required amount of bentonite or polymer to the corresponding amount of tap water with continuous mixing using a high-speed electrical mixer until consistent and uniform solution was achieved. The solutions were kept for minimum of 24 hours before use according to the manufacturer's instructions to ensure full dispersion of the suspension particles in water and to avoid flocculation.

3.4.2 Tests for Swelling Behaviour

To investigate the swelling behaviour of the Milton and Niagara Queenston shales in lubricant fluids, three swell tests were employed: i) free swell test, ii) semi-confined swell test (Lo et al., 1978), and iii) null swell test (Lo and Hefny, 1999). These swell tests were originally developed in the Geotechnical Research Centre at the University of Western Ontario. For detailed description of the test apparatus and test procedures see Lo and Hefny (1999). The free swell test was performed to investigate the swelling behaviour of Milton and Niagara Queenston shales in lubricant fluids when no confining stress is applied on specimens during the test. The semi-confined swell test was performed to investigate the stress-dependency of the swelling behaviour of Milton and Niagara Queenston shales in lubricant fluids. In this test, specimens were subjected to different confining stresses while the corresponding swelling strains in the same direction of the applied stresses were measured. The null swell test was performed on Queenston shales specimens from Milton and Niagara to measure the pressure required to suppress the swelling of specimens in the direction of the applied pressure when they were submerged in lubricant fluids. The standard ambient fluid in these tests was water. To investigate the anisotropy of the swelling behaviour of Milton and Niagara Queenston shales in lubricant fluids, the semi-confined swell test and null swell test were performed on vertically cored and horizontally cored specimens with respect to the rock bedding. In the free swell test, swelling strains were measured for each specimen in the vertical direction and in two orthogonal horizontal directions with respect to the rock bedding. All of the swelling tests were performed at 10° Celsius in a temperature-controlled room similar to the rock temperature in-situ.

3.5 COMPLEMENTARY TESTS

Additional complementary tests were performed on most tested swelling specimens. These complementary tests are important in assessing the Queenston shale swelling behaviour in the adopted lubricant fluids.

3.5.1 Mineralogical Tests

3.5.1.1 X-Ray Diffraction

To determine the mineralogical composition of Milton and Niagara Queenston shales, X-Ray diffraction analyses were performed on four specimens of Milton Queenston shale and two specimens of Niagara Queenston shale that were selected from different depths to represent the entire rock column. These analyses were performed on randomly oriented powder (bulk) specimens and on oriented clay minerals (wet) specimens that included the separated clay-size portion only. The bulk specimens were prepared following the procedure described by Zhang et al., (2003), while the wet specimens were prepared following the procedure proposed by Moore and Reynolds (1989). The X-Ray diffraction analyses were performed using a Rigaku rotating-anode X-Ray diffractometer. It employed $\text{CoK}\alpha$ radiation, with monochromation achieved using curved crystal, diffracted beam, and graphite monochromator. The instrument was operated at 45 kV and 160 mA, using the normal scan rate of $10^\circ 2\theta/\text{min}$ (equivalent to $0.5^\circ 2\theta$ on conventional diffractometers). X-rays were collimated using 1° divergent and scatter slits, and a 0.15 mm receiving slit. Bulk sample scans were completed from 2° to $82^\circ 2\theta$, at a rate of $10^\circ/\text{min}$.

The mineralogical composition of the tested Milton and Niagara Queenston shales was assessed using the semi-quantitative X-Ray diffraction analyses following Bragg's law. Specimens from the Milton Queenston shale were taken from depths of 16.570, 21.158, 25.140, and 31.039 m from the borehole in Milton. The Niagara Queenston shale specimens were taken from depths of 6.1 and 11.2 m from two boreholes drilled at the tunnel invert at the lowest point in the Niagara Tunnel. The approximate percentage

of each mineral was calculated by dividing the area of the most intense mineral's peak by the sum of areas of all minerals' peaks at their highest intensities. Due to the difficulty in identifying the minerals in clay-size crystals, additional X-Ray diffraction traces were obtained for the separated clay-size fraction specimens. The X-Ray diffraction traces for the bulk and clay-separated fractions for both the Milton and Niagara Queenston shales are shown in Figure 3.1 and the results of the X-Ray diffraction analyses are summarized in Table 3.1.

In the process of identifying and quantifying the clay-size minerals, the corrections on the percentages of chlorite, illite, and kaolinite suggested by Hein and Longstaffe (1983) were applied. Chlorite has a basal series of diffraction that peaks on the first order reflection of 14.2 Å. When heating the specimen to 550 °C for 1 hour, the first-order peak became sharper and stronger while peaks at the second, third, and fourth orders became weaker and could be eliminated (Moore and Reynolds, 1989) as revealed from Figs. 3.1 (b) and 3.1 (d) for traces of the separated clay-size fraction of the Milton and Niagara Queenston shales, respectively. However, the peak intensity of chlorite at the first, second, and third order reflections in the X-Ray diffraction traces of Niagara Queenston shale is slightly higher than that in the Milton Queenston shale, which indicates a higher presence of chlorite salt in Niagara Queenston shale. The illite was identified in both the Milton and Niagara Queenston shales through the maintained peaks at 10.06 Å of the saturated specimens with ethylene glycol vapor and the specimens heated to 300 and 550 °C, respectively. The intensities of the peaks of Niagara Queenston shale are greater than Milton Queenston shale, indicating a higher percentage of illite in Niagara Queenston shale. The illite content of Niagara Queenston shale ranges between 16.3% and 23.0%, which is almost double the amount of illite in Milton Queenston shale.

The distinct behaviour of kaolinite is clearly indicated in the traces of both Milton and Niagara Queenston shale specimens, where the first-order reflection peak at 7.14 Å disappears after heating the specimens to 550 °C for two hours. The Niagara Queenston shale has a slightly higher percentage of kaolinite than Milton Queenston shale, as indicated in Table 3.1. Although kaolinite possesses relatively low swelling capacity, it may contribute to the resulting higher swelling deformation of Niagara Queenston shale

in comparison with Milton Queenston shale. The feldspar was identified through the first-order reflection at $32.35^\circ 2\theta$ in the traces of the bulk specimen. Moore and Reynolds (1989) suggested that the feldspar that reflects at this angle is potassium-rich monoclinic feldspar from the orthoclase family. The presence of the feldspar in Milton Queenston shale is somewhat greater than in Niagara Queenston shale, as indicated in the X-Ray diffraction traces shown in Figures. 3.1(a, c). The low, or α -quartz, is by far the most common silica mineral in sedimentary rocks. The large amounts of quartz in the $<2 \mu\text{m}$ fraction, for properly prepared samples, indicates the presence of either a glacial rock flour or siliceous microfossil type, such as radiolarians and diatoms (Moore and Reynolds 1989). According to the X-Ray diffraction traces of both the Milton and Niagara Queenston shales, the first- and second-order peaks of the quartz happen at 4.28 and 3.35 Å, respectively. The presence of α -quartz in Niagara Queenston shale is about 25%-32% greater than in Milton Queenston shale, and generally forms about 45%-60% of the minerals of both Queenston shales.

The calcite peaks in the second order were at 3.03 and 3.04 Å in the traces of bulk specimens for the Milton and Niagara Queenston shales, respectively. The second-order peaks were the strongest, and therefore they were used in predicting the percentage of calcite. The X-Ray diffraction analyses revealed that the percentage of calcite in Milton Queenston shale is more than double in comparison with that in Niagara Queenston shale. Results of the semi-quantitative determination of the calcite contents from the X-Ray diffraction analyses, summarized in Table 3.1, strongly agree with the results of the quantitative determination of carbonates using the gasometric (Chittick) apparatus. The strong agreement in the results of both analyses promotes confidence in the predicted minerals from the semi-quantitative X-Ray diffraction analyses. The percentage of dolomite was derived from the third- and second-order peaks at 2.9 and 3.67 Å in the traces of bulk specimens of Milton and Niagara Queenston shales, respectively. The dolomite content determined from the X-Ray diffraction analyses agree fairly well with results from the Chittick apparatus, except for two Milton Queenston shale specimens at depths of 16.57 and 25.14 m. The slight difference may be attributed to the disturbance that might have occurred during sample preparation of the bulk specimens. The amount

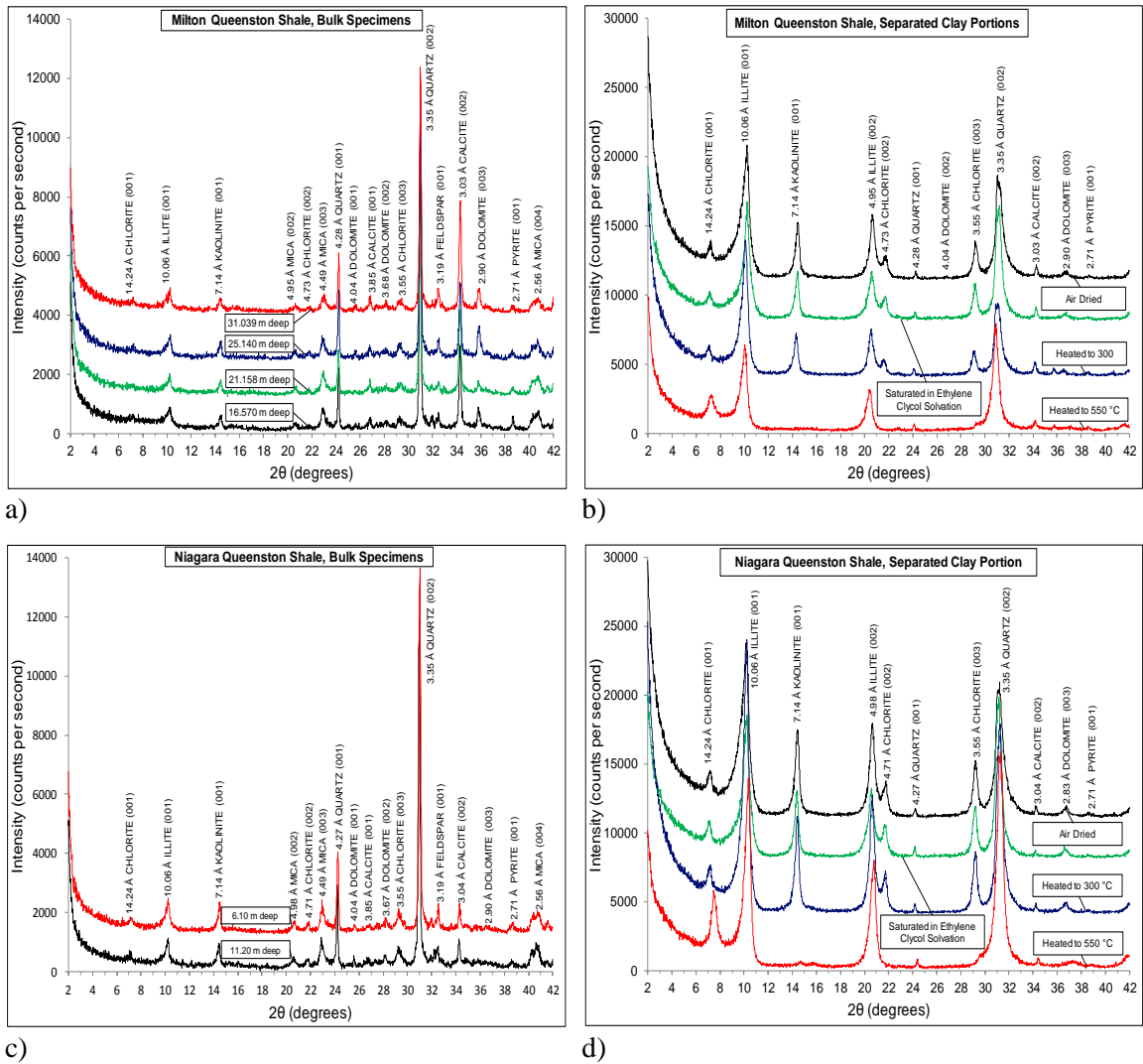


Figure 3.1. X-ray diffraction traces of Milton Queenston shale and Niagara Queenston shale: (a, c) bulk specimens; (b, d) separated clay-size fractions.

of dolomite in Milton Queenston shale is almost double the amount in the Niagara Queenston shale, as indicated in Table 3.1. The existence of both calcite and dolomite in the Queenston shale governs the swelling deformation of these rocks. These carbonates form concretionary masses in the Queenston shale and result in a more resistive microstructure to the swelling deformations. The greater the calcite content in the shaly rocks, the lower the value of swelling deformation (Lo et al., 1987).

The pyrite has a first-order reflection peak at 2.71 Å, as indicated in the X-Ray diffraction traces shown in Figure 3.1. The amount of the existing pyrite is quite similar in the Niagara and Milton Queenston shales, and it ranges between 2.2% and 3.7%. The minerals that exist in both Queenston shales are listed with their percentages in Table 3.1. It is quite obvious that there are no gypsum and anhydrites that may cause a considerable volume change upon contact with water. On the one hand, the amounts of illite and chlorite are higher in Niagara Queenston shale than in Milton Queenston shale; and on the other, the amounts of calcite and dolomite in Milton Queenston shale are more than double their amounts in Niagara Queenston shale. This mineralogical combination in both the Milton and Niagara Queenston shales may cause considerable variation in the swelling deformations of both of these shales.

3.5.1.2 Scanning Electron Microscopy

The scanning electron microscopy (SEM) was performed using a Hitachi S-3400N variable pressure SEM machine on four sets of Milton Queenston shale specimens with orientations parallel and perpendicular to the rock beddings (i.e., horizontally and vertically cut specimens). One set of these specimens was cut from intact Milton Queenston shale while the other sets were cut from terminated swelling tests in fresh water, bentonite solution, and polymer solution. The specimens were cut in a dry condition using a thin-blade diamond saw without cooling agent to avoid washing of bentonite and polymers. The cut specimens were mounted on the metal base of the SEM machine using adhesive epoxy. To produce clear images, the specimens were coated with a very thin layer of gold using a gold sputter coater. The scanning electron microscopy

was performed at three spots on each specimen: i) at the outer surface of the specimen, which was in direct contact with the ambient fluid; ii) at 15 mm away from the specimen's surface towards the centre; and iii) at 30 mm away from the surface towards the specimen's centre (i.e., near the centre). The sample preparation and locations of imaging are illustrated schematically in Figure 3.2.

The SEM images taken at the outer surface of Milton Queenston shale specimens after terminating the free swell test in bentonite and polymer solutions are presented in Figures 3.3 (a) through 3.3 (d). The dark colour mass represents Milton Queenston shale, while the white-grey colour on the surface of the specimen represents either bentonite or polymer particles, which were accumulated during the free swell test. The accumulation of bentonite and polymer particles has resulted in the formation of coating layers on the outer surface of the Milton Queenston shale specimens. These coating layers might have been acting as barriers that have relatively reduced further penetration of water particles, which exist in the ambient fluid, into these specimens. Comparing images for the specimens exposed to bentonite and polymer solutions, it can be noted that the coating layer of polymer particles is considerably thicker than the coating layer of the bentonite particles. The images indicate that the polymer particles penetrated deeper into the superficial micro-cracks of Milton Queenston shale, forming a thick surface coating layer, as indicated in Figures 3a and 3b, which effectively sealed the outer surface of these specimens and hence reduced the swelling of the specimens in the polymer solution, as it will be presented in the swelling results.

Figures 3.4 and 3.5 compare the microstructure of Milton Queenston shale in vertical and horizontal directions, respectively, with respect to the rock beddings, before and after exposure to the ambient fluids. Figure 3.4 (a) shows that the outer surface of the intact Milton Queenston shale specimen had micro-cracks, which may be attributed to sample disturbance during the cutting process because the images of the spots away from surface (Figure 3.4 (b, c)) do not show micro-cracks. Figures 3.4 (d, e, f) show the vertical sections in Milton Queenston shale after terminating the free swell test in the polymer solution. In comparison with the intact specimen, the micro-cracks near the outer

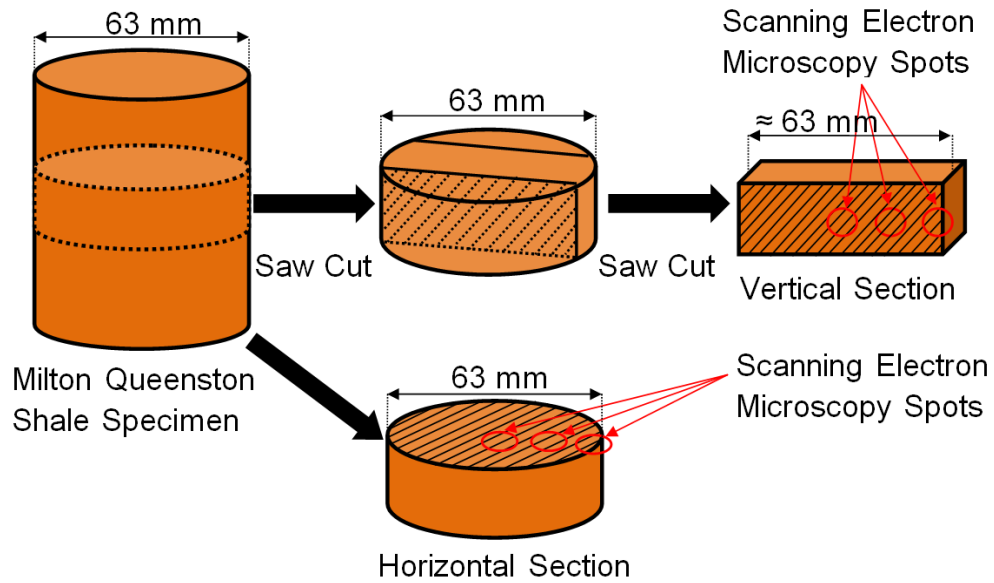


Figure 3.2. Preparations of specimens and locations of scanning electron microscopy imaging.

surface of the specimen are relatively wider and spread deeper into the specimen up to 15 mm from the outer surface. It can also be noted from Figure 3.4 (e) that polymer particles have accumulated on the micro-crack boundaries, forming a micro-film that may prevent the water from moving deeper into the specimen (Figure 3.4 (f, g, h, i) show that the micro-cracks developed along the entire width of the specimen after exposure to the bentonite solution. These micro-cracks resulted in more swelling deformations. The effect of water as ambient fluid on Milton Queenston shale is manifested in Figures 3.4 (j), 3.4 (k), and 3.4 (l), which show the micro-cracks widening near the surface of the specimen up to 15 mm away from the surface. At the specimen centre, the micro-pores were enlarged, but there was no formation of new micro-cracks.

Based on the observations mentioned above, it can be concluded that both the bentonite solution and fresh water have similar effects on Milton Queenston shale, and expanded the surface micro-cracks, compared to the polymer solution. At 15 mm from the outer surface, the bentonite solution resulted in the widest micro-cracks, While no micro-cracks can be noticed at the specimen centre. The micro-pores at the centre of the specimen exposed to water were enlarged in volume.

Figure 3.5 shows the SEM images made on horizontal sections (i.e., parallel to rock bedding) of the same specimens. The fabric of Milton Queenston shale in the horizontal direction appears more compact, and it has less disturbance than the vertical direction (Figures 3.5 (a, b, c)). The overall effect of ambient fluids on the microstructure of Milton Queenston shale in the horizontal direction is similar, but lower in magnitude, compared to the vertical direction. The bentonite solution caused the widest micro-cracks across the entire depth of the specimen, as indicated in Figures 3.5 (g, h, i), while the polymer solution caused the least micro-cracks and only near the surface as indicated in Figure 3.5 (d). The fresh water had significant effect near the surface (Figure 3.5 (j)), but its effect was less than the bentonite solution at deeper spots (Figures 3.5 (k, l)).

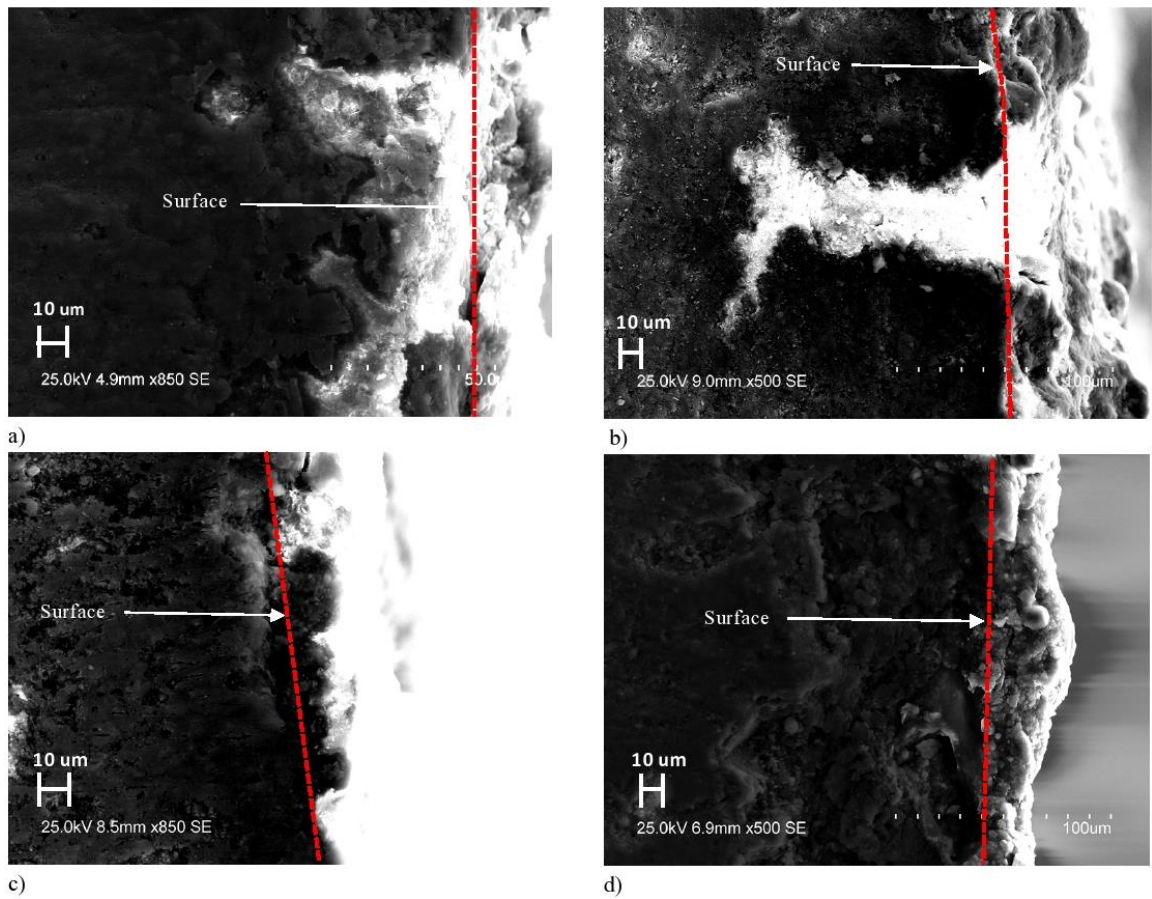


Figure 3.3. Scanning electron microscopy images at surfaces of Milton Queenston shale specimens: (a, b) vertical and horizontal sections of specimen soaked in polymer solution; (c, d) vertical and horizontal sections of specimen soaked in bentonite solution.

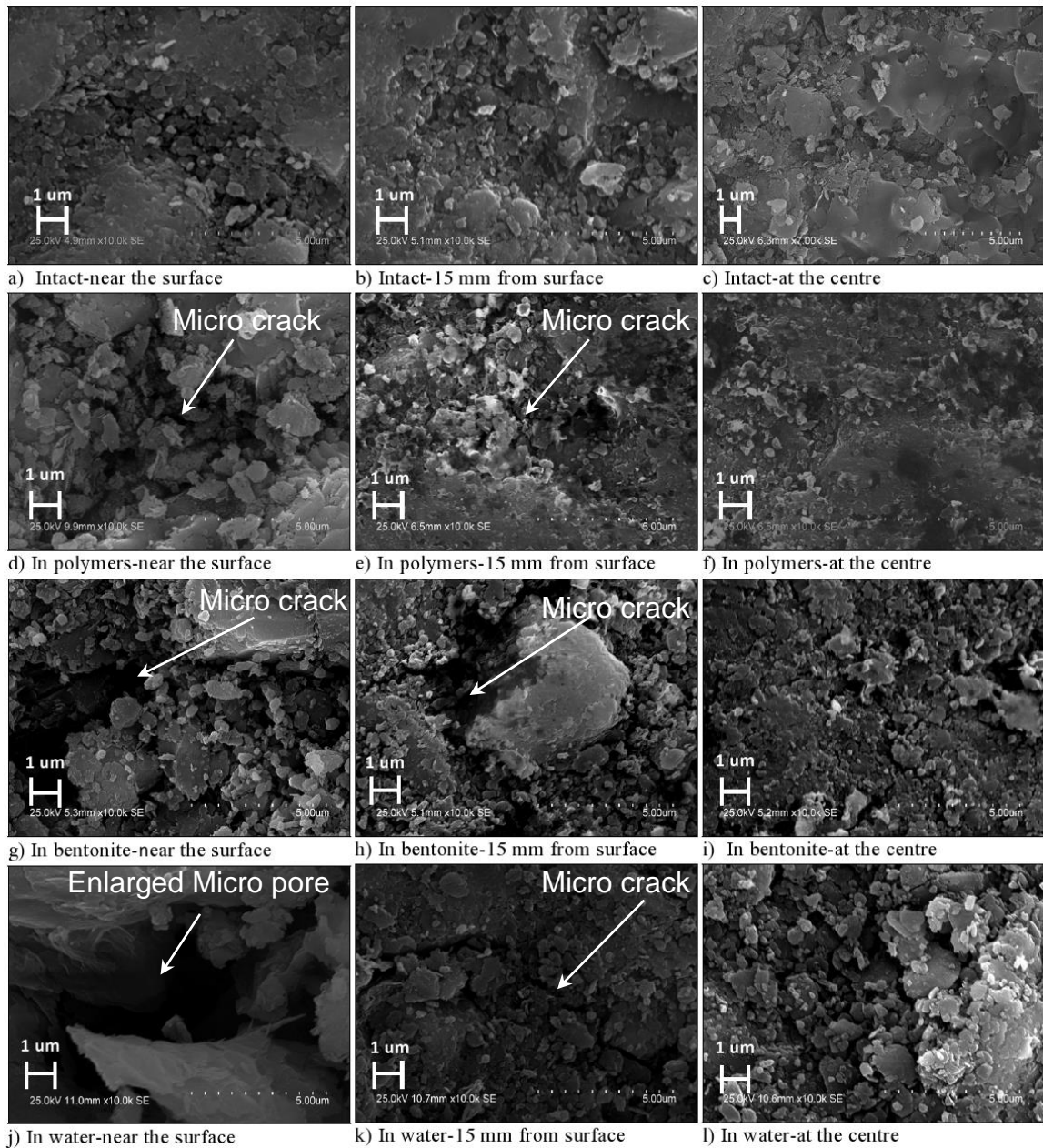


Figure 3.4. Scanning electron microscopy images on vertical sections of Milton Queenston shale: (a, b, c) intact near outer surface, at 15 mm , and at centre; (d, e, f) after 100 days of soaking in polymer solution; (g, h, i) after 100 days of soaking in bentonite solution; (j, k, l) after 100 days of soaking in water.

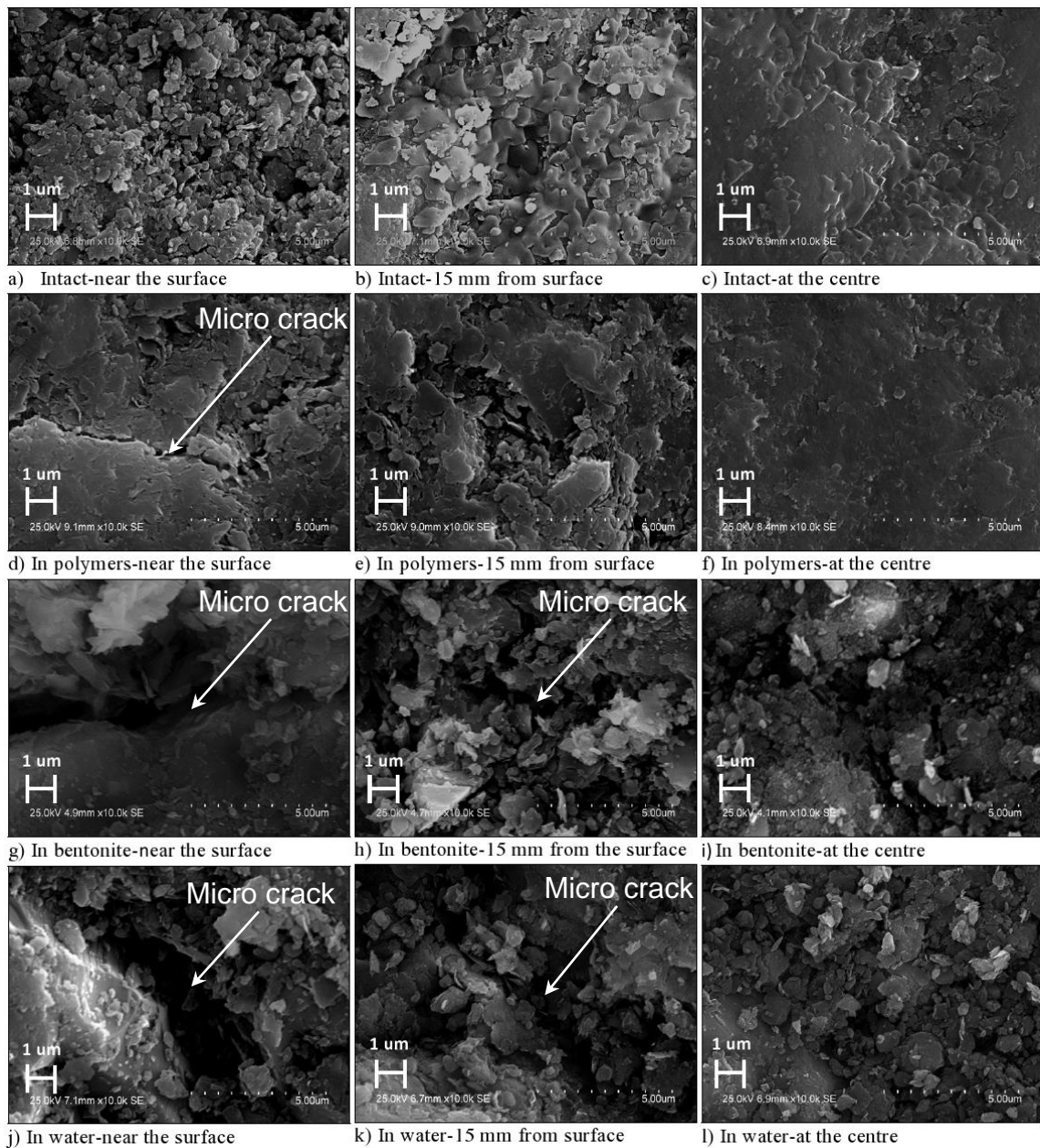


Figure 3.5. Scanning electron microscopy images on horizontal sections of Milton Queenston shale: (a, b, c) intact near outer surface, at 15 mm, and at centre; (d, e, f) after 200 days of soaking in polymer solution; (g, h, i) after 100 days of soaking in bentonite solution; (j, k, l) after 100 days of soaking in water.

3.5.1.3 Cation Exchange Capacity Test

The cation exchange capacity (CEC) generally refers to the quantity of the measured cations that are reversibly adsorbed (expressed as moles of positive charge) per unit weight of mineral (McBride 1994). In the sedimentary rocks that involve clayey minerals, the CEC is representative of the concentration of unfixed cations in the interlayers and surface layers (diffuse layer) of the mineral, which depends on the magnitude of the total layer charge (structural plus surface). The CEC can also be considered as a measure of the replacement of a given cation on a given surface by another cation, which can be of a similar valence (Evangelou 1998). The CEC can be expressed in milliequivalents per 100 grams of powdered rock or soil, where the equivalent represents the cation molecular weight divided by its valence.

The CEC of Milton and Niagara Queenston shales was measured through mixing air-dried powder of Queenston shale specimens with potassium chloride and ammonium acetate solutions of known concentrations, separately. The mixing continued for 24 h to allow for the cations that exist in the specimens to exchange either with the potassium or ammonium cations in the solutions. The amounts of freed cations in the solutions, such as potassium (K^+), sodium (Na^+), magnesium (Mg^{2+}), and calcium (Ca^{2+}), were then measured using a computerized inductively coupled plasma (ICP) analyzer (Vista Pro ICP-OES with a SPS-3 auto-sampler from Varian, Australia). The measured quantities of these cations represent the CEC of Milton and Niagara Queenston shales. In a similar manner, the CEC of the bentonite solution, which was used as the ambient fluid in the swelling tests, was also measured. The CEC was measured for Milton and Niagara Queenston shales before and after the exposure to the bentonite solution, as well as on fresh bentonite solution and bentonite solutions that were in direct contact with Milton and Niagara Queenston shales during the swelling tests. In the following discussions in this chapter and throughout this thesis, the chemistry of the surface water of the Queenston shale will not be considered, as it is beyond the scope of this study.

In aqueous suspension, ions (i.e. cations and anions) may exchange with ions in the bulk solution and they are known as exchangeable cations (Luckham and Rossi,

1999). The exchange in the ions may occur when submerging the Queenston shale in bentonite solution during the time-dependent deformation tests. The average of the exchangeable cations, such as Ca^{2+} , K^+ , Mg^{2+} , and Na^+ , measured in Milton Queenston shale, Niagara Queenston shale, and bentonite solution, are summarized in Table 3.2. Results presented in Table 3.2 indicate that the exchangeable Ca^{2+} cations in both Niagara and Milton Queenston shales found to be more, while the exchangeable Mg^{2+} cations found to be less, after their exposure to the bentonite solution. The exchangeable K^+ and Na^+ cations in Niagara Queenston shale found to be less after the exposure to bentonite solution, and the overall CEC of Niagara Queenston shale found to be higher by 15% compared to its value before the exposure., from 45.13 to 38.3 meq/100 g. In Milton Queenston shale, the exposure to bentonite solution increased the exchangeable Na^+ cations and slightly decreased the exchangeable K^+ cations, and the overall CEC found to be 10.5% higher than its value before the exposure, from 37.56 to 41.51 meq/100 g. The overall CEC of bentonite solution used in free swell test of Niagara Queenston shale found to be higher than its initial value (i.e. for fresh bentonite solution), while the opposite was observed for Milton Queenston shale. These observations reveal that the diffusion of cations during the free swell test was from Niagara Queenston shale to the bentonite solution, but from the bentonite solution to the Milton Queenston shale. This difference in diffusion direction between Niagara Queenston shale and Milton Queenston shale may explain the reversed influence of the bentonite solution on swelling deformations of these shales, as it will be presented in the results of the swelling tests.

3.5.2 Ancillary Tests

3.5.2.1 Determination of Calcite and Dolomite Contents

For each specimen of the free swell test, semi-confined swell test, and null swell test, quantitative determination of calcite and dolomite content was performed using the Chittick apparatus following the procedure described in Dreimanis (1962). For most of the specimens, the calcite and dolomite contents were determined before and after

performing the swelling deformation tests. For each swelling deformation test specimen, an additional specimen was taken from the same rock core to determine the initial calcite and dolomite contents. The specimens were air-dried for 7 days and then were grinded and sieved on a No. 200 ASTM sieve (75 μm). The portions finer than 75 μm were used to perform the gasometric Chittick analyses. This test measures the volume of the evolved CO₂ from the reaction of the hydrochloric acid and carbonates in the specimen. This volume is used to calculate the corresponding percentages of calcite and dolomite in the specimen. The calcite and dolomite contents of most specimens were determined after the swelling deformation tests were terminated to evaluate the exact carbonate contents in each specimen.

The calcite and dolomite contents determined from Chittick apparatus are presented in Tables 3.3 through 3.9 for the Milton and Niagara Queenston shales. From these tables it can be noted that the percentage of calcite content in Milton Queenston shale ranges between 12% and 37%, and the majority of specimens have a calcite content of 20%–25%, while the calcite content of Niagara Queenston shale ranges between 7% and 10.5%. It is quite clear that the percentage of the calcite content in Milton Queenston shale is more than double that in Niagara Queenston shale. The high presence of calcite in Milton Queenston shale forms concretionary masses in the microstructure of these shales, resulting in more resistance to the swelling deformations. This resistance to deformation affects the swelling potential of Milton Queenston shale. The calcite and dolomite contents of both the Milton and Niagara Queenston shales from the Chitteck apparatus were generally consistent with the results of semi-quantitative X-ray diffraction analyses.

3.5.2.2 Moisture Content Determination

The moisture content was determined according to ASTM-D2216 (2010) standard. For each free swell test, semi-confined swell test, and null swell test, the moisture content of the test specimen was calculated before and after performing the swelling deformation test. Moisture content results of Milton and Niagara Queenston shale specimens are presented in Tables 3.3 through 3.9. The natural moisture content of

Milton Queenston shale ranged between 2% and 3%, while the natural moisture content of Niagara Queenston shale was 0.9%–1.6%. Moisture contents of the Milton and Niagara Queenston shales measured before and after the swelling tests were used to determine the pore water salinity of the specimens of both shales. It can be noted from the results of the moisture content of both the Milton and Niagara Queenston shales, measured after performing the swelling tests, that the moisture content generally increased, which indicates occurrence of the osmosis process. However, the magnitude of the increase in the moisture content was not similar in water, polymer solution, and bentonite solution for both shales.

3.5.2.3 Rock Pore Water Salinity Determination

The pore water salinity of the Milton and Niagara Queenston shale specimens was calculated before and after performing the swelling tests following an earlier-established procedure as described by Lee (1988). This was achieved by measuring the electrical conductivity of a suspension of rock powder and water, then correlate the measured value to the corresponding pore water salinity using calibrated NaCl solutions. This is accomplished as follows. A chunk was extracted from the same rock core next to the swelling test specimens for the determination of the initial pore water salinity. The rock chunks were air dried for seven days, and then were pulverized and passed No. 60 ASTM Sieve (250 μm). Obtained from the clay portion ($< 250 \mu\text{m}$), 20 g of QS powder was added to 100 g of distilled water and the mixture was shaken for a minimum of 30 minutes, and was then left for 24 hours to ensure that the pores salts completely dissolved in water. In order to separate the suspended powder from the water, the suspension was centrifuged using a Sorvall RC-5B Refrigerated Super-speed Centrifuge (Du Pont Instruments) running at 7000 rpm for 20 minutes.

The collected clear saline water was poured into a beaker to measure its electrical

conductivity. The water electrical conductivity was measured using a pH/ION 340i meter and a conductivity probe type TetraCon® 325 (WTW Wissenschaftlich-Technische Werkstätten GmbH, Weilheim, Germany). The electrical conductivity of NaCl reference solutions of known NaCl concentration was also measured. The results of the reference solutions were plotted in terms of electrical conductivity versus corresponding salinity and the best straight line fit was established. Employing this best-fit line, the salinity of the specimen saline water was determined considering its electrical conductivity. The determined salinity of the saline water is equivalent to NaCl in grams per liter of water. This salinity was corrected to reflect the exact pore water salinity of the test specimens by considering the volume of the used suspension (0.1 L), the weight of the powdered rock (20 g) and the specimen moisture content. The limitation of this test is that the rock pore water salinity is calculated based on equivalent amount of NaCl in the rock pores.

The pore water salinity of both Queenston shale specimens measured before and after the swelling tests is presented in Tables 3.3 through 3.9. The percentage reduction in pore water salinity of Milton and Niagara Queenston shale specimens, due to the exposure to water, bentonite solution, and polymer solution, during the swelling tests is also presented in Tables 3.3 through 3.9.

In general, the natural pore water salinity of Milton Queenston shale ranged between 71 and 268 g/L, with an average of 100 g/L, while the natural pore water salinity of Niagara Queenston shale specimens ranged between 290 and 435 g/L, with an average of 370 g/L. Results show that the pore water salinity of both Queenston shale specimens increased gradually with depth. The results also demonstrate that the percentage reduction in pore water salinity upon exposure of Milton Queenston shale to the bentonite solution was higher than that for water, and the opposite is true for Niagara Queenston shale. In Milton Queenston shale, the pore water salinity of the specimens

exposed to bentonite decreased by 69%-87% (average of 77%) from its initial (natural) value, while specimens exposed to water experienced 48%-73% reduction in pore water salinity by 48%-73% (average of 65%). For Niagara Queenston shale, exposure to water decreased the pore water salinity by 65%-76%, averaging 70%, while the exposure to bentonite solution decreased it by 48%-55%, averaging 50%. This difference in the behaviour of Milton and Niagara Queenston shales may be attributed to their mineralogical composition and the variation in their cation concentrations. In contrast, the polymer solution reduced the affected pore water salinity of both Queenston shale specimens almost equally and resulted in lower average percentages of 31% and 25% for the Milton and Niagara Queenston shales, respectively.

The presented pore water salinity measurements of Milton and Niagara Queenston shales are consistent with the conditions of swelling of Queenston shale proposed by Lee and Lo (1993). They attributed the swelling of the Queenston shale to the diffusion process of pore water salinity and the osmosis process that occurs between the shale pores and the ambient fluids. The results obtained herein indicate diffusion of pore water salinity of both the Milton and Niagara Queenston shales, manifested in a reduction of pore water salinity, which occurred upon the exposure to water, bentonite solution, and polymer solution. However, the amount of the diffusion varied for the three ambient fluids.

3.5.2.4 Rate of Absorption of Water

The rate of absorption of water for Milton and Niagara Queenston shales was determined following the test method described in ASTM- C1585 (2013) standard. This test method is used to determine the rate of absorption (sorptivity) of water by hydraulic cement concrete through measuring the increase in the mass of a specimen resulting from absorption of water as a function of time when only one surface of the specimen is exposed to water. However, this test method was used in this research to measure the rate of absorption of water, polymer solution, and bentonite solution by Milton and Niagara Queenston shales. The specimens were cut into cylinders 50 mm high. The height and diameter of each specimen was measured to the nearest 0.001 mm. The aim of this test

was to evaluate the rate of absorption of Milton and Niagara Queenston shales under their natural moisture contents to simulate their in-situ conditions. Thus, the specimens were coated with paraffin wax on all surfaces, leaving only the bottom of the specimens uncoated, where they would be in contact with the solution. The weights of the specimens were recorded to the nearest 0.01 g. The specimens were then placed in containers similar to those for the semi-confined and null swell tests. The specimens were seated on a plastic wire cage placed in the containers to have the solutions freely contacts with the bottom of the specimens. Fresh water was then added to one container while bentonite solution and polymer solution were added to the other containers up to the required level. The containers were covered with plastic sheets to prevent evaporation of the solutions. The test was performed in a temperature-controlled room at 10 ± 1 °C. The increase in the specimen's weight was measured in time intervals up to 8 days. The test was repeated in each solution for both of Milton and Niagara Queenston shales to have the average value of the rate of absorption in water, bentonite solution, and in polymers solution, when the successive tests produced consistent results.

The rate of water absorption by Milton and Niagara Queenston shales from the ambient fluids (i.e., water, polymer solution, and bentonite solution) was measured in the first 8 days and the results are presented in Table 3.10. The initial rate of absorption (initial sorptivity, S_i) was measured during the first hours of the test, while the secondary rate of absorption (secondary sorptivity, S_c) was measured during the next 7 days of the test. It can be noted from Table 3-10 that both the initial and secondary sorptivities of Niagara Queenston shale in water were higher than that in the polymer and bentonite solutions. Moreover, the initial and secondary sorptivities of the Milton Queenston shale in the bentonite solution were relatively high, and were higher than that in the water and polymer solution. The secondary sorptivity in the polymer solution was the lowest for both the Niagara and Milton Queenston shales (<0.0005 mm/vs), while the secondary sorptivity of both Queenston shale specimens in water was approximately 0.001 mm/vs. Finally, the secondary sorptivity of Milton Queenston shale in the bentonite solution (0.0011 mm/vs) was higher than the secondary sorptivity of Niagara Queenston shale in the bentonite solution (0.0008 mm/vs). The relative rates of water absorption of both the

Niagara and Milton Queenston shales in the ambient fluids presented in Table 3.10 are consistent with the swelling results that will be presented in the next section.

3.6 RESULTS AND DISCUSSION

3.6.1 Free Swell Test

The results of the free swell tests performed on Milton and Niagara Queenston shales are presented in Tables 3.3 and 3.4, respectively, in terms of vertical swelling potential (VSP) and horizontal swelling potential (HSP). The presented HSP was the average of the swelling potential in two orthogonal horizontal directions, (i.e., x and y directions). The VSP and HSP are defined as the rate of swelling strain of the rock specimen that occurs in the vertical direction and in two orthogonal horizontal directions, respectively, in a log cycle of time upon exposure to ambient fluid, (i.e., water, polymer solution, and bentonite solution) (Lo et al. 1978). The log cycle of time is defined as a time period between day 10 and day 100 from the beginning of the test, where most of swelling strains occur. The strain that occurs in the rock specimen during the first 10 days of the free swell test is not considered an accurate representation of the actual swelling strain of the specimen, and therefore it is disregarded. This period is required for the rock specimen to reach environmental equilibrium between in-situ and laboratory conditions (Lo et al. 1978).

To investigate the influence of the polymer and bentonite concentrations in lubricant fluids used in the micro-tunneling process, free swell tests were performed on Milton Queenston shale specimens submerged in different concentrations of solutions. In this group, a total of 21 free swell test was performed in polymer concentrations of 0.2%, 0.4%, 0.6%, 0.8%, 1.0%, and 1.2%; bentonite concentrations of 2.4%, 2.8%, 3.2%, 3.6%, 4.0%, and 8.0%; in mixed polymer and bentonite solutions; and in fresh water. Results of these free swell tests are presented in Table 3-3. These results demonstrate that as the concentration increased, the swelling strains of Milton Queenston shale decreased, while the opposite, to some extent, was observed for bentonite solutions. The polymer solution with 0.8% concentration, which is used in some micro-tunneling applications, suppressed

the swelling of Milton Queenston shale in both vertical and horizontal directions significantly. Therefore, this polymer concentration was adopted for the remainder of the swelling tests in this research. Similarly, the bentonite solution with 8.0% concentration was adopted in the testing program because it is used in micro-tunneling projects to provide the required lubrication between the Queenston shale and the outer surface of the pipe segments. Using higher concentrations of polymer and bentonite solutions may cause blockage of the slurry pipes and (or) damage to the pumping system.

Results of free swell tests on Milton Queenston shale in water, 0.8% polymer solution, and 8% bentonite solution are presented in Figure 3.6. The slope of the best-fit straight line of the swelling strain versus log time curves in the vertical and horizontal directions during day 10 to day 100 represents VSP and HSP, respectively. Figure 3.6

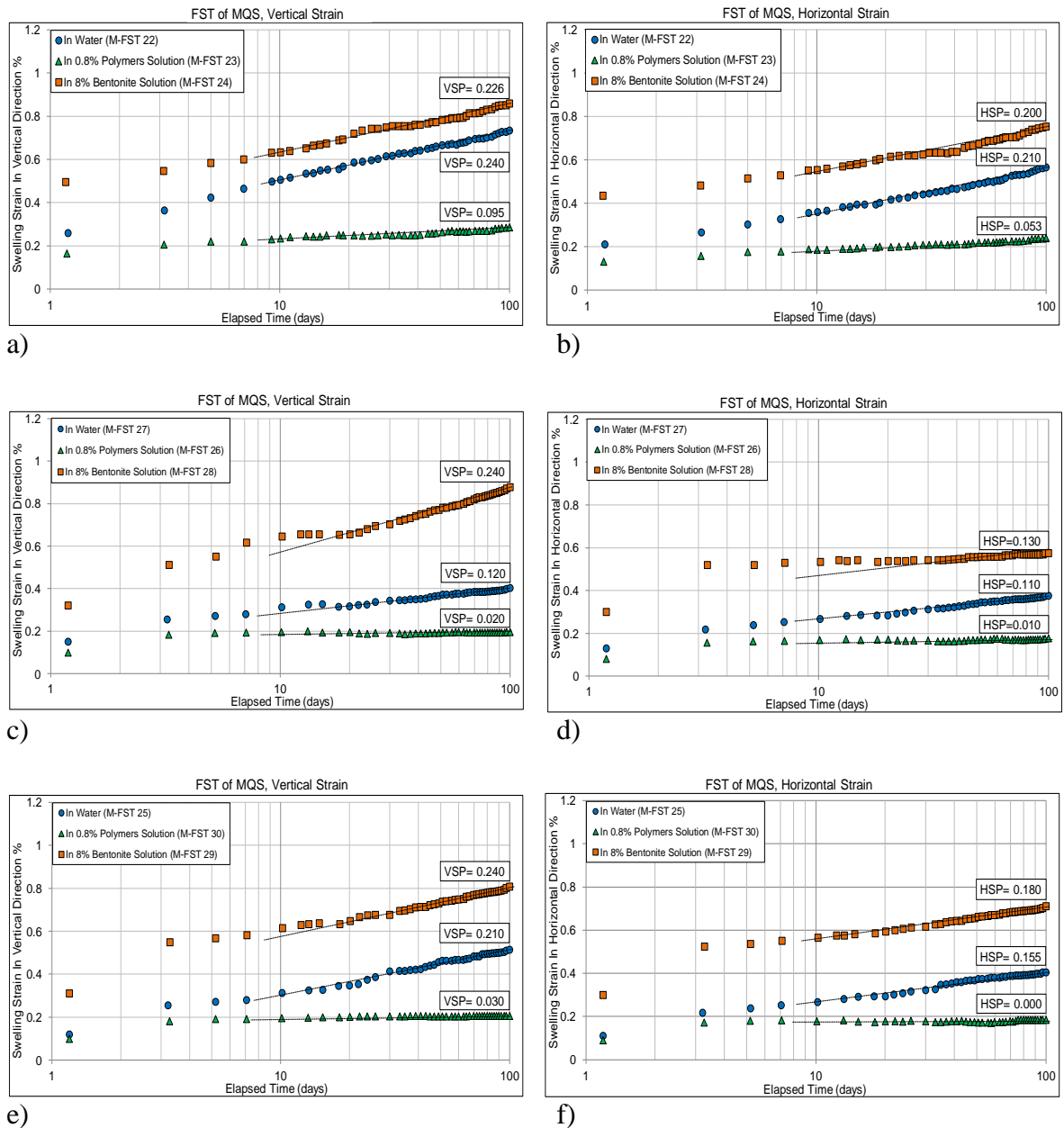


Figure 3.6. Free swell test on Milton Queenston shale (MQS) in water, polymer and bentonite solutions (from M-FST22 TO M-FST30): (a, c, e) vertical swelling strains, (b, d, f) horizontal swelling strains.

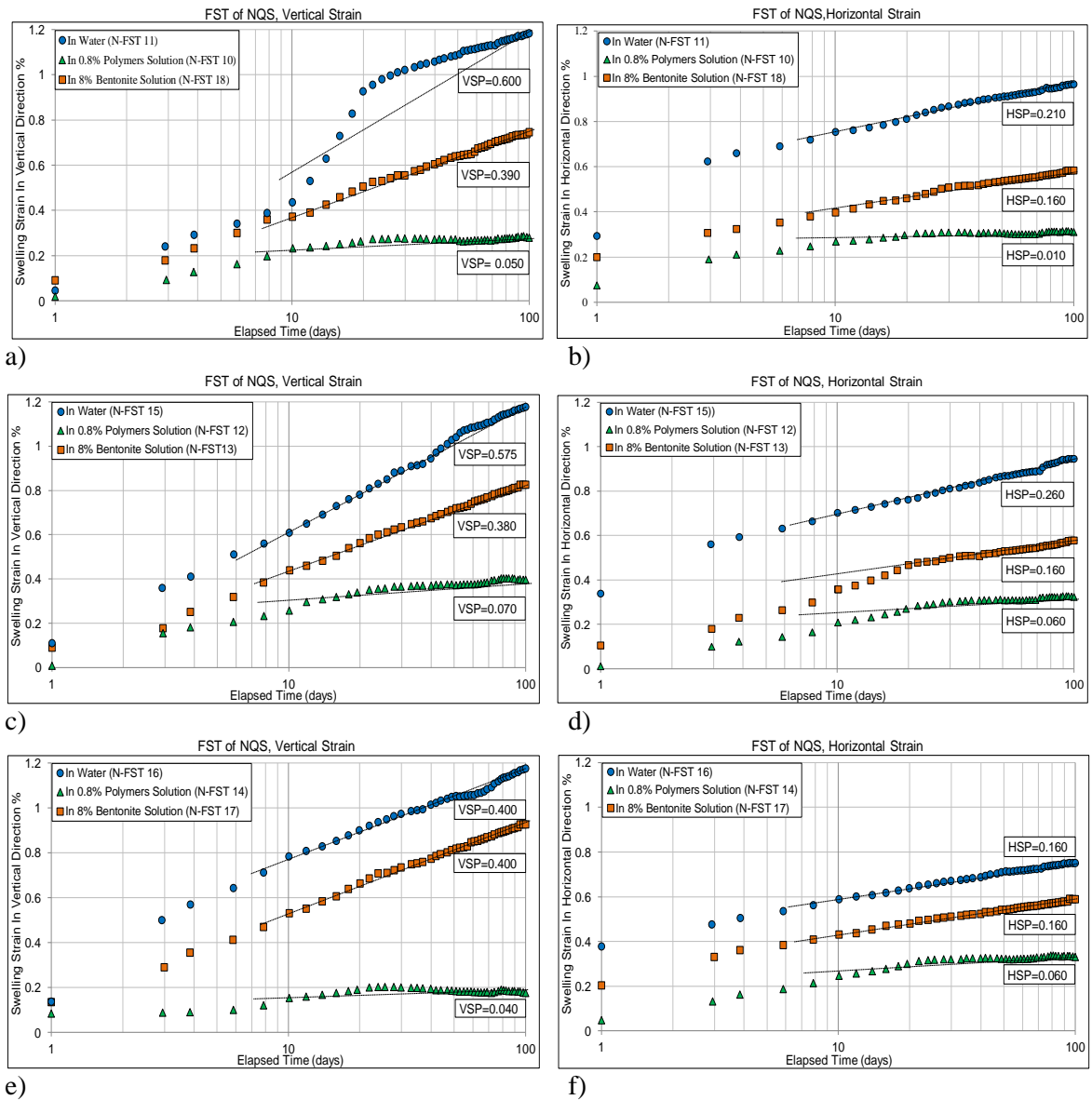


Figure 3.7. Free swell test on Niagara Queenston shale (NQS) in water, polymer and bentonite solutions (from N-FST10 TO M-FST18): (a, c, e) vertical swelling strains; (b, d, f) horizontal swelling strains.

shows that the swelling of Milton Queenston shale in the polymer solution was significantly reduced in both directions in comparison to its swelling in fresh water. The average VSP of Milton Queenston shale in water was 0.19% strain / log cycle of time, while it was 0.065% strain / log cycle of time in the polymer solution, i.e., 66% suppression of swelling strains in the vertical direction. Similarly, the average HSP of Milton Queenston shale in water was 0.156% strain / log cycle of time, while the HSP of Milton Queenston shale in the polymer solution was only 0.027% strain / log cycle of time, i.e., 83% suppression of swelling strains in the horizontal direction, which suggests that the polymer solution is more effective in suppressing swelling strain of Milton Queenston shale in the horizontal direction. This finding is consistent with the observation made from SEM images that the generated micro-cracks in the horizontal sections were relatively smaller than those in the vertical sections. In contrast, the average VSP of Milton Queenston shale in the bentonite solution was 0.235% strain / log cycle of time, which means an increase of 24% over the average VSP in water, and the HSP of Milton Queenston shale in the bentonite solution was 0.17% strain / log cycle of time, which represents an increase of 10% over that in water. This impact of bentonite solution on swelling of Milton Queenston shale has to be considered when adopting this fluid as a lubricant for micro-tunneling projects in Milton Queenston shale. The SEM images explain the behaviour of Milton Queenston shale in the free swell tests in bentonite solution. These images demonstrate that both the size and depth of micro-cracks of the Milton Queenston shale specimen increased after being exposed to the bentonite solution.

Results of the free swell test performed on Niagara Queenston shale are presented in Table 3.4 and Figure 3.7. The presented results reveal that water resulted in the highest swelling potential in both vertical and horizontal directions, in comparison to polymer and bentonite solutions. In the specimens that were collected from borehole 1 (N-FST10 to N-FST18), the average VSP of Niagara Queenston shale in water was 0.525% strain / log cycle of time; while it was 0.39% strain / log cycle of time in the bentonite solution and only 0.053% strain / log cycle of time in the polymer solution, with a reduction of 26% and 90%, respectively. In the horizontal direction, the average HSP of Niagara

Queenston shale in water was 0.21% strain / log cycle of time; while it was 0.16% strain / log cycle of time in the bentonite solution and only 0.043% strain / log cycle of time in the polymer solution, with a reduction of 24% and 80%, respectively. These results demonstrate that both polymer and bentonite solutions were efficient in suppressing the swelling strains of Niagara Queenston shale in both vertical and horizontal directions in comparison to the swelling strains in water. However, the polymer solution was superior in suppressing the swelling deformation of Niagara Queenston shale. For the specimens that were collected from borehole 2 (N-FST1 to N-FST9), the average VSP of Niagara Queenston shale in water was 0.31% strain / log cycle of time; while it was 0.23% strain / log cycle of time and 0.06% strain / log cycle of time in the bentonite and polymer solutions, i.e., a reduction of 26% and 81%, respectively. In addition, the average HSP of Niagara Queenston shale in water was 0.17% strain / log cycle of time; while it was 0.163% strain / log cycle of time and 0.047% strain / log cycle of time in the bentonite and polymer solutions, i.e., reduction of 45% and 72%, respectively.

The above results clearly show that the swelling strains of both the Milton and Niagara Queenston shales in water, polymer solution, and bentonite solution are anisotropic, with the vertical strain (i.e., perpendicular to rock bedding) higher than the horizontal strain (i.e., parallel to rock bedding). It can also be concluded that the polymer solution significantly reduced the swelling deformations of both the Milton and Niagara Queenston shales, while the bentonite solution was less efficient in reducing the swelling strains of Niagara Queenston shale, and resulted in a slight increase in the deformation strains of Milton Queenston shale. This finding is of significance. The polymer solution can be used as an effective means to reduce and control the swelling strain of Queenston shale and to mitigate the time-dependent effects of these shales on the micro-tunneling machine and on the installed pipe. It has to be noted that time is one of the limitations of this test. The free swell test is performed in 100 days and its result is assumed to be valid for longer time. The other limitation is the size of test specimen compared to the size of the rock in-situ, which may cause a difference in the swelling behavior of the rock in both cases.

3.6.2 Semi-Confined Swell Test

To investigate the influence of applied pressure on the swelling strains of Milton and Niagara Queenston shales in water, polymer solution, and bentonite solution, semi-confined swell tests were performed. Each tested specimen was subjected to a constant pressure in one direction, while it was submerged in the solution, and the swelling strain in the same direction of the applied pressure was continuously recorded for 100 days. For Milton Queenston shale, each test was repeated three times and the average value of the swelling potential for each corresponding applied pressure was calculated. Due to the limited supply of available Niagara Queenston shale samples, only one specimen from borehole 1 was tested for each corresponding applied pressure in both directions. Results of the semi-confined swell tests are presented in Tables 3.5 through 3.7 and in Figures 3.8 and 3.9 for the Milton and Niagara Queenston shales, respectively. Figures 3.8 and 3.9 show that, as expected, the swelling strain of both the Milton and Niagara Queenston shales in both directions and in all fluids is a function of the applied pressure. As the applied pressure increased, the VSP and the HSP decreased gradually from their values in the free swell tests.

The swelling occurs in steps in the semi-confined swell test as indicated in the presented figures. In the semi-confined swell test, the sample is subjected to a specified pressure applied in the direction of swelling measurement. This pressure prevents the gradual swelling of the sample as it is the case in the free swell test. When the generated osmotic pressure in the rock pores exceeds the applied pressure, the swelling occurs forming a sudden jump in the swelling curve. On the other hand, this swelling provides relative relief to the osmotic pressure in the rock pores dropping its value below the applied pressure. At this stage the sample shows no increase in its swelling in the direction of the applied load. However, in the presence of water, the osmosis process continues causing an increase in the swelling pressure of the sample. When the swelling pressure exceeds the applied pressure, the swelling occurs causing another jump in the swelling curve.

Moreover, the general trends observed in free swell tests for both the Milton and Niagara Queenston shales are also observed in the semi-confined swell tests: Niagara Queenston

shale exhibited higher VSP and HSP than Milton Queenston shale; the polymer solution significantly reduced the swelling strains in both the Milton and Niagara Queenston shales, and the bentonite solution had opposite effects on the swelling strains of the Milton and Niagara Queenston shales.

Under an applied pressure of 0.01 MPa, the water resulted in a VSP of 0.18% strain / log cycle of time and HSP of 0.13% strain / log cycle of time in Milton Queenston shale, while in Niagara Queenston shale it resulted in a VSP of 0.515% strain / log cycle of time and HSP of 0.205% strain / log cycle of time. Under the same applied pressure of 0.01 MPa, the polymer solution reduced the VSP and HSP of Milton Queenston shale by 64% and 85%, respectively, and reduced the VSP and HSP for Niagara Queenston shale by 26% and 80%, respectively. As the applied pressure varied from 0.01 to 0.05, 0.1, and 1.0 MPa in Milton Queenston shale, the suppression effect of the polymer solution on HSP was more evident and reached 100% with 0.7 MPa, while VSP was reduced by 54%, 60%, and 25%, respectively. In Niagara Queenston shale, the polymer solution reduced the HSP by 83% under applied pressure of 0.3 MPa, while it reduced the VSP by 91% under applied pressure of 0.1 MPa. In contrast, the bentonite solution increased the VSP and HSP of Milton Queenston shale by 22% and 8%, respectively, while it reduced the VSP and HSP by 42% and 24%, respectively, under applied pressure of 0.01 MPa.

These results clearly show that swelling strains are anisotropic with respect to the rock bedding and they depend strongly on the applied pressure. The polymer solution significantly suppressed the swelling strains of both shales in both orthogonal directions, under variable amounts of applied pressure. The bentonite solution was less efficient in suppressing the swelling strains of Niagara Queenston shale, but increased the swelling strains of Milton Queenston shale under variable amounts of applied pressure. This test has same limitations of the free swell test in addition to the lack of confinement of the sample in the transverse direction of the measured swelling.

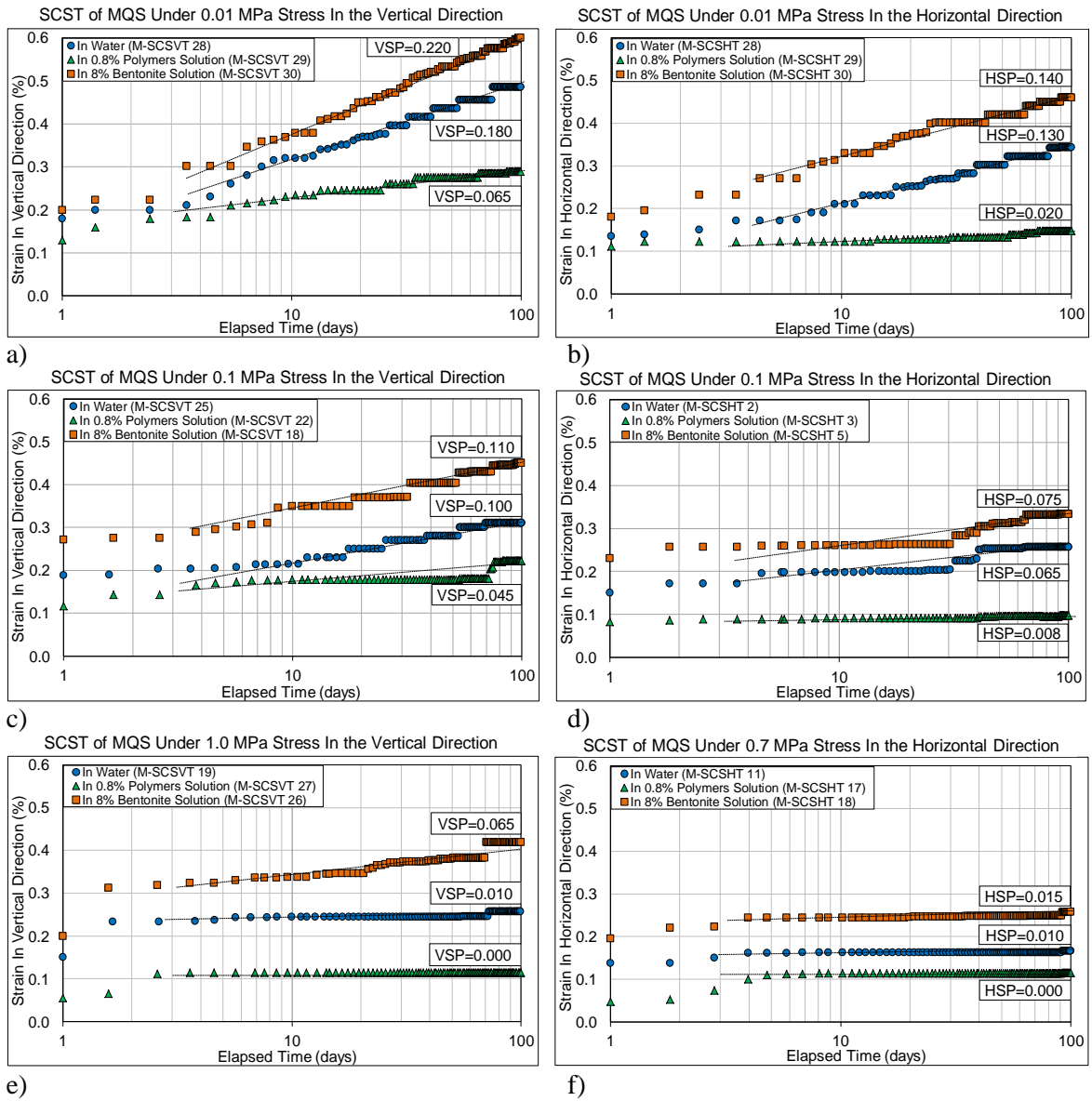


Figure 3.8. Semi-confined swell tests on Milton Queenston shale (MQS) in water, polymer and bentonite solutions: (a, c, e), vertical swelling strains under stress of 0.01, 0.1 & 1.0 MPa; (b, d, f) horizontal swelling strains under stress of 0.01, 0.1 and 0.7 MPa.

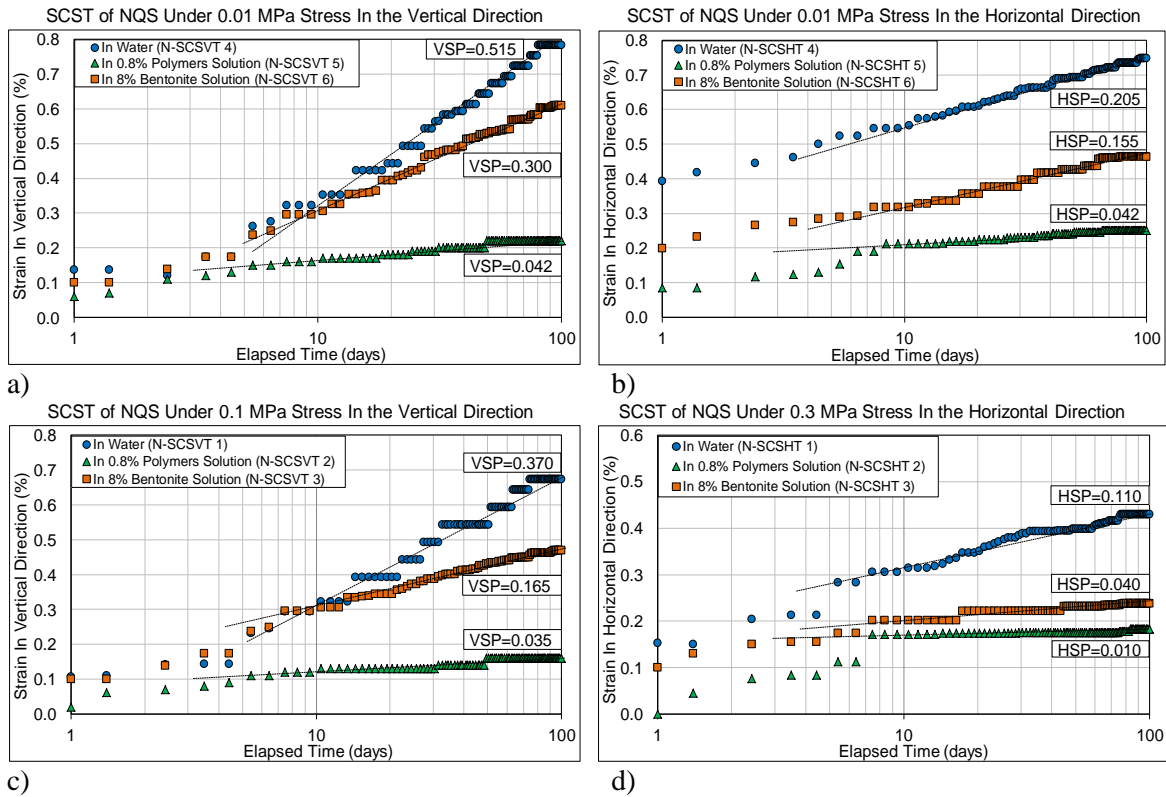


Figure 3.9. Semi-confined swell tests on Niagara Queenston shale (NQS) in water, polymer and bentonite solutions: (a, c) vertical swelling strains under stress of 0.01 & 0.1 MPa; (b, d) horizontal swelling strains under stress of 0.01, & 0.3 MPa.

3.6.3 Null Swell Test

Results of the null swell tests performed on Milton and Niagara Queenston shales from borehole 1 are presented in Tables 3.8 and 3.9 and in Figures 3.10 and 3.11, respectively. The shale specimens were prevented from swelling in one direction, while they were submerged in the solution, by adding gradual loads in the same direction through the apparatus. The tests were terminated when the specimens reached the equilibrium stage (i.e., no more load was required to prevent their swelling). The load at that stage divided by the cross-sectional area of the specimen is the suppression pressure, which was termed as “the critical stress (σ_c)” by Lo and Hefny (1996).

Figures 3.10 and 3.11 show that the average null swell pressure in water was 2.14 and 2.06 MPa in the vertical and horizontal directions, respectively, for Milton Queenston shale and was 2.07 and 1.59 MPa, respectively, for Niagara Queenston shale. Figures 3.10 and 3.11 also show general trends consistent with those observed in the free swell tests and the semi-confined swell tests: the suppression pressures of both the Milton and Niagara Queenston shales in the polymer solution were the least among other fluids, and bentonite solution had opposite effects on the suppression pressures of the Milton and Niagara Queenston shales.

In comparison to water, the polymer solution effectively reduced the average null swell pressure in both the Milton and Niagara Queenston shales by 30% and 27%, and by 28% and 51% in the vertical and horizontal directions, respectively. In contrast, the null swell pressures of Milton Queenston shale in the bentonite solution were greater than that in water, while the opposite was observed for Niagara Queenston shale. Null swell pressures of Milton Queenston shale in the bentonite solution increased by 10% and 9% in the vertical and horizontal directions, respectively, compared to water, while for Niagara Queenston shale they decreased by 13% and 29%. Finally, it is noted that although the swelling strains of Niagara Queenston shale were, in general, greater than that in Milton Queenston shale in both the free swell tests and semi-confined swell tests, the average null swell pressure in Niagara Queenston shale was less than that in Milton Queenston shale in all fluids used. Same limitations of the semi-confined swell test are applicable for the null swell test.

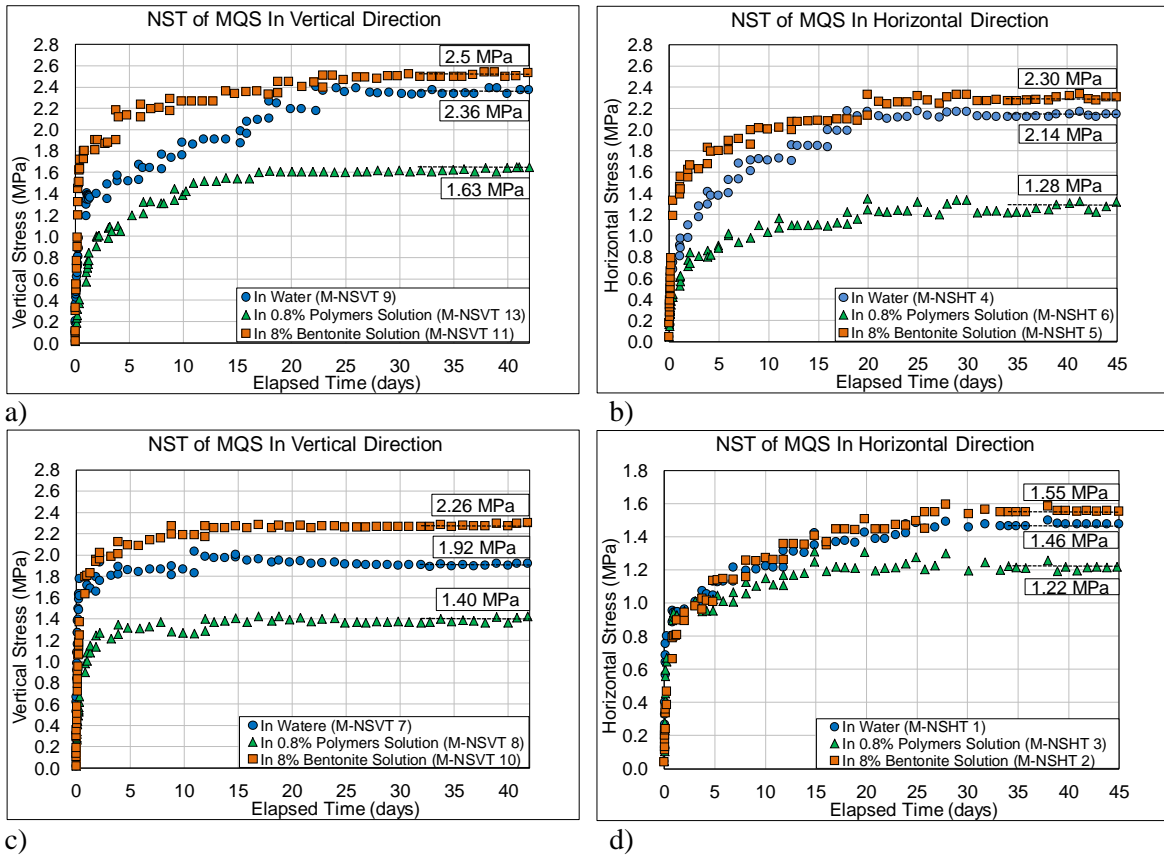


Figure 3.10. Null-swell tests on Milton Queenston shale (MQS) in water, polymer and bentonite solutions: (a, c) null-swell stress in the vertical direction; (b, d) null-swell stress in the horizontal direction.

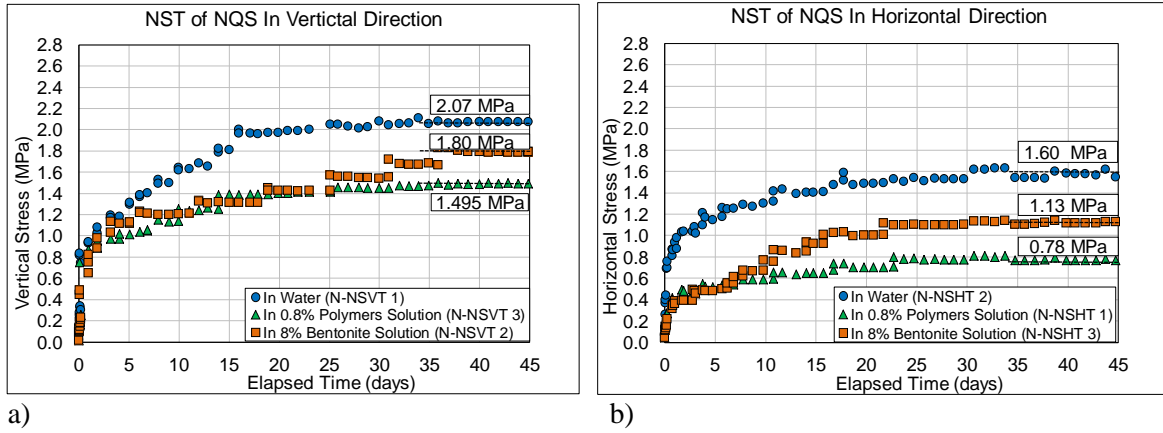


Figure 3.11. Null-swell tests on Niagara Queenston shale (NQS) in water, polymer and bentonite solutions: (a) null-swell stress in the vertical direction; (b) null-swell stress in the horizontal direction.

3.7 CONSTRUCTION OF SWELLING ENVELOPES

Results of the swelling test program in this research can be summarized in swelling envelopes defined in the model proposed by Lo and Hefny (1996). In this model, the average free swell potentials (VSP and HSP), and the average of VSP and HSP under different applied pressures are plotted on the y-axis versus the applied pressure in a log scale on the x-axis. The average null swell pressures in the vertical and horizontal directions, where the swell was completely suppressed, are also presented in this model. The average values of free swell tests, semi-confined swell tests, and null swell tests are summarized and presented in Table 3.11. For Milton Queenston shale, the average was calculated from tests performed on the adopted ambient fluids (i.e., water, 0.8% polymer solution, and 8% bentonite solution). Other tests performed on variable concentrations of polymer and bentonite solutions were not included in calculating the average. For Niagara Queenston shale, only test results from borehole 1, where there were enough samples to perform the three types of swelling tests, were considered in calculating the average. Based on these average values, the swelling envelopes of Milton and Niagara Queenston shales were constructed in both vertical and horizontal directions, and are presented in Figures 3.12 and 3.13, respectively. In these figures, the horizontal lines represent the average swell potentials from the free swell tests, while the inclined lines represent the swell potentials under different values of applied pressure (suppression pressure). The x-intercepts represent the average null-swell pressures, defined by Lo and Hefny (1996) as the critical stresses (σ_c). The critical stress represents the minimum stress that is required to suppress the swelling strain completely in the direction of the applied stress. Intercepts of the horizontal line and inclined line represent the threshold stress (σ_{th}), as defined in the aforementioned model. The threshold stress represents the minimum required stress to be applied on the rock to initiate the suppression influence on the swelling deformation in the same direction of the applied stress. The stresses that lie between the threshold stress and critical stress represent the required stresses for partial suppression of the swelling deformation of the tested rock.

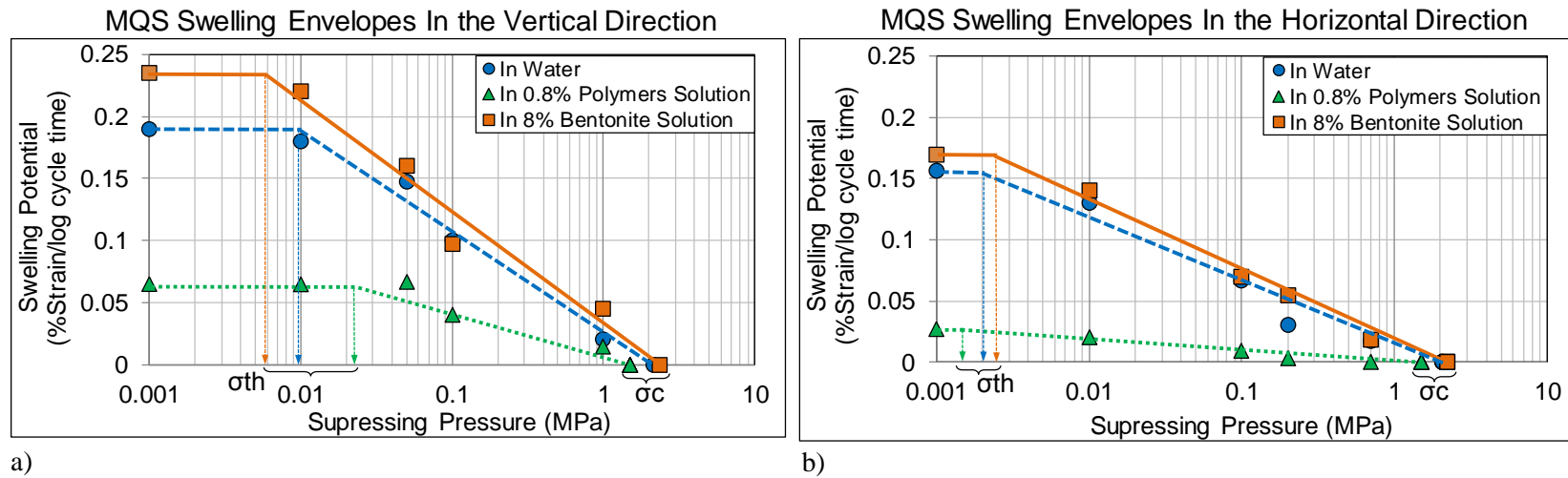


Figure 3.12. Swelling envelopes of Milton Queenston shale (MQS): (a) in the vertical direction; (b) in the horizontal direction.

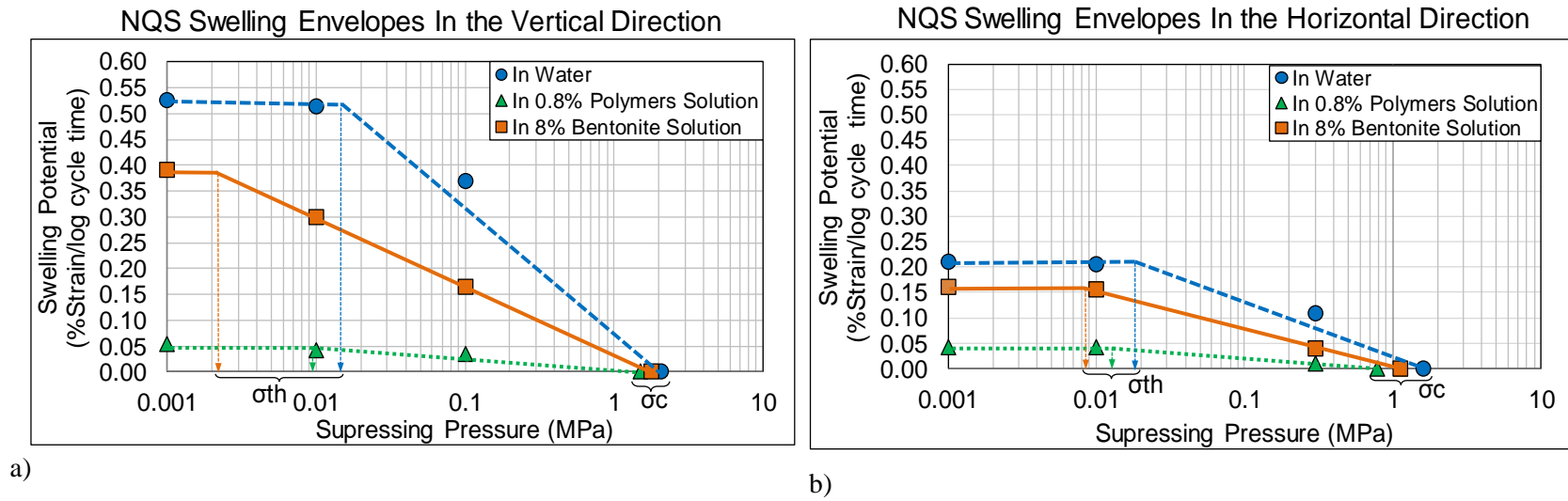


Figure 3.13. Swelling envelopes of Niagara Queenston shale (NQS): (a) in the vertical direction; (b) in the horizontal direction.

The swelling envelopes of the Milton and Niagara Queenston shales displayed in Figures 3.12 and 3.13, respectively, demonstrate that the polymer and bentonite solutions can have significant influence on the swelling behaviour of these shales in comparison to their swelling behaviour in water. As part of the design process of buried structures in swelling rocks, such as the Milton and Niagara Queenston shales, water is usually used as the only ambient fluid in the experimental program to develop the swelling envelopes of these rocks, and to derive the consequent design parameters. Findings of the current study clearly show that using fluid other than water can significantly change the shape of the swelling envelopes, and hence change the derived design parameters. The polymer solution effectively suppressed the swelling strains of both the Milton and Niagara Queenston shales, and thus significantly reduced the swelling envelopes of both shales. The bentonite solution was less effective than the polymer solution in suppressing the swelling strains of Niagara Queenston shale, while it negatively increased the swelling strains of Milton Queenston shale. In general, it can be noted that the variation in threshold stresses for the three fluids used in the horizontal swelling envelopes was smaller than the variation in the threshold stresses of the vertical envelopes. This means that Milton and Niagara Queenston shales are more susceptible to the type of fluids in the vertical direction than in the horizontal direction under different applied suppressing stresses.

3.8 SUMMARY AND CONCLUSIONS

A comprehensive testing program was performed on Queenston shale from the Milton and Niagara regions in southern Ontario to investigate the influence of lubricant fluids, such as polymers and bentonite solutions used in the micro-tunneling process, on the swelling behaviour of these shales. Water, which is the standard ambient fluid for swell tests, was also used in these tests for comparison purposes with the lubricant fluids. The testing program was performed utilizing the free swell test, semi-confined swell test, and the uniaxial null swell test, which were developed at the University of Western Ontario by Lo and co-workers between 1978 and 1999. In the testing program, 48 free

swell tests, 72 semi-confined swell tests, and 24 null swell tests (in addition to complementary tests) were performed on both of the tested shales. To obtain the swelling parameters of Queenston shale in lubricant fluids used in the micro-tunneling process, the standard ambient fluid used in swelling tests (i.e., water) was replaced with lubricant fluids (i.e., polymer solution and bentonite solution) in this research. Swelling parameters (i.e., vertical and horizontal swelling potentials, threshold pressure, and critical pressure) in lubricant fluids and in water were derived accordingly. The suggested mechanism of the swelling behavior due to lubricant fluids of Queenston shale can be summarized as follows. Both the polymer solution and bentonite solution create coating layers on the outer surface of rock and reduce osmosis water molecule penetration deep into the rock. However, the thickness of these layers is different. Polymers tend to penetrate deeper into the surface micro-cracks and tend to accumulate in a thicker layer compared to bentonite. This makes the polymer solution more efficient than bentonite in preventing more water molecule penetration, and hence causes less swelling of Queenston shale.

The swelling envelopes in the vertical and horizontal directions for both Milton and Niagara Queenston shales were developed. From the results of the testing program performed, the following conclusions can be drawn:

- 1) Lubricant fluids used in the micro-tunneling process, such as polymer and bentonite solutions, can cause a considerable influence on the swelling behaviour of Milton and Niagara Queenston shales.
- 2) In comparison to water, the polymer solution effectively reduced the swelling strains of Milton and Niagara Queenston shales in both vertical and horizontal directions, with greater effect in the horizontal direction. The percentage of reduction in the swelling strains could be as high as 90%.
- 3) The bentonite solution was less efficient than the polymer solution in reducing the swelling strains of Niagara Queenston shale, by 24%–26% in comparison to water, and caused an increase in the swelling strains of Milton Queenston shale by 10%-24%.

- 4) The swelling behaviour of Milton and Niagara Queenston shales in lubricant fluids, as in the case of water, is anisotropic with respect to the rock bedding, with the swelling strain in the vertical direction, in general, higher than in the horizontal direction.
- 5) The reverse influence of the bentonite solution on the swelling strain of Milton and Niagara Queenston shales may be attributed to the movement of cations from the shale to the bentonite solution and vice versa. However, more detailed investigation needs to be performed.
- 6) The stress-dependent behaviour of both Milton and Niagara Queenston shales in lubricant fluids can be represented by the Lo and Hefny (1996) model.

It appears that the swelling behaviour of swelling rocks in lubricant fluids can be significantly different from their behaviour in water, and therefore it is recommended to extend this research to include more types of swelling rocks.

3.9 REFERENCES

- Al-Maamori, H.M.S., El Naggar, M.H., and Silvana, M. 2014. A compilation of the geo-mechanical properties of rocks in southern Ontario and the neighbouring regions. *Open Journal of Geology*, **4**: 210-227.
- ASTM. 2008. Standard practices for preparing rock core as cylindrical test specimens and verifying conformance to dimensional and shape tolerances. ASTM standard D4543-08. ASTM International, West Conshohocken, Pa.
- ASTM. 2010. Standard test methods for laboratory determination of water (moisture) content of soil and rock by mass. ASTM standard D2216-10. ASTM International, West Conshohocken, Pa.
- ASTM. 2013. Standard test method for measurement of rate of absorption of water by hydraulic-cement concretes. ASTM standard C1585-13. West Conshohocken, Pa.
- Bowen, C.F.P., Hewson, F.I., MacDonald, D.H., and Tanner, R.G. 1976. Rock squeeze at Thorold Tunnel. *Canadian Geotechnical Journal*, **13**(2): 111-126.

- Das, B.M. 1998. Principles of geotechnical engineering. 4th ed. International Thomson Publishing Inc., London.
- Dreimanis, A. 1962. Quantitative gasometric determination of calcite and dolomite by using Chittick apparatus. *Journal of Sedimentary Petrology*, **32**(3): 520-529.
- Einstein, H.H., and Bischoff, N. 1975. Design of tunnels in swelling rocks. In *Proceedings of the 16th Symposium on Rock Mechanics*, University of Minnesota, Minneapolis, Minn. pp. 185-197.
- Evangelou, V.P. 1998. Environmental soil and water chemistry: principles and applications. John Wiley & Sons, Inc., Toronto, Ont.
- Hawlder, B.C., Lee, Y.N., and Lo, K.Y. 2003. Three-dimensional stress effects on time-dependent swelling behaviour of shaly rocks. *Canadian Geotechnical Journal*, **40** (3): 501-511.
- Hefny, A., Lo, K.Y., and Huang, J.A. 1996. Modelling of long-term time-dependent deformation and stress-dependency of Queenston shale. In *Proceedings of Canadian Tunnelling 1996*. The Tunnelling Association of Canada. pp. 115-146.
- Hein, F.J., and Longstaffe, F.J. 1983. Geotechnical, sedimentological and mineralogical investigations in Arctic Fjords. In *Sedimentology of Arctic Fjords Experiment: HU 82-031m Data Report I*. Compiled by J.P.M. Syvitski and C.P. Blakeney. *Can. Data Rep. Hydrogr. Ocean Sci.* 12. pp. 11.1-11.158.
- Huang, J.A. 1993. Long-term deformation behaviour of Queenston Shale. M.Sc. thesis, Western University, London, Ont.
- Lee, Y.N. 1988. Stress-strain-time relationship of Queenston shale. Ph.D. thesis, Civil and Environmental Engineering Department, The University of Western Ontario, London, Ont.

- Lee, Y.N., and Lo, K.Y. 1993. The swelling mechanism of Queenston shale. In Proceedings of Canadian Tunnelling 1993. The Tunnelling Association of Canada. pp. 75-97.
- Lo, K.Y. 1978. Regional distribution of in situ horizontal stresses in rocks of Southern Ontario. Canadian Geotechnical Journal, **15**(3): 371-381.
- Lo, K.Y., and Hefny, A. 1996. Design of tunnels in rock with long-term time-dependent and nonlinearly stress-dependent deformation. In Proceedings of Canadian Tunnelling 1996 The Tunnelling Association of Canada, Toronto, Ont. pp. 179-214.
- Lo, K.Y., and Hefny, A.M. 1999. Measurements of residual expansion rates result from alkali-aggregate reaction in existing concrete dams. ACI Materials Journal, **96** (3): 339-345.
- Lo, K.Y., and Lee, Y.N. 1990. Time-dependent deformation behaviour of Queenston shale. Canadian Geotechnical Journal, **27** (4): 461-471.
- Lo, K.Y., and Yuen, C.M.K. 1981. Design of tunnel lining in rock for long term time effects. Canadian Geotechnical Journal, **18** (1): 24-39.
- Lo, K.Y., Lee, C.F., Palmer, J.H.L., and Quigley, R.M. 1975. Stress relief and time-dependent deformation of rocks. Final Report, National Research Council of Canada Special Project No. 730., Faculty of Engineering Science, The University of Western Ontario, London, Ont.
- Lo, K.Y., Wai, R.S.C., Palmer, J.H.L., and Quigley, R.M. 1978. Time-dependent deformation of shaly rocks in southern Ontario. Canadian Geotechnical Journal, **15** (4): 537-547.
- Lo, K.Y., Lukajic, B., and Ogawa, T. 1984. Interpretation of stress-displacement measurements. In Proceedings of Geotech '84 - Tunnelling in Soil and Rock. ASCE. pp. 128-155.

- Lo, K.Y., Cooke, B.H., and Dunbar, D.D. 1987. Design of buried structures in squeezing rock in Toronto, Canada. *Canadian Geotechnical Journal*, **24** (2): 232-241.
- Luckham, P.F., Rossi, S., 1999. The colloidal and rheological properties of bentonite suspensions. *Advances in Colloid and Interface Science*, 82:43-92.
- McBride, M.B. 1994. *Environmental chemistry of soils*. Oxford University Press, Inc., New York.
- Moore, D.M., and Reynolds, R.C., Jr. 1989. *X-ray diffraction and the identification and analysis of clay minerals*. Oxford University Press, Oxford, New York.
- Morison, W.G. 1957. Rock squeeze investigation. Ontario Hydro Research Division Report No. 57-13. Toronto Power Generating Station, Ontario Hydro Research Division, Toronto, Ont.
- Wai, R.S.C. 1977. Time-dependent deformation of some shaly rocks. M.Sc. thesis, The University of Western Ontario, London, Ont.
- Zhang, G., Germaine, J.T., Martin, R.T., and Whittle, A.J. 2003. A simple sample mounting method for random powder x-ray diffraction. *Clays and Clay Minerals*, **51**(2): 218-225.

Table 3.1. Percentage minerals of Milton and Niagara Queenston shales from x-ray diffraction analyses

Milton Queenstown shale								
Sample Depth (m)	Chlorite (%)	Illite (%)	Kaolinite (%)	Quartz (%)	Feldspar (%)	Calcite (%)	Dolomite (%)	Pyrite (%)
16.57	0.8	16.5	2.4	45.5	4.7	20.9/25.1*	6.2 / 2.8*	3.0
21.16	0.6	11.8	1.1	47.4	3.3	28.2/21.9*	3.9 / 3.0*	3.7
25.14	1.0	16.8	1.7	43.1	5.9	19.3/21.4*	9.2 / 2.9*	3.0
31.04	1.1	10.4	1.3	47.4	6.7	24.9/24.1*	6 / 7.9*	2.2
Percentage Range	0.8-1.1	10.4-6.8	1.1 - 2.4	43.1-47.4	3.3 - 6.7	19.3-28.2	3.9 - 9.2	2.2-3.7
Niagara Queenston shale								
Sample Depth (m)	Chlorite (%)	Illite (%)	Kaolinite (%)	Quartz (%)	Feldspar (%)	Calcite (%)	Dolomite (%)	Pyrite (%)
6.1	1.6	23.0	1.8	56.7	2.8	8.1 / 8.9*	2.4 / 2.3*	3.6
11.2	1.4	16.3	1.9	59.7	5.5	9.4 / 9.5*	3.2 / 2.3*	2.6
Percentage Range	1.4-1.6	16.3-3.0	1.8-1.9	56.7-59.7	2.8-5.5	8.1-9.4	2.4-3.2	3.6

Note: * value obtained from Chittick apparatus (gasometric analysis)

Table 3.2. Cation exchange capacity of Milton and Niagara Queenston shales and bentonite solution

Cation Exchange Capacity (CEC) In (meq/100 g)	CEC Ca ²⁺		CEC K ⁺		CEC Mg ²⁺		CEC Na ⁺		CEC Total	
	Before	After	Before	After	Before	After	Before	After	Before	After
Niagara Queenston Shale (NQS)	30.5	31.275	2.3	2.12	1.745	1.39	10.585	3.515	45.13	38.3
Milton Queenston Shale (MQS)	31.98	33.185	1.89	1.92	1.965	1.72	1.725	4.685	37.56	41.51
Fresh Bentonite Solution	2.83	-	0.2	-	0.585	-	6.765	-	10.38	-
Bentonite Solution After NQS Test	-	4.84	-	0.22	-	0.97	-	5.97	-	12
Bentonite Solution After MQS Test	-	4.11	-	0.15	-	0.85	-	5.15	-	10.26

Table 3.3. Free swell test and complementary tests results of Milton Queenston shale

Specimen No.	Ambient Fluid	Depth (m)	Calcite Content (%)	Dolomite Content (%)	Moisture Content Before Test (%)	Moisture Content After Test (%)	Pore Salinity Before Test (g/L)	Pore Salinity After Test (g/L)	Percent Decrease In Pore Salinity (%)	Mass Density (g/cm ³)	Horizontal Swelling Potential (% strain/ log cycle of time)	Vertical Swelling Potential (% strain/ log cycle of time)
M-FST 4	Air	20.40	22.5	2.3	2.00	2.31	75.0	-	-	2.601	0.04	0.025
M-FST 16	Water	20.63	22.8	2.1	2.92	3.58	73.7	21.9	70	2.629	0.16	0.2
M-FST 21	Water	20.75	16.5	2.5	2.00	2.67	75.0	28.0	63	2.623	0.145	0.18
M-FST 22	Water	30.02	15	3.9	2.84	3.51	149.7	76.2	49	2.623	0.21	0.24
M-FST 25	Water	26.31	30.3	1.8	19.30	3.73	81.7	42.2	48	2.633	0.155	0.21
M-FST 27	Water	26.59	30.3	1.8	2.55	3.20	93.1	46.6	50	2.626	0.11	0.12
M-FST 1	1% bentonite & 0.1% polymers	15.98	24.3	0.7	2.91	3.41	86.0	40.3	53	2.405	0.1 *	0.14 *
M-FST 2	1% bentonite & 0.2% polymers	16.15	22.8	2.1	2.10	2.39	95.2	39.4	59	2.616	0.07 *	0.08 *
M-FST 3	1% bentonite & 0.3% polymers	16.31	23.0	1.8	2.05	2.38	73.2	0.1	100	2.617	0.09 *	0.1 *
M-FST 5	2.4% Bentonite Solution	17.83	22.8	2.1	2.70	3.39	83.3	25.3	70	2.656	0.03 *	0.02 *
M-FST 6	2.8% Bentonite Solution	17.81	23.3	1.6	2.50	3.22	100.0	25.7	74	2.648	0.07 *	0.1 *
M-FST 7	3.6% Bentonite Solution	18.24	23.0	1.8	2.56	3.32	97.7	26.0	73	2.657	0.08 *	0.19 *
M-FST 8	3.2% Bentonite Solution	18.75	23.5	1.4	3.00	3.68	83.4	24.5	71	2.559	0.075 *	0.125 *
M-FST 9	4.0% Bentonite Solution	19.96	23.8	1.1	2.60	3.29	96.0	29.5	69	2.608	0.085 *	0.195 *
M-FST 15	3.6% Bentonite Solution	20.60	23.5	1.4	2.11	2.31	95.0	28.9	70	2.637	0.08 *	0.15 *

Continued

M-FST 24	8% Bentonite Solution	30.71	12.1	2.3	3.13	3.82	145.9	20.4	86	2.636	0.2	0.226
M-FST 28	8% Bentonite Solution	26.70	29.4	1.8	2.50	3.38	148.6	34.8	77	2.632	0.13	0.24
M-FST 29	8% Bentonite Solution	26.62	29.3	3.2	2.20	2.89	118.3	25.6	78	2.631	0.18	0.24
M-FST 10	0.2 % Polymers Solution	19.94	22.3	2.5	2.10	2.37	71.4	48.1	33	2.647	0.12 *	0.125 *
M-FST 11	0.4 % Polymers Solution	20.02	23.8	1.1	2.10	2.40	73.8	49.9	32	2.637	0.1 *	0.11 *
M-FST 12	0.6 % Polymers Solution	20.09	24.1	0.9	2.77	3.20	74.0	49.0	34	2.644	0.065 *	0.105 *
M-FST 17	0.6 % Polymers Solution	19.30	18.1	2.1	2.14	2.57	72.6	50.4	31	2.613	0.024 *	0.12 *
M-FST 13	1 % Polymers Solution	20.17	23.8	1.1	2.10	2.40	71.4	52.0	27	2.672	0.05 *	0.06 *
M-FST 19	1.0 % Polymers Solution	20.50	17.9	2.5	2.05	2.48	73.3	56.9	22	2.632	-0.002 *	-0.002 *
M-FST 20	1.2 % Polymers Solution	20.70	17.9	2.5	1.99	2.43	77.8	63.2	19	2.62	0.02 *	-0.03 *
M-FST 14	0.8 % Polymers Solution	20.32	24.3	0.7	3.02	3.64	74.5	47.5	36	2.646	0.06	0.1
M-FST 18	0.8 % Polymers Solution	20.37	18.4	1.8	2.14	2.57	70.2	50.5	28	2.625	0.01	0.08
M-FST 23	0.8% Polymers Solution	30.58	13.4	3.3	2.30	2.96	173.4	119.2	31	2.63	0.053	0.095
M-FST 26	0.8% Polymers Solution	26.43	28.6	3.8	3.65	4.09	232.9	173.0	26	2.641	0.01	0.02
M-FST 30	0.8% Polymers Solution	26.85	29.3	3.2	2.40	2.84	107.7	76.2	29	2.654	0	0.030

Note: * value not included in calculating the average

Table 3.4. Free swell test and complementary tests results of Niagara Queenston shale

Specimen No.	Ambient Fluid	Depth (m)	Calcite Content (%)	Dolomite Content (%)	Moisture Content Before Test (%)	Moisture Content After Test (%)	Pore Salinity Before Test (g/L)	Pore Salinity After Test (g/L)	Percent Decrease In Pore Salinity (%)	Mass Density (g/cm ³)	Horizontal Swelling Potential (% strain/ log cycle of time)	Vertical Swelling Potential (% strain/ log cycle of time)
N-FST 1	Water	11.20	9.5	2.3	1.50	2.71	314.8	110.8	65	2.815	0.19 *	0.32 *
N-FST 5	Water	11.66	7.6	5.0	1.10	2.31	423.9	115.6	73	2.240	0.2 *	0.31 *
N-FST 7	Water	9.25	7.7	4.9	1.41	2.62	379.4	109.5	71	2.689	0.12 *	0.30 *
N-FST 11	Water	6.20	8.7	4.0	1.18	2.39	377.5	114.5	70	2.682	0.21	0.60
N-FST 15	Water	6.55	8.4	4.3	1.16	2.37	375.9	118.3	69	2.686	0.26	0.575
N-FST 16	Water	6.65	7.8	4.8	0.95	2.16	394.7	120.5	69	2.675	0.16	0.40
N-FST 3	8% Bentonite Solution	11.54	8.2	4.5	1.07	2.28	434.5	208.1	52	2.691	0.16 *	0.21 *
N-FST 6	8% Bentonite Solution	9.18	8.3	4.3	1.27	2.48	370.1	183.6	50	2.676	0.19 *	0.2 *
N-FST 8	8% Bentonite Solution	9.31	7.9	4.8	1.03	2.24	362.7	180.2	50	2.684	0.14 *	0.28 *
N-FST 13	8% Bentonite Solution	6.40	8.5	4.1	1.44	2.65	369.8	188.2	49	2.697	0.16	0.38
N-FST 17	8% Bentonite Solution	6.70	7.7	4.9	0.92	2.13	379.1	184.3	51	2.785	0.16	0.40
N-FST 18	8% Bentonite Solution	6.80	7.8	4.8	1.20	2.20	370.8	178.5	52	2.781	0.16	0.39
N-FST 2	0.8 % Polymers Solution	11.47	7.9	4.7	1.07	2.17	435.7	323.6	26	2.708	0.04 *	0.02 *
N-FST 4	0.8 % Polymers Solution	11.60	7.4	5.1	1.07	2.17	435.3	341.3	22	2.706	0.04 *	0.08 *

Continued

N-FST 9	0.8 % Polymers Solution	9.38	8.0	4.6	1.13	2.34	414.8	316.7	24	2.695	0.06 *	0.08 *
N-FST 10	0.8 % Polymers Solution	6.10	8.4	4.2	1.33	2.54	375.9	320.0	15	2.682	0.01	0.05
N-FST 12	0.8 % Polymers Solution	6.30	8.9	3.8	0.94	2.04	397.1	311.3	22	2.688	0.06	0.07
N-FST 14	0.8 % Polymers Solution	6.50	8.2	4.4	1.44	2.54	369.8	277.9	25	2.695	0.06	0.04

Note: * value not included in calculating the average, (samples from borehole2)

Table 3.5. Semi-confined swell test in vertical direction, and complementary tests results of Milton Queenston shale

Specimen No.	Ambient Fluid	Depth (m)	Calcite Content (%)	Dolomite Content (%)	Moisture Content Before Test (%)	Moisture Content After Test (%)	Pore Salinity Before Test (g/L)	Pore Salinity After Test (g/L)	Percent Decrease In Pore Salinity (%)	Mass Density (g/cm ³)	Applied Pressure (MPa)	Vertical Swelling Potential (% strain/ log cycle of time)
M-SCSVT 28	Water	32.28	12.6	2.2	2.70	3.36	192.1	60.7	68	2.604	0.01	0.180
M-SCSVT 2	Water	31.12	27.1	3.2	2.55	3.06	127.6	66.7	48	2.633	0.05	0.140
M-SCSVT 13	Water	17.98	23.2	10.3	2.30	2.90	73.9	30.3	59	2.622	0.05	0.14
M-SCSVT 14	Water	32.97	22.6	8.0	2.86	3.40	130.9	46.2	65	2.627	0.05	0.16
M-SCSVT 1	Water	30.66	18.8	7.5	2.28	3.80	145.9	54.9	62	2.633	0.1	0.125
M-SCSVT 7	Water	23.77	18.4	3.9	2.83	3.31	85.9	31.8	63	2.626	0.1	0.075
M-SCSVT 25	Water	18.62	25.8	13.5	2.25	2.65	73.3	19.6	73	2.592	0.1	0.100
M-SCSVT 10	Water	26.39	23.2	10.3	2.14	2.84	114.3	36.5	68	2.620	1	0.040
M-SCSVT 19	Water	16.64	24.0	2.5	2.09	2.79	119.4	51.2	57	2.636	1	0.010
M-SCSVT 20	Water	16.41	19.7	3.2	2.35	3.02	85.0	33.8	60	2.444	1	0.010
M-SCSVT 30	8% Bentonite Solution	32.36	13.6	1.3	2.70	3.39	203.7	26.7	87	2.627	0.01	0.220
M-SCSVT 5	8% Bentonite Solution	30.53	20.9	3.6	2.53	3.07	156.3	42.4	73	2.642	0.05	0.215
M-SCSVT 6	8% Bentonite Solution	30.23	17.7	2.7	2.55	3.24	221.8	90.5	59	2.623	0.05	0.150
M-SCSVT 23	8% Bentonite Solution	16.46	21.2	1.8	2.27	2.96	110.2	29.6	73	2.763	0.05	0.115
M-SCSVT 12	8% Bentonite Solution	26.94	20.0	2.7	2.45	3.10	92.2	23.8	74	2.624	0.1	0.100
M-SCSVT 18	8% Bentonite Solution	18.01	19.7	3.2	2.05	2.65	134.6	25.2	81	2.612	0.1	0.110

Continued

M-SCSVT 24	8% Bentonite Solution	16.69	22.6	8.0	2.46	3.03	79.4	27.2	66	2.624	0.1	0.080
M-SCSVT 9	8% Bentonite Solution	24.10	21.3	4.6	2.65	3.27	169.7	36.1	79	2.637	1	0.010
M-SCSVT 17	8% Bentonite Solution	20.14	22.5	9.8	2.21	2.90	72.4	21.8	70	2.630	1	0.060
M-SCSVT 26	8% Bentonite Solution	18.64	25.5	13.8	2.05	2.65	75.6	21.2	72	2.598	1	0.065
M-SCSVT 29	0.8% Polymers Solution	32.31	13.1	1.8	2.65	3.09	197.2	127.3	35	2.620	0.01	0.065
M-SCSVT 3	0.8 % Polymers Solution	30.33	20.6	6.1	2.58	2.68	153.5	95.3	38	2.634	0.05	0.060
M-SCSVT 8	0.8 % Polymers Solution	23.81	20.4	3.9	2.85	3.29	140.4	92.8	34	2.626	0.05	0.070
M-SCSVT 16	0.8 % Polymers Solution	20.12	22.3	10.1	2.11	2.35	73.5	51.8	29	2.594	0.05	0.070
M-SCSVT 4	0.8 % Polymers Solution	30.38	19.0	7.3	2.65	3.08	164.8	101.6	38	2.630	0.1	0.040
M-SCSVT 15	0.8 % Polymers Solution	18.31	25.5	2.5	2.22	2.52	135.1	91.9	52	2.627	0.1	0.035
M-SCSVT 22	0.8 % Polymers Solution	16.43	20.4	2.5	2.27	2.70	88.1	69.1	22	2.602	0.1	0.045
M-SCSVT 11	0.8 % Polymers Solution	26.90	19.7	3.2	2.19	2.34	102.9	67.1	35	2.636	1	0.015
M-SCSVT 21	0.8 % Polymers Solution	16.66	23.5	3.0	1.86	2.10	134.2	101.9	24	2.602	1	0.030
M-SCSVT 27	0.8% Polymers Solution	18.90	22.0	9.0	3.20	3.47	78.1	51.0	35	2.628	1	0.000

Table 3.6. Semi-confined swell test in horizontal direction, and complementary tests results of Milton Queenston shale

Specimen No.	Ambient Fluid	Depth (m)	Calcite Content (%)	Dolomite Content (%)	Moisture Content Before Test (%)	Moisture Content After Test (%)	Pore Salinity Before Test (g/L)	Pore Salinity After Test (g/L)	Percent Decrease In Pore Salinity (%)	Mass Density (g/cm ³)	Applied Pressure (MPa)	Horizontal Swelling Potential (% strain/ log cycle of time)
M-SCSHT 28	Water	32.39	17.5	2.5	2.30	2.80	127.6	43.2	66	2.641	0.01	0.130
M-SCSHT 1	Water	28.25	24.4	1.8	3.02	3.43	82.8	39.8	52	2.633	0.1	0.075
M-SCSHT 2	Water	28.50	21.6	2.2	3.03	3.42	88.5	41.3	53	2.633	0.1	0.065
M-SCSHT 7	Water	28.70	25.0	1.0	7.00	7.72	157.1	40.7	74	2.613	0.1	0.060
M-SCSHT 10	Water	19.03	28.9	1.3	2.83	3.50	70.6	18.0	75	2.630	0.2	0.030
M-SCSHT 22	Water	16.05	22.9	8.3	2.54	3.20	87.3	39.2	55	2.616	0.2	0.020
M-SCSHT 23	Water	15.95	20.6	7.7	2.36	2.90	93.1	29.8	68	2.620	0.2	0.040
M-SCSHT 11	Water	19.61	33.6	1.8	2.13	2.79	105.9	39.4	63	2.495	0.7	0.010
M-SCSHT 12	Water	19.66	30.3	1.8	2.56	3.22	97.9	34.1	65	2.596	0.7	0.030
M-SCSHT 13	Water	21.06	31.6	2.7	2.57	3.23	116.9	46.6	60	2.566	0.7	0.010
M-SCSHT 30	8% Bentonite Solution	32.18	18.0	2.0	2.67	3.25	110.6	25.2	77	2.618	0.01	0.140
M-SCSHT 9	8% Bentonite Solution	30.81	23.5	1.6	2.78	3.45	95.2	27.2	71	2.625	0.1	0.065
M-SCSHT 5	8% Bentonite Solution	28.42	24.1	7.9	2.37	2.42	103.7	27.6	73	2.642	0.1	0.075
M-SCSHT 6	8% Bentonite Solution	28.60	22.8	2.4	3.04	3.99	130.3	25.6	80	2.623	0.1	0.070
M-SCSHT 20	8% Bentonite Solution	19.25	32.9	3.2	2.77	3.46	75.8	27.8	63	2.593	0.2	0.055
M-SCSHT 26	8% Bentonite Solution	16.00	20.7	5.8	2.40	3.20	87.5	24.7	72	2.612	0.2	0.060
M-SCSHT 27	8% Bentonite Solution	15.95	20.6	7.7	2.66	3.44	75.2	20.0	73	2.598	0.2	0.050
M-SCSHT 18	8% Bentonite Solution	19.56	32.4	2.5	2.28	2.97	109.5	30.5	72	2.591	0.7	0.015

Continued

M-SCSHT 19	8% Bentonite Solution	21.13	27.2	2.4	3.17	3.85	110.5	23.8	78	2.627	0.7	0.010
M-SCSHT 21	8% Bentonite Solution	19.00	28.4	2.0	2.95	3.64	74.6	24.7	67	2.570	0.7	0.030
M-SCSHT 29	0.8% Polymers Solution	32.41	17.8	2.2	2.39	2.77	121.6	72.6	40	2.609	0.01	0.020
M-SCSHT 3	0.8 % Polymers Solution	28.35	27.9	2.2	2.07	2.54	122.3	79.3	35	2.634	0.1	0.008
M-SCSHT 14	0.8 % Polymers Solution	19.32	28.7	1.1	2.78	3.21	72.0	56.2	22	2.650	0.1	0.010
M-SCSHT 15	0.8 % Polymers Solution	19.43	29.2	0.7	2.40	2.84	104.1	75.5	28	2.494	0.1	0.010
M-SCSHT 16	0.8 % Polymers Solution	19.63	32.5	5.6	2.00	2.43	112.7	82.0	27	2.569	0.2	0.003
M-SCSHT 24	0.8 % Polymers Solution	16.05	22.9	8.3	2.54	2.60	108.4	68.2	37	2.609	0.2	0.002
M-SCSHT 25	0.8 % Polymers Solution	16.00	22.9	8.3	2.16	2.60	101.7	68.0	33	2.599	0.2	0.004
M-SCSHT 4	0.8 % Polymers Solution	28.55	21.4	2.4	3.03	3.60	95.1	66.2	30	2.630	0.7	0.000
M-SCSHT 8	0.8 % Polymers Solution	28.80	22.8	2.2	3.37	3.76	122.9	89.5	27	2.602	0.7	0.000
M-SCSHT 17	0.8 % Polymers Solution	20.90	28.7	1.6	2.91	3.34	120.4	79.5	34	2.613	0.7	0.000

Table 3.7. Semi-confined swell test in vertical and horizontal directions and complementary tests results of Niagara Queenston shale

Specimen No.	Ambient Fluid	Depth (m)	Calcite Content (%)	Dolomite Content (%)	Moisture Content Before Test (%)	Moisture Content After Test (%)	Pore Salinity Before Test (g/L)	Pore Salinity After Test (g/L)	Percent Decrease In Pore Salinity (%)	Mass Density (g/cm ³)	Applied Pressure In The Direction of Swelling (MPa)	Swelling Potential (% strain/ log cycle of time)
N-SCSVT 4	Water	3.35	9.3	2.9	2.65	3.08	319.7	101.1	68	2.699	0.01	0.515 <i>v</i>
N-SCSVT 1	Water	3.30	10.2	2.9	1.30	3.21	308.2	93.5	70	2.700	0.1	0.370 <i>v</i>
N-SCSVT 6	8% Bentonite Solution	3.45	9.0	2.7	2.55	3.24	311.5	157.0	50	2.700	0.01	0.300 <i>v</i>
N-SCSVT 3	8% Bentonite Solution	3.24	9.9	3.1	1.29	3.38	311.3	139.4	55	2.699	0.1	0.165 <i>v</i>
N-SCSVT 5	0.8 % Polymers Solution	3.40	9.5	2.5	2.53	3.07	310.0	219.7	29	2.698	0.01	0.042 <i>v</i>
N-SCSVT 2	0.8 % Polymers Solution	3.27	10.3	2.9	1.30	3.02	308.2	222.6	28	2.697	0.1	0.035 <i>v</i>
N-SCSHT 4	Water	3.50	9.3	2.4	1.27	3.20	382.0	108.7	72	2.654	0.01	0.205 <i>h</i>
N-SCSHT 1	Water	3.12	9.7	2.9	1.37	2.00	350.8	85.3	76	2.683	0.3	0.110 <i>h</i>
N-SCSHT 6	8% Bentonite Solution	3.60	9.2	2.6	1.29	2.00	373.0	176.6	53	2.657	0.01	0.155 <i>h</i>
N-SCSHT 3	8% Bentonite Solution	3.04	9.6	3.0	1.36	2.57	354.4	183.3	48	2.653	0.3	0.040 <i>h</i>
N-SCSHT 5	0.8 % Polymers Solution	3.55	9.3	2.3	1.30	2.40	372.0	257.7	31	2.665	0.01	0.042 <i>h</i>
N-SCSHT 2	0.8 % Polymers Solution	3.18	9.2	3.4	1.35	2.45	357.0	259.3	27	2.657	0.3	0.010 <i>h</i>

Note: *v* = swelling potential in the vertical direction; *h* = swelling potential in the horizontal direction with respect to the rock bedding.

Table 3.8. Null- swell test in vertical and horizontal directions, and complementary tests results of Milton Queenston shale

Specimen No.	Ambient Fluid	Depth (m)	Calcite Content (%)	Dolomite Content (%)	Moisture Content Before Test (%)	Moisture Content After Test (%)	Pore Salinity Before Test (g/L)	Pore Salinity After Test (g/L)	Percent Decrease In Pore Salinity (%)	Mass Density (g/cm ³)	Direction of Test	Null-Swell Pressure (MPa)
M-NSVT 5	Water	27.68	23.8	3.8	2.67	3.33	98.6	25.9	74	2.637	Vertical	2.14
M-NSVT 7	Water	24.47	22.1	7.1	2.61	3.28	120.6	40.7	66	2.634	Vertical	1.92
M-NSVT 9	Water	25.17	26.2	2.0	2.25	2.91	133.6	47.5	64	2.622	Vertical	2.36
M-NSVT 6	8% Bentonite Solution	27.78	24.3	3.4	2.66	3.50	111.3	25.0	78	2.640	Vertical	2.30
M-NSVT 10	8% Bentonite Solution	25.86	25.8	2.0	2.97	3.10	228.6	38.0	83	2.645	Vertical	2.26
M-NSVT 11	8% Bentonite Solution	18.85	23.0	5.4	3.12	3.81	100.4	21.7	78	2.601	Vertical	2.50
M-NSVT 1	0.8 % Polymers Solution	30.18	17.7	2.6	2.55	2.98	268.7	169.9	37	2.621	Vertical	1.485
M-NSVT 8	0.8 % Polymers Solution	24.90	21.4	9.3	2.67	3.11	224.7	140.5	37	2.618	Vertical	1.40
M-NSVT 13	0.8 % Polymers Solution	32.94	22.0	6.4	2.86	3.30	109.6	71.5	35	2.640	Vertical	1.63
M-NSHT 1	Water	31.06	22.60	8.0	2.30	2.97	131.9	52.9	60	2.695	Horizontal	1.46
M-NSHT 4	Water	31.19	25.3	2.4	2.24	2.91	112.5	35.1	69	2.647	Horizontal	2.14
M-NSHT 10	Water	32.59	15.2	2.5	3.02	3.68	131.5	46.9	64	2.595	Horizontal	2.57
M-NSHT 2	8% Bentonite Solution	30.89	22.4	8.0	2.25	3.00	131.8	39.3	70	2.632	Horizontal	1.55
M-NSHT 5	8% Bentonite Solution	31.04	24.1	7.9	2.79	3.48	87.9	33.8	62	2.646	Horizontal	2.3
M-NSHT 12	8% Bentonite Solution	32.64	14.7	2.9	2.98	3.67	132.7	23.6	82	2.611	Horizontal	2.85
M-NSHT 3	0.8 % Polymers Solution	30.96	22.8	8.0	2.24	2.67	135.4	96.1	29	2.636	Horizontal	1.22
M-NSHT 6	0.8 % Polymers Solution	30.81	25.1	3.3	2.20	2.60	122.0	82.0	33	2.626	Horizontal	1.28
M-NSHT 11	0.8 % Polymers Solution	32.56	14.9	2.7	2.90	3.34	136.4	88.2	35	2.545	Horizontal	1.99

Table 3.9. Null- swell test in vertical and horizontal directions, and complementary tests results of Niagara Queenston shale

Specimen No.	Ambient Fluid	Depth (m)	Calcite Content (%)	Dolomite Content (%)	Moisture Content Before Test (%)	Moisture Content After Test (%)	Pore Salinity Before Test (g/L)	Pore Salinity After Test (g/L)	Percent Decrease In Pore Salinity (%)	Mass Density (g/cm ³)	Direction of Test	Null-Swell Pressure (MPa)
N-NSVT 1	Water	3.21	8.2	4.5	1.30	1.97	290.1	101.9	65	2.673	Vertical	2.07
N-NSVT 2	8% Bentonite Solution	3.18	8.5	4.3	1.30	1.62	347.5	157.3	55	2.670	Vertical	1.8
N-NSVT 3	0.8 % Polymers Solution	3.14	8.1	4.6	1.30	1.87	324.1	227.2	30	2.686	Vertical	1.495
N-NSHT 2	Water	5.52	8.9	2.3	1.26	2.90	319.7	96.7	70	2.691	Horizontal	1.60
N-NSHT 3	8% Bentonite Solution	3.04	9.2	1.8	1.36	2.57	354.4	183.3	48	2.653	Horizontal	1.13
N-NSHT 1	0.8 % Polymers Solution	5.42	9.2	3.4	1.26	2.28	319.4	238.2	25	2.678	Horizontal	0.78

Table 3.10. Rate of absorption of water of Niagara and Milton Queenston shales in ambient fluids

Ambient Fluid	Rate of Absorption In Water		Rate of Absorption In Polymers Solution		Rate of Absorption In Bentonite Solution	
	Initial, Si (mm/ \sqrt{s})	Secondary, Ss (mm/ \sqrt{s})	Initial, Si (mm/ \sqrt{s})	Secondary, Ss (mm/ \sqrt{s})	Initial, Si (mm/ \sqrt{s})	Secondary, Ss (mm/ \sqrt{s})
Niagara Queenston Shale (NQS)	0.0058	0.0011	0.0003	0.0005	0.0003	0.0008
Milton Queenston Shale (MQS)	0.0011	0.001	0.0005	0.0004	0.0012	0.0011

Table 3.11. Summary results of free swell tests, semi-confined swell tests, and null swell tests performed on Milton and Niagara Queenston shale

Ambient Fluid	Water				0.8% Polymer Solution				8% Bentonite Solution			
Direction of Test	Vertical		Horizontal		Vertical		Horizontal		Vertical		Horizontal	
Type of Shale	Applied Pressure (MPa)	Average Swelling Potential (% strain/ log cycle of time)	Applied Pressure (MPa)	Average Swelling Potential (% strain/ log cycle of time)	Applied Pressure (MPa)	Average Swelling Potential (% strain/ log cycle of time)	Applied Pressure (MPa)	Average Swelling Potential (% strain/ log cycle of time)	Applied Pressure (MPa)	Average Swelling Potential (% strain/ log cycle of time)	Applied Pressure (MPa)	Average Swelling Potential (% strain/ log cycle of time)
Milton Queenston Shale (MQS)	0	0.19 (5)	0	0.156 (5)	0	0.065 (5)	0	0.027 (5)	0	0.235 (3)	0	0.17 (3)
	0.01	0.18 (1)	0.01	0.13 (1)	0.01	0.065 (1)	0.01	0.02 (1)	0.01	0.22 (1)	0.01	0.14 (1)
	0.05	0.147 (3)	0.1	0.067 (3)	0.05	0.067 (3)	0.1	0.009 (3)	0.05	0.16 (3)	0.1	0.07 (3)
	0.1	0.1 (3)	0.2	0.03 (3)	0.1	0.04 (3)	0.2	0.003 (3)	0.1	0.097 (3)	0.2	0.055 (3)
	1	0.02 (3)	0.7	0.017 (3)	1	0.015 (3)	0.7	0 (3)	1	0.045 (3)	0.7	0.018 (3)
	2.14	0 (3)	2.057	0 (3)	1.505	0 (3)	1.497	0 (3)	2.353	0 (3)	2.233	0 (3)
Niagara Queenston Shale (NQS)	0	0.525 (3)	0	0.21 (3)	0	0.053 (3)	0.000	0.043 (3)	0	0.39 (3)	0	0.16 (3)
	0.01	0.515 (1)	0.01	0.205 (1)	0.01	0.042 (1)	0.01	0.042 (1)	0.01	0.3 (1)	0.01	0.155 (1)
	0.1	0.37 (1)	0.3	0.11 (1)	0.1	0.035 (1)	0.3	0.01 (1)	0.1	0.165 (1)	0.3	0.04 (1)
	2.07	0 (3)	1.6	0 (3)	1.495	0 (3)	0.78	0 (3)	1.8	0 (3)	1.13	0 (3)

Note: Value in brackets represents number of tests considered in calculating the average

Chapter 4

THE INFLUENCE OF WATER AND LUBRICANT FLUIDS ON THE PEAK STRENGTH OF QUEENSTON SHALE FROM SOUTHERN ONTARIO³

4.1 INTRODUCTION

Micro-tunneling is an effective construction technique to install pipelines and tunnels of variable diameters in various types of soil. However adopting this technique to install pipelines and tunnels in weak rocks, such as Queenston shale of Southern Ontario is still ambiguous and needs to be investigated. Lubricant fluids, such as bentonite and polymer solutions are used in micro-tunneling technique during the installation of the pipe/tunnel sections. This process may last for several weeks where the excavated rock is in direct contact with lubricant fluids used. Based on the recognized swelling behaviour of Queenston shale when it contacts water, and the associated development of micro-cracks (Lee and Lo, 1993), it is suggested here to investigate the strength of Milton Queenston shale when exposed to water and lubricant fluids.

Previous studies on the strength behaviour of sedimentary rocks have focused primarily on the following aspects: strength anisotropy (Dan et al. 2013; Gorski et al. 2007; Claesson and Bohlooli 2002 and Lo and Hori 1979); strength-volume relationship (Lee 1988 and Lo et al. 1987); strength-temperature relationship (Wai et al. 1981); post peak failure behaviour and the influence of brine and water on the strength (Wasantha and Ranjith 2014; Liang et al. 2012; Paterson and Wong 2005; Baud et al. 2000; Paterson 1978 and Colback and Wiid 1965). Dan et al. (2013), and Lo and Hori (1979) investigated the strength anisotropy of sedimentary rocks by employing the Brazilian split, unconfined compression and triaxial compression tests. They concluded that

³ Aversion of this chapter has been submitted for publication in the Canadian Geotechnical Journal in April, 2016

sedimentary rocks generally exhibit anisotropic strength behaviour, which is highly dependent on the direction of applied stress with respect to the rock beddings. Gorski et al. (2007) found that the tensile strength of granite from Forsmark, Sweden, measured in direct tension test was 39-69% of the tensile strength measured in Brazilian split test. Claesson and Bohloli (2002) suggested a formula to calculate the principal tensile strength at centre of disc in Brazilian split test in anisotropic rocks. Lee (1988) proposed a stress-strain relationship for Queenston Shale using the results of Brazilian split and uniaxial compression tests. Lo et al. (1987) studied the effect of specimen's size on the strength and concluded that the deformation modulus of shaly limestone decreases with increasing the size of specimen, approaching the mass modulus. Wai et al. (1981) investigated heating effect on the strength of some sedimentary rocks of Southern Ontario. It was revealed that the shaly limestone maintains a constant strength when heated up to 350°C and then gained more strength beyond 350°C, while the granitic gneiss showed variable strength while heated. Wasantha and Ranjith (2014), and Liang et al. (2012) studied the decrease in strength of gypsum and Hawkesbury sandstone due to saturation in water and brine leaching, and reported that a considerable amount of the strength of both rocks was lost. Paterson and Wong (2005); Baud et al. (2000), Paterson (1978) and Colback and Wiid, (1965) attributed weakening effects of water on the strength of rocks to the pressurized pore water that decreases the effective strength and weakens the rock structure.

4.1.1 Work Objective and Scope

Although many studies have investigated water effects on the strength of different rocks in different parts of the world, the region of southern Ontario is still lacking in this aspect. Of particular interest, the influence of lubricant fluids used in micro-tunneling applications, such as bentonite and polymer solutions, on the strength of Queenston shale need to be investigated thoroughly. Results of such investigation can be of high significance for micro-tunneling applications, as this technique is quite new in shales of this region. The work reported herein is part of a comprehensive study to investigate the feasibility of the micro-tunneling technique in shales of southern Ontario. The presented

work aims to investigate the influence of soaking in water and lubricant fluids used in micro-tunneling applications on the strength of Milton Queenston shale. Specimens were cut parallel and perpendicular to the rock bedding to investigate strength anisotropy before and after soaking. Vertical and horizontal specimens of Milton Queenston shale were kept submerged in water and lubricant fluids for 100 days. A total of 101 specimens were tested in Brazilian split, unconfined compression, and triaxial compression tests, before and after soaking. The changes occurred in Milton Queenston shale strength due to soaking effects are presented and discussed in this chapter. The measured strength was utilized to develop strength envelopes of Milton Queenston shale before and after soaking in water and lubricant fluids in both parallel and perpendicular directions to the rock bedding. The developed strength envelopes of Milton Queenston shale after soaking can give an insight of the amount of strength that can be lost due to soaking in water and lubricant fluids.

4.2 BOREHOLE

Samples were collected from a single vertical borehole drilled near the interchange between Regional Road 25 and Louis St. Laurent Avenue in Milton, Ontario. The borehole was located 150 m to the east of the interchange, and 10 m to the south of Regional Road 25. The recovered Milton Queenston shale samples were collected from depth of 15.50 to 34.50 m below the ground level. Thirteen runs of recovered rock columns were collected in two days. Immediately after coring, samples were identified and wrapped with saran wrap followed with electrical tape, and bubble wrap to preserve the moisture. Wrapped samples were placed inside hard polyvinyl chloride (PVC) pipes with two rubber end caps for each rock piece followed by a mechanical clamping to protect samples during transporting to the laboratory at the University of Western Ontario.

The collected samples were Queenston shale interbedded with thin layers of shaly limestone. The rock quality designation (RQD) value varied between 50.0 % and 99.2 %, indicating rock condition varying from fair to good to excellent with increasing depth as

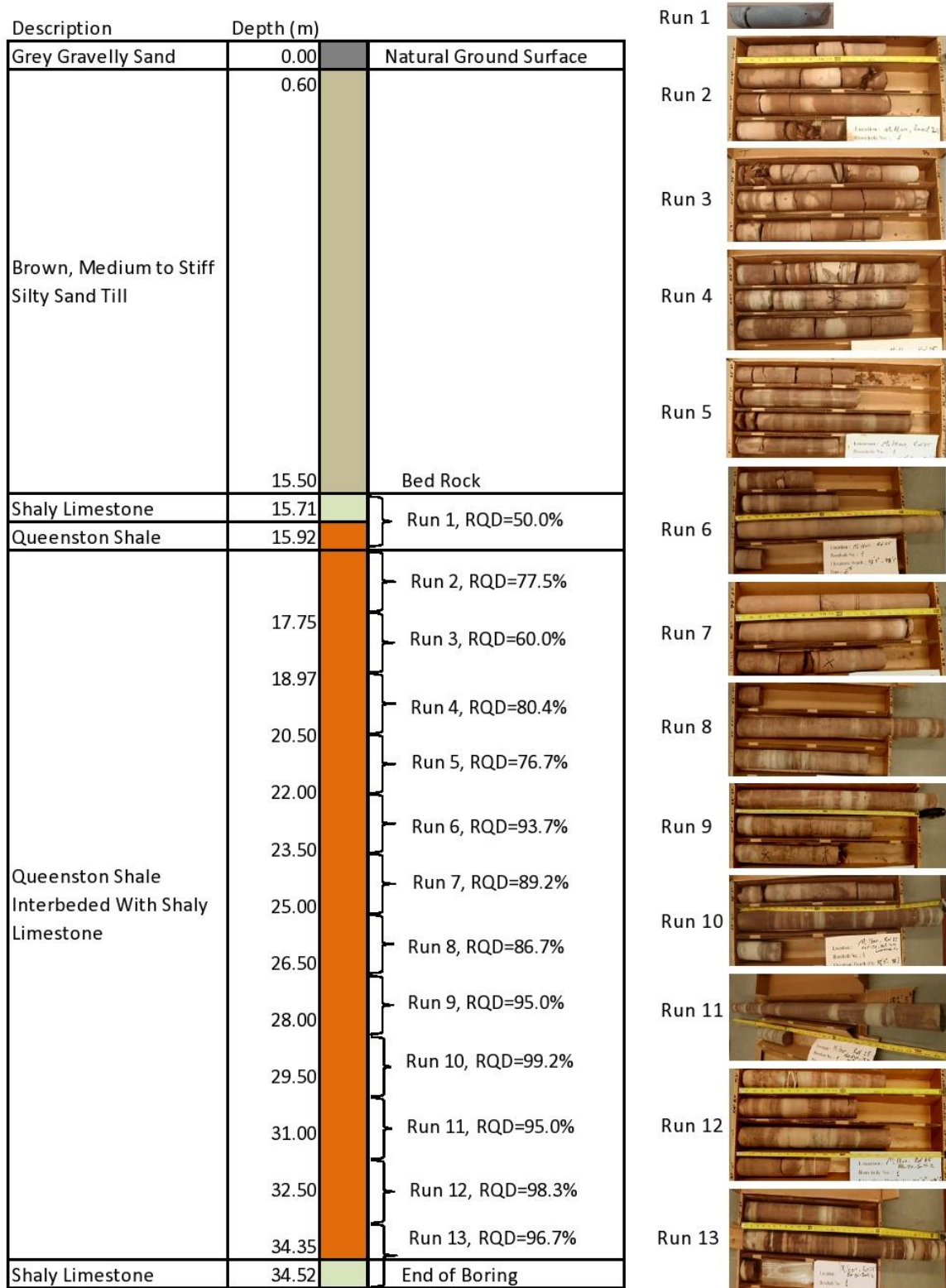


Figure 4.1. Borehole logging of the recovered samples of Queenston shale from Milton, Ontario.

indicated in Figure 4.1. The borehole logging indicated that the Queenston shale layer has occasionally 2-4 mm thick gypsum nodulus that exist along the entire layer at average intervals of 1.0 m-1.4 m. Based on the recurrence of joints, and RQD value of each run, the Queenston shale layer can be divided into three sub-layers: i) top layer from depth of 15.5 m to 22.5 m BGL, with an average RQD value of 68.9 %, and majority of 2 mm-5 mm of compacted clay joints that occur at an average of 4 joints/m; ii) intermediate layer from 22.5 m to 26.5 m BGL with an average RQD value of 89.9 %, and 2 mm-5 mm compacted clay joints that occur at an average of 1 joint/m and iii) lower layer from 26.5 m to 34.52 m BGL with average RQD value of 96.8 %, and joints of compacted clay occurring at 1 joint/4m.

4.3 MINERALOGICAL COMPOSITION OF MQS

The x-ray diffraction analyses were performed on Milton Queenston shale specimens collected from four different depths to cover the entire rock column. Bragg's law was utilized in these analyses. The procedure of preparing test specimen and performing analyses was presented in Chapter 3. The analyses revealed that Milton Queenston shale composed of the following minerals: 0.8-1.1% Chlorite; 10.4-16.8% Illite; 1.1-2.4 Kaolinite; 43.1-47.4% Quartz; 3.3-6.7% Feldspar; 19.3-28.2% Calcite; 3.9-9.2% Dolomite and 2.2-3.7% Pyrite. It can be noted that no significant swelling clay minerals exist in Milton Queenston shale where both illite and kaolinite have low swelling capacity. Other minerals that can be affected by the presence of water, such as gypsum or anhydrite do not exist as well. The swelling capacity of the pyrite can cause volumetric changes in shales. However its effect on the swelling behavior of Milton Queenston shale can be limited due to its low presence. This can indicate that the influence of water and lubricant fluids on Milton Queenston shale can be expected to be similar to the well-recognized swelling mechanism of shales in southern Ontario. The swelling in these shales was found to be attributed to the following three reasons: i) the relief of initial in-situ stresses; ii) the accessibility of water and iii) salinity gradient between the rock pore fluid and the ambient fluid (Lee and Lo, 1993). Al-Maamori et al.

(2016) concluded that the diffusion of Milton Queenston shale pore fluid salinity can be affected by bentonite solution causing this shale to swell slightly more than its swelling in water. While polymer solution was found to cause less swelling due to its both physical action on the surface of Milton Queenston shale and its influence in reducing the diffusion process of the pore fluid salinity.

4.4 TEST METHODOLOGY

Micro-tunneling technique utilizes lubricant fluids during the construction period of tunnels and pipelines to facilitate the installation of the tunnel/pipe sections. These fluids are used to reduce the frictional forces between the excavated ground and the tunnel/pipe sections, and hence reduce the required driving forces applied by the jacking system. Additional function of the lubricant fluids is to support the excavated ground to maintain tunnel stability. The installation period of a tunnel or a pipeline depends on how hard the ground is and the run distance between successive shafts. Adopting micro-tunneling technique to install tunnels/pipelines in rocks such as Milton Queenston shale may have to account for strength loosening or strength softening. As part of a comprehensive research program in the University of Western Ontario to study the feasibility of micro-tunneling technique in Queenston shale of Southern Ontario, it was concluded that lubricant fluids utilized in this technique minimized the swelling of this shale (Al-Maamori et al., 2016) but did not eliminate it completely. Motivated by this finding and the continuous exposure of Queenston shale to lubricant fluids during the installation period of the tunnel/pipeline, this chapter investigates the influence of lubricant fluids on the strength behaviour of Milton Queenston shale.

One of the suggested procedures to mitigate the influence of the time-dependent deformation of Queenston shale and other swelling rocks in Southern Ontario on underground structures is to delay the installation of the permanent structure until sufficient rock deformation has occurred, so that any further deformation after construction is within manageable limits (Lo et al., 1987). In micro-tunneling technique

the permanent structure (tunnel/pipeline sections) is installed simultaneously while the micro-tunneling boring machine advances. The gap between the tunnel/pipeline and the excavated shale, which is continuously filled with lubricant fluid, is permanently filled with cement grout at the end of installation period. In micro-tunneling technique, to apply the mitigation procedure of the swelling effects suggested by Lo et al. (1987), the application of the permanent cement grout can be delayed until a sufficient amount of rock deformation has occurred.

The lubricant fluids, polymer solution and bentonite solution, used in this research are the same as those used in the field with the same mixing proportions. The polymer solution was prepared by adding 0.8 % of liquid polymer concentrate type TK60 (anionic polyacrylamide suspension in a water-in-oil emulsion from Morrison Mud, Division of Mudtech Ltd.-UK) to tap water with a continuous high speed mixing. Similarly, the bentonite solution was prepared by mixing 8 % of dry powder sodium bentonite clay type (HYDRAUL-EZ from CETCO-USA) with tap water. A soaking period of 100 days was selected in this research to represent a reasonable period for time-dependent deformation of Milton Queenston shale before replacing lubricant fluids with permanent cement grout. Three tests were utilized to cover the full strength envelope of Milton Queenston shale: Brazilian split test; unconfined compression test and triaxial compression test with different confining pressure up to 20 MPa. In addition, to evaluate the strength anisotropy, the strength behaviour of Milton Queenston shale in the vertical and horizontal directions was investigated. Total of 35 Brazilian split tests; 25 unconfined compression tests and 30 triaxial compression tests were performed on Milton Queenston shale samples. Tests were conducted on specimens that were cut and prepared as received from in-situ with the natural moisture content (denoted herein intact specimens), and on specimens soaked for hundred days in lubricant fluids (i.e. polymer and bentonite solutions) and in water. Water was used as a control fluid where it is usually used as the ambient fluid to measure swelling deformation of rocks. Due to the limited supplied samples, only one additional direct tension test was performed on intact vertical specimen for the purpose of selecting the appropriate reduction on the Brazilian splitting strength to convert it to the corresponding direct tension strength. The measured tensile, unconfined

compression and triaxial compression strength results were used to produce the strength envelopes of Milton Queenston shale before and after soaking, in both vertical and horizontal directions. Cutting test specimens and re-coring samples to get horizontal specimens was done in the laboratory of the University of Western Ontario using diamond slab saw and a coring machine. For each test specimen, additional tests were performed, such as: calcite content; moisture content; mass density and pore water salinity. The Brazilian split test was performed according to the procedure described in ASTM-D3967 (2008). The unconfined compression test was conducted according to method “C” and “D” described in ASTM-D7012 (2010) while the triaxial compression test was performed according to method “A” and “B” described in ASTM-D7012 (2010).

The ultimate tensile strength, the ultimate unconfined compression strength, and the ultimate compression strength were measured in both vertical and horizontal directions under different confining pressure (i.e. 2.5 MPa, 5.0 MPa, 7.5 MPa, 10.0 MPa, 15.0 MPa and 20.0 MPa). The high confining pressure used represents the high in-situ horizontal stresses that exist in Queenston shale of Southern Ontario (Al-Maamori et al. 2014). The Poisson’s ratio was calculated in these tests based on the vertical and horizontal deformation curves of the elastic deformation portion. The elastic modulus was also calculated using method “b” described in ASTM- D7012 (2010), and the shear modulus was accordingly calculated. The measured strength and the calculated parameters for intact and soaked Milton Queenston shale in lubricant fluids and water are presented and discussed in detail in the discussion section.

4.4.1 Maintaining Specimens During Soaking Period

It is well recognized that the Queenston shale develops micro-cracks when submerged in water due to the increase in the volume of macro-pores and ultra-micro-pores (Lee and Lo 1993). These micro-cracks can be developed along the entire small size specimen and hence renders maintaining specimen soundness quite difficult. A procedure was developed in this research to maintain the test specimens during the

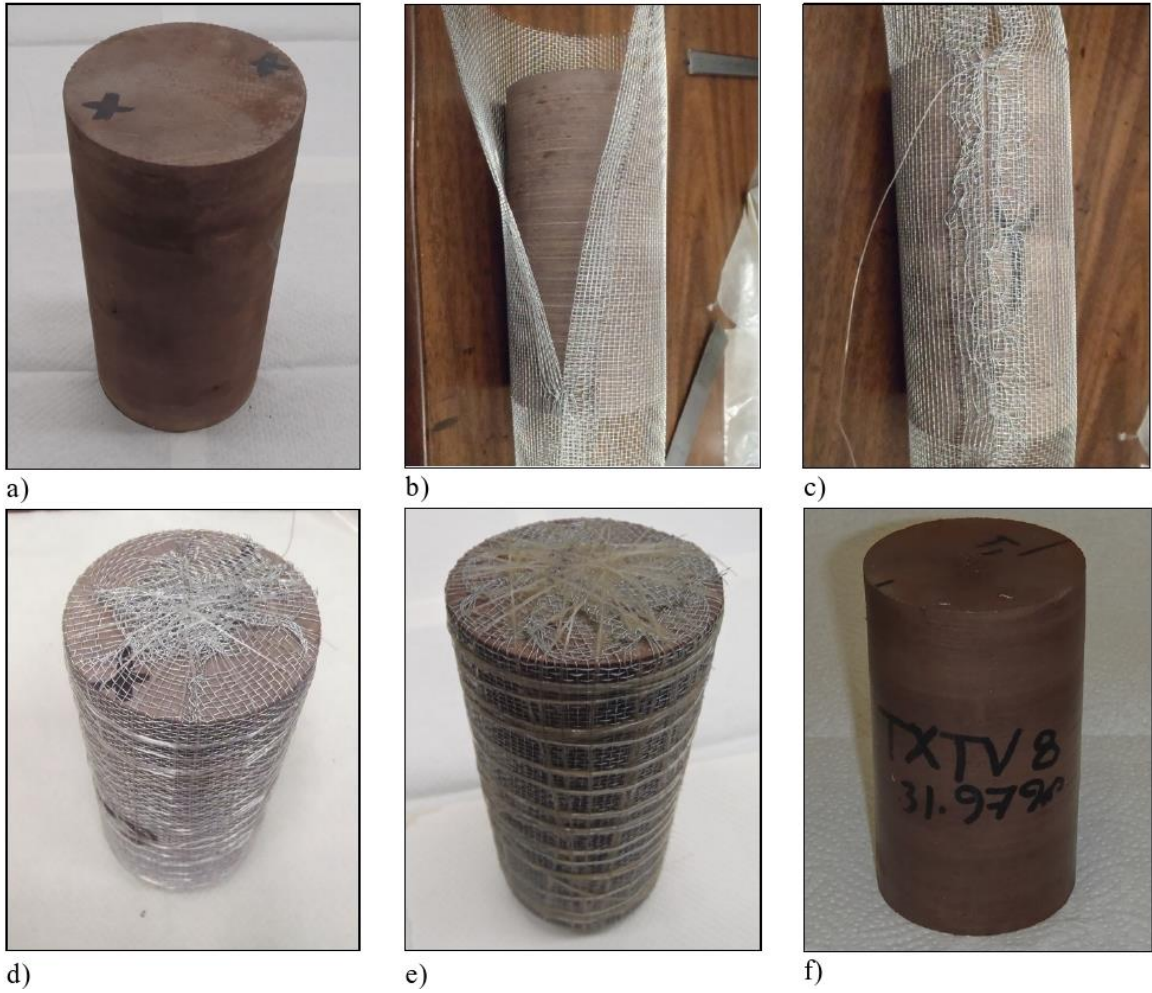


Figure 4.2. Steps followed to protect specimens during soaking period: (a) Intact specimen; (b, c, d) steps of preserving the specimen; (e, f) preserved specimen after soaking period.

soaking period. After cutting the specimen, a layer of screen wire mesh was used to coat the entire specimen. Terminals of the coating screen wire mesh were sewed firmly together by hand using fish wire of 60-Pounds line. Many winding layers with the fish wire in the longitudinal direction of the specimen were added. This was followed by several transverse winding layers with the fish wire. This procedure allowed lubricant fluids and water to contact the specimen through the holes in the screen wire mesh, while maintaining the specimen intact. These steps are illustrated in Figure 4.2.

4.4.2 Modified High Capacity Triaxial Cell

Figure 4.3 shows the high capacity triaxial cell used to perform the triaxial compression tests on Milton Queenston shale. The cell was designed earlier in the University of Western Ontario to investigate the strength parameters of concrete-rock contact at dam-foundation interface (Lo et al. 1991). The cell consists of: 1) cell body made of hardened steel; 2) cell base made of hardened steel and contains three channels connect the inner chamber of the cell to the outside through inlet/outlet opening; 3) Central pedestal mounted on the cell base; 4) piston to apply the vertical stress made of hardened steel with spherically concave base and contains a rubber washer and stopper; 5) ventilation valve located on top of the piston to remove entrapped air bubbles in the confining fluid; 6) inlet/outlet junction connected to the cell base; 7) one-way inlet valve connected to the base through inlet/outlet junction for adding the required confining pressure fluid through a hydraulic jack; 8) outlet adjusting valve; 9) outlet needle valve for adjusting the confining pressure connected through the inlet/outlet junction to the cell chamber and 10) specimen's assembly cap with spherical convex head to ensure centric applied load. The cell was modified by designing additional mechanical pieces to accommodate rock specimens of variable sizes; to ensure centering the specimen on the cell pedestal; to adopt high confining pressure up to 20 MPa and to adjust the confining pressure manually during the test, if needed. These additional pieces are:

1) Multi-step adjusting seat mounted on the base pedestal through a depression in its bottom, which ensures centric specimen placement on the pedestal to minimize load

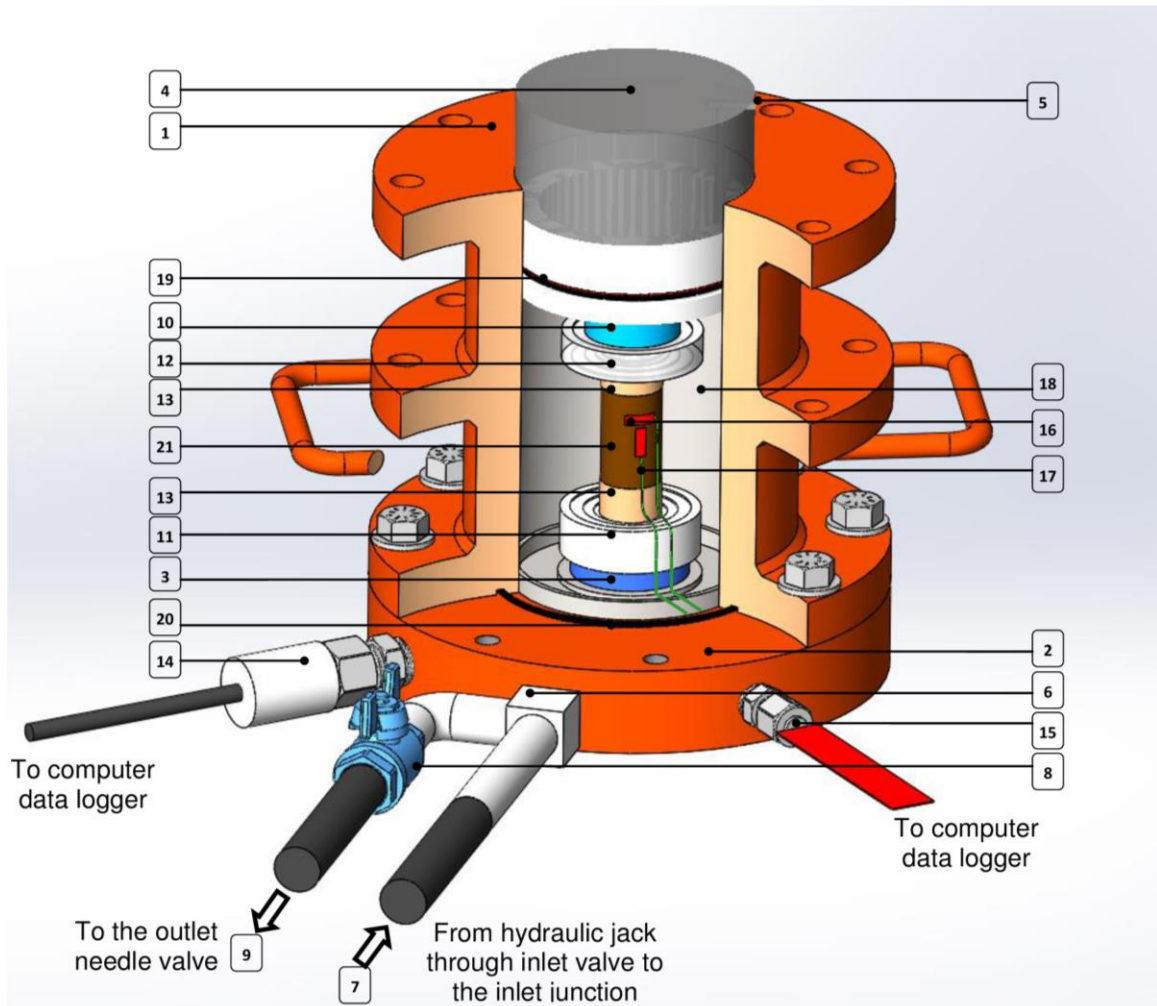


Figure 4-3. Sectional view of the modified triaxial compression cell: 1) cell body, 2) cell base, 3) central pedestal, 4) piston, 5) ventilation valve, 6) inlet/outlet junction, 7) one-way inlet valve, 8) outlet adjusting valve, 9) outlet needle valve, 10) assembly cap, 11) adjusting seat, 12) adjusting cap, 13) specimen's platen, 14) pressure transducer, 15) sealing gland, 16) electronic foil strain gauge, 17) strain gauge wires, 18) cell chamber, 19) rubber washer and stopper, 20) rubber casket: and 21) rock specimen.

eccentricity. It has multiple circular steps on its top to accommodate specimen diameter of 63, 49, 39, and 33 mm.

2) Multi-step adjusting cap that is seated on top of the specimen's end cap through the multiple circular steps in its bottom. It has two circular steps on its top to accommodate the specimen's assembly cap (10). The cap ensures that the spherical specimen's assembly cap is centered atop the specimen during the test to minimize load eccentricity

3) Two platens placed directly at top and bottom of the specimen.

4) Pressure transducer, with 10,000 psi capacity (type AST4000A10000PAD0000, American Sensor Technology, NY) connected to the cell base to measure the confining pressure up to 68.9 MPa with an accuracy of $\pm 0.5\%$.

5) Sealing gland with eight wires connection and Teflon sealant (type MCH4, Conax Technologies, Buffalo) connected to cell base to allow the wires of electronic strain gauges that are mounted on the rock specimen to pass through without oil leakage from the cell chamber.

To avoid contact between bare connections of electronic strain gauges, dielectric transformer oil type MODEF60 from (Aevitas Inc., Brantford, ON) used as ambient fluid to apply the required confining pressure. The in-situ horizontal stress recorded in the Queenston shale layer of Niagara Falls (nearby similar formation) at a depth of 93.9 m-123.8 m was 14.3 MPa-17.1 MPa (Al-Maamori et al., 2014). Therefore, the triaxial tests were performed under confining pressure ranging up to 20 MPa.

4.4.3 Electronic Strain Gauges

Electronic foil strain gauges type N11-FA-10-120-11, and terminals for foil strain gauges type FG-10T from (SHOWA Measuring Instruments Company Ltd., Tokyo, Japan) were used to measure the vertical and horizontal strains of the rock specimen during the unconfined compression test and the triaxial compression test. Four electronic foil strain gauges were glued on each test specimen using instant adhesive glue type (Loctite 454 from Loctite Corporation North American Group, USA). The strain gauges were glued in T-shape arrangement on two opposite side of the specimen. Two strain

gauges were glued parallel to the longitudinal axis of the specimen to measure the vertical strain. The other two circumferential strain gauges were glued on the circumference of the specimen perpendicular to its longitudinal axis to measure the horizontal strain.

4.4.4 Triaxial Compression Test Procedure

To perform the triaxial compression test, the end caps are placed on top and bottom of the test specimen followed by 0.64 mm thick triaxial membrane with silicone and two O-rings to prevent the penetration of confining fluid into the rock specimen. The test specimen is placed on the multi-step adjusting seat that is mounted to the cell pedestal, and the multi-step adjusting cap is placed on the top platen of the specimen followed by the specimen's assembly cap. Wires of strain gauges were connected to the wires of the sealing gland which in turn were connected to a computer data logger. Transformer oil was added to fill the cell chamber covering the whole specimen's assembly, and the cell piston is finally placed on top of the specimen's assembly spherical cap with the ventilation valve kept opened to allow for dissipating the entrapped air bubbles. When the piston is positioned in the cell, the ventilation valve is closed, and the cell is placed in the MTS machine to apply the vertical loading. A suitable vertical seating load of less than 1% of anticipated ultimate strength is applied on the specimen to ensure contact between all parts. The confining pressure is gradually added through a manual hydraulic jack while the readings of the pressure transducer are monitored. When the required confining pressure is reached, all valves are kept closed and the vertical loading is applied in a constant rate until specimen's failure is achieved. The load is applied according to the procedure described in ASTM-D7012 (2010) to achieve failure within 2-15 minutes. The loading rate was 0.16 kN/s equivalent to a displacement rate of 0.045 mm/min. The confining pressure is kept constant during the test and any required adjustments are made through the outlet needle valve. All tests were successfully performed under the specified confining pressures using the modified triaxial cell without any leak of the ambient fluid.

4.5 RESULTS AND DISCUSSION

4.5.1 Brazilian Split Test

The Brazilian split test was performed on Milton Queenston shale specimens in both vertical and horizontal directions with respect to the rock beddings. Figure 4.4 shows schematic details of the orientation of test specimens to measure the split strength in the vertical and horizontal directions. Vertically cored specimens were used to measure the split strength in the horizontal direction, while horizontally cored specimens were used to measure the split strength in the vertical direction. Cutting the test specimen was done in accordance with the ASTM-D4543 (2008). Dimensions of the test specimens were kept within requirements of ASTM-D3967 (2008) (i.e. thickness-to-diameter ratio between 0.2 and 0.75) and tests were performed according to the procedure given therein. Wooden plates were used to distribute the applied load evenly along the entire length of the specimen and to avoid localized forces. Total of 35 Brazilian tests were performed on Milton Queenston shale specimens: 12 in the horizontal direction and 23 in the vertical direction. The average value of minimum three successful tests was considered as the average splitting strength. For each test specimen, the moisture content and pore water salinity were measured before and after the soaking period, following ASTM-D2216 (2010) and the procedure described by Lee (1988), respectively. The Chittick carbon dioxide apparatus was utilized to determine the percentage of total carbonates content (i.e. calcite content and dolomite content) in each test specimen following the procedure described by Dreimanis (1962).

The test results of the Brazilian split strength in the vertical and horizontal directions, and the corresponding supplementary test results are presented in Tables 4.1 and 4.2. In these tables, the percentage decrease in the Brazilian split strength due to soaking effect in lubricant fluids and in water is also presented.

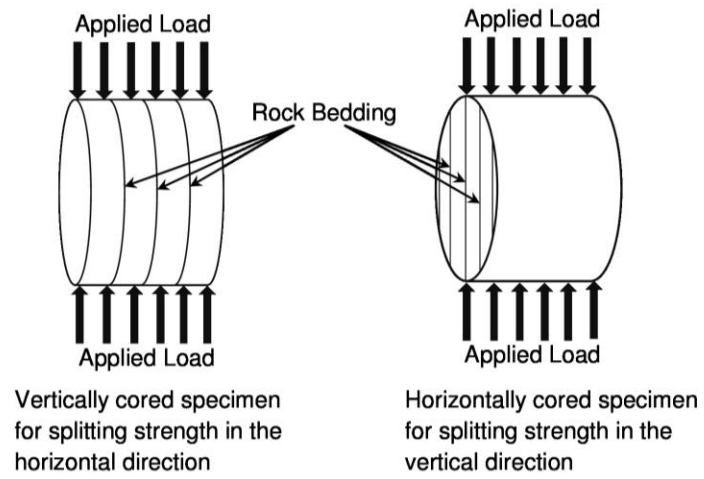


Figure 4.4. Schematic drawing of the orientation of specimens in the Brazilian split test.

4.5.1.1 Discussion

The results presented in Tables 4.1 and 4.2 indicate that the split strength is anisotropic with respect to the rock bedding. In general, the Brazilian split strength was higher in the vertical direction than the Brazilian split strength in the horizontal direction. It can also be noted from Tables 1 and 2 that the Brazilian split strength of Milton Queenston shale has decreased significantly after soaking. However, the percentage decrease in the strength was not the same in vertical and horizontal directions, and depended on the ambient fluid. Soaking Milton Queenston shale in water caused 29 % and 57 % strength reduction in the vertical and horizontal directions, respectively, compared to the strength of intact specimens. Similarly, soaking Milton Queenston shale in bentonite solution caused 39 %, and 55 % strength reduction in the vertical and horizontal directions, respectively, compared to the strength of intact specimens. Whereas soaking Milton Queenston shale specimens in polymer solution caused a strength decrease of only 10 % and 34 % in the vertical and horizontal directions, respectively, compared to their intact strength.

It is clear that the strength decrease due to soaking Milton Queenston shale in water and lubricant fluids was more significant along the horizontal direction, which indicates that Milton Queenston shale is more susceptible to the influence of ambient fluids in the horizontal direction than in the vertical direction. This difference in the influence of ambient fluids can be attributed to the fabric of Milton Queenston shale particles. Milton Queenston shale has a strong clayey fabric with the preferred orientation of horizontal layering, as indicated in Figure 4.5 (a, b). The remarkable orientation of clayey fabric in the horizontal layering may cause a difference in the penetration of ambient fluids deep into Milton Queenston shale.

Ambient fluids may tend to penetrate deeper in the direction parallel to particles (i.e. horizontal direction) than in the perpendicular direction to the particles (i.e. vertical direction). This assumption can be true when dealing with the same fluid. However, with different fluids, such as those adopted in this research (i.e. water, polymer and bentonite solutions) the penetration can also be affected by the size of suspended particles in the fluid. Both polymer and bentonite solutions are composed of either polymer particles or

bentonite particles suspended in water. When lubricant fluids contacts Milton Queenston shale, polymer (or bentonite) particles tend to accumulate on the outer surface of the shale creating coating layers, as indicated in Figure 4.5 (c, d). However, the thickness of these coating layers is different. Polymer solution penetrates deeper into the surficial pores and surficial micro-cracks than bentonite solution. This behaviour makes the coating layer formed from polymer particles thicker than the coating layer formed from bentonite particles, as indicated in Figure 4.5 (c, d). It seems that the polymer coating layer was relatively more efficient than bentonite coating layer in preventing excessive water particles from penetration deeper into Milton Queenston shale.

The pore water salinity was measured before and after soaking Milton Queenston shale specimens in water and lubricant fluids, and the test results together with the percentage decrease in the pore salinity are presented in Tables 4.1 and 4.2. The percentage decrease in the pore salinity of Milton Queenston shale due to soaking in bentonite solution was the highest (60-81 %) compared to water (55-77 %) and polymer solution (28-41 %). This means that the processes of diffusion and osmosis in Milton Queenston shale were more dominant in bentonite solution compared to water and polymer solution. The osmosis and diffusion processes are conditions for swelling of Queenston shale of southern Ontario to occur (Lee and Lo 1993). The coating layer on the outer surface of Milton Queenston shale and the effect of osmosis and diffusion could be the reasons that bentonite solution caused more decrease in the Brazilian split strength of this shale compared to water and polymer solution.

Figure 4.6 shows the failure modes and cracks developed in Milton Queenston shale after reaching the split strength of both intact specimens and specimens soaked for 100 days in lubricant fluids and water. The failure of Milton Queenston shale in the vertical direction (i.e. in a direction perpendicular to the rock bedding) was mainly generated along weak bonds between bedding planes, and the failure appears to have occurred simultaneously in multiple planes for the soaked specimens (Figure 4.6 (1-b, 1-c, 1-d)). However, the vertical intact specimens failed mainly in a single crack developed along weak bonds between rock bedding, as shown in Figure 4.6 (1-a). The Brazilian split failure of Milton Queenston shale in the vertical direction appears

Table 4.1. Brazilian splitting strength of Milton Queenston shale in vertical direction and supplementary test results

Specimen No.	Ambient Fluid	Depth (m)	Calcite Content (%)	Dolomite Content (%)	Moisture Content Before Soaking (%)	Moisture Content After Soaking (%)	Pore Salinity Before Soaking (g/L)	Pore Salinity After Soaking (g/L)	Percent Decrease In Pore Salinity (%)	Brazilian Splitting Strength (MPa)	Average Brazilian Splitting Strength (MPa)	Percentage Decrease In Brazilian Split Strength	Equivalent Direct Tension Strength σ_v (MPa)
BZVT 1	-	9.921	20.2	5.8	2.454	-	206.8	-	-	8.189			
BZVT 2	-	8.517	33.5	2.3	2.406	-	72.7	-	-	9.783			
BZVT 3	-	28.03	24.4	7.9	2.410	-	93.4	-	-	9.056	8.7	0	4.5
BZVT 4	-	28.4	22.0	0.9	2.483	-	105.7	-	-	8.739			
BZVT 5	-	5.621	25.3	2.5	2.200	-	159.1	-	-	7.942			
BZVT 6	Water	9.934	31.4	4.8	3.122	3.810	242.6	109.4	55	6.523			
BZVT 7	Water	27.92	24.4	7.9	2.932	3.50	134.0	44.9	67	5.516			
BZVT 8	Water	9.921	20.9	5.0	2.71	3.60	187.3	85.1	55	5.462			
BZVT 9	Water	5.697	33.4	1.6	2.20	2.81	184.8	65.4	65	7.854	6.2	29	3.2
BZVT 10	Water	8.517	31.4	4.8	2.012	2.55	74.6	24.0	68	6.024			
BZVT 11	Water	28.03	19.6	8.6	2.46	3.1	195.1	69.4	64	5.682			

Continued

BZVT 12	0.8 % Polymers Solution	29.934	23.9	5.2	2.297	3.130	250.3	150.5	40	7.399			
BZVT 13	0.8 % Polymers Solution	27.92	23.5	6.1	2.210	2.882	164.0	104.5	36	7.587			
BZVT 14	0.8 % Polymers Solution	29.921	19.1	4.3	2.888	3.766	175.7	104.2	41	7.464			
BZVT 15	0.8 % Polymers Solution	18.567	20.8	7.3	2.184	3.493	160.3	111.3	31	7.700	7.8	10	4.1
BZVT 16	0.8 % Polymers Solution	15.697	31.4	4.8	2.237	2.672	78.8	47.7	39	8.749			
BZVT 17	0.8 % Polymers Solution	26.48	21.6	8.0	2.275	2.39	73.2	52.6	28	7.786			
BZVT 18	8% Bentonite Solution	29.934	23.1	9.1	2.855	3.70	227.7	43.7	81	5.094			
BZVT 19	8% Bentonite Solution	27.92	23.2	2.5	2.30	2.99	157.6	35.8	77	5.021			
BZVT 20	8% Bentonite Solution	18.567	25.3	2.0	2.184	3.841	183.2	56.4	69	5.199			
BZVT 21	8% Bentonite Solution	15.697	33.5	2.3	2.210	2.990	70.1	14.6	79	6.218	5.3	39	2.8
BZVT 22	8% Bentonite Solution	26.48	24.0	9.1	2.385	3.319	136.3	36.6	73	5.364			
BZVT 23	8% Bentonite Solution	15.621	23.0	5.4	2.855	3.038	145.9	40.1	73	5.004			

Table 4.2. Brazilian splitting strength of Milton Queenston shale in horizontal direction and supplementary test results

Specimen No.	Ambient Fluid	Depth (m)	Calcite Content (%)	Dolomite Content (%)	Moisture Content Before Soaking (%)	Moisture Content After Soaking (%)	Pore Salinity Before Soaking (g/L)	Pore Salinity After Soaking (g/L)	Percent Decrease In Pore Salinity (%)	Brazilian Splitting Strength (MPa)	Average Brazilian Splitting Strength (MPa)	Percentage Decrease In Brazilian Split Strength	Equivalent Direct Tension Strength (MPa)
BZHT 1	-	22.331	26.9	2.5	2.604	-	87.4	-	-	8.948			
BZHT 2	-	22.518	26.0	2.2	2.786	-	125.6	-	-	7.499	7.6	0	4.0
BZHT 3	-	23.14	22.9	6.4	2.516	-	196.7	-	-	6.463			
BZHT 4	Water	22.4	31.6	2.7	2.165	2.564	144.8	55.1	62	3.277			
BZHT 5	Water	22.523	33.5	2.3	2.484	3.225	72.9	29.2	60	3.439	3.3	57	1.7
BZHT 6	Water	23.25	25.7	2.3	2.516	2.717	180.8	57.8	68	3.126			
BZHT 7	0.8 % Polymers Solution	22.429	29.7	3.9	2.551	2.564	78.4	47.6	39	4.871			
BZHT 8	0.8 % Polymers Solution	22.7	36.2	2.7	1.952	1.952	124.3	88.7	29	5.711	5.0	34	2.6
BZHT 9	0.8 % Polymers Solution	22.97	21.7	6.1	2.091	2.683	152.2	102.4	33	4.452			
BZHT 10	8% Bentonite Solution	22.6	27.5	2.90	2.20	3.36	109.8	37.6	66	3.658			
BZHT 11	8% Bentonite Solution	22.96	26.6	3.9	2.035	2.889	154.3	36.0	77	3.242	3.4	55	1.8
BZHT 12	8% Bentonite Solution	23.24	22.9	6.4	2.516	3.120	125.4	34.0	73	3.274			

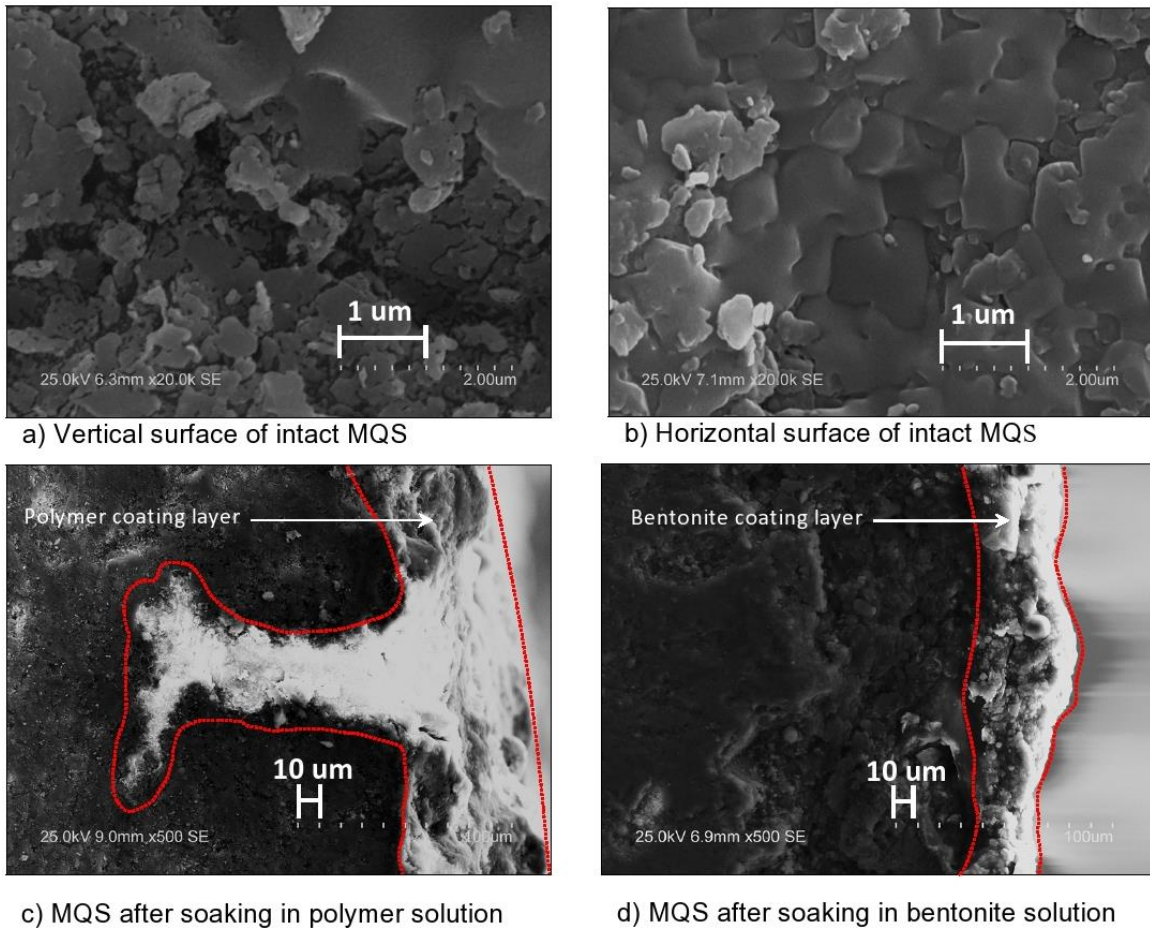
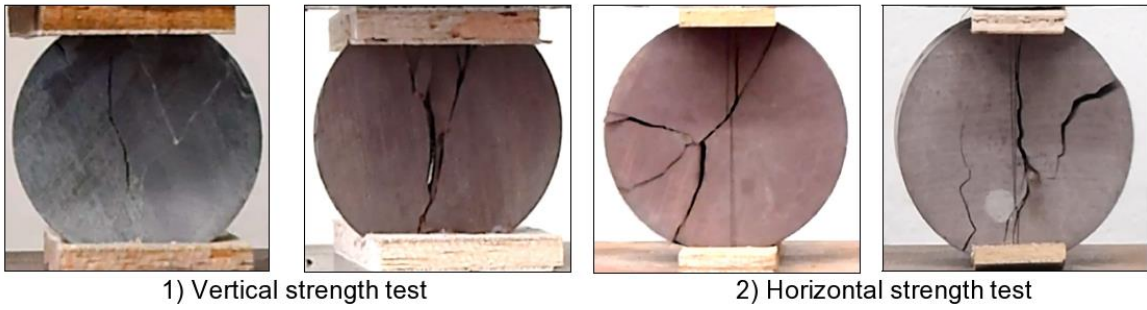


Figure 4.5. Scanning electron microscopy images of Milton Queenston shale (MQS): (a) vertical surface of intact specimen; (b) horizontal surface of intact specimen, c) polymer coating on MQS and (d) bentonite coating on MQS.

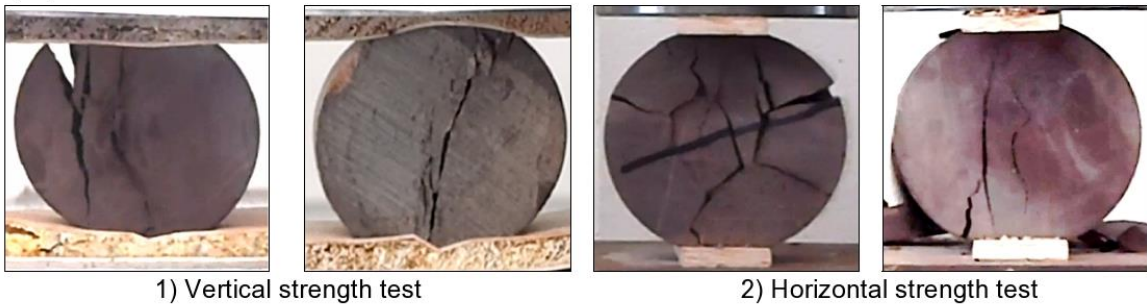
to be mainly pure tensile failure (i.e. straight cracks) in between bedding planes with some tensile-shear failures (i.e. curved cracks). Some wedges can also be noted, which may be attributed to the boundary effects of the loading platens and the wooden pads. On the other hand, failure of Milton Queenston shale in the horizontal direction (i.e. in the direction parallel to the rock bedding) developed in the form of tensile-shear failure with some wedges near the loading platens. During the test, the main failure cracks were noticed to develop first in the direction of the applied load. As the deformation increased with loading, more cracks developed in the direction perpendicular to the applied load. Splitting along bedding planes was also noticed in most of the soaked specimen followed by complete collapse of the test specimens. The occurrence of splitting cracks prior to the occurrence of splitting between rock bedding in the horizontal specimens indicates that the tensile strength of Milton Queenston shale in the horizontal direction is smaller than the tensile strength in the vertical direction. This is quite consistent with the results presented in Table 4.1 and Table 4.2.

Due to the biaxial state of stresses induced in the rock specimen in Brazilian split test and its boundary effects, the measured tensile strength may overestimate the real tensile strength of the rock. In contrast, the direct tension test generates single state of tensile stress that acts on the rock specimen until it fails with minimal boundary effects influencing its result. Gorski et al. (2007) noted this difference when measured the tensile strength of granite in both Brazilian split test and direct tension test. The tensile strength of the granite measured in direct tension test was 39-69%, and averaging 54% of its value measured in Brazilian split test. This observation was also reported for other materials,

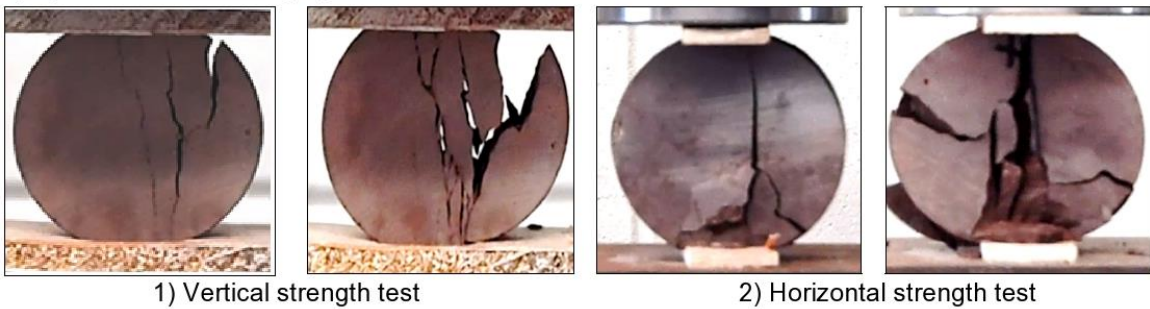
a) Intact specimens:



b) Specimens soaked in water:



c) Specimens soaked in polymer solution:



d) Specimens soaked in bentonite solution:

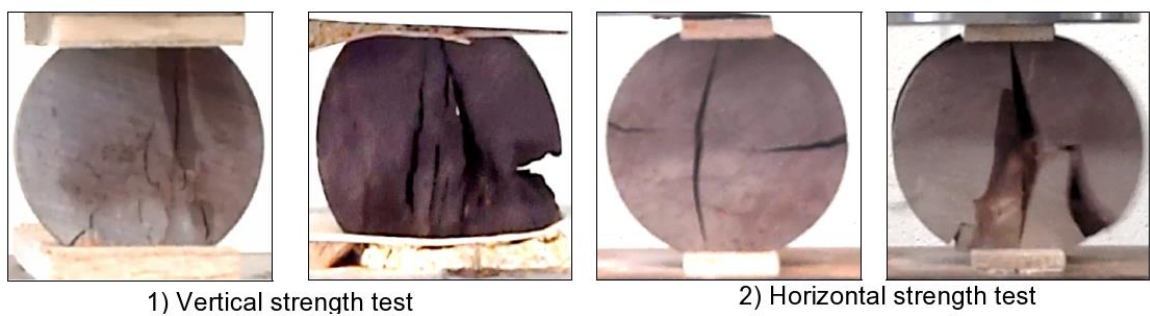


Figure 4.6. Brazilian splitting test performed on: (a) intact specimens and specimens soaked for hundred days in (b) water; (c) polymer solution and (d) bentonite solution; (1) vertical specimens; (2) horizontal specimen.

such as concrete (Neville 1996). The tensile strength of concrete measured in Brazilian split test found overestimated by 5-12% of that measured in direct tension test. Based on these observations, it is more convenient to adopt the tensile strength of rocks measured in direct tension test. However, this is not possible in our case, where it was quite difficult to do the sophisticated preparations for the test specimen in direct tension test after soaking specimens for 100 days. Therefore, the tensile strength of Milton Queenston shale measured in Brazilian split test will be reduced by a 52%. This reduction is based on the direct tension test result performed on intact Milton Queenston shale, as it will be presented in a later section. The values of the equivalent tensile strength of Milton Queenston shale before and after soaking in water and lubricant fluids are listed in Tables 4-1 and 4-2. The values of the equivalent tensile strength of Milton Queenston shale will be used to develop the strength envelopes of this shale.

4.5.2 Direct Tension Test

The direct tension test was performed on intact vertical Milton Queenston shale specimen according to ASTM-D2936 (2008), and following the procedure described in Lo et al (1991). The specimen was cut to a length/diameter ratio of 2. Care was taken to produce parallel contacts. Two end caps were glued on top and bottom of the specimen using two-part Epoxy resin and polyamide hardener adhesive from (Loctite and Hysol, Henkel Corporation, U.S.A.). The specimen was then mounted on MTS system through universal joints to eliminate load eccentricities. Tensile load was applied gradually on the specimen with a constant displacement rate of 0.024 mm/min until failure. The tensile strength was calculated from dividing the failure load by the cross-sectional area of the specimen. The test was repeated three times for the same specimen where the fractured edge was cut and prepared for successive test. In this case it was possible to have an average value of three direct tension tests. The average tensile strength of Milton Queenston shale in the vertical direction was 4.5 MPa. This value represents 52% of the tensile strength of intact Milton Queenston shale measured in Brazilian split test in vertical direction (8.7 MPa), listed in Table 4.1. This percentage is very consistent with

that reported by Gorski et al. (2007). Therefore, it is assumed here that this reduction percentage of 52% is valid in both vertical and horizontal specimens of Milton Queenston shale. This strength reduction assumption is adopted to calculate the equivalent direct tension strength of soaked specimens.

4.5.3 Unconfined Compression Test

The unconfined compression strength test was carried out on intact specimens and on specimens soaked for 100 days in lubricant fluids and water in both vertical and horizontal directions. Twenty five unconfined compression tests were carried out, 12 on vertically oriented specimens and 13 on horizontally oriented specimens. A constant rate of loading of 0.16 kN/s equivalent to a displacement rate of 0.045 mm/min was applied until failure was achieved within 2-15 minutes according to the procedure described in methods “C” and “D” in ASTM-D7012 (2010). Four electronic foil strain gauges were glued in T arrangement on two opposite sides of each test specimen to measure deformation strains along and perpendicular to the longitudinal axis of the test specimen, as illustrated in Figure 4.3. For the horizontally oriented specimens, the strain gauges were glued on two orthogonal sides of the specimen: parallel to and across the rock bedding. With this arrangement, it was possible to measure two values of Poisson’s ratio in the horizontal direction. The first value calculated from strain gauges on the side parallel to rock bedding is the Poisson’s ratio for the effect of horizontal stress on horizontal strain, denoted as ν_h , while the second calculated value from strain gauges across the rock bedding is the Poisson’s ratio for the effect of horizontal stress on vertical strain, denoted as ν_{hv} (Lo and Hori, 1979).

The test results are presented in Tables 4.3 and 4.4 for vertically and horizontally oriented specimens, respectively. Typical results of the unconfined compression test performed on Milton Queenston shale are presented in Figure 4.7 and Figure 4.8 for vertically and horizontally oriented specimens, respectively.

4.5.3.1 Discussion

The results presented in Tables 4.3 and 4.4 indicate that Milton Queenston shale exhibited anisotropic behaviour in their unconfined compressive strength with respect to the rock bedding. This behaviour is noticed for both intact specimens and specimens soaked for 100 days in water and in lubricant fluids. The unconfined compressive strength of intact Milton Queenston shale in the vertical direction was higher than the strength of intact shale in the horizontal direction. Soaking effects are also evident in the presented results where strength reduction was observed for different soaking fluids. The unconfined compressive strength of Milton Queenston shale in the vertical direction (i.e. perpendicular to the rock beddings) has considerably decreased by 62 %, 56 % and 57 % of the intact shale strength, after being soaked in water, polymer solution and bentonite solution, respectively. However, in the horizontal direction (i.e. parallel to the rock beddings), the soaking effects were less evident, as the unconfined compressive strength decreased by 33 %, 22 %, and 51 % of the intact shale strength, after soaking in water, polymer solution and bentonite solution, respectively. Thus, it can be concluded that soaking effects of polymer solution on the unconfined compressive strength of Milton Queenston shale was less than other fluids in both directions. Whereas that bentonite solution caused higher decrease than water in the horizontal direction and less decrease than water in the vertical direction compared to the strength of intact shale.

This trend of behaviour is consistent with the trend noted in the results of the Brazilian split test. The expected mechanism of soaking fluids on the unconfined compressive strength of Milton Queenston shale is suggested to be similar to that explained in the discussion of Brazilian split test results. The polymer solution appears to be more efficient than bentonite solution in creating thicker coating layer on the contact surface of Milton Queenston shale. The thick polymer coating layer prevents water from penetration deeper into the shale and hence reducing micro cracks that affect the shale strength. The variation in the pore water salinity of Milton Queenston shale after soaking period is also presented in Table 4.3 and Table 4.4. A higher difference in the pore water salinity of Milton Queenston shale can be noticed due to soaking in bentonite solution compared to water and polymer solution. This means a higher diffusion and osmosis of

Milton Queenston shale can occur in bentonite solution compared to water and polymer solution. The more diffusion and osmosis can result in more swelling deformations of Milton Queenston shale to occur, which in turn may cause its strength to drop down due to the developed micro-cracks in the shale structure (Lee and Lo 1993).

Figure 4.9 shows the cracks developed in Milton Queenston shale and failure modes of intact and soaked specimens tested vertically and horizontally with respect to rock beddings. Figure 4.9 shows that the failure of Milton Queenston shale was in general brittle. The brittle failure was more obvious in intact specimens than soaked specimens. In general, failures occurred in vertical planes across the rock beddings for vertically cored specimens, whereas for horizontally cored specimens, most failures occurred in the rock beddings. No pure shear failure was noticed in both directions. However, for horizontally cored specimens, some shear wedges appeared after one or more cracks been developed in the rock beddings. This indicates that Milton Queenston shale has a strong fabric structure and the failure occurred when a considerable compression stress was reached to induce tensile stresses on the perpendicular directions to the applied load (i.e. similar to the tensile stresses induced in Brazilian split test). When the ultimate tensile strength in weak bonds was reached, tension failures started to develop along weak planes. Tension failures across the direction of the applied load were developed consecutively until the final collapse of the specimen in compression was occurred. The process of developing the tensile cracks that induced the final collapse of the test specimens occurred so fast which supports the observed brittle failure of Milton Queenston shale.

Table 4.3. Unconfined compression strength and strength parameters of Milton Queenston shale in vertical direction and supplementary test results

Specimen No.	Ambient Fluid	Depth	Calcite Content (%)	Dolomite Content (%)	Moisture Content Before Soaking (%)	Moisture Content After Soaking (%)	Pore Salinity Before Soaking (g/L)	Pore Salinity After Soaking (g/L)	Percent Decrease in Pore Salinity (%)	Unconfined Compression Strength (MPa)	Average Unconfined Compression Strength (MPa)	Poisson's Ratio ν_{vh}	Average Poisson's Ratio ν_{vh}	Elastic Modulus E_v (GPa)	Average Elastic Modulus E_v (GPa)	Shear Modulus G_v (GPa)	Average Shear Modulus G_v (GPa)
UCVT 1	Air	24.48	22.1	7.1	2.81	-	213.4	-	-	53.100	-	0.273	-	15.150	-	5.951	-
UCVT 2	Air	31.54	16.1	3.0	2.38	-	221.3	-	-	43.751	42.861	0.231	0.268	20.732	16.794	8.421	6.650
UCVT 3	Air	31.70	17.2	2.2	2.95	-	156.7	-	-	31.732	-	0.300	-	14.500	-	5.577	-
UCVT 4	Water	24.63	25.2	2.7	2.60	2.67	149.2	52.9	65	24.769	-	0.356	-	7.656	-	2.823	-
UCVT 5	Water	26.97	23.7	2.7	2.97	3.73	87.2	31.6	64	11.881	16.364 (-62%)	0.470	0.434 (62%)	6.000	6.773 (-60%)	2.041	2.374 (-64%)
UCVT 6	Water	29.38	20.1	3.2	2.84	3.53	158.9	52.6	67	12.443	-	0.476	-	6.664	-	2.257	-
UCVT 7	0.8 % Polymers Solution	27.40	24.9	2.7	2.60	3.00	91.8	73.6	20	25.433	-	0.477	-	8.065	-	2.730	-
UCVT 8	0.8 % Polymers Solution	29.57	26.2	2.0	2.76	2.90	118.7	88.4	25	15.689	18.917 (-56%)	0.351	0.434 (62%)	7.914	7.292 (-57%)	2.929	2.553 (-62%)
UCVT 9	0.8 % Polymers Solution	24.76	22.3	3.6	2.67	3.25	206.0	124.7	39	15.630	-	0.475	-	5.896	-	1.999	-
UCVT 10	8% Bentonite Solution	25.66	25.9	3.2	2.97	3.20	228.6	69.4	70	25.610	-	0.384	-	4.032	-	1.457	-
UCVT 11	8% Bentonite Solution	25.79	25.4	3.0	2.97	3.00	229.0	33.8	85	15.100	18.471 (-57%)	0.458	0.389 (45%)	2.893	4.183 (-75%)	0.992	1.524 (-77%)
UCVT 12	8% Bentonite Solution	29.69	22.5	4.8	2.78	3.10	119.4	24.4	80	14.702	-	0.325	-	5.625	-	2.123	-

Note: values in brackets represent percentage variation in the strength and elastic deformation parameters due to soaking in lubricant fluids and in water compared to intact specimens.

Table 4.4. Unconfined compression strength and strength parameters of Milton Queenston shale in horizontal direction and supplementary test results

Specimen No.	Ambient Fluid	Depth (m)	Calcite Content (%)	Dolomite Content (%)	Moisture Content Before Soaking (%)	Moisture Content After Soaking (%)	Pore Salinity Before Soaking (g/L)	Pore Salinity After Soaking (g/L)	Percent Decrease in Pore Salinity (%)	Unconfined Compression Strength (MPa)	Average Unconfined Compression Strength (MPa)	Poisson's Ratio (parallel to bedding, $\frac{U_h}{U_v}$ /perpendicular to bedding, $\frac{U_h}{U_v}$)	Average Poisson's Ratio $\frac{U_h}{U_v}$	Elastic Modulus E_h (GPa)	Average Elastic Modulus E_h (GPa)	Shear Modulus G_h (GPa)	Average Shear Modulus G_h (GPa)
UCHT 1	Air	15.65	24.6	11.7	2.20	-	72.7	-	-	44.956		0.250 / 0.357		21.853		8.741	
UCHT 2	Air	25.14	21.4	2.9	3.88	-	91.2	-	-	23.171	30.885	0.222 / 0.333	0.249/0.333	22.200	23.093	9.083	9.241
UCHT 3	Air	27.50	20.6	4.8	2.73	-	103.8	-	-	22.161		0.270 / 0.313		26.647		10.491	
UCHT 4	Air	15.67	30.1	1.8	2.55	-	78.4	-	-	33.251		0.253 / 0.330		21.670		8.647	
UCHT 5	Water	17.76	28.6	3.8	2.30	2.50	155.4	62.8	60	27.144		0.309 / 0.393		12.356		4.720	
UCHT 6	Water	25.90	30.3	1.8	2.01	2.66	224.3	86.9	61	17.131	20.825 (-33%)	0.222/ 0.278	0.246/0.397 (-1%/19%)	33.330	19.007 (-18%)	13.637	7.683 (-17%)
UCHT 7	Water	27.98	25.3	2.5	2.60	3.30	152.7	55.7	64	18.200		0.208 / 0.519		11.334		4.691	
UCHT 8	0.8 % Polymers Solution	15.60	26.6	4.3	2.47	2.92	91.1	60.5	34	18.440		0.235 / 0.329		16.920		6.850	
UCHT 9	0.8 % Polymers Solution	25.05	23.3	4.3	2.40	2.73	72.9	43.1	41	25.210	24.112 (-22%)	0.200 / 0.338	0.225/0.325 (-10%/-2%)	18.014	20.539 (-11%)	7.506	8.372 (-9%)
UCHT 10	0.8 % Polymers Solution	28.01	19.9	5.0	2.40	2.52	97.7	69.3	29	28.685		0.240 / 0.307		26.682		10.759	
UCHT 11	8% Bentonite Solution	15.57	25.1	2.8	3.11	3.63	99.3	29.0	71	13.303		0.250 / 0.353		11.565		4.626	
UCHT 12	8% Bentonite Solution	24.98	25.4	3.0	2.72	3.42	97.7	30.4	69	14.794	15.052 (-51%)	0.264 / 0.361	0.242/0.334 (-3%/0%)	17.779	11.677 (-49%)	7.033	4.669 (-49%)
UCHT 13	8% Bentonite Solution	28.38	20.9	5.4	2.61	3.09	101.9	20.1	80	17.058		0.211 / 0.289		5.686		2.348	

Note: values in brackets represent percentage variation in the strength and elastic deformation parameters due to soaking in lubricant fluids and in water compared to intact specimens.

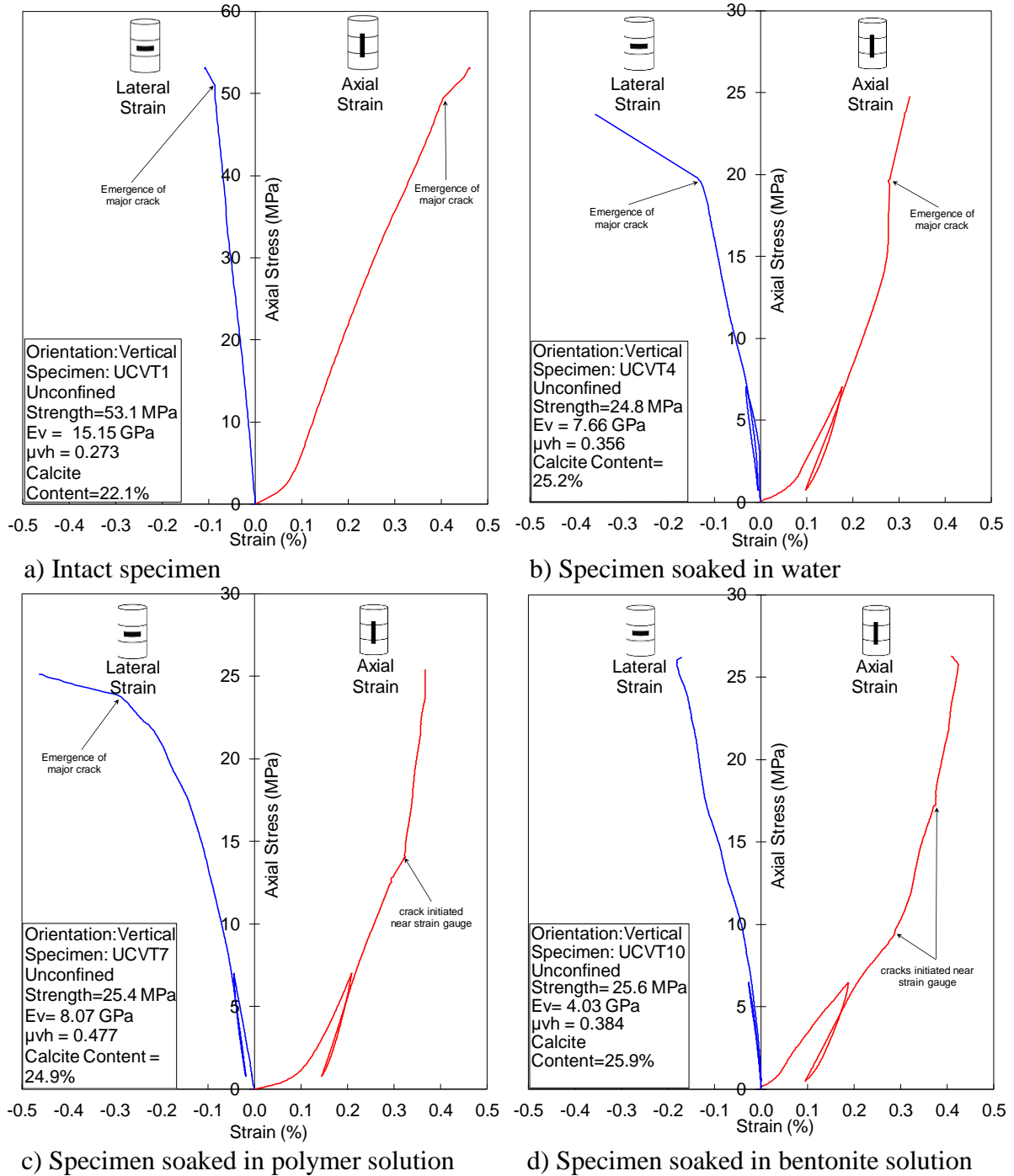


Figure 4.7. Results of unconfined compressive strength performed on vertically cored Milton Queenston shale specimens: (a) intact specimen; specimens soaked for hundred days in: (b) water, (c) polymer solution and (d) bentonite solution, respectively.

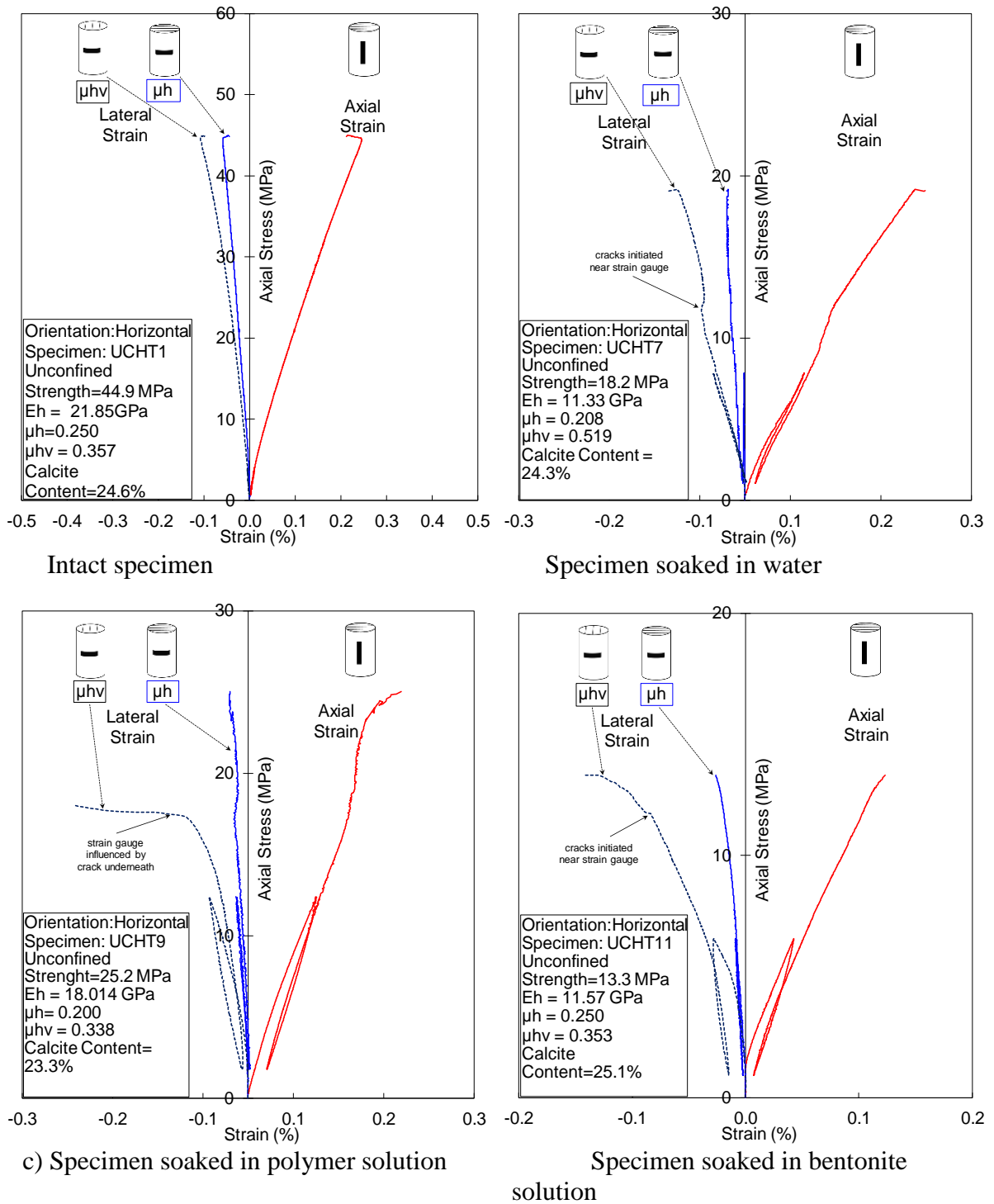
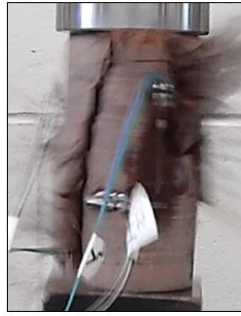


Figure 4.8. Results of unconfined compressive strength performed on horizontally cored Milton Queenston shale specimens: (a) intact specimen; specimens soaked for hundred days in: (b) water, (c) polymer solution and (d) bentonite solution, respectively.

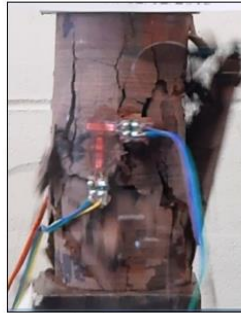
a) Intact specimens:



1) Vertical strength test

2) Horizontal strength test

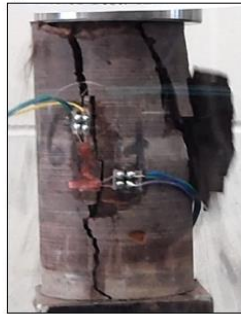
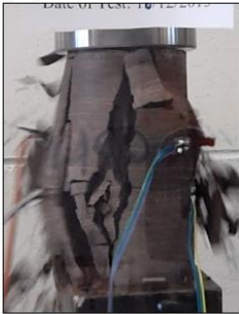
b) Specimens soaked in water:



1) Vertical strength test

2) Horizontal strength test

c) Specimens soaked in polymer solution:



1) Vertical strength test

2) Horizontal strength test

d) Specimens soaked in bentonite solution:



1) Vertical strength test

2) Horizontal strength test

Figure 4.9. Unconfined compressive strength test performed on: (a) intact specimens and specimens soaked for hundred days in: (b) water; (c) polymer solution and (d) bentonite solution; 1) vertical specimens, 2) horizontal specimen.

4.5.3.2 Poisson's Ratio; Elastic Modulus and Shear Modulus

Milton Queenston shale is a rock formation of sedimentary origins and as such its elastic deformation parameters, such as Poisson's ratio; elastic modulus and shear modulus are expected to vary in the orthogonal directions with respect to rock beddings. Thus, Poisson's ratio was measured for both vertical and horizontal specimens. For horizontal specimens, it was measured in two perpendicular directions (i.e. parallel to rock beddings denoted as ν_h and across rock beddings denoted as ν_{hv}). Based on the elastic deformations of Milton Queenston shale during the unconfined compression tests, Poisson's ratio and elastic and shear moduli were calculated employing the relationships given in Lo and Hori (1979). The unconfined compression test results show that lateral deformations occurred in vertical specimens (Figure 4.7) were generally greater than lateral deformations occurred in horizontal specimens (Figure 4.8). Moreover, lateral deformations of soaked specimens were greater in the vertical specimens than horizontal specimens.

From the data presented in Table 4.3 and Table 4.4, it can be noted that the variation in Poisson's ratio, elastic modulus and shear modulus due to soaking were more evident in the vertical direction (i.e. perpendicular to rock beddings) than in the horizontal direction (i.e. parallel to rock beddings). Soaking Milton Queenston shale in water; polymer and bentonite solutions caused Poisson's ratio to increase by (62 %, 62 %, and 45 %) in the vertical direction (ν_{hv}), and to decrease by (1-10 %) in the horizontal direction (ν_h), respectively. However, water caused an increase of 19 % in Poisson's ratio in the horizontal direction perpendicular to rock beddings (i.e. ν_{hv}). In contrast, soaking Milton Queenston shale in water and lubricant fluids caused the elastic modulus and shear modulus to decrease compared to its value in intact specimens. The change was generally greater in the vertical direction than the change in the horizontal direction. The polymer solution caused a decrease of (57 % and 62 %) in the elastic modulus and shear modulus in the vertical direction and (11 % and 9 %) in the horizontal direction, while bentonite solution caused a decrease of (75 % and 77 %) in the vertical direction, and (49 %) in the horizontal direction.

It can be concluded that Milton Queenston shale showed a considerable variation in the unconfined compressive strength and the elastic properties, such as Poisson's ratio; elastic modulus and shear modulus when exposed to water and lubricant fluids for a period of time. These variations should be considered in the design of underground structures in Milton Queenston shale when water and other fluids are expected to be acting in the vicinity of excavation. However, the extent of these variations that may occur in Milton Queenston shale from the source of fluids needs to be investigated.

4.5.4 Triaxial Compression Test

The triaxial compression test was carried out on vertically and horizontally oriented Milton Queenston shale specimens following the procedure described in methods "A" and "B" in ASTM-D7012 (2010). The deformation strain was measured using electronic foil strain gauges. Elastic membrane was used to jacket the test specimen and part of the platens with silicon and O-rings to seal the specimen from the confining fluid. Silicon was applied 24 hours prior to the beginning of the test to allow for adequate setting time. After placing the specimen in the cell with the confining fluid filling the cell chamber, a suitable seating load less than 1% of anticipated ultimate strength was applied to ensure contact between all parts. The confining pressure was applied gradually until the desired value was achieved, and then the vertical loading was increased at a constant rate until failure was achieved within 2-15 minutes (ASTM-D7012, 2010). The loading rate was 0.16 kN/s equivalent to a displacement rate of 0.045 mm/min. Since the piston of the cell has bigger diameter than the test specimen, a correction was made to the vertical applied load through accounting for the difference in the cross-sectional areas of the test specimen and the cell piston. The triaxial test was performed on intact Milton Queenston shale specimens and on specimens that been soaked for 100 days in lubricant fluids and in water. Twenty four tests were conducted on horizontally oriented Milton Queenston shale specimens under confining pressure of 2.5, 5.0, 7.5, 10.0, 15.0, and 20.0 MPa. Due to the limited supplied samples, only 16 tests were performed on vertically oriented Milton Queenston shale specimens, under confining pressure of 2.5, 5.0, 10.0, and 20.0 MPa. The desired confining pressure was maintained stable during the test within the allowable

tolerance indicated in ASTM-D7012 (2010). The test results are presented in Tables 4.5 and 4.6, and Figure 4.10 displays the failure modes. Sample results of the triaxial compression test performed on Milton Queenston shale before and after soaking in lubricant fluids and in water are presented in Figure 4.11 and Figure 4.12.

4.5.4.1 Discussion

The triaxial test data presented in Tables 4.5 and 4.6 revealed that the influence of increasing the confining pressure from 2.5 MPa to 20 MPa on the strength was more evident in the horizontal direction. Soaking effects are also listed in these tables as the percentage of decrease in the compressive strength. The percentage decrease in the compressive strength of vertical specimens due to soaking in water and in lubricant fluids was generally greater than the decrease in horizontal specimens. Moreover, polymer solution caused the least decrease in the strength of Milton Queenston shale compared to water and bentonite solution, which had approximately similar percentage strength decrease in both directions.

The calculated Poisson's ratio was generally increased after soaking in water and lubricant fluids in both vertical and horizontal directions. However, some of horizontal specimens exhibit smaller values of Poisson's ratio compared to intact Milton Queenston shale which could be attributed to the variation in shale. As defined by Lo and Hori (1979), Poisson's ratio for the effect of horizontal stress on vertical strain (i.e. ν_{hv}) was generally greater than Poisson's ratio of the effect of horizontal stress on horizontal strain (i.e. ν_h) for horizontal specimens. The elastic modulus and shear modulus were generally decreased after soaking Milton Queenston in water and lubricant fluids. The decrease in both factors was more evident in vertical specimens. Some specimens showed an increase in the elastic modulus and shear modulus, which might be attributed to the variation in Milton Queenston shale.

Figure 4.10 shows the cracks developed and failure modes of vertical and horizontal Milton Queenston shale specimens under confining pressure of 20 MPa. Similar to the unconfined compression tests, the failure generally developed along

vertical planes across rock beddings for vertical specimens and in multiple planes along rock beddings for horizontal specimens. Shear failures occurred only in intact vertical

specimens (Figure 4.10 (a-1)) at an angle of 60-70° with the horizontal. Soaked specimens showed similar failure trend with no distinct difference for different fluids. However, failures were less brittle than failures in unconfined compression test.

Table 4.5. Triaxial compression strength and strength parameters of Milton Queenston shale in vertical direction and supplementary test results

Specimen No.	Ambient Fluid	Depth (m)	Calcite Content (%)	Dolomite Content (%)	Moisture Content Before Soaking (%)	Moisture Content After Soaking (%)	Pore Salinity Before Soaking (g/L)	Pore Salinity After Soaking (g/L)	Percent Decrease in Pore Salinity (%)	Confining Pressure (MPa)	Triaxial Compression Strength (MPa)	Percentage Decrease in Triaxial Compression Strength	Poisson's Ratio ν_{vh}	Percentage increase in Poisson's Ratio (%)	Elastic Modulus E_v (GPa)	Percentage decrease in Elastic Modulus (%)	Shear Modulus = $E_v / 2(1 + \nu_{vh})$ (GPa)
TXCVT 3	Air	26.01	27.5	2.2	2.60	-	88.7	-	-	2.5	59.200	-	0.322	-	15.130	-	5.722
TXCVT 1	Air	22.80	22.1	2.7	2.49	-	140.8	-	-	5.0	63.255	-	0.259	-	19.240	-	7.641
TXCVT 2	Air	25.30	21.2	7.6	2.59	-	210.8	-	-	10.0	91.870	-	0.225	-	17.500	-	7.143
TXCVT 4	Air	32.09	16.3	4.8	2.26	-	154.6	-	-	20.0	112.360	-	0.217	-	26.908	-	11.055
TXCVT 7	Water	31.82	18.2	4.8	2.74	3.10	174.6	70.9	59	2.5	24.730	58	0.333	3	7.333	52	2.751
TXCVT 6	Water	28.20	20.6	5.9	2.97	3.73	109.2	39.0	64	5.0	25.425	60	0.493	47	6.746	65	2.259
TXCVT 5	Water	32.21	20.5	2.2	2.40	2.85	156.7	101.9	35	10.0	27.941	70	0.270	17	5.184	70	2.041
TXCVT 8	Water	31.98	18.6	4.3	2.65	3.25	141.9	37.2	74	20.0	34.966	68.9	0.300	28	34.000	-26	13.077
TXCVT 9	0.8 % Polymers Solution	23.26	21.0	6.4	2.52	3.10	198.7	122.1	39	2.5	19.987	66	0.368	13	7.368	51	2.693
TXCVT 10	0.8 % Polymers Solution	27.10	26.1	6.2	2.85	3.04	88.5	72.5	18	5.0	25.112	60	0.429	40	12.012	38	4.203
TXCVT 12	0.8 % Polymers Solution	23.09	23.5	11.5	2.48	3.40	171.5	65.2	62	10.0	33.107	64	0.293	23	14.064	20	5.439
TXCVT 11	0.8 % Polymers Solution	29.20	23.6	9.3	2.35	2.51	133.4	85.2	36	20.0	48.644	56.7	0.302	28	25.397	9	9.753
TXCVT 15	8% Bentonite Solution	29.10	16.4	4.5	2.51	3.84	124.9	30.1	76	2.5	19.735	67	0.353	9	4.707	83	1.739
TXCVT 16	8% Bentonite Solution	32.78	15.5	3.2	2.60	3.40	211.5	31.9	85	5.0	20.370	68	0.467	45	3.336	98	1.137
TXCVT 14	8% Bentonite Solution	25.50	25.4	3.0	2.82	2.97	240.8	38.2	84	10.0	23.033	75	0.400	44	24.000	-37	8.571
TXCVT 13	8% Bentonite Solution	23.89	19.3	4.1	2.23	3.56	145.2	31.9	78	20.0	27.186	75.8	0.283	23	3.773	92	1.470

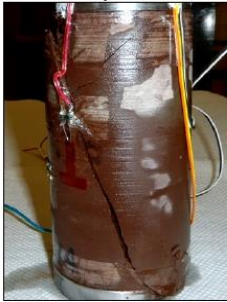
Table 4.6. Triaxial compression strength and strength parameters of Milton Queenston shale in horizontal direction and supplementary test results

Specimen No.	Ambient Fluid	Depth (m)	Calcite Content (%)	Dolomite Content (%)	Moisture Content Before Soaking (%)	Moisture Content After Soaking (%)	Pore Salinity Before Soaking (g/L)	Pore Salinity After Soaking (g/L)	Percent Decrease in Pore Salinity (%)	Confining Pressure (MPa)	Triaxial Compression Strength (MPa)	Percentage Decrease in triaxial Compression strength (%)	Poisson's Ratio (parallel to bedding, ν_h /perpendicular to bedding, ν_{hv})	Percentage Increase in Poisson's Ratio (%)	Elastic Modulus E_h (GPa)	Shear Modulus = $E_h / 2(1 + \nu_h)$ (GPa)
TXCHT 3	Air	21.03	18.4	6.9	3.54	-	73.8	-	-	2.5	36.883	-	0.250 / 0.375	-	50.000	20.000
TXCHT 4	Air	26.30	21.6	4.8	2.98	-	70.4	-	-	5.0	38.477	-	0.313 / 0.328	-	31.269	11.907
TXCHT 5	Air	26.46	22.1	6.1	3.06	-	195.9	-	-	7.5	54.861	-	0.276 / 0.395	-	32.887	12.887
TXCHT 2	Air	20.96	23.5	10.3	3.20	-	151.9	-	-	10.0	58.781	-	0.164 / 0.309	-	47.318	20.326
TXCHT 1	Air	19.05	21.5	12.4	2.47	-	80.5	-	-	15.0	91.042	-	0.211 / 0.253	-	27.419	11.321
TXCHT 6	Air	19.48	33.5	2.3	2.55	-	88.2	-	-	20.0	114.700	-	0.230 / 0.230	-	69.622	28.302
TXCHT 9	Water	21.16	21.9	3.0	2.90	3.70	134.0	50.1	63	2.5	23.932	35	0.259 / 0.324	4 / -14	29.443	16.400
TXCHT 11	Water	26.34	19.9	4.8	2.35	3.51	210.6	55.1	74	5.0	26.949	30	0.286 / 0.393	-9 / 20	66.712	25.938
TXCHT 10	Water	28.35	20.7	5.2	2.55	2.85	148.8	64.5	57	7.5	27.454	64	0.214 / 0.500	-22 / 27	15.704	6.468
TXCHT 12	Water	27.88	19.3	3.4	2.43	3.79	161.6	49.7	69	10.0	37.017	37	0.217 / 0.478	32 / 55	34.741	14.273
TXCHT 8	Water	20.83	23.3	4.5	3.21	3.60	94.9	39.2	59	15.0	38.400	58	0.389 / 0.424	84 / 68	111.127	40.003
TXCHT 7	Water	19.08	25.3	2.3	2.22	2.95	141.2	58.6	59	20.0	69.821	40	0.311 / 0.335	35 / 31	33.593	12.812
TXCHT 13	0.8 % Polymers Solution	19.23	22.1	9.8	2.80	2.99	80.3	59.9	25	2.5	32.216	13	0.239 / 0.392	-4 / 5	21.752	8.778
TXCHT 17	0.8 % Polymers Solution	27.95	19.0	7.5	2.13	2.68	105.3	61.6	41	5.0	34.138	11	0.320 / -	2 / -	160.000	60.606
TXCHT 14	0.8 % Polymers Solution	20.88	22.0	6.3	3.18	3.32	70.9	51.1	28	7.5	44.288	19	0.416 / 0.444	51 / 12	832.250	293.874
TXCHT 18	0.8 % Polymers Solution	19.53	32.9	2.9	2.35	2.75	95.7	64.2	33	10.0	50.669	14	0.385 / 0.423	135 / 37	153.909	55.563
TXCHT 15	0.8 % Polymers Solution	26.38	26.9	10.7	2.53	2.80	77.0	55.9	27	15.0	62.113	32	0.286 / 0.381	36 / 51	26.205	10.189
TXCHT 16	0.8 % Polymers Solution	27.53	23.6	9.3	2.35	2.51	133.4	85.2	36	20.0	71.635	38	0.378 / 0.378	64 / 64	1188.000	431.060

Continued

TXCHT 20	8% Bentonite Solution	21.01	21.7	5.0	2.50	3.34	76.4	14.1	82	2.5	16.713	55	0.323 / 0.355	29 / -5	27.121	10.250
TXCHT 22	8% Bentonite Solution	27.56	21.1	6.8	2.41	2.68	95.0	26.0	73	5.0	28.052	27	0.211 / 0.268	-33 / -18	25.751	10.632
TXCHT 21	8% Bentonite Solution	26.42	21.2	5.0	2.54	3.37	161.9	36.6	77	7.5	34.706	37	0.385 / 0.423	39 / 16	67.335	24.309
TXCHT 19	8% Bentonite Solution	19.30	24.4	12.5	2.01	2.69	141.4	37.2	74	10.0	45.335	23	0.370 / 0.370	126 / 20	18.500	6.752
TXCHT 24	8% Bentonite Solution	19.58	26.0	2.0	2.10	2.90	76.4	19.0	75	15.0	55.183	39	0.259 / 0.353	23 / 40	29.424	11.685
TXCHT 23	8% Bentonite Solution	28.06	19.3	4.1	2.23	3.56	145.2	31.9	78	20.0	60.765	47	0.262 / 0.299	14 / 30	39.739	15.744

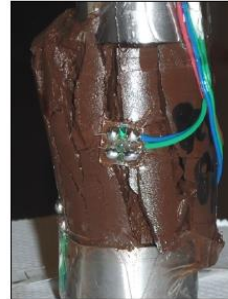
a) Intact specimen:



1) Vertical strength test

2) Horizontal strength test

b) Specimen soaked in water:



1) Vertical strength test

2) Horizontal strength test

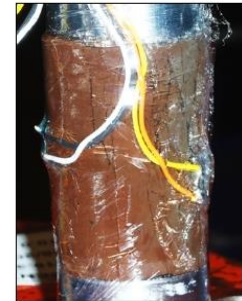
c) Specimen soaked in polymer solution:



1) Vertical strength test

2) Horizontal strength test

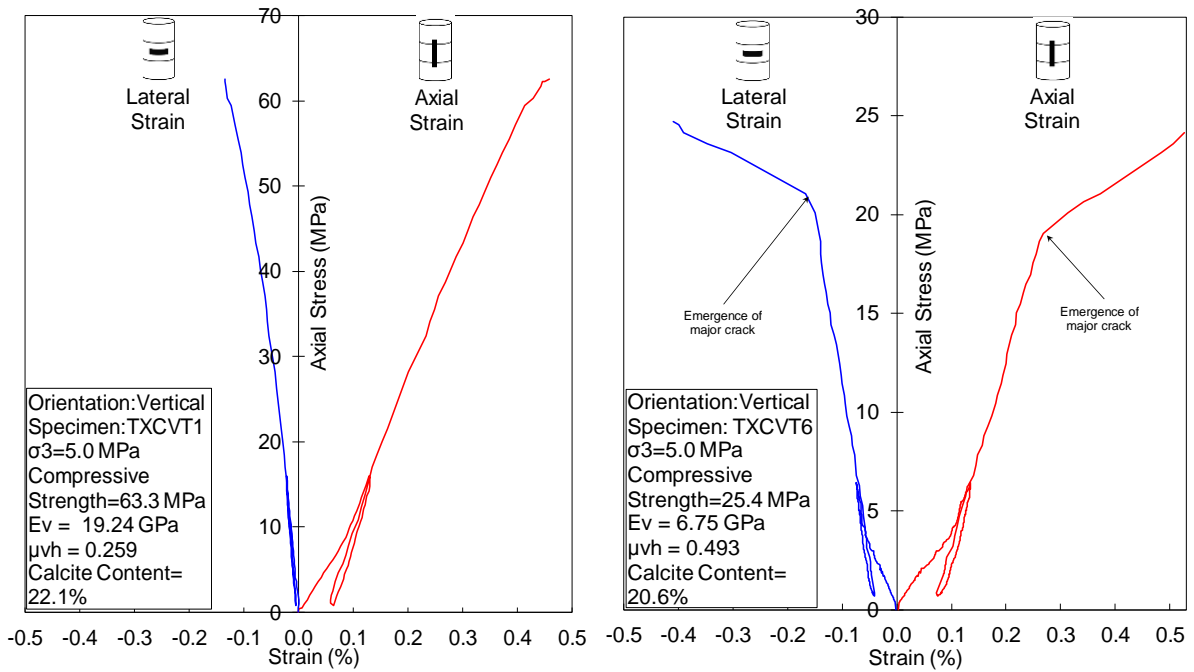
d) Specimen soaked in bentonite solution:



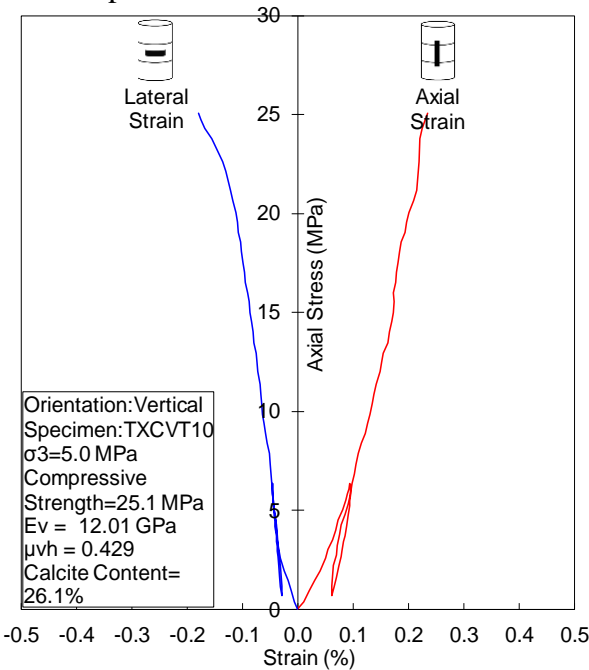
1) Vertical strength test

2) Horizontal strength test

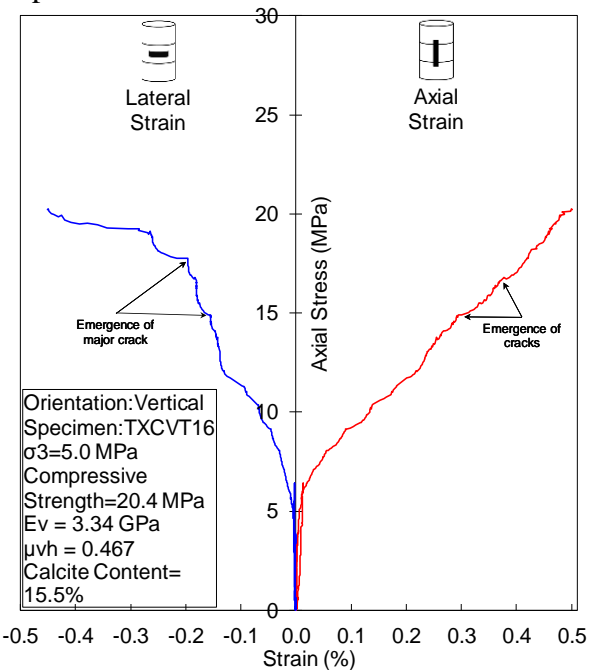
Figure 4.10. Triaxial compressive strength test performed on: (a) intact specimens and specimens soaked for hundred days in: (b) water; (c) polymer solution and (d) bentonite solution; (1) vertical specimens, (2) horizontal specimen.



Intact specimen



Specimen soaked in water



Specimen soaked in polymer solution

Specimen soaked in bentonite solution

Figure 4.11. Results of triaxial compression strength performed on vertically cored Milton Queenston shale specimens at $\sigma_3=5.0$ MPa: (a) intact specimen; specimens soaked for hundred days in: (b) water, (c) polymer solution and (d) bentonite solution, respectively.

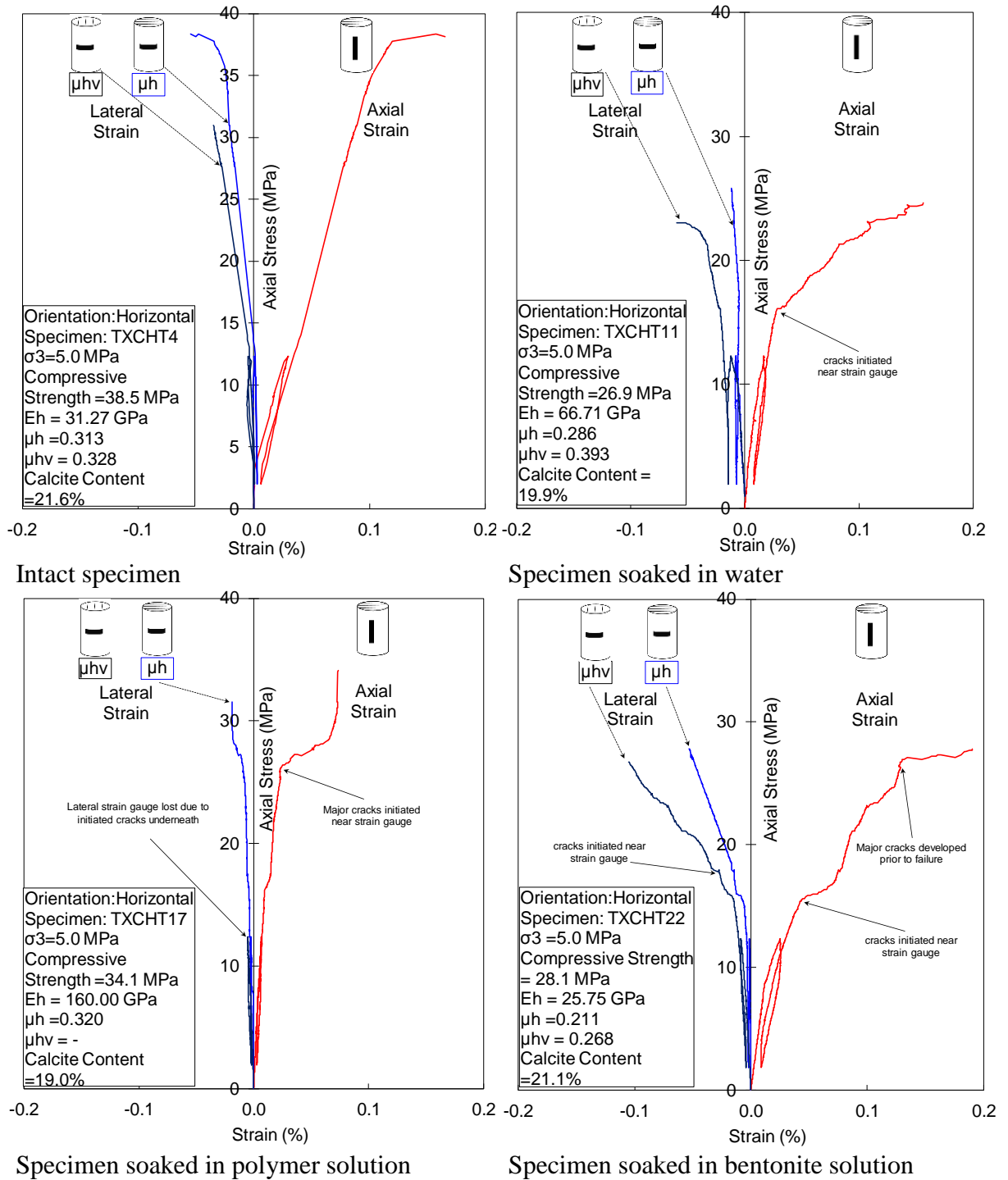
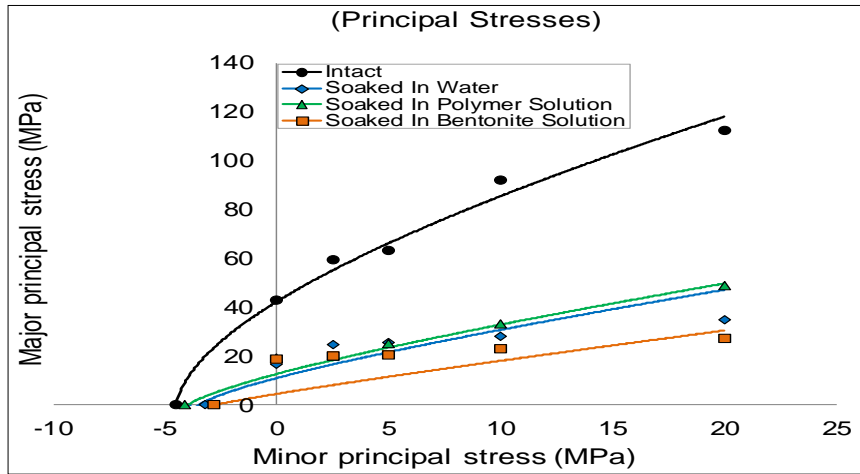


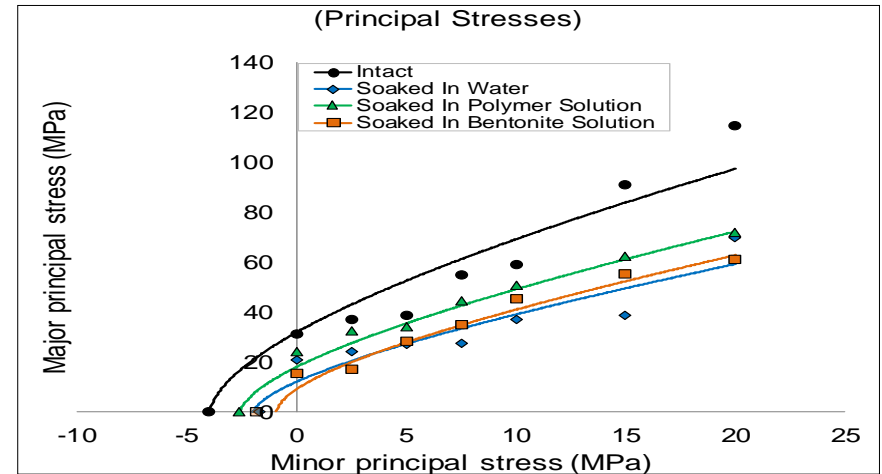
Figure 4.12. Results of triaxial compression strength performed on horizontally cored Milton Queenston shale specimens at $\sigma_3 = 5.0$ MPa: (a) intact specimen; specimens soaked for hundred days in: (b) water, (c) polymer solution and (d) bentonite solution, respectively.

4.6 CONSTRUCTING STRENGTH ENVELOPES OF MILTON QUEENSTON SHALE

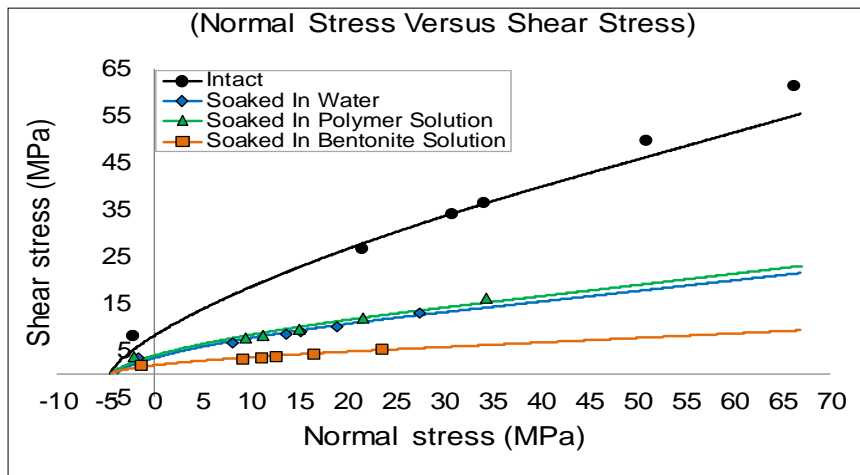
The measured strength of Milton Queenston shale from the comprehensive test program performed in this research was used to develop strength envelopes of Milton Queenston shale in the vertical and horizontal directions utilizing RocLab software. The strength envelopes were developed for intact Milton Queenston shale and for Milton Queenston shale after being exposed for 100 days to water, polymer solution and bentonite solution. The change in Milton Queenston shale strength with increasing the confining pressure is presented in the form of principal stresses in Figure 4.13. The solid curves in this figure represent the strength envelopes of Milton Queenston shale developed using RocLab software while the solid points represent measured values from the test program performed in this research. The developed strength envelopes represent peak strength of Milton Queenston shale in both tension and compression states. It can be revealed that the change in strength of Milton Queenston shale after soaking in water and lubricant fluids is generally more evident in the vertical direction (Figure 4.13 (a)). The decrease in Milton Queenston shale strength after soaking in water and lubricant fluids was less in the horizontal direction (Figure 4.13 (b)) than the decrease in strength in the vertical direction (Figure 4-13 (a)). Strength envelope of Milton Queenston shale after soaking in polymer solution was relatively higher compared to other fluids. The strength envelopes for Milton Queenston shale after being exposed to water and lubricant fluids show significant variation in the strength compared to intact rock strength. These findings are consistent with those observed by Wasantha and Ranjith (2014); Liang et al. (2012); and Lo et al. (1979). These findings should be useful for the design of infrastructure constructed in these shales. It is clearly indicated in the strength envelopes developed for Milton Queenston shale that a considerable amount of the strength of these shales can be lost after the exposure to water and lubricant fluids. The minimal impact on the strength of Milton Queenston shale was caused by polymer solution compared to water and bentonite solution. By developing these strength envelopes, it is quite clear that adopting the intact strength envelope of Milton Queenston shale may lead to overestimation of the



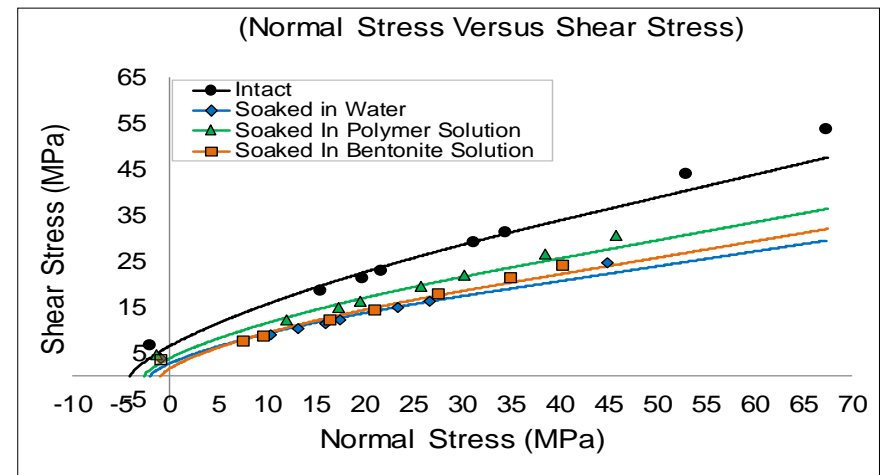
Strength envelopes in the vertical direction



Strength envelopes in the horizontal direction



c) Strength envelopes in the vertical direction



d) Strength envelopes in the horizontal direction

Figure 4.13. Strength envelopes of Milton Queenston shale (Intact and after soaking in water; polymer solution and bentonite solution): (a, b) principal stresses; (c, d) normal and shear stresses.

rock strength in the zone influenced by water or lubricant fluids, which in turn may lead to less accurate design of structures built in these shales. One of the limitations of the performed strength tests and their results is the lack of confinement on the tested samples during soaking period compared to the rock condition in-situ.

4.7 SUMMARY AND CONCLUSIONS

As part of a research to investigate the feasibility of micro-tunneling technique in Queenston shale of southern Ontario, a comprehensive test program was conducted on Milton Queenston shale utilizing Brazilian split; direct tension; unconfined compression and triaxial compression tests. These tests were performed on vertical and horizontal specimens with respect to rock beddings to account for strength anisotropy. Specimens were divided into four groups in both directions prior to perform the aforementioned tests: intact (i.e. as received from site), and soaked for 100 days in water; polymer solution and bentonite solution. Total of 101 tests were performed on Milton Queenston shale and results were used in RocLab software to develop the strength envelopes in both directions for the four cases. The developed strength envelopes can be used to represent the strength of Milton Queenston shale in vertical and horizontal directions, at any confining stress (i.e. horizontal in-situ stress) up to 20 MPa, for the affected zone by water and lubricant fluids, and the unaffected zone. These strength envelopes can lead to more accurate design of structures built in Milton Queenston shale. From this study, the following conclusions can be drawn:

- 1) Milton Queenston shale showed a significant decrease in its strength after soaking in water; bentonite solution and polymer solution. This finding is consistent with that reported in the literature for similar shales in southern Ontario (Lo et al. 1979) and for other type of rocks in other parts of the world (Wasantha and Ranjith 2014 and Liang et al. 2012).
- 2) Milton Queenston shale kept exhibiting the anisotropic strength behaviour after soaking in water; bentonite solution and polymer solution. With respect to rock

beddings, the strength of intact Milton Queenston shale in vertical direction is greater than the strength in horizontal direction, while the reverse is true after soaking.

- 3) The compression failure of Milton Queenston shale was in general brittle indicating tension failure occurred in weak bonds across rock beddings in the vertical direction, and along rock beddings in horizontal direction.
- 4) Poisson's ratio increased in both vertical and horizontal directions while elastic modulus and shear modulus decreased after soaking Milton Queenston shale in water; bentonite solution and polymer solution.
- 5) Among fluids used in this research, polymer solution caused the least decrease in strength of Milton Queenston shale, while bentonite solution caused slightly higher decrease in the strength compared to water.
- 6) The developed strength envelopes of Milton Queenston shale in both vertical and horizontal directions were found to be considerably influenced by the exposure to water and lubricant fluids. The developed strength envelopes can provide a clear insight of the amount of Milton Queenston shale strength that can be lost due to the continuous exposure to water and lubricant fluids. However, the extent of influence of water and lubricant fluids into these shales needs further investigation.

4.8 REFERENCES

- Al-Maamori, H.M.S., El Naggar, M.H., and Micic, S. 2014. A compilation of the geo-mechanical properties of rocks in Southern Ontario and the neighbouring regions. *Open Journal of Geology*, **4**: 10-27.
- Al-Maamori, H.M.S., El Naggar, M.H., Micic, S., and Lo, K.Y. 2016. Influence of lubricant fluids on swelling behaviour of Queenston shale in southern Ontario. *Canadian Jeotechnical Journal*, , **53** (7): 1059-1080.
- ASTM- D7012, 2010. Standard test method for compressive strength and elastic moduli of intact rock core specimens under varying states of stress and temperatures. ASTM International, West Conshohocken, Pa.

- ASTM- D2216, 2010. Standard Test Methods for Laboratory Determination of Water (Moisture) Content of Soil and Rock by Mass. ASTM International, West Conshohocken, Pa.
- ASTM- D2936, 2008. Standard test method for direct tensile strength of intact rock core specimens. ASTM International, West Conshohocken, Pa.
- ASTM- D3967, 2008. Standard test method for splitting tensile strength of intact rock core specimens. ASTM International, West Conshohocken, Pa.
- ASTM-D4543, 2008. Standard practices for preparing rock core as cylindrical test specimens and verifying conformance to dimensional and shape tolerances. ASTM International, West Conshohocken, Pa.
- Baud, P., Zhu, W., Wong, T., 2000. Failure Mode and Weakening Effect of Water on Sandstone. *Journal of Geophysical Research*, **105**: 16371–16389.
- Claesson, J., and Bohloli, B. 2002. Brazilian test: stress field and tensile strength of anisotropic rocks using an analytical solution. *International Journal of Rock Mechanics and Mining Sciences*, **39**: 991-1004.
- Colback, P.S.B., Wiid, B.L., 1965. The Influence of Moisture Content on the Compressive Strength of Rock. *Rock Mechanics Symposium, Ottawa 1965*. University of Toronto, Department of Mines and Technical Surveys, pp. 65–84.
- Dan, D.Q., Konietzky, H., and Herbst, M. 2013. Brazilian tensile strength tests on some anisotropic rocks. *International Journal of Rock Mechanics and Mining Sciences*, **58**: 1-7.
- Dreimanis, A. 1962. Quantitative Gasometric Determination of Calcite and Dolomite By Using Chittick Apparatus. *Journal of Sedimentary Petrology*, **32** (3): 520 - 529.
- Gorski, B., Conlon, B., Ljunggren, B., and AB, T. 2007. Determination of the direct and indirect tensile strength on cores from borehole KFM01D. Forsmark Site Investigation Report ISSN 1651-4416, SKB P-07-76, AP PF 400-06-067.

CANMET-MMSL, Mining and Mineral Sciences Laboratories, Natural Resources Canada, Svensk Kärnbränslehantering AB, Swedish Nuclear Fuel and Waste Management Co, Stockholm, Sweden.

- Lee, Y.N. 1988. Stress-strain-time relationship of Queenston shale. Ph.D. thesis, Civil and Environmental Engineering Department, The University of Western Ontario, London, Ontario.
- Lee, Y.N., and Lo, K.Y. 1993. The swelling mechanism of Queenston shale. Tunnelling Association of Canada Annual Publication. Canadian Tunnelling, pp. 75-97.
- Liang, W., Yang, X., Gao, H., Zhang, C., and Zhao, Y. 2012. Experimental study of mechanical properties of gypsum soaked in brine. International Journal of Rock Mechanics and Mining Sciences, **53**: 42-50. doi:10.1016/j.ijrmms.2012.05.015.
- Lo, K.Y., and Hori, M. 1979. Deformation and strength properties of some rocks in Southern Ontario. Canadian Geotechnical Journal, **16** (1): 108-120. doi: 10.1139/t79-010.
- Lo, K.Y., Cooke, B.H., and Dunbar, D.D. 1987. Design of buried structures in squeezing rock in Toronto, Canada. Canadian Geotechnical Journal, **24** (2): 32-41. doi: 10.1139/t87-028.
- Lo, K.Y., Devata, M., Yuen, C.M.K. 1979. Performance of shallow tunnel in a shaly rock with high horizontal stresses. Tunnelling '79, Proceedings of the Second International Symposium on Tunnelling. Institution of Mining and Metallurgy, London, England, Paper 9, pp. 1-12.
- Lo, K.Y., Yung, T.C.B., Lukajic, B. 1987. A field method for the determination of rock-mass modulus. Canadian Geotechnical Journal, **24** (3): 6-13. doi: 10.1139/t87-051.

- Lo, K.Y., Ogawa, T., Lukajic, B., and Dupak, D.D. 1991. Measurements of strength parameters of concrete-rock contact at the dam-foundation interface. *Geotechnical Testing Journal*, **14** (4): 83-94. Url: <http://worldcat.org/issn/01496115>.
- Neville, A.M. 1996. *Properties of Concrete*. 4th edition, Pearson Education Limited, Harlow, England.
- Paterson, M.S. 1978. *Experimental Rock Deformation: The Brittle Field*. Springer-Verlag, Berlin.
- Paterson, M.S., and Wong, T.F. 2005. *Experimental Rock Deformation - The Brittle Field*, 2nd Edition. Springer-Verlag, Berlin, Heidelberg, New York. doi:10.1017/S0016756806242973.
- Wai, R.S.C., Lo, K.Y., and Rowe, R.K., 1981, Thermal stresses in rocks with nonlinear properties. Research report, Faculty of Engineering Science, The University of Western Ontario, GEOT-8-81.
- Wasantha, P.L.P., Ranjith, P.G. 2014. Water-weakening behavior of Hawkesbury sandstone in brittle regime. *Engineering Geology*, **178**: 91-1. doi:10.1016/j.enggeo.2014.05.015.

Chapter 5

STRENGTH ENVELOPES OF NIAGARA QUEENSTON SHALE UNDER DIFFERENT WETTING CONDITIONS UTILIZING MULTISTAGE TRIAXIAL COMPRESSION TEST⁴

5.1 INTRODUCTION

In micro-tunneling technique, bentonite solution and polymer solution are used as lubricant fluids to facilitate the installation of tunnel and/or pipeline segments. The construction period in micro-tunneling applications may last for several weeks depending on ground conditions and the run distance between successive shafts. On the one hand, the lubricant fluids used in this application may remain around the tunnel/ pipeline for a period of time, allowing for time-dependent deformation of Queenston shale to occur prior to replacing them with cement grout permanently (Lo et al. 1987). On the other hand, the existence of lubricant fluids and water may influence the strength of the excavated exposed swelling rock. Lee and Lo (1993) stated that the time-dependent deformation behaviour of Queenston shale is associated with developing micro-cracks. These micro-cracks may influence the strength of affected shales. Al-Maamori et al. (2016) found that lubricant fluids used in micro-tunnelling applications and water can have different influence on the micro-structure of the Queenston shale and the resulting swelling deformations. These fluids caused different amounts of osmosis and diffusion to occur within the Queenston shale. The pressurized pore water in these micro-cracks weakens the rock skeleton as it decreases its effective strength (Colback and Wiid 1965, Paterson, 1978, Baud et al., 2000, Paterson and Wong, 2005, Alkan et al., 2007, Heap et al., 2009, Yang et al., 2011, Liang et al. 2012 and Wasantha and Ranjith 2014). The strength weakening was also observed in some rock in southern Ontario, such as the

⁴ A version of this chapter has been submitted for publication in the Canadian Geotechnical Journal in March, 2016.

Georgian Bay shales in Heart Lake Tunnel through field investigations where results of unconfined compression tests performed on samples collected after 24 years of tunnel operation showed significant decrease compared to their strength at the time of tunnel construction (Lo et al. 1979 and Lo 2005).

Multistage triaxial compression test is used when no sufficient rock samples are available to perform the single stage triaxial compression test, or to eliminate the variation in rock samples. Heuze (1967) justified results of multistage triaxial compression test performed on Chino limestone and found a good agreement with those obtained from single stage triaxial tests. Kovari and Tisa (1975) concluded that the decrease in the peak strength of different types of Buchberg sandstone and Carrara marble was practically negligible when increased subsequent failure states in multistage triaxial compression test. Kim and Ko (1979) performed multistage triaxial compression test successfully on ductile and somewhat brittle rock such as Pierre shale and Raton shale. Bro (1997) proposed an approach to analyze multistage triaxial compression test results of rocks with strain hardening behaviour.

Youn and Tonon (2010) suggested radial strain control to predict the imminent failure strength of each loading stage in multistage triaxial compression test of brittle rocks, such as Edwards limestone that tend to suddenly fragment without displaying any failure warning. The suggested approach gave good approximation to the single-stage triaxial tests. Yang, S.-Q, 2012 studied the strength of red sandstone and proposed a correlation to predict its single-stage triaxial strength from multistage triaxial strength test results. Hashiba and Fukui (2014) successfully combined multistage triaxial compression and alternating loading rate for testing small rock samples. It can be concluded from earlier research that multistage triaxial compression test can be performed on various types of rocks varying from strong rock such as marble and limestone to weak rock such as shales. However, using multistage triaxial compression test has to be examined for its suitability for testing the Queenston shale. Since this test requires less samples compared to the traditional single stage triaxial test, the prudent selection of the test sample is crucial.

Moreover, the correct identification of the imminent peak strength at each loading stage is the key parameter to perform a successful multistage triaxial compression test.

5.1.1 Objectives and Scope of Work

The evaluation of strength weakening is important to assess the strength of Niagara Queenston shale in the close vicinity of underground excavation, which should lead to better design of the hosted infrastructure. In this research, the strength weakening of Niagara Queenston shale due to the influence of water and lubricant fluids used in micro-tunneling applications is investigated. Multistage triaxial compression test is performed on Niagara Queenston shale before and after soaking in water and lubricant fluids using the modified triaxial cell. Brazilian split test; unconfined compression test and direct tension test are also conducted on the rock specimens. These tests were performed on vertical samples (i.e. in the direction perpendicular to the rock bedding). The strength envelopes of Niagara Queenston shale are constructed before and after soaking in water and lubricant fluids and the results are amply discussed.

5.2 TEST PROGRAM AND PROCEDURE

Queenston shale samples from the Niagara region in southern Ontario were tested in this research in four conditions:

- 1) As received from site, with their preserved natural moisture content, denoted herein as intact specimens.
- 2) Samples soaked in water for 100 days.
- 3) Samples soaked in bentonite solution for 100 days, and
- 4) Samples soaked in polymer solution for 100 days.

Many samples of Niagara Queenston shale are required to perform the ordinary single stage triaxial compression tests necessary to establish the strength envelope of this shale. Alternatively, the multistage triaxial compression test can be used as the testing

program would require fewer specimens in this case. In multistage triaxial test, one specimen can be tested under different values of confining pressure and measure the corresponding peak strength. In cases where rock samples are limited, this test is practically valuable to facilitate completing the testing program. In addition, it reduces cost and time compared to ordinary single stage triaxial compression test. Therefore, multistage triaxial compression test was utilized in combination with unconfined compression test, Brazilian split test and direct tension test in this study to define the strength envelopes of Niagara Queenston shale.

The Niagara Queenston shale samples used in this study were collected from single borehole drilled from the invert of Niagara Tunnel at its lowest part, approximately 3.00 m to 12.00 m depth (i.e. 125 m to 137 m below the ground level). The test specimens were cut and prepared using diamond cutting saw in accordance with ASTM-D4543(2008). All test specimens had 62 mm diameter as they were drilled from the borehole. The test specimen's length/diameter ratio was maintained to be 2 for multistage triaxial compression test; unconfined compression test and direct tension test while for Brazilian split test the thickness/diameter ratio was between 0.2 and 0.75.

To preserve specimens during soaking period, they were wrapped with a layer of screen wire mesh, followed by several longitudinal and transverse winding layers of fish wire of 60-pounds line. Specimens were then kept separately submerged in water; bentonite solution and polymer solution, for 100 days. This period was selected where it may fairly represent a long construction period in micro-tunneling technique applications.

Bentonite and polymer solutions were prepared with similar proportions to those used in micro-tunneling process in the field. Bentonite solution was prepared by mixing 8% of dry powder, sodium bentonite clay type (HYDRAUL-EZ) from CETCO-USA with tap water using high speed mixer. Polymer solution was produced by mixing tap water, using a high speed mixer, with 0.8% of liquid polymer concentrate type (TK60, anionic polyacrylamide suspension in a water-in-oil emulsion) from Morrison Mud, Division of Mudtech Ltd.-UK.

The Brazilian split test was performed in correspondence with ASTM-D3967 (2008), while the unconfined compression test performed according to ASTM-D7012

(2010). The procedure described in ASTM-D2936 (2008), and Lo et al. (1991) was followed in the direct tension test. The multistage triaxial compression test was performed according to ASTM-7012 (2010).

The triaxial cell used in this research was fabricated earlier in the Geotechnical Research Centre at the University of Western Ontario to evaluate rock strength parameters (Lo et al. 1991). In this research, the triaxial cell was modified to facilitate high confining pressure and its adjustment during the test, if required, and to test rock specimen of different sizes and ensure specimen centricity on the cell pedestal. Figure 5.1 shows the triaxial cell, which consists of: hardened steel body to endure high confining pressure; piston that moves freely in the vertical direction to apply the vertical pressure, and can be removed to place the rock specimen; inlet junction to add confining fluid; main and needle valves for confining pressure adjustment; and hydraulic jack to supply confining pressure fluid. The following additional pieces were added to upgrade the cell: i) multistep adjusting seat; ii) multistep cap; iii) specimen's platen; iv) pressure transducer type AST4000A10000PAD0000 (from American Sensor Technology, USA) to measure confining pressure up to 70 MPa with an accuracy of $\pm 0.5\%$; and v) eight wires sealing gland with Teflon sealant (type MCH4 from Conax Technologies, USA) to pass wires of electronic foil strain gauges to the computer data logger. By adding parts (i, ii, iii) it became possible to keep the triaxial cell assembled throughout the test program. The rock specimen can be seated in the centre of the cell from the top after removing the piston only, which saves a lot of time and efforts for test setup. Dielectric transformer oil (type MODEF60 from Aevitas Inc., Canada) was used as ambient fluid to overcome bare connections in the foil strain gauges lead wires and the sealing gland.

The vertical and horizontal strains of the test specimen were measured using electronic foil strain gauges (type N11-FA-10-120-11 from SHOWA Measuring Instruments Company Ltd., Japan). Instant adhesive (type Loctite 454 from Loctite Corporation North American Group, USA) was used to glue the electronic foil strain gauges on opposite sides of each test specimen in T-shape arrangement.

In the multistage triaxial compression test, samples were cut to length/diameter ratio of 2. The diameter of samples was 62 mm as they were drilled in the borehole.

During the test, the specimen is subjected to constant confining pressure in each stage while the axial loading is gradually increased with constant displacement rate until the peak strength is achieved. At the end of each stage, the displacement-controlled loading is kept unchanged while the confining pressure is increased gradually to the second level. Upon reaching the second level of confining pressure, it is kept unchanged and the displacement-controlled loading is resumed applying axial loading at the same displacement rate until the second peak strength is reached. This procedure was repeated six times to measure the peak compressive strength of Niagara Queenston shale that corresponded to confining pressures of 2.5, 5.0, 7.5, 10.0, 15.0, and 20.0 MPa. These confining pressures were selected to be within the range of in-situ horizontal stress in Niagara Queenston shale (see Chapter 2). The axial and lateral deformation curves of the test specimen were carefully monitored during each stage of loading. When the vertical deformation curve plateaued, the strength was recorded as the peak strength corresponding to this level of confining pressure. Following this procedure, several peak strength values for the same specimen were measured under different values of confining pressure. Using values of peak strength measured from multistage triaxial compression test in addition to unconfined compression test; Brazilian split test and direct tension test result, the full strength envelope that covers a wide range

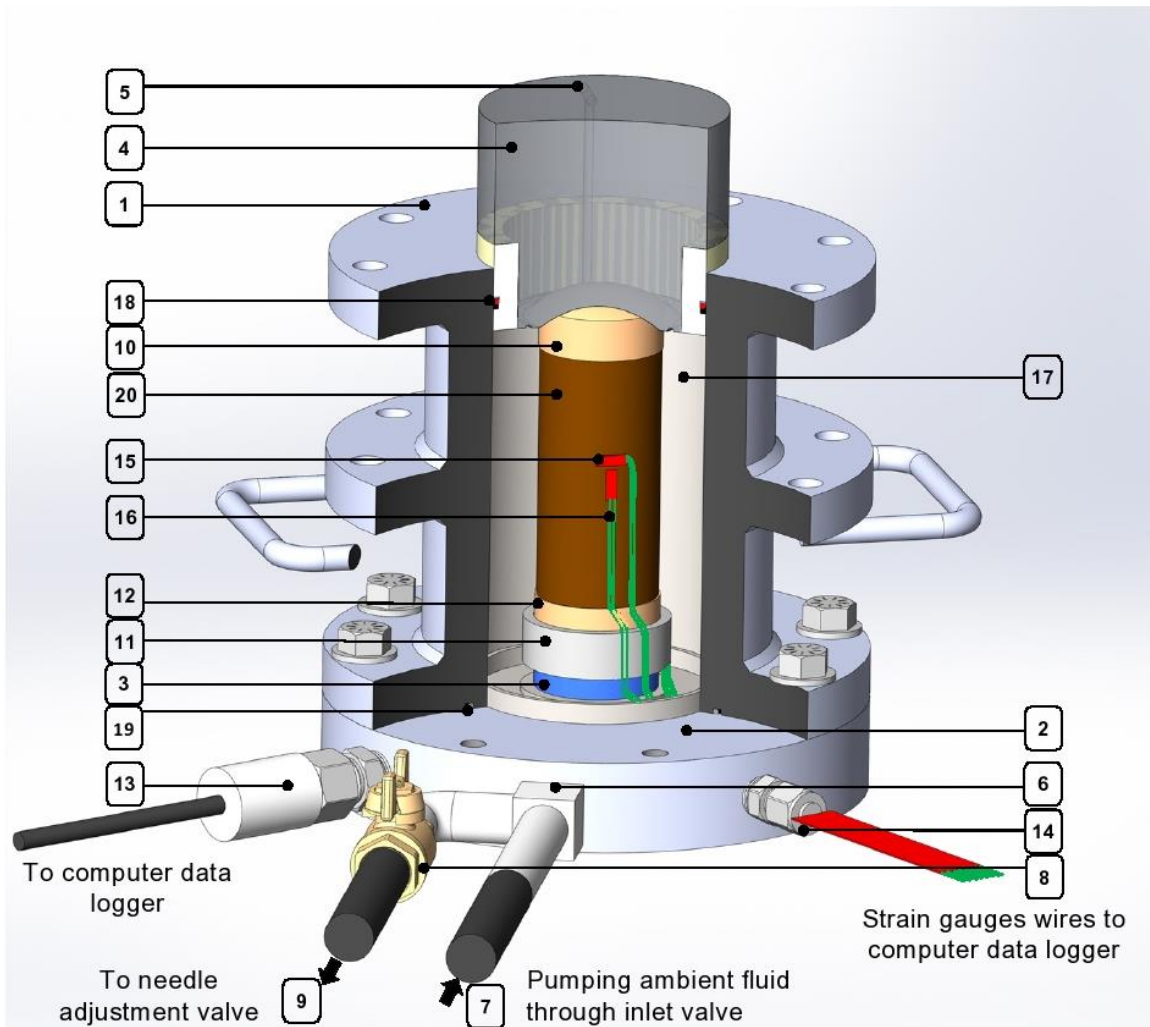


Figure 5-1. Longitudinal section in the modified triaxial cell: (1) cell body; (2) cell base; (3) central pedestal; (4) piston; (5) ventilation valve; (6) inlet/outlet junction; (7) one-way inlet valve; (8) main adjustment valve; (9) needle adjustment valve; (10) specimen's cap; (11) adjusting seat; (12) specimen's platen; (13) pressure transducer; (14) sealing gland; (15) electronic foil strain gauge; (16) strain gauge wires; (17) cell chamber; (18) rubber washer and stopper; (19) rubber casket and (20) rock specimen.

of confining pressure was developed for Niagara Queenston shale before and after soaking in water and lubricant fluids.

In addition to the strength tests, supplementary tests, including: x-ray diffraction analyses, calcite content, moisture content, and rock pore fluid salinity were performed on Niagara Queenston shale. The x-ray diffraction analyses were performed to identify the mineralogical composition of Niagara Queenston shale in the tested samples. The moisture content test was performed according to ASTM 2216 (2010). Rock pore fluid salinity was evaluated according to the procedure described in Lee (1988), while the calcite content was measured by Chittick carbon dioxide apparatus and following the procedure described in Dreimanis (1962). Both moisture content and rock pore fluid salinity were measured before and after soaking Niagara Queenston shale specimens in water and lubricant fluids in order to evaluate the change in their rock pore fluid salinity.

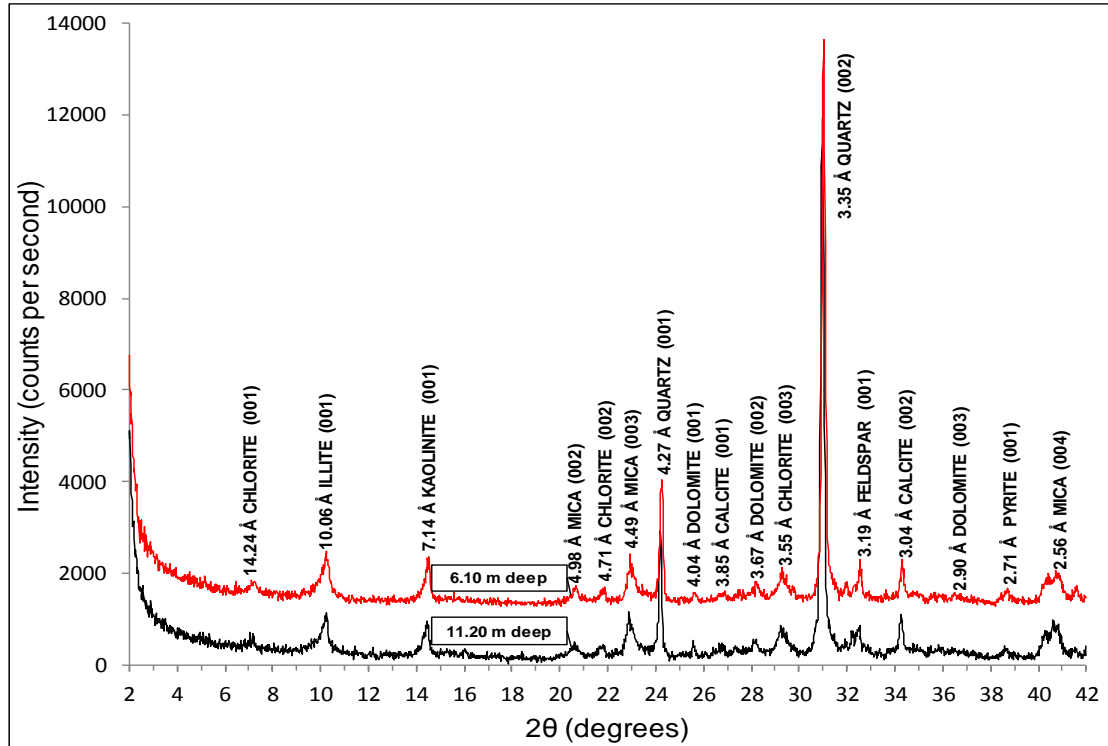
5.3 RESULTS AND DISCUSSION

5.3.1 X-Ray Diffraction Analyses

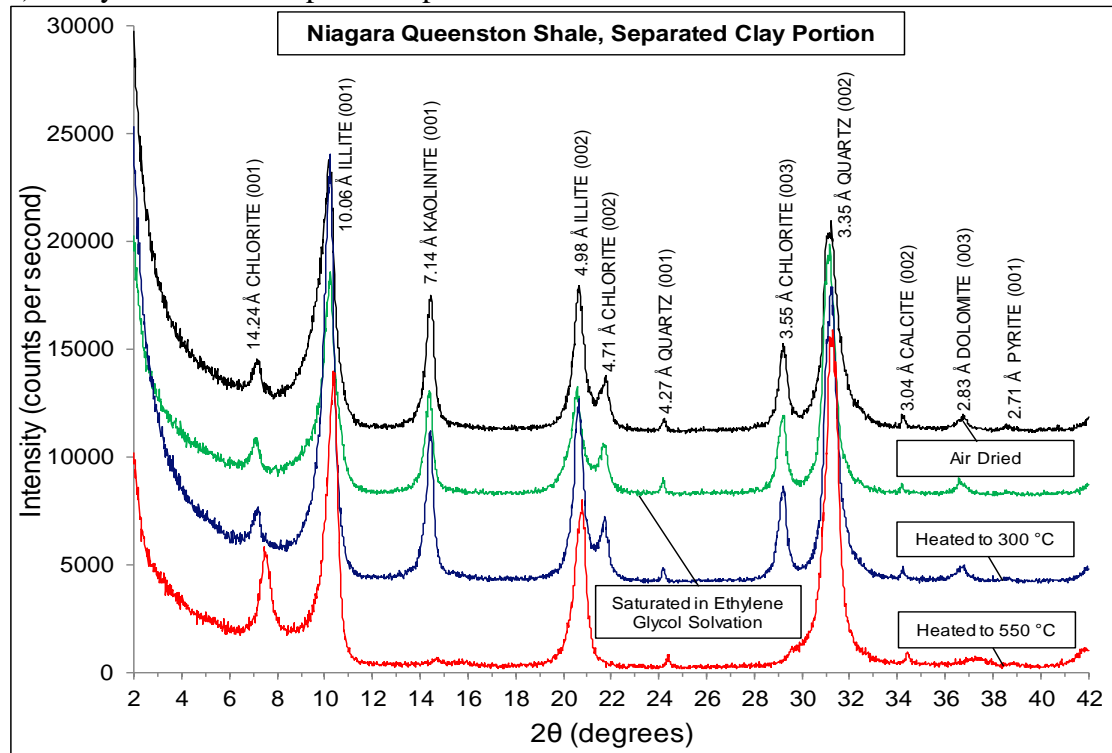
The mineralogical composition of Niagara Queenston shale was determined using the x-ray diffraction analyses. These analyses were performed on two samples of Niagara Queenston shale collected at 6.10 m and 11.20 m depth from the borehole in Niagara tunnel used in this research. The x-ray diffraction analyses were performed on randomly oriented powder (i.e. bulk) specimens and on oriented clay minerals (i.e. wet) specimens of the separated clay-size portion only. These analyses identified the minerals composition of Niagara Queenston shale. The traces of x-ray diffraction analyses on both types of analyses are shown in Figure 5.2 and the analyses results are summarized in Table 5.1.

Table 5.1. Mineralogical composition of Niagara Queenston shale

Sample Depth (m)	Chlorite (%)	Illite (%)	Kaolinite (%)	Quartz (%)	Feldspar (%)	Calcite (%)	Dolomite (%)	Pyrite (%)
6.1	1.6	23.0	1.8	56.7	2.8	8.1	2.4	3.6
11.2	1.4	16.3	1.9	59.7	5.5	9.4	3.2	2.6
Range (%)	1.4 - 1.6	16.3 - 23.0	1.8 - 1.9	56.7 - 59.7	2.8 - 5.5	8.1 - 9.4	2.4 - 3.2	2.6 - 3.6



a) X-ray traces of bulk powder specimens



b) X-ray traces of clay-size portion specimens

Figure 5.2. X-ray diffraction traces of Niagara Queenston shale powder: (a) Bulk powder specimens; (b) Separated clay-size portions specimens.

The calcite content has a significant effect on the strength and time-dependent deformation of Queenston shale upon exposure to water (Lo et al. 1987). Other minerals, such as anhydrite and gypsum expand in volume upon exposure to water and can result in high time-dependent deformation of this shale. The time-dependent deformation of shales from southern Ontario was found to be associated with developing micro cracks in the rock skeleton (Lee and Lo 1993). Therefore, the more time-dependent deformation of Niagara Queenston shale during soaking process would cause higher weakening to these shales. Table 5.1 shows that no significant swelling clay minerals were found in Niagara Queenston shale. Calcite content was found to be between 8.1 % and 9.4 %. Within this minimal variation in the calcite content; chlorite content and other clay minerals in the tested Niagara Queenston shale, it is not expected to have an influence on their strength other than soaking in water and lubricant fluids.

5.3.2 Development of Micro Cracks

The development of micro cracks in the Queenston shale due to its swelling effects is presented in Figure 5.3. The scanning electron microscopy images taken near the surface of intact Queenston sample are shown in Figure 5.3 (a), while Figures 5.3 (b,c,d) show SEM images of near the surface of Queenston shale samples after been soaked for 100 days in water, polymer solution and bentonite solution. It is clearly indicated that the surface of intact sample is free from micro cracks. However, micro cracks can be easily noted in the surface of soaked samples. These micro cracks were generated in the Queenston shale micro structure due to the swelling effects (Al-Maamori et al, 2016 and Lee and Lo, 1993). The size and intensity of the generated micro cracks in the soaked samples is different in the fluids used. Water caused the largest micro cracks compared to other fluids and it also caused an increase of the size of micro pores, as indicated in Figure 5.3 (d). These effects may cause a decrease in the strength of the soaked Queenston shale. The effects of bentonite solution on the micro structure of Queenston shale was less than the effect of water. However, it also caused micro cracks that are big in size, which may influence the strength of the soaked shale.

,The minimal impact of soaking effects can be noted in the sample soaked in polymer solution (Figure 5.3 (b)). Compared to other fluids used, polymer solution caused micro cracks that are smaller in size and the Queenston shale micro structure seems to be still more intact. Based on these images and the observed developed micro cracks due to soaking effects under different fluids, it can be assumed that polymer solution may cause the lesser impact, bentonite solution may cause moderate impact, while water may cause the higher impact on the strength of the Queenston shale. This assumption is made based on the fact of development of micro cracks in the micro structure of the Queenston shale due to its swelling behaviour (Lee and Lo, 1993) and the observations made from Figure 5.3. This assumption is used throughout the discussion of the following sections.

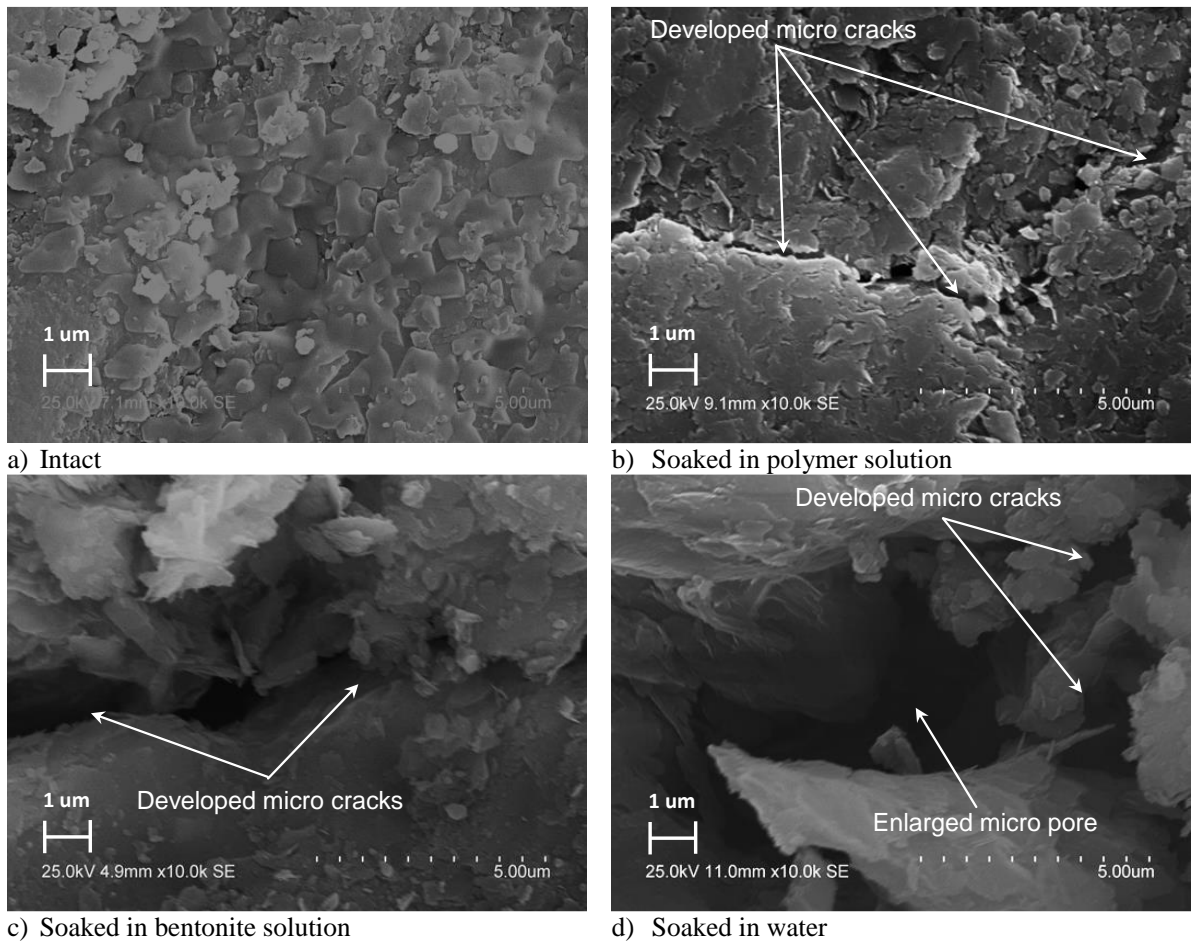


Figure 5.3. Scanning electron microscopy images on horizontal sections of Queenston shale before and after soaking for 100 days in water, polymer solution and bentonite solution.

5.3.3 Brazilian Split Strength

The Brazilian split strength results of Niagara Queenston shale are presented in Table 5.2. This table shows the average strength of three tests of Niagara Queenston shale before and after soaking in water and lubricant fluids together with the percentage decrease in the strength due to soaking effects. The moisture content and rock pore water salinity before and after soaking are also provided in Table 5.2. The presented Brazilian strength represents average of three test in each case.

As a guide to select the proper reduction to the Brazilian split test results, a direct tension test was performed on an intact Niagara Queenston shale specimen. Based on the tensile strength of intact Niagara Queenston shale from both tests (i.e. Brazilian split test and direct tension test), a suitable reduction could be then applied to the Brazilian split strength of shale soaked in water and lubricant fluids. In this case, the reduced Brazilian strength represents the equivalent tensile strength in the direct tension test. This assumption is supported by a suggested percentage reduction of the Brazilian split strength of materials, such as concrete (Neville 1996). He concluded that the tensile strength of concrete obtained from the Brazilian split test found to be overestimated by 5 % to 12 % compared to concrete tensile strength obtained from the direct tension test.

The measured tensile strength of intact Niagara Queenston shale from direct tension test was 4.7 MPa (average of three tests), while the tensile strength obtained from the Brazilian split test was 11.3 MPa. Therefore, a reduction of 42 % was adopted in this research to convert the measured Brazilian split strength of soaked Niagara Queenston shale to the equivalent tensile strength. However, choosing the right test to produce the tensile strength in sedimentary rocks such as Niagara Queenston shale is a debatable issue and requires comprehensive study. The reason of utilizing the Brazilian test, and then applying this reduction approach was due to the great difficulty in attaching the steel caps of the loading machine in the direct tension test to the Niagara Queenston shale specimen after soaking period.

Table 5.2. Brazilian split strength test results of Niagara Queenston shale

Specimen No.	Ambient Fluid	Depth (m)	Calcite Content (%)	Dolomite Content (%)	Moisture Content Before Soaking (%)	Moisture Content After Soaking (%)	Pore Water Salinity Before Soaking (g/L)	Pore Water Salinity After Soaking (g/L)	Decrease In Pore Water Salinity (%)	Brazilian Split Strength (MPa)	Decrease In Brazilian Split Strength (%)	Equivalent Direct Tension Strength σ_t (MPa)
BZT 1	Air	6.04	8.0	1.6	1.17	-	343.5	-	-	11.30	-	4.70
BZT 2	Water	7.60	12.1	1.6	1.21	2.78	307.1	72.7	76	0.46	96	0.19
BZT 3	0.8 % Polymers Solution	7.90	10.9	1.6	1.26	2.66	317.4	210.8	34	1.63	86	0.68
BZT 4	8 % Bentonite Solution	9.67	13.3	2.0	1.20	1.93	366.6	168.4	54	1.36	88	0.57

The results presented in Table 5.2 clearly indicate that the Brazilian split strength of Niagara Queenston shale has decreased significantly after soaking in water and lubricant fluids. The percentage decrease in Niagara Queenston shale split strength was 96 %; 88 % and 86 % after 100 days of soaking in water; bentonite solution and polymer solution, respectively, compared to intact specimen split strength. This significant decrease may be attributed to micro cracks developed in Niagara Queenston shale specimens after soaking in water and lubricant fluids. It is noted that even though the strength reduction was generally high in all fluids used, polymer solution caused the least decrease. The measured pore water salinity of Niagara Queenston shale before and after soaking in water and lubricant fluids indicates a remarkable difference. The decrease in pore fluid salinity of Niagara Queenston shale was 76 % in water; 54 % in bentonite solution and 34 % in polymer solution. Moreover, the moisture content of Niagara Queenston shale was initially 1.21 %; 1.20 % and 1.26 % and increased to 2.78 %; 2.66 % and 1.93 % (i.e. with an increase of 130 %; 111 % and 61 %), respectively, after soaking in water; bentonite solution and polymer solution. This indicates a diffusion of the pore water salinity and wetting of Niagara Queenston shale have occurred after the soaking period.

The wetting process (i.e. osmosis) and the diffusion of pore water salinity are essential to cause the time-dependent deformation of shales in southern Ontario (Lee and Lo 1993). However, the time-dependent deformation behaviour of Niagara Queenston shale and the associated development of micro-cracks were found to be different in water and lubricant fluids as it is explained in Chapter 3. It was found that water caused the highest while polymer solution caused the least time-dependent deformation of Niagara Queenston shale. A similar trend can be observed in the data presented in Table 5.2. The different degrees of osmosis and diffusion processes occurred in Niagara Queenston shale, and the associated micro-cracks developed in its skeleton, explain the difference in the Brazilian split strength reduction after soaking in water and lubricant fluids. The increased osmosis and the enhanced diffusion processes during soaking period may enlarge the micro-pores of Niagara Queenston shale and hence inducing more micro-cracks that are spread in its skeleton causing the reduction in the strength.

5.3.4 Unconfined Compression Strength

Table 5.3 presents the results of the unconfined compression tests. In addition, the values of moisture content and the pore water salinity of Niagara Queenston shale before and after soaking as well as the change in Poisson's ratio, elastic modulus, and shear modulus due to soaking effects are provided in Table 5.3. The presented values in this table represents the average of three tests for each case. Samples were subjected to a uniform loading rate of 0.16 kN/s, which is equivalent to a displacement rate of 0.045 mm/min to achieve failure within 5-15 minutes, according to the ASTM D7012(2010).

Figure 5.4 shows axial stress versus axial and lateral strains of unconfined compression tests performed on intact Niagara Queenston shale specimens and specimens soaked for 100 days in water and lubricant fluids. The unconfined compression strength of Niagara Queenston shale showed remarkable drop after soaking in water and lubricant fluids (i.e. 82 %; 85 % and 63 % after soaking in water; bentonite solution and polymer solution, respectively) compared to its value of intact samples. The strength reduction was accompanied with a decrease in pore water salinity of Niagara Queenston shale (i.e. 69 %; 49% and 23% after soaking in water; bentonite solution and polymer, respectively). These results are consistent with the results of the Brazilian split strength tests. The decrease in unconfined compression strength can, therefore, be attributed to the same reasons, i.e. the diffusion of pore water salinity and the osmosis process caused Niagara Queenston shale to deform and develop micro-cracks at varying levels in water and lubricant fluids.

Table 5.3. Unconfined compression strength test results and strength parameters of Niagara Queenston shale

Specimen No.	Ambient Fluid	Depth (m)	Calcite Content (%)	Dolomite Content (%)	Moisture Content Before Soaking (%)	Moisture Content After Soaking (%)	Pore Water Salinity Before Soaking (g/L)	Pore Water Salinity After Soaking (g/L)	Decrease In Pore Salinity (%)	Unconfined Compression Strength (MPa)	Decrease In Unconfined Compressive Strength (%)	Poisson's Ratio ν	Elastic Modulus E (GPa)	Decrease In Elastic Modulus E (%)	Shear Modulus G (GPa)	Decrease In Shear Modulus G (%)
UCT 1	Air	6.00	9.4	2.0	1.17	-	361.8	-	-	37.40	-	0.23	28.57	-	11.61	-
UCT 2	Water	7.65	11.6	2.3	1.30	2.31	280.3	88.5	69	6.74	82	0.50	2.00	93	0.67	94
UCT 3	0.8 % Polymers Solution	7.80	13.4	1.8	1.32	2.39	304.6	235.2	23	13.77	63	0.35	6.18	78	2.29	80
UCT 4	8 % Bentonite Solution	9.5	11.9	1.8	1.23	2.38	328.5	165.9	49	5.52	85	0.42	3.27	89	1.15	90

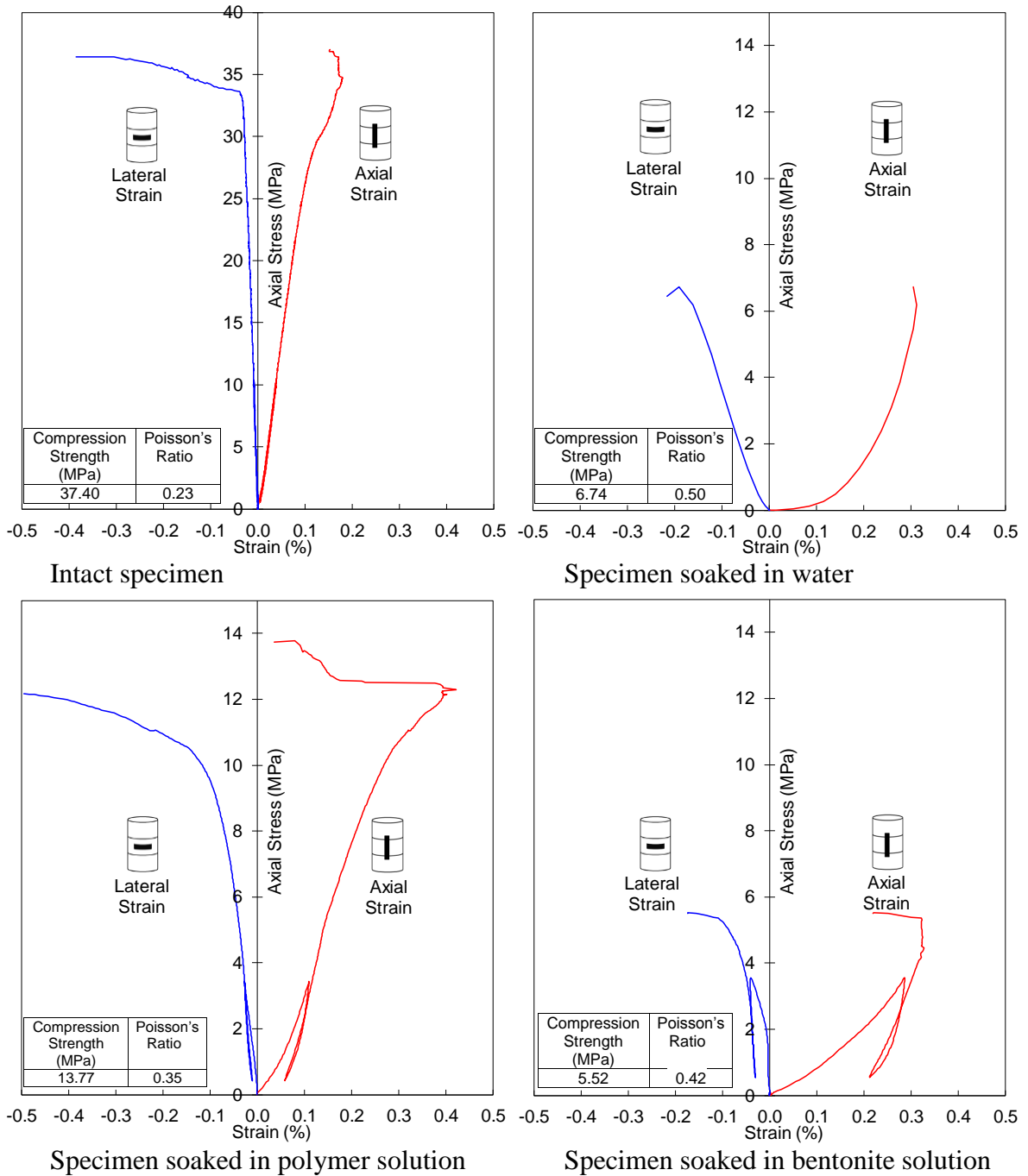


Figure 5.4. Typical results of unconfined compression strength test of Niagara Queenston shale: (a) intact specimen; (b) soaked in water; (c) soaked in polymer solution and (d) soaked in bentonite solution, for 100 days.

Figure 5.4 also indicates that soaking Niagara Queenston shale in water and lubricant fluids has changed the shape of its stress-strain curves, i.e., increased the strain of soaked specimens (Figure 5.4 (b, c, d)) compared to intact specimen (Figure 5.4 (a)). The higher strain exhibited by soaked Niagara Queenston shale specimens prior to failure may be attributed to closing of micro-cracks developed during soaking period. This can be observed clearly in the axial strain curves of soaked specimens where the load is acting in the same direction of the measured strain. The elastic zone of the stress-strain curves (i.e. the initial straight line at early stage of loading) of intact Niagara Queenston shale can be distinguished clearly in Figure 5.4 (a) while it was less obvious for the soaked Niagara Queenston shale as demonstrated in Figures 5.4 (b, c, d). At early stage of loading, the closure of developed micro cracks in the soaked samples caused the sample to show lower strength than intact samples. As loading increased, the structure of the Niagara Queenston shale became more compacted due to the closure of developed micro cracks in the direction of loading, causing an increase in the strength of the shale. However, at failure the Niagara Queenston shale structure collapsed as it could not sustain the applied load due to discontinuities created by micro-cracks developed during soaking in water and lubricant fluids.

5.3.5 Multistage Triaxial Compression Strength

The results of multistage triaxial compression tests performed on Niagara Queenston shale and the derived Poisson's ratio; elastic modulus and shear modulus are summarized in Table 5.4. The change in strength of Niagara Queenston shale due to variation of the confining pressure was also calculated and is included in Table 5-4. In addition, the stress-strain curves are shown in Figures 5.5 through 5.8.

As it can be seen in Table 5.4 and Figures 5.5 to 5.8, the triaxial compression strength of Niagara Queenston shale has decreased significantly after soaking in water and lubricant fluids compared to intact strength. Soaking in water caused the highest decrease in Niagara Queenston shale triaxial compression strength (76; 70; 62; 59; 53 and 42 %) and polymer solution caused the least decrease in the compression strength (64; 57;

44; 54; 39 and 36%), under confining pressure of 2.5; 5.0; 7.5; 10.0; 15.0 and 20.0 MPa, respectively. The decrease in the triaxial compression strength due to soaking Niagara Queenston shale in bentonite solution was similar to the decrease caused by water.

It can also be noticed that the strength reduction was less as the confining pressure increased in all fluids used. As the confining pressure increases, the micro structure of the soaked NQS samples becomes more compacted and more dense due to the closure of developed micro cracks in all directions of the sample causing it to exhibit higher strength. At high confining pressure, this effect became higher and hence the decrease in the compression strength of soaked Niagara Queenston shale compared to the intact samples was less.

Table 5.4. Test results multistage triaxial compression strength and strength parameters of Niagara Queenston shale

Specimen No.	Ambient Fluid	Depth (m)	Calcite Content (%)	Dolomite Content (%)	Moisture Content Before Soaking (%)	Moisture Content After Soaking (%)	Pore Water Salinity Before Soaking (g/L)	Pore Water Salinity After Soaking (g/L)	Increase in Pore Water Salinity (%)	Confining Pressure (MPa)	Compression Strength (MPa)	Increase in Compression Strength (%)	Poisson's Ratio ν	Increase in Poisson's Ratio (%)	Elastic Modulus (GPa)	Shear Modulus $G = E / 2(1 + \nu)$ (GPa)
TXCT 1	Air	5.80	8.7	1.6	1.505	-	352.8	-	-	2.5	42.04	-	0.26	-	102.56	40.83
										5.0	48.90	-	0.35	-	26.93	10.00
										7.5	53.01	-	0.24	-	10.81	4.35
										10.0	59.50	-	0.44	-	8.96	3.11
										15.0	67.64	-	0.48	-	8.00	2.70
										20.0	77.79	-	-	-	4.12	-
TXCT 2	Water	9.95	9.1	1.3	1.40	2.74	272.9	65.8	76	2.5	10.08	76	0.38	47	16.67	6.27
										5.0	14.91	70	0.42	20	8.07	2.84
										7.5	20.12	62	0.44	81	8.62	3.00
										10.0	24.50	59	0.46	5	7.08	2.42
										15.0	31.72	53	0.49	2	9.15	3.07
										20.0	45.48	42	0.50	-	7.50	2.51

Continued

TXCT 3 0.8 %	7.90	10.5	1.8	1.18	2.67	355.9	252.2	29	2.5	15.01	64	0.38	46	23.85	8.64
Polymers Solution									5.0	21.06	57	0.41	17	8.57	3.04
									7.5	26.58	44	0.45	88	6.98	2.41
									10.0	31.73	54	0.47	7	8.57	2.91
									15.0	41.54	39	0.48	0	11.05	3.73
									20.0	50.12	36	0.47	-	10.70	3.64
TXCT 4 8 %	9.6	11.4	1.5	1.6	3.25	245.0	120.6	51	2.5	10.71	75	0.40	54	20.00	7.14
Bentonite Solution									5.0	15.90	67	0.44	26	12.00	4.17
									7.5	20.81	61	0.47	96	7.81	2.66
									10.0	24.87	58	0.45	2	4.40	1.52
									15.0	33.59	50	0.49	2	7.44	2.50
									20.0	44.12	43	0.47	-	7.04	2.39

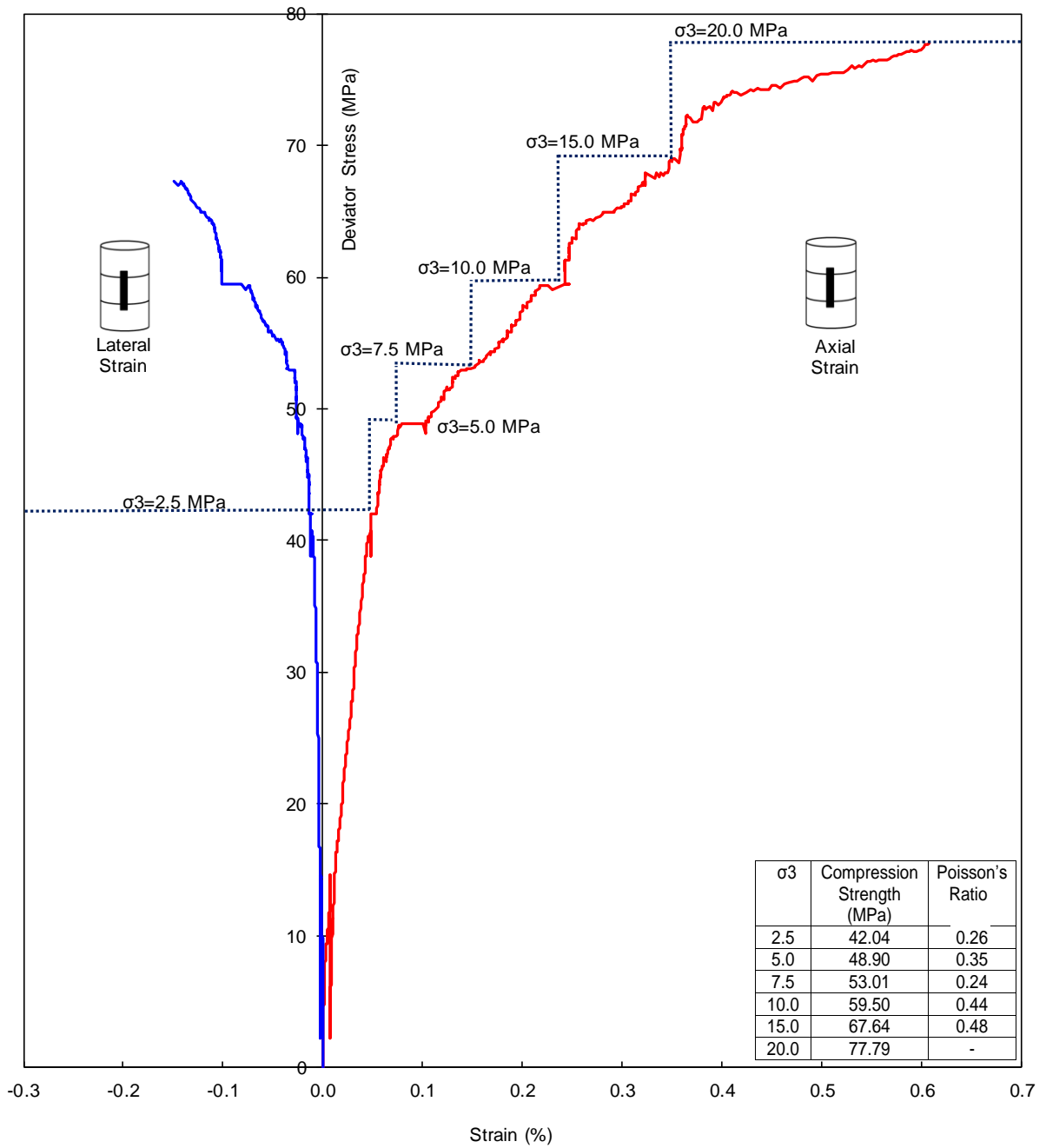


Figure 5.5. Multistage triaxial compression strength test performed on intact Niagara Queenston shale.

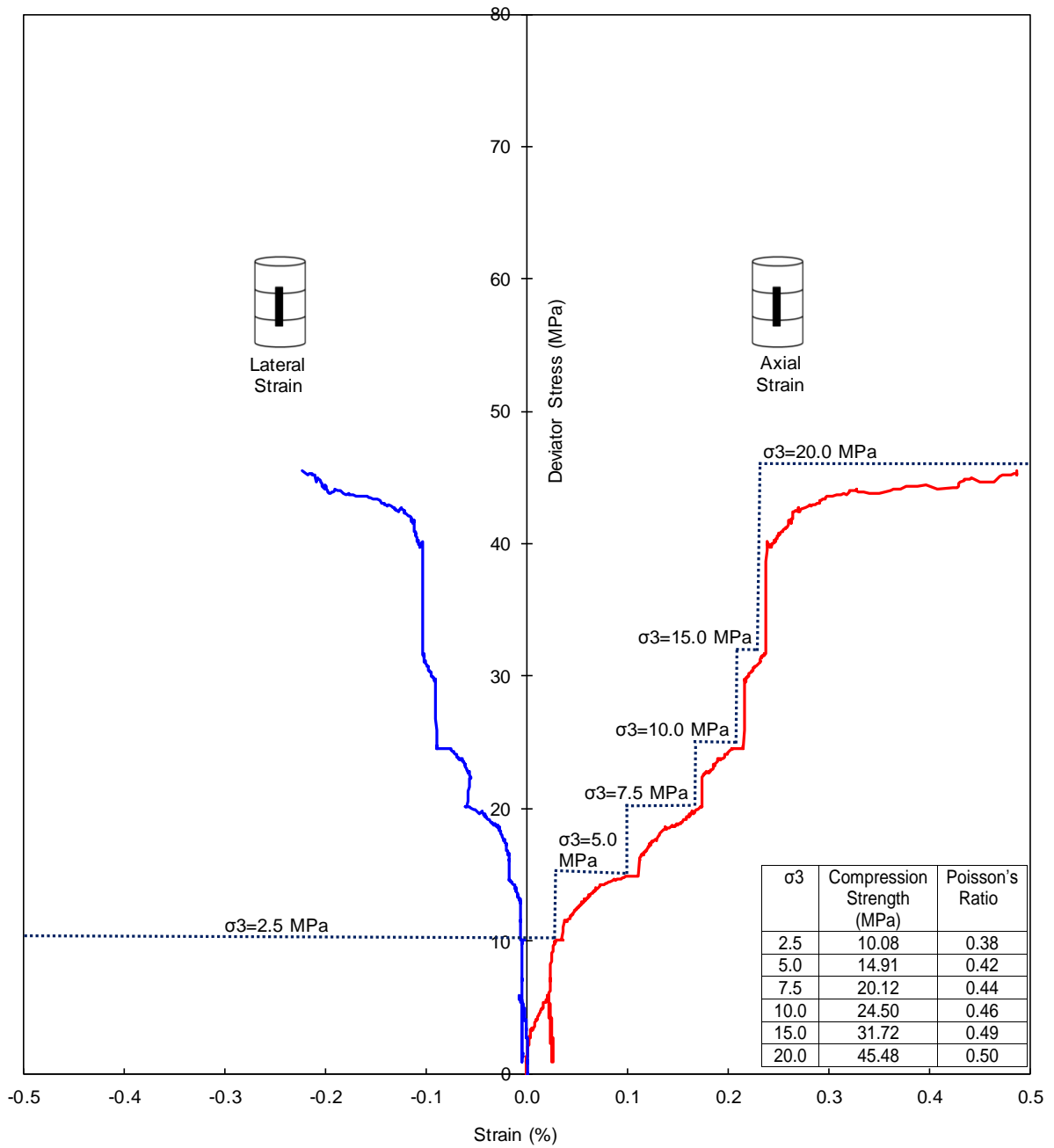


Figure 5.6. Multistage triaxial compression strength test performed on Niagara Queenston shale soaked for 100 days in water.

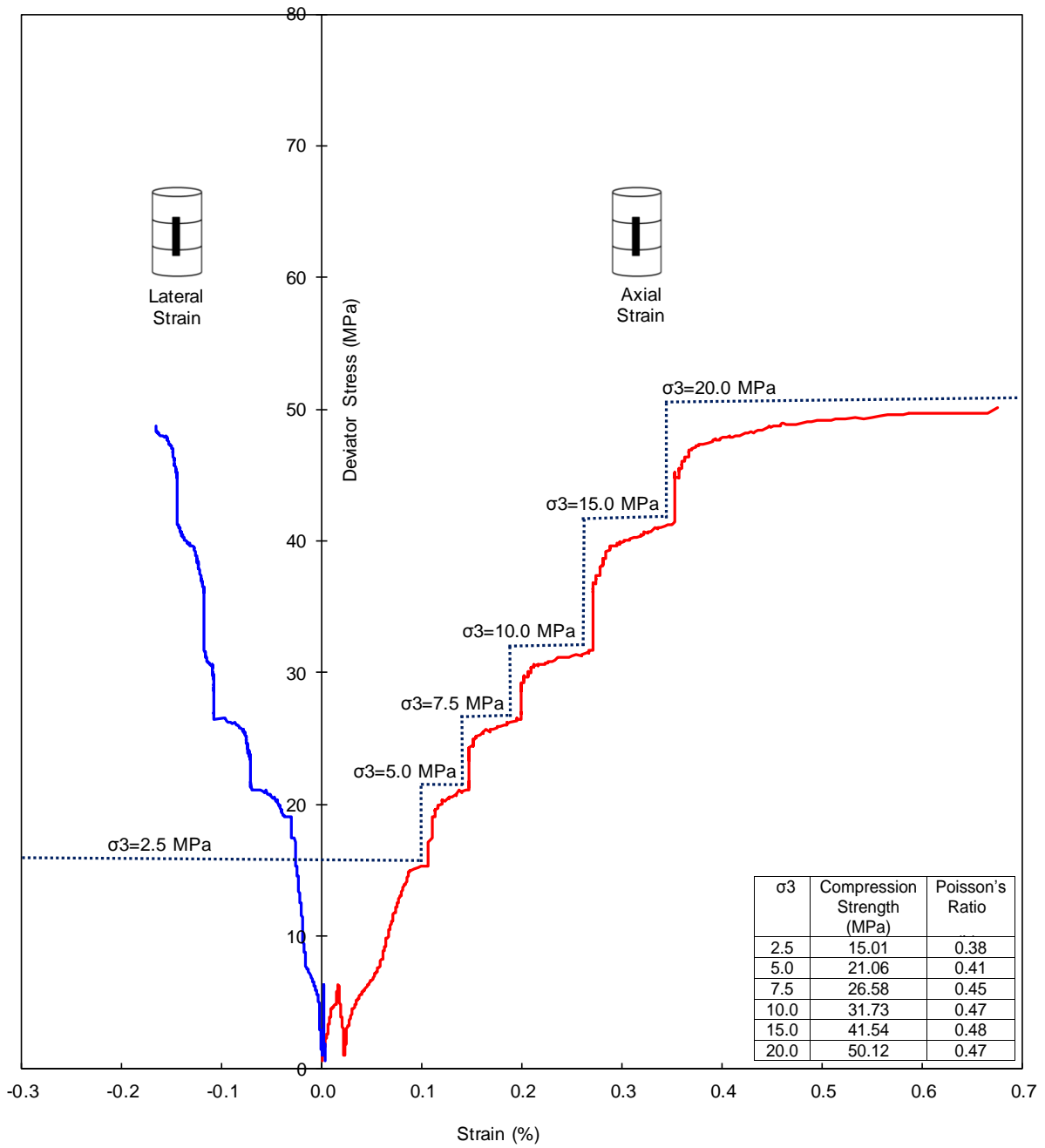


Figure 5.7. Multistage triaxial compression strength test performed on Niagara Queenston shale soaked for 100 days in polymer solution.

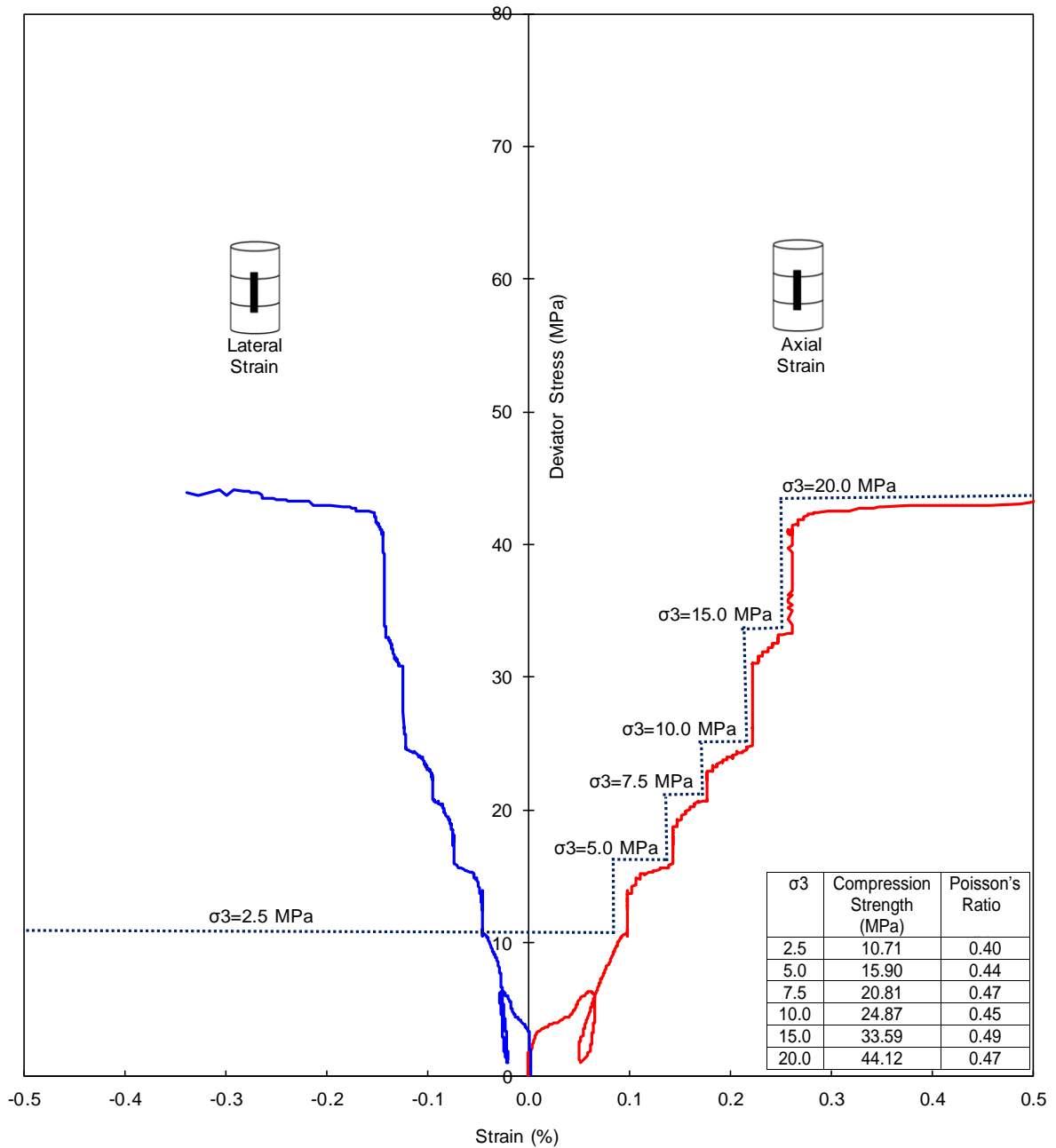


Figure 5.8. Multistage triaxial compression strength test performed on Niagara Queenston shale soaked for 100 days in bentonite solution.

5.3.6 Poisson's Ratio

The Poisson's ratio values derived from unconfined compression and triaxial compression tests performed on Niagara Queenston shale are summarized in Table 5.3, and Table 5.4. The results show that Poisson's ratio generally increased after soaking Niagara Queenston shale specimens in water and lubricant fluids. Considering the failure mechanism discussed earlier, soaking Niagara Queenston shale in water and lubricant fluids have increased the volume of micro-pores and developed more micro-cracks in the test specimens, which caused more deformations prior to failure as indicated in Figures 5.4 through 5.8. For unconfined compression and multistage triaxial compression tests under low confining pressure (i.e. 2.5 MPa), the change in Poisson's ratio was more evident. For high confining pressure (i.e. 20.0 MPa), minimal difference in Poisson's ratio of soaked Niagara Queenston shale was observed (0.50, 0.47, and 0.47). Moreover, when the confining pressure was increased in multistage triaxial compression tests, Poisson's ratio increased compared to its value at low confining pressure. It is worth mentioning that in multistage triaxial compression test, the strength corresponding to a confining pressure is given by the stress at the onset of the stress-strain curve plateau due to the development of failure cracks. At each higher confining pressure, additional micro-cracks have developed at the plateau of the stress-strain curve. With the accumulation of these micro-cracks, the structure of Niagara Queenston shale becomes more deformable and may cause higher Poisson's ratio. It is suggested that further investigation is required to evaluate measuring Poisson's ratio in the stages following first stage in multistage triaxial compression test.

5.3.7 Elastic Modulus and Shear Modulus

The average elastic modulus of Niagara Queenston shale was calculated using method (b) described in ASTM-D7012 (2010), while the shear modulus was calculated using theory of elasticity relationships. The elastic modulus decreased significantly by (95%; 89% and 78%) after soaking Niagara Queenston shale in water; bentonite solution and polymer solution, respectively. The shear modulus similarly decreased after soaking

Niagara Queenston shale in these fluids. These changes in elastic and shear moduli of Niagara Queenston shale can be attributed to the developed micro-cracks in the structure of the shale after soaking in water and lubricant fluids as it is explained earlier. Generally, as the confining pressure increased in the multistage triaxial compression test, the percentage decrease in elastic and shear moduli compared to their values in intact Niagara Queenston shale under similar confining pressure became smaller. This behaviour may be attributed to the confining effect and the closure of the developed micro cracks resulting in more compacted structure of the Niagara Queenston shale at high confining pressure compared to its structure at low confining pressure.

5.4 DEVELOPING STRENGTH ENVELOPES OF NIAGARA QUEENSTON SHALE

In order to evaluate the influence of water and lubricant fluids on the strength of Niagara Queenston shale, strength envelopes were developed for intact shale and for shale after soaking in water and in bentonite and polymer solutions. The strength envelopes were developed utilizing all strength results from Brazilian split test; unconfined compression test and multistage triaxial compression test employing RocLab software (available from www.rocscience.com). The Brazilian split strength was reduced by 42 % to convert it to an equivalent tensile strength in direct tension test, as it is explained earlier. The strength envelopes are presented in Figure 5.9 in the form of principal stresses (Figure 5.9 (a)) and in the form of normal and shear stresses (Figure 5.9 (b)). The solid points represent values measured from the conducted laboratory tests, while solid curves represent strength envelopes produced from RocLab software based on the lab test results. The weakening effect of water and lubricant fluids is clearly evident in Figure 5.9.

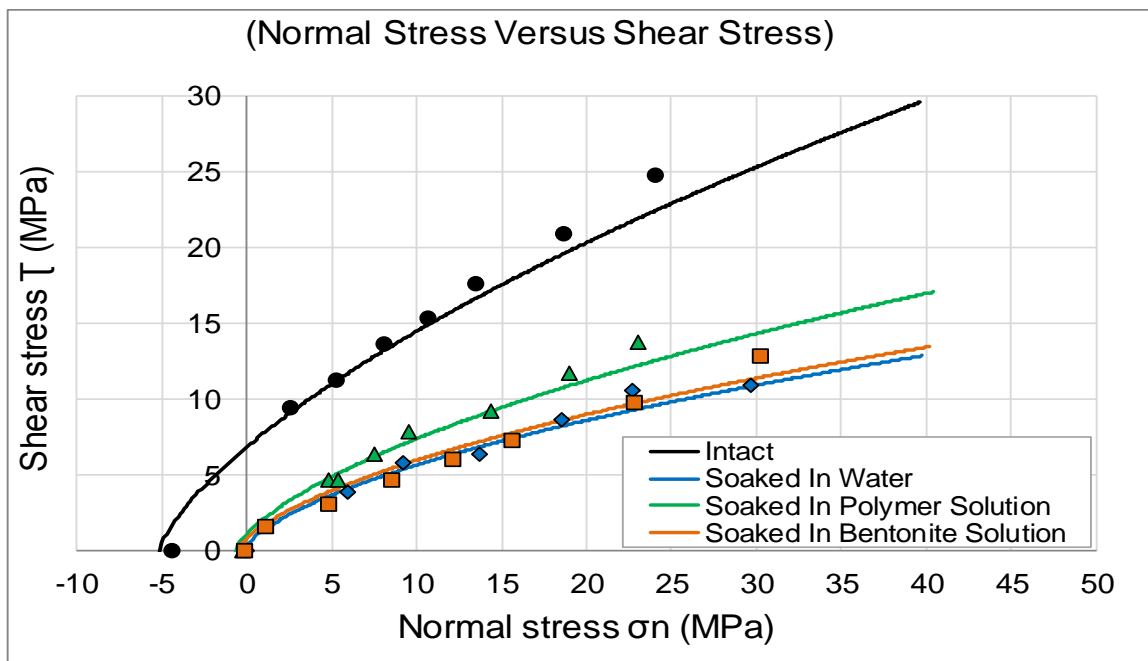
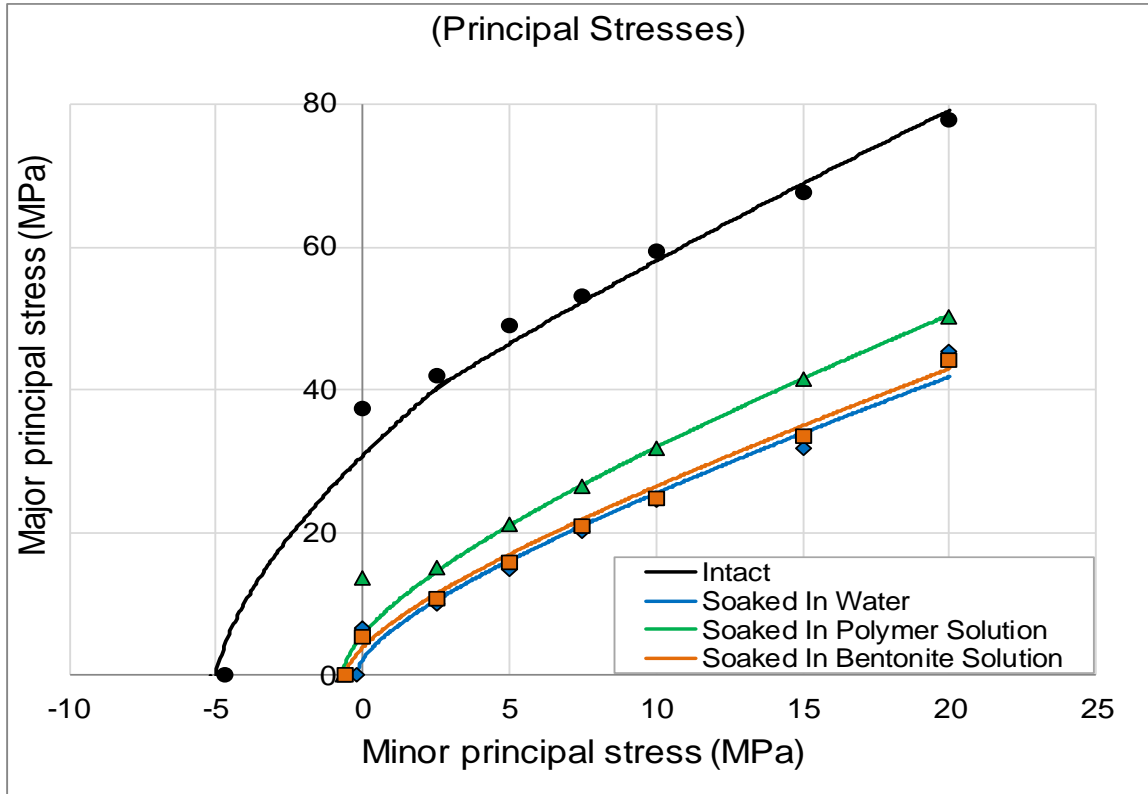
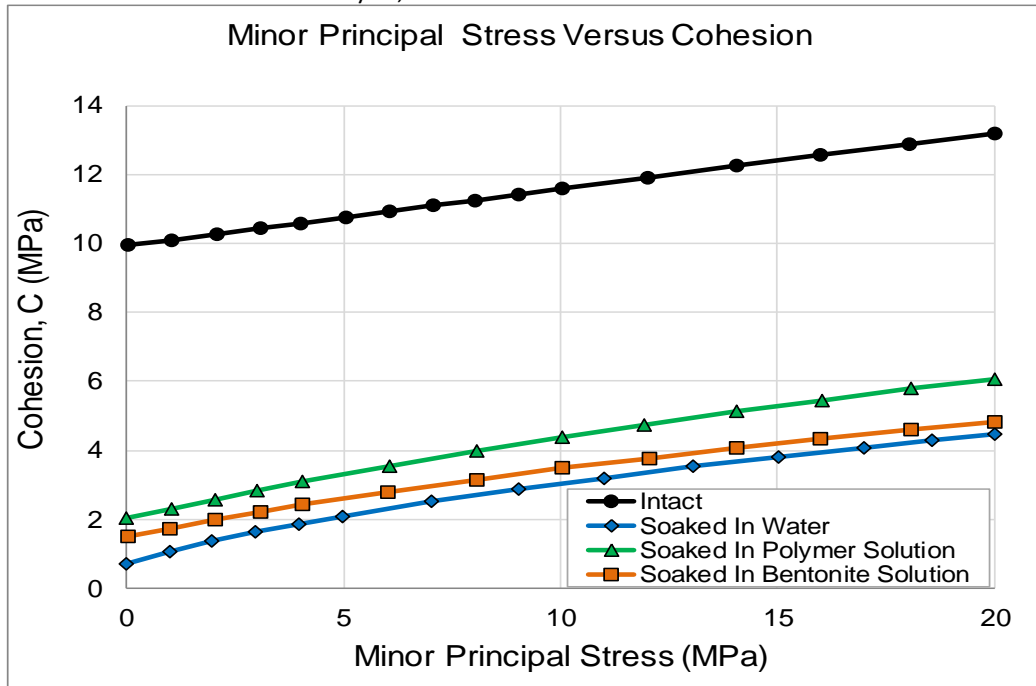


Figure 5.9. Strength Envelopes of Niagara Queenston shale: (a) Principal stresses and (b) Normal and shear stresses.

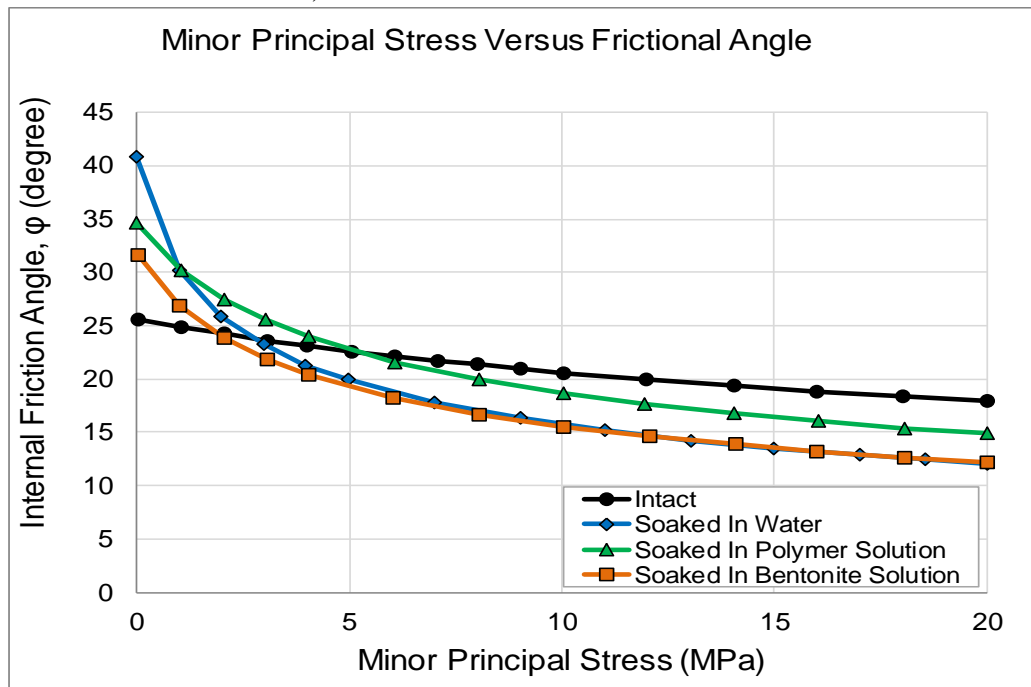
Although, weakening effects are similar, polymer solution caused the least decrease in the strength of as manifested by the higher strength envelope for Niagara Queenston shale specimens soaked in polymer solution compared to specimens soaked in water and bentonite solution. This weakening effect is more evident in Figure 5.9 (b).

It is important to consider this drop in the strength of Niagara Queenston shale in the design of underground structures. Most tunneling excavations involve either water or lubricant fluids in their applications. Weakening effects of these fluids may decrease the strength of the Queenston shale in the close vicinity of the constructed tunnel or micro-tunnel. However, rock samples were submerged in water and lubricant fluids during the soaking period, which may not be the same of their condition in-situ. This is one of the limitations of results derived from the performed tests.

The changes in instant cohesion (C) and instant frictional angle (ϕ) of Niagara Queenston shale obtained from RocLab software are presented in Figure 5.10. Instant cohesion and frictional angle are derived based on the tangent line to the strength envelope at a specific value of minor principal stress. The minor principal stress represents the confining pressure applied on Niagara Queenston shale specimen during the test, which may represent the in-situ stress. The instant cohesion (C) increases with increasing the confining pressure, while the reverse is true for the instant frictional angle (ϕ). The increase in the instant cohesion may be attributed to the more compacted structure of Niagara Queenston shale under higher confining pressure. The influence of polymer solution on the instant cohesion and frictional angle of Niagara Queenston shale was the least among other fluids used.



a) Cohesion of Niagara Queenston shale (before and after soaking in water and lubricant fluids)



b) Frictional angle of Niagara Queenston shale (before and after soaking in water and lubricant fluids)

Figure 5.10. Mohr-Coulomb parameters of Niagara Queenston shale: (a) change in cohesion with minor principal stress and (b) change in internal frictional angle with minor principal stress.

5.5 COMPARISON OF STRENGTH MEASURED IN MULTISTAGE AND SINGLE-STAGE TRIAXIAL COMPRESSION TESTS

Due to the limited samples of Niagara Queenston shale, the comparison between the results of multistage triaxial compression test and the single-stage triaxial compression test is presented here for Queenston shale samples collected from Milton in Ontario. In Chapter 4, a testing program was performed on Milton Queenston shale, where the single-stage triaxial test under different confining pressure in addition to the Braziliab split test and the unconfined compression test were used. For the purpose of comparison of both triaxial tests results, an additional multistage triaxial compression test was also performed on intact sample from Milton Queenston shale.

The results of the multistage triaxial test and the single-stage triaxial test are presented in Figure 11. The black solid curve represents results of multistage triaxial compression test while the other colored curves represent results of single-stage triaxial tests performed under different confining pressure (i.e. 2.5, 5.0, 10.0 and 20 MPa). For clarity reasons, only axial deformation curves are plotted in Figure 11. This figure clearly indicates that the strength of the Queenston shale at each confining pressure is quite similar in both tests. It also shows that both tests produced axial deformation curves of similar trend and similar slopes, indicating that similar elastic modulus can be calculated from both tests. There is a small difference in the peak strength from both tests which can be attributed to the variation in rock samples or to the effect of successive loading of same sample in the multistage triaxial test. This figure shows that the compressive strength of the Queenston shale can be measured in multistage triaxial compression test with minimal impact on the measured strength compared to the traditional single-stage triaxial test. This impact is small and practically can be ignored.

The strength envelope of Milton Queenston shale was developed using the average values of the tensile strength and the unconfined compression strength in addition to the compression strength measured from the multistage triaxial compression test and the single-stage triaxial compression test under different confining pressures. These envelopes are presented in Figure 12. In this figure, the solid curve represents the

strength envelope of Milton Queenston shale based on results of multistage triaxial test and the dotted curve represents the envelope of Milton Queenston shale based on results of single-stage triaxial test. Both envelopes are quite similar and they are almost identical indicating minimal impact of the multistage triaxial test on the measured strength of Milton Queenston shale and on its overall strength envelope. The small difference between both envelopes can be ignored.

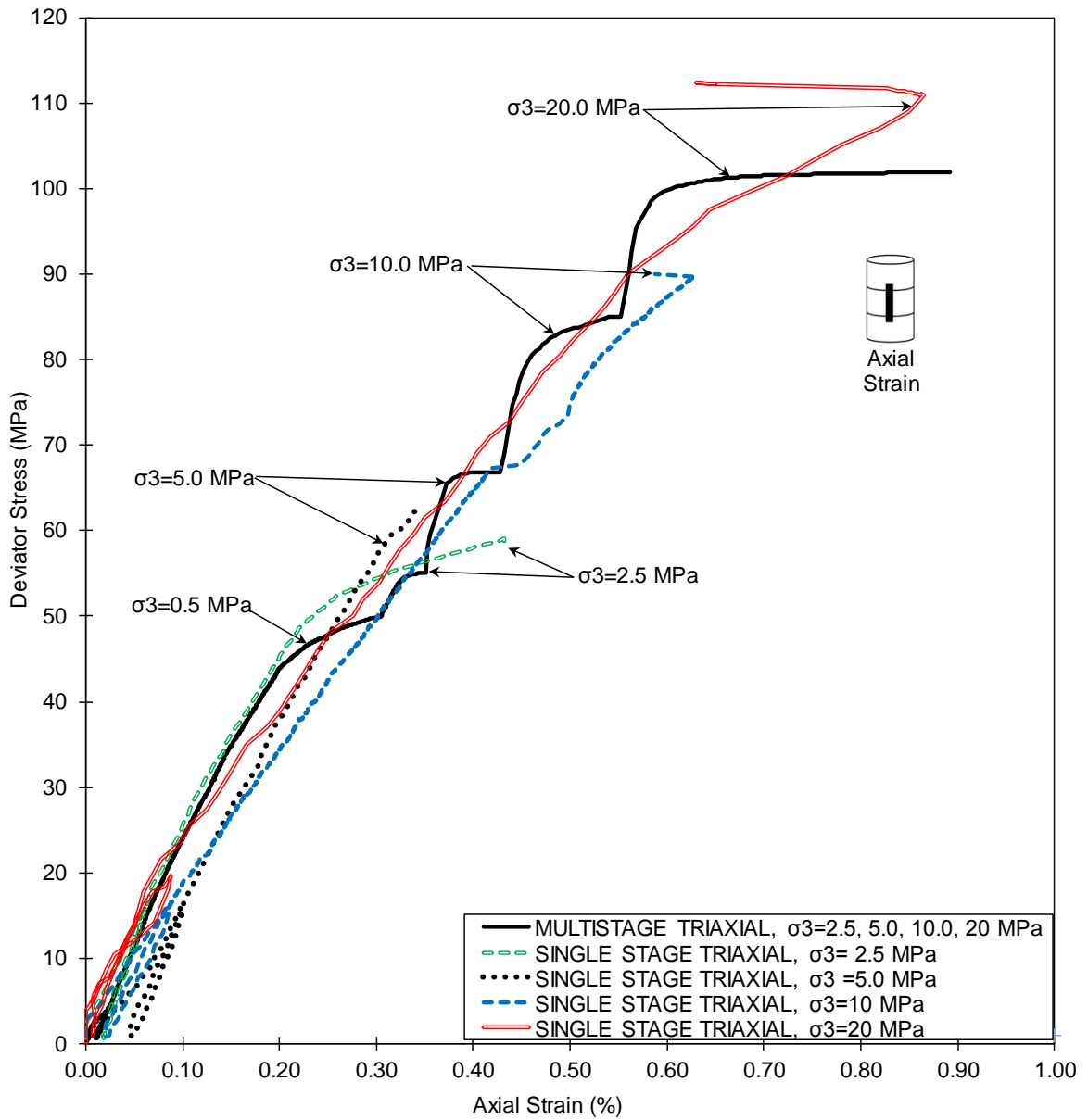


Figure 5.11. Comparative display of the strength of intact Milton Queenston shale measured from multistage triaxial and single-stage triaxial tests.

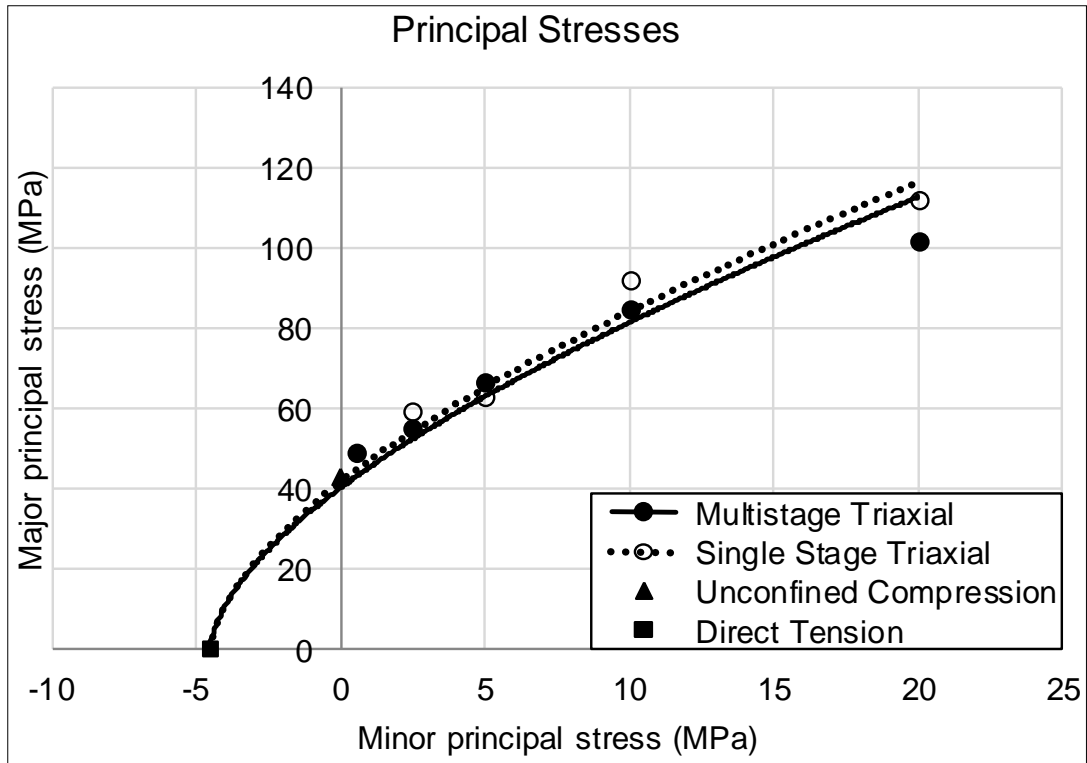
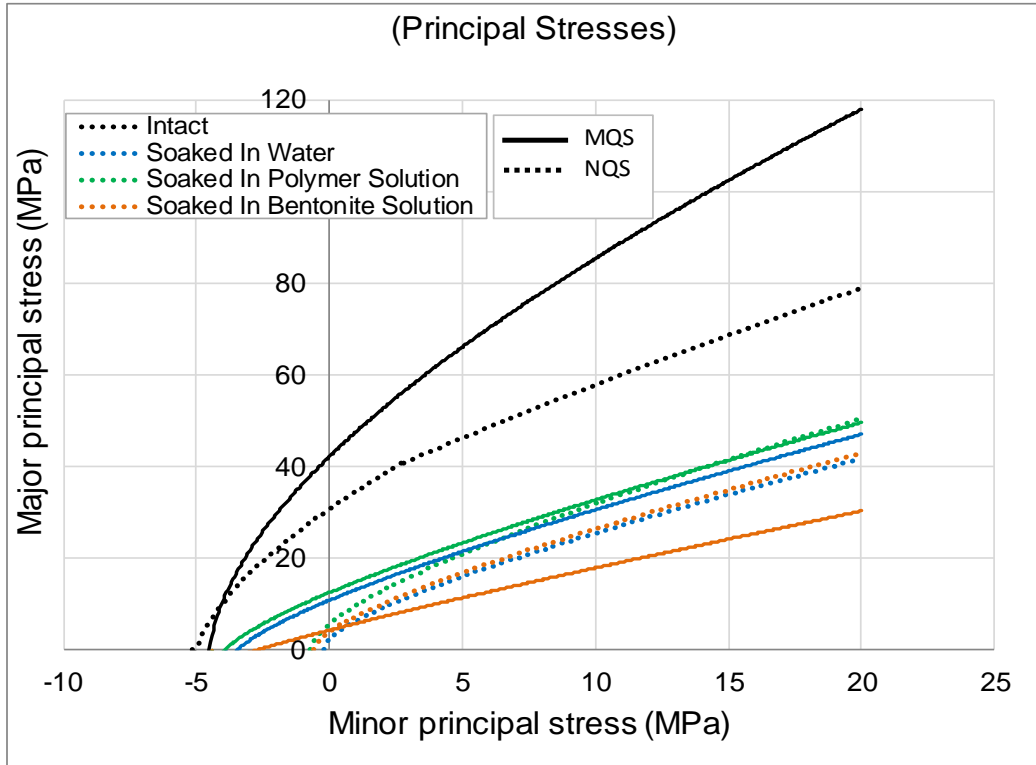


Figure 5.12. Strength envelope of Milton Queenston shale based on multistage triaxial compression test and single-stage triaxial compression test results.

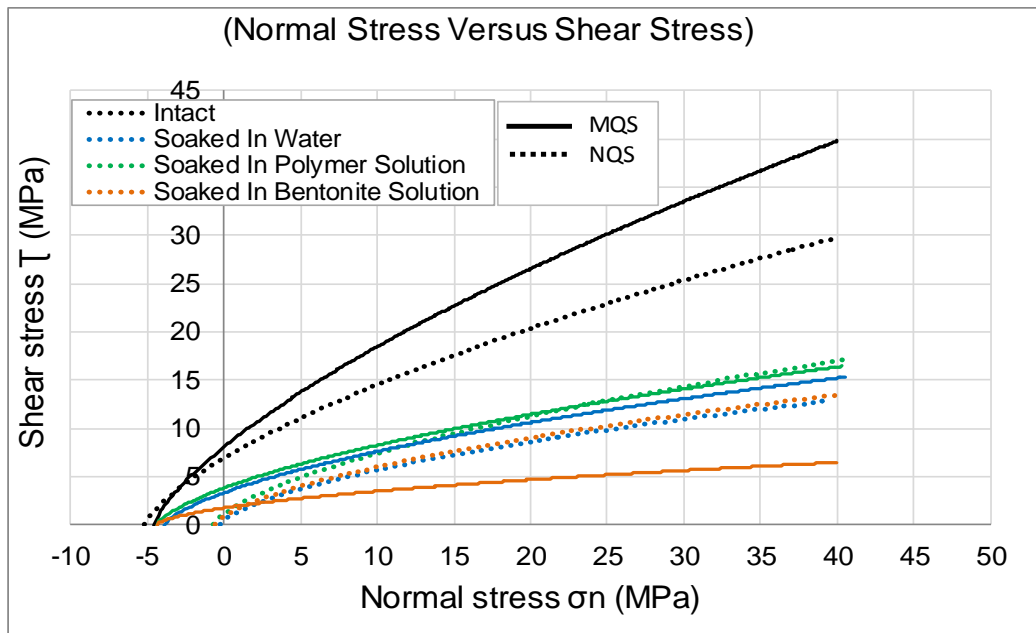
5.6 COMPARISON OF STRENGTH ENVELOPS OF NIAGARA AND MILTON QUEENSTON SHALE

The developed strength envelopes of Niagara Queenston shale before and after soaking in water and lubricant fluids are compared in this section with the strength envelopes of Milton Queenston shale. The strength envelopes of Milton Queenston shale were derived based on single stage triaxial compression tests, using multiple specimens. However, only the strength envelopes are used in this comparison.

Figure 5.13 shows the strength envelopes of both Niagara Queenston shale plotted in dotted lines, and Milton Queenston shale plotted in solid lines. The envelopes are presented in principal stresses form (Figure 5.13 (a)), and in normal and shear stresses form (Figure 5.13 (b)). The strength behaviour of both Queenston shales is fairly similar, except the fact that Milton Queenston shale strength is higher than the strength of Niagara Queenston shale. At zero confining pressure, the strength of intact Niagara Queenston shale is almost three quarters the strength of Milton Queenston shale. This difference remains constant with increasing the confining pressure in both shales (Figure 5.13 (a)). The constant difference in intact strength envelopes of both Queenston shales indicates the negligible influence of the type of triaxial test used to measure the strength of these shales. A similar observation can be made for the strength envelopes of Niagara and Milton Queenston shale after soaking in water and polymer solution, i.e., the difference in strength remains constant with increasing the confining pressure as shown in Figure 5.13 (a) and 5.13 (b). The difference in strength of soaked Niagara Queenston shale and Milton Queenston shale in bentonite solution increased with increasing the confining pressure. Compared to the constant differences in strength of both Queenston shales of (intact and soaked in water and polymer solution), this observation may be attributed to other factors and not due to using multistage triaxial test. These observations suggest that using multistage triaxial compression test has negligible influence on the strength of Queenston shale. The soaking effect on the tensile strength of Niagara Queenston shale is more evident than soaking effect on the tensile strength of Milton Queenston shale, which indicates a stronger fabric structure of Milton Queenston shale.



a) Strength envelopes of Niagara and Milton Queenston shales (Principal Stresses)



b) Strength envelopes of Niagara and Milton Queenston shales (Normal Stress Versus Shear Stress)

Figure 5.13. Comparison of strength envelopes of Niagara and Milton Queenston shales: (a) principal stresses and (b) normal and shear stresses.

The envelopes of soaked Niagara Queenston shale and Milton Queenston shale form a bundle of curves that are fairly close to each other, specifically in the compression side of the envelopes. In all of these strength envelopes, the polymer solution produced the higher strength relative to other used fluids in both shales. This observation together with the finding of very low swelling deformations of both Niagara Queenston shale and Milton Queenston shale caused by polymer solution (see Chapter 3 and Al-Maamori et al. 2016), it is suggested here to use the polymer solution in micro-tunnelling applications in Queenston shales.

5.7 SUMMARY AND CONCLUSIONS

The weakening effect of water, bentonite solution and polymer solution used in micro-tunnelling applications on the strength of Niagara Queenston shale was investigated. Specimens were soaked in these fluids for 100 days. A full suite of laboratory tests including Brazilian split test; unconfined compression test; multistage triaxial compression test and direct tension test were performed on intact and soaked specimens. The strength envelopes of Niagara Queenston shale were developed for intact and soaked shales. From the results of this study, the following conclusions can be drawn:

- 1) The tensile and compressive strength of Niagara Queenston shale decreased significantly after soaking for 100 days in water; bentonite solution and polymer solution. The decrease was dissimilar in these fluids. Relative to other used fluids, polymer solution caused the minimal decrease in the strength. The decrease was also evident in the elastic and shear moduli of soaked Niagara Queenston shale.
- 2) Soaking Niagara Queenston shale in water and lubricant fluids caused an increase in their deformation before failure compared to intact specimens. The Poisson's ratio of Niagara Queenston shale increased after soaking in water and lubricant fluids approaching 0.5.
- 3) Strength envelopes were developed for both intact Niagara Queenston shale and after soaking in water and lubricant fluids. The strength envelopes demonstrated a

remarkable decrease in strength of this shale after soaking in water and lubricant fluids.

- 4) Based on the developed strength envelopes of Niagara Queenston shale, the instant cohesion found to be increasing with increasing the confining pressure, while the reverse was noticed in the instant frictional angle.
- 5) The multistage triaxial compression test was found to be suitable for Niagara Queenston shale, and it has almost a negligible influence on the measured strength. However, adopting this test requires an accurate monitoring of the deformation curves during loading to identify the maximum strength corresponds to each confining pressure. It is limited to the correct identification of the imminent strength in each loading stage. If the imminent strength is missed, the test loses its vantage upon traditional single-stage triaxial compression test.

The presented research indicated a significant weakening influence of water and lubricant fluids on the strength of Niagara Queenston shale. However the extent (i.e. the depth) of these influences in-situ needs further investigation.

5.8 REFERENCES

- Alkan, H., Cinar, Y., and Pusch, G. 2007. Rock salt dilatancy boundary from combined acoustic emission and triaxial compression tests. *International Journal of Rock Mechanics & Mining Sciences* 44:108-119.
- Al-Maamori, H.M.S., El Naggar, M.H., and Micic, Silvana 2014. A compilation of the geo-mechanical properties of rocks in Southern Ontario and the neighbouring regions. *Open Journal Of Geology*. **4**: 210-227.
- Al-Maamori, H.M.S., El Naggar, M.H., Micic, Silvana and Lo, K.Y., 2016. Influence of Lubricant Fluids on Swelling Behaviour of Queenston Shale In Southern Ontario. *Canadian Geotechnical Journal*, **53** (7): 1059-1080.

- ASTM. 2008. Standard Practices for Preparing Rock Core As Cylindrical Test Specimens and Verifying Conformance to Dimensional and Shape Tolerances. ASTM standard D4543–08. ASTM International, West Conshohocken, PA.
- ASTM. 2008. Standard Test Method for Splitting Tensile Strength of Intact Rock Core Specimens. ASTM standard D3967–08. ASTM International, West Conshohocken, PA.
- ASTM. 2010. Standard Test Method For Compressive Strength and Elastic Moduli of Intact Rock Core Specimens Under Varying States of Stress and Temperatures. ASTM standard D7012–10. ASTM International, West Conshohocken, PA.
- ASTM. 2008. Standard Test Method for Direct Tensile Strength of Intact Rock Core Specimens. ASTM standard D2936–08. ASTM International, West Conshohocken, PA.
- ASTM. 2010. Standard Test Methods for Laboratory Determination of Water (Moisture) Content of Soil and Rock by Mass. ASTM standard D2216-10. ASTM International, West Conshohocken, PA.
- Baud, P., Zhu, W., Wong, T., 2000. Failure Mode and Weakening Effect of Water on Sandstone. *Journal of Geophysical Research*, **105**: 16371-16389.
- Bro, A. 1997. Analysis of Multistage Triaxial Test Results for a Strain-Hardening Rock. *International Journal of Rock Mechanics and Mining Sciences*, **34** (1): 143-145.
- Colback, P.S.B., Wiid, B.L., 1965. The Influence of Moisture Content on the Compressive Strength of Rock. *Rock Mechanics Symposium, Ottawa 1965*. University of Toronto, Department of Mines and Technical Surveys, pp. 65-84.
- Dreimanis, A. 1962. Quantitative Gasometric Determination of Calcite and Dolomite by Using Chittick Apparatus. *Journal of Sedimentary Petrology*, **32** (3): 520-529.

- Hashiba, K., Fukui, K. 2014. Effect of water on the deformation and failure of rock in uniaxial tension. *Rock Mechanics and Rock Engineering*, **47**: 1-11.
- Heap, M. J., P. Baud, P. G. Meredith, A. F. Bell, and I. G. Main, 2009. Time-dependent brittle creep in Darley Dale sandstone. *Journal of Geophysical Research*, **114**: B07203.
- Heuze F.E., 1967. Mechanical Properties and In-Situ Behaviour of the Chino Limestone, Riverside, California. ,” M.Sc. Thesis, Department of Civil Engineering, University of California, Berkeley, USA.
- Kim, M. M. and Ko, H. Y. 1997. Multistage Triaxial Testing of Rocks. *Geotechnical Testing Journal*, **2**: 98-105.
- Kovari, K. and Tisa, A., 1975. Multiple Failure State and Strain Controlled Triaxial Tests. *Rock Mechanics*, **7**: 17-33.
- Lee, Y.N. 1988. Stress-Strain-Time Relationship of Queenston Shale. Ph.D. thesis, Civil and Environmental Engineering Department, The University of Western Ontario, London, ON., Canada.
- Lee, Y.N., and Lo, K.Y. 1993. The Swelling Mechanism of Queenston Shale. In *Proceedings of The Canadian Tunnelling, 1993, The Tunnelling Association of Canada*, pp. 75-97.
- Liang, W., Yang, X., Gao, H., Zhang, C. and Zhao, Y. 2012. Experimental Study of Mechanical Properties of Gypsum Soaked In Brine. *International Journal of Rock Mechanics and Mining Sciences*, **53**: 142-150.
- Lo, K. Y. 2005. *From Soft Clay To Hard Rock In Geotechnical Engineering*. Western University, London, Ontario, Canada.
- Lo, K.Y., Cooke, B.H. and Dunbar, D.D. 1987. Design of Buried Structure In Squeezing Rock In Toronto, Canada. *Canadian Geotechnical Journal*, **24**(2): 232-241.

- Lo, K.Y., Devata, M. and Yuen, C.M.K. 1979. Performance of Shallow Tunnel In A Shaly Rock With High Horizontal Stresses. In Proceedings of the Second International Symposium on Tunnelling. Tunnelling '79. Institution of Mining and Metallurgy, London, England, Paper 9, pp. 1-12.
- Lo, K.Y. and Hori, M. 1979. Deformation and Strength Properties of Some Rocks in Southern Ontario. Canadian Geotechnical Journal, **16** (1): 108-120.
- Lo, K.Y., Ogawa, T., Lukajic, B., and Dupak, D.D. 1991. Measurements of strength parameters of concrete-rock contact at the dam-foundation interface. Geotechnical Testing Journal, **14** (4): 383-394.
- Neville, A.M. 1996. Properties of Concrete, 4th Edition. Pearson Education Limited, Harlow, England.
- Paterson, M.S. 1978. Experimental Rock Deformation: The Brittle Field. Springer-Verlag, Berlin.
- Wasantha, P.L.P. and Ranjith, P.G. 2014. Water-Weakening Behavior of Hawkesbury Sandstone In Brittle Regime. Engineering Geology, **178**: 91-101.
- Yang, S.-Q. 2012. Strength and deformation behavior of red sandstone under multi-stage triaxial compression. Canadian Geotechnical Journal, **49**: 694-709.
- Yang, S.-Q., Jing, H.W., Li, Y.S., and Han, L.J. 2011. Experimental Investigation on Mechanical Behavior of Coarse Marble Under Six Different Loading Paths. Experimental Mechanics, **51**:315-334.
- Doi:10.1007/s11340-010-9362-2.
- Youn, H. and Tonon, F. 2010. Multi-stage triaxial test on brittle rock. International Journal of Rock Mechanics & Mining Sciences, **47**: 678-684.

Chapter 6

DEPTH OF PENETRATION OF LUBRICANT FLUIDS AND WATER IN QUEENSTON SHALE OF SOUTHERN ONTARIO⁵

6.1 INTRODUCTION

The Queenston shale is a sedimentary rock in southern Ontario exhibiting time-dependent deformation behaviour (i.e. swelling). This swelling occurs due to the water osmosis and diffusion in salinity of the rock pore fluid (Lee and Lo, 1993). It is different than creep process that occurs in other rocks, such as potash and rock salt when loading condition changes. When these rocks creep, their particles undergo a movement of dislocation that leads to gliding in the intracrystalline structure manifested in the form of swelling deformation (Al-Maamori et al, 2016). The swelling of the Queenston shale was found to occur when three conditions are met: i) the relief of the initial in-situ stress that serves as an initiating mechanism, ii) the accessibility of water, and iii) an outward salt concentration gradient from the rock pore fluid to the ambient fluid (Lee and Lo 1993). It was concluded that swelling of the Queenston shale occurs when these three conditions are met, while no swelling occurs if none of these conditions are satisfied.

The swelling of this shale may or may not occur if one or two of these conditions are not fulfilled. The second and third conditions are essentially related to each other. Increasing the moisture content of shales decreases its pore fluid salinity, and vice versa (Lee 1988). Therefore, it is important to evaluate the depth of influence of water and other fluids into the shale to predict the extent of its swelling zone. The swelling of the Queenston shales was also found to be associated with the development of micro-cracks in their structure. These micro-cracks are induced in the Queenston shale structure due to the increase in

⁵ A version of this chapter has been submitted for publication in the Canadian Geotechnical Journal in March, 2016.

the volume of macropores and ultra-micropores during the exposure of this shale to fresh water (Lee and Lo, 1993). The developed micro-cracks during the swelling process may act as pathways for water and other fluids to percolate deeper into this shale.

Most of the available research studies in the literature dealt with drilling fluids, such as bentonite slurry in different types of soil. The effect of using bentonite slurry enriched with polymer and other additives decreased its fluid loss into the ground and enhanced its ability to hold higher pressure, compared to pure bentonite slurry (Fritz, P., 2006, Flint, G.R., 1992, and Flint, G.R., and Foreman, W., 1992). This action was achieved through the thick filter cake created on the surface of excavation and it was used successfully in earth pressure balance machines to construct large tunnels in weak soils heavily charged with ground water. Al-Maamori et al. (2016) investigated the influence of lubricant fluids, such as bentonite and polymer solutions used in micro-tunneling applications on the swelling behaviour of the Queenston shale in southern Ontario. These fluids were found to cause different degrees of swelling (i.e. different swelling potentials) compared to water. The influence of lubricant fluids on the swelling behaviour was attributed to their coating effect on the exposed surface of the Queenston shale, and on their effect on the exchange process of free cations in this shale and the ambient fluid. Therefore, it is suggested in this research to investigate the penetration of water and lubricant fluids in the Queenston shale considering long time effects. During the period of the suggested penetration test (i.e. 100 days), some of the swelling deformation of the Queenston shale can occur, inducing the development of micro-cracks in their structure, which in turn, may influence the rates of fluids penetration.

Hydraulic conductivity (formerly known as coefficient of permeability) is the ratio of the fluid velocity through a medium divided the hydraulic gradient (Lambe and Whitman, 1979). In rock mechanics, two values of hydraulic conductivity are defined: i) primary hydraulic conductivity of intact rock and ii) secondary hydraulic conductivity of the rock mass that contains joints, fissures and faults. At high depth, it is believed that both values are similar where high overburden pressure closes existing joints. The hydraulic conductivity of various rocks in Canada was reported from in-situ measurement. Raven et al., (1992) reported that the Queenston shale at 127-140 m depth

exhibits hydraulic conductivity of 10^{-9} to 10^{-10} m/s, and it decreases with increasing the depth. The Queenston shale of the Niagara Escarpment in Ontario indicated similar value of the hydraulic conductivity of 10^{-9} m/s measured at 54-60 m depth (Nadon and Gale, 1984). Similar observation was indicated for the Gabbro in Okanagan Highland, where the average hydraulic conductivity was 4.3×10^{-9} m/s and it decreases with increasing depth (Lawson 1968). The Georgian Bay shale in Toronto exhibited secondary hydraulic conductivity of 10^{-6} – 10^{-5} m/s that decreases to 3×10^{-9} – 4×10^{-7} m/s at higher depths (Lo et al., 1987) indicating the closure of existing joints. The measured hydraulic conductivity of the shaly limestone of Trenton formation was between 4×10^{-12} and less than 1×10^{-13} m/s, and for Ordovician argillaceous limestone it was between 10^{-13} and 10^{-14} m/s and decreases with increasing the depth (Raven et al., 1992).

The Opalinus Clay rock at the Mont Terri rock lab exhibited hydraulic conductivity between 2×10^{-14} and 2×10^{-12} m/s (Daniel et al., 2007 and Marshal et al., 2004). They indicated that nearfield effects can cause desaturation of the exposed rock near excavation causing overestimation of the measured hydraulic conductivity. Gale and Reardon (1984) indicated that hydraulic conductivity of fractured granite grouted with Portland cement grout can be reduced using effluent of high concentration $\text{Ca}(\text{HCO}_3)_2$. The confining pressure of the rock can influence its hydraulic conductivity. Changing the stress state acting on a rock from compression to tension can increase its hydraulic conductivity (Heystee and Roegiers, 1981). Liu et al., (2013) back calculated the hydraulic conductivity of clay liners, which was found to be less than 5×10^{-11} m/s from its fluid loss and produced reasonable values indicating the possibility to use indirect measurements to calculate the hydraulic conductivity.

6.2 RESEARCH OBJECTIVE

The objective of this research study is to evaluate the depth of influence of water and lubricant fluids used in micro-tunneling applications (i.e. bentonite and polymer solutions) in the Queenston shale through measuring their depth of penetration under similar conditions for a period of 100 days.

6.3 MATERIALS

6.3.1 Rock Cores

The Queenston shale samples used in this research were collected from a borehole drilled in Milton, Ontario, Canada. The borehole was located near the Regional Road 25 and Louis St. Laurent Avenue at 150 m to the east of the interchange, and 10 m to the south of Regional Road 25. The Universal Transverse Mercator (UTM) coordinates of the borehole are: 17T 593246 m E, 4816478 m N. The drilling was performed using truck-mounted double tube swivel type core barrels. The overburden soil was 15.5 m and the recovered rock column was HQ size (i.e. 63 mm diameter) 19 m long, from 15.5 m depth to 34.5 m depth below the ground level. The rock layer was Queenston shale with thin interbedded layers of shaly limestone at various intervals, and occasional gypsum nodulus along the rock column. The recovered samples were properly maintained immediately after drilling to preserve moisture, and to protect samples against breakage.

The Queenston shale layer where samples were collected can be divided into three sub-layers based on their Rock Quality Designation (RQD), which is defined as the percentage of intact core pieces longer than 100 mm in the total length of the core:

- i) Top 7 m with an average of 69 %, and 2-5 mm wide joints of compacted clay at an average of 4 joints/m.
- ii) Intermediate 4 m with an average RQD of 90 %, and 2-5 mm wide joints of compacted clay at an average of 1 joint/m, and
- iii) Lower 8 m with an average RQD of 97 %, and 2 mm wide joints of compacted clay at an average of 1 joint/4m.

6.3.2 Lubricant Fluids

The lubricant fluids (i.e. bentonite and polymer solutions) used in this research were prepared in the lab using similar mixing proportions to those used in the field in most of micro-tunnelling applications. The bentonite solution was prepared by mixing 8

% of dry powder sodium bentonite clay type (HYDRAUL-EZ from CETCO-USA) with tap water, while polymer solution was prepared by mixing 0.8 % of liquid polymer concentrate type TK60 (anionic polyacrylamide suspension in a water-in-oil emulsion from Morrison Mud, Division of Mudtech Ltd.-UK) with tap water. Both solutions were kept for 24 hours to achieve full suspension in water prior to using them in the test.

6.4 TEST METHODOLOGY

6.4.1 Fluid Penetration Test Setup

Figure 6.1 shows a schematic drawing of the test setup. In this test, three cylindrical Queenston shale specimens were cut to approximate length of 0.24 m. These specimens were cut from the recovered rock column at depth 32-33 m below the ground level. The diameter of test specimens was kept at 0.063 m as samples were drilled in-situ. Holes of 0.01 m diameter were drilled to a depth of 0.01 m in one side of each specimen at 0.025 m intervals centre to centre along the specimen's length. To eliminate the variation in moisture content of the Queenston shale specimens that may exist initially, or may have occurred during the preparation of the 0.01 m holes, the test specimens were oven dried for 14 days at 60 ° Celsius temperature. This temperature was selected to avoid overheating of test specimens that may influence the shale structure. Drying the test specimens diminishes the variation in their initial moisture content which may influence the rate of fluid penetration. Zero moisture content of sample was achieved when its weight was constant in three successive measurements in three days in the drying process. The test specimens were then kept in a desiccator to allow them to cool to the room temperature. The weight of each test specimen was taken, and the dimensions were recorded as initial dimensions, as indicated in Table 6.2. Fine silica gel powder was used as a moisture or humidity indicator. The silica gel powder changes its colour instantaneously from purple to pink when subjected to moisture, as indicated in Figure 6.2. This is another reason for drying the test specimens at the start of test, as their initial moisture content may change the colour of the silica gel powder, which may produce misleading results. The drilled holes in each specimen were filled with the silica gel

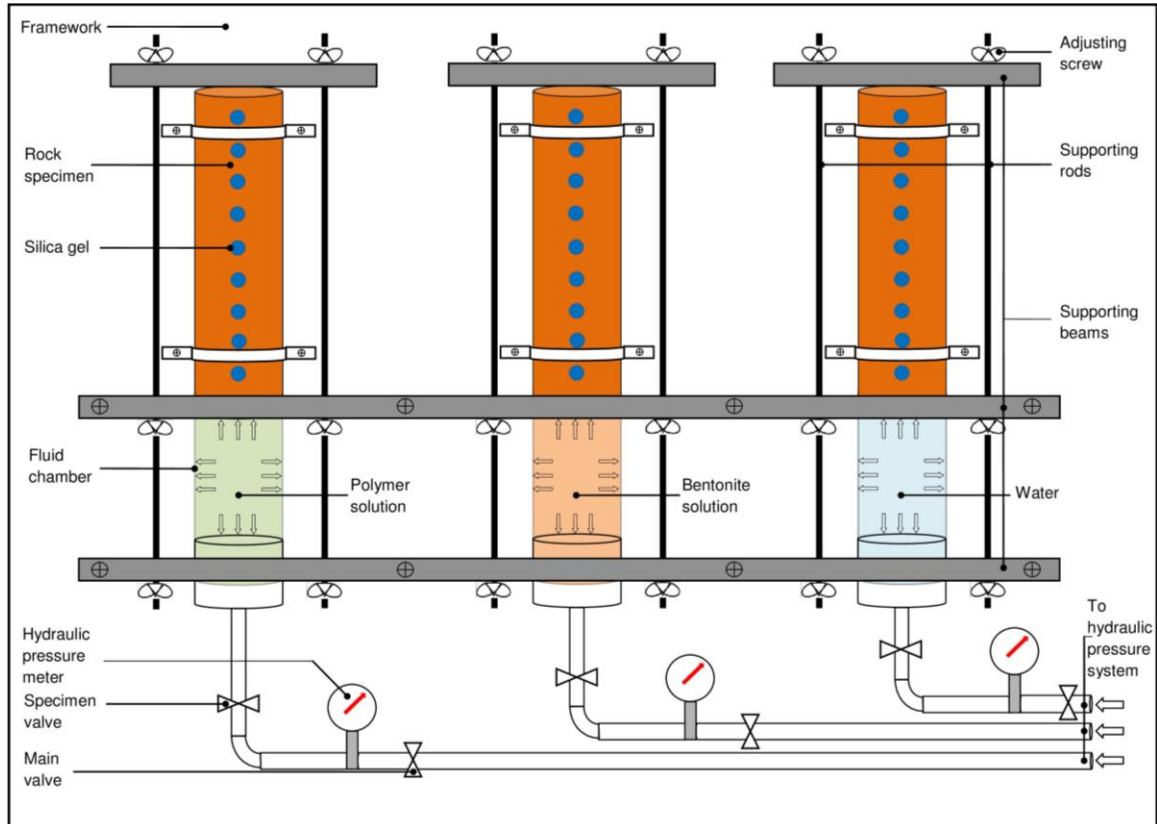


Figure 6.1. Test setup to investigate depth of penetration of lubricant fluids into shale.

powder, and the specimens were then coated with melted Paraffin wax from all sides leaving the front side uncoated. This side will be used to apply the fluid under pressure. Transparent masking tape was placed on top of the silica gel powder in the drilled holes to avoid contamination with the melted wax. The Paraffin wax coat was used to seal the test specimens in order to avoid air humidity in the lab from interfering test results. The test specimens were then placed in the test setup, as indicated in Figure 6.1. Each specimen was connected from the bare end to its fluid chamber, using mechanical clamp and silicone gel to ensure sealing against leakage. Three fluid chambers were filled with water, bentonite solution, and polymer solution, separately. Each fluid chamber was then connected to high strength PVC tube which in turn was connected to the hydraulic pressure system in the soil mechanics laboratory at Western University. Care was exercised to avoid any entrapped air bubbles in the used fluids inside the fluid chamber and in the tubing. Pressure was applied through the hydraulic system to the fluid chamber of each specimen. The pressure was gradually increased within one hour until it reached 200 kPa and was then kept constant throughout the test period allowing the fluid to percolate into the specimen. The hydraulic pressure system maintains the applied pressure onto the fluid chamber constant throughout the test period. The colour of the silica gel powder in the holes of each specimen was monitored throughout the test period. The time at which the colour changed to pink indicated the time required for the fluid to reach that depth in the Queenston shale specimen. A record of the depth of penetration (d) of each fluid and the corresponding time was maintained for 100 days.

6.4.2 Supplementary Tests

6.4.2.1 Moisture Content Determination

The moisture content was measured at several locations along the Queenston shale cylinders to investigate the increase in moisture content with depth, away from the source of fluid application. Upon the termination of the penetration tests after 100 days, each Queenston shale specimen was sliced into several segments, based on the location of the silica gel indicator (i.e. at 0.025 m intervals). Each segment was then divided into

three parts for the determination of moisture content, rock pore fluid salinity, and the calcite content. The moisture content test was performed following the procedure given in ASTM- D2216 (2010).

6.4.2.2 Rock Pore Fluid Salinity

The pore fluid salinity of Queenston shale specimens was measured at the end of the fluid penetration test, using the procedure described in Lee (1988). In a similar manner to that followed in moisture content determination, the pore fluid salinity was measured at several intervals along the length of each fluid penetration specimen.

Measuring the pore fluid salinity of the Queenston shale samples after performing the fluid penetration tests was achieved by measuring the electrical conductivity of a suspension of Queenston shale powder and water. The measured conductivity was then correlated to the corresponding pore water salinity using calibrated NaCl solutions. This is accomplished as follows. A Queenston shale chunk was extracted from the rock sample of the terminating fluid penetration test at several intervals along the sample. The Queenston shale chunks were air dried for seven days, and then were pulverized and passed No. 60 ASTM Sieve (250 μm). Obtained from the clay portion (< 250 μm), 20 g of Queenston shale powder was added to 100 g of distilled water and the mixture was shaken for a minimum of 30 minutes, and was then left for 24 hours to ensure that the pores salts completely dissolved in water. In order to separate the suspended powder from the water, the suspension was centrifuged for 20 minutes using centrifuge machine type (Sorvall RC-5B Refrigerated Super-speed Centrifuge, from Du Pont Instruments, Wilmington, Delaware, USA). The collected clear saline water was poured into a beaker to measure its electrical conductivity using a pH/ION 340i meter and a conductivity probe type TetraCon® 325 (WTW Wissenschaftlich-Technische Werkstätten GmbH, Weilheim, Germany). The electrical conductivity of NaCl reference solutions of known NaCl concentration was also measured. The results of the reference solutions were plotted in terms of electrical conductivity versus corresponding salinity and the best straight line fit was established. Employing this best-fit line, the salinity of the specimen

saline water was determined considering its electrical conductivity. The salinity was corrected to reflect the exact pore water salinity of the test specimens by considering the volume of the used suspension (0.1 L), the weight of the powdered Queenston shale (20 g) and the specimen moisture content.

6.4.2.3 Calcite Content

Calcite content plays a major role in cementing and strengthening the Queenston shale micro structure, and hence it may influence the fluid penetration tests results. The swelling potential of Queenston shale and other shales in southern Ontario was found to be influenced by the calcite content (Lo, 1989). When these shales possess a relatively high calcite content, their swelling potentials were found to be relatively smaller. This was attributed to the strong micro structure of these shales when they exhibit high calcite content. Therefore, it is important to determine the calcite content at several locations along the fluid penetration test specimens to ensure that no significant variation in the calcite content exists. The quantitative determination of the calcite content test in each segment after terminating the penetration test was performed using Chittick carbon dioxide apparatus, and following the procedure described in Dreimanis (1962). The specimens were air dried for seven days prior to performing the test.

6.4.3 A Suggested Approach of Calculating Hydraulic Conductivity of the Queenston Shale

The test method developed in this study for measuring the depth of influence of water and lubricant fluids in Queenston shale can also be used to predict the hydraulic conductivity of the Queenston shale in the tested fluids. In rocks mechanics, two types of hydraulic conductivity can be defined: the primary hydraulic conductivity, also known as the intrinsic hydraulic conductivity which is conductivity of intact rock; and the secondary hydraulic conductivity, that is the conductivity of the rock mass. Measuring the secondary hydraulic conductivity of rocks is a complicated process, where the condition of discontinuities and the material inside them play major roles in defining its

value. According to Hudson and Harrison (1997), the secondary hydraulic conductivity of fractured rock mass depends on:

- i) the aperture of the fracture, which in turn depends on
- ii) the normal stress acting across the fractures, which in turn depends on
- iii) the depth below the ground surface.

At high depths, both the primary and the secondary hydraulic conductivities are similar due to the closure of existing fractures under large overburden stress. Moreover, the high in-situ horizontal stresses that exist in the region of southern Ontario may have significant influence on the closure of vertical discontinuities in the rock mass. In this research, the primary hydraulic conductivity of Queenston shale from Milton, Ontario was calculated using results of the developed test method of measuring the fluids penetration depths. Adopting the calculated hydraulic conductivity suggested in this section is limited for rocks at high depths where joints in the rock mass are closed and secondary hydraulic conductivity approaches the primary hydraulic conductivity.

The following steps were followed in calculating the hydraulic conductivity of the Queenston shale in water, bentonite solution, and polymer solution:

The weight and dimensions of each specimen were measured after oven drying stage. The calculated density at that stage represents the dry density of the Queenston shale specimen, and the measured weight represents the mass of solids in it. The weight of solids remains constant throughout the test period. Any increase in the weight of the specimen was attributed to the weight of penetrated fluid. The mass density of water and lubricant fluids used in this research was also measured in room temperature, as summarized in Table 6.2. At the end of the test period (100 days), each specimen was divided into nine pieces at the locus of the drilled holes of the powder silica gel moisture indicator. Small pieces of test specimens were segregated from the exposed side at the end of fluids penetration tests. Therefore, moisture content along test specimens was used as a tool to calculate the amount of fluid penetrated. The moisture content of each piece

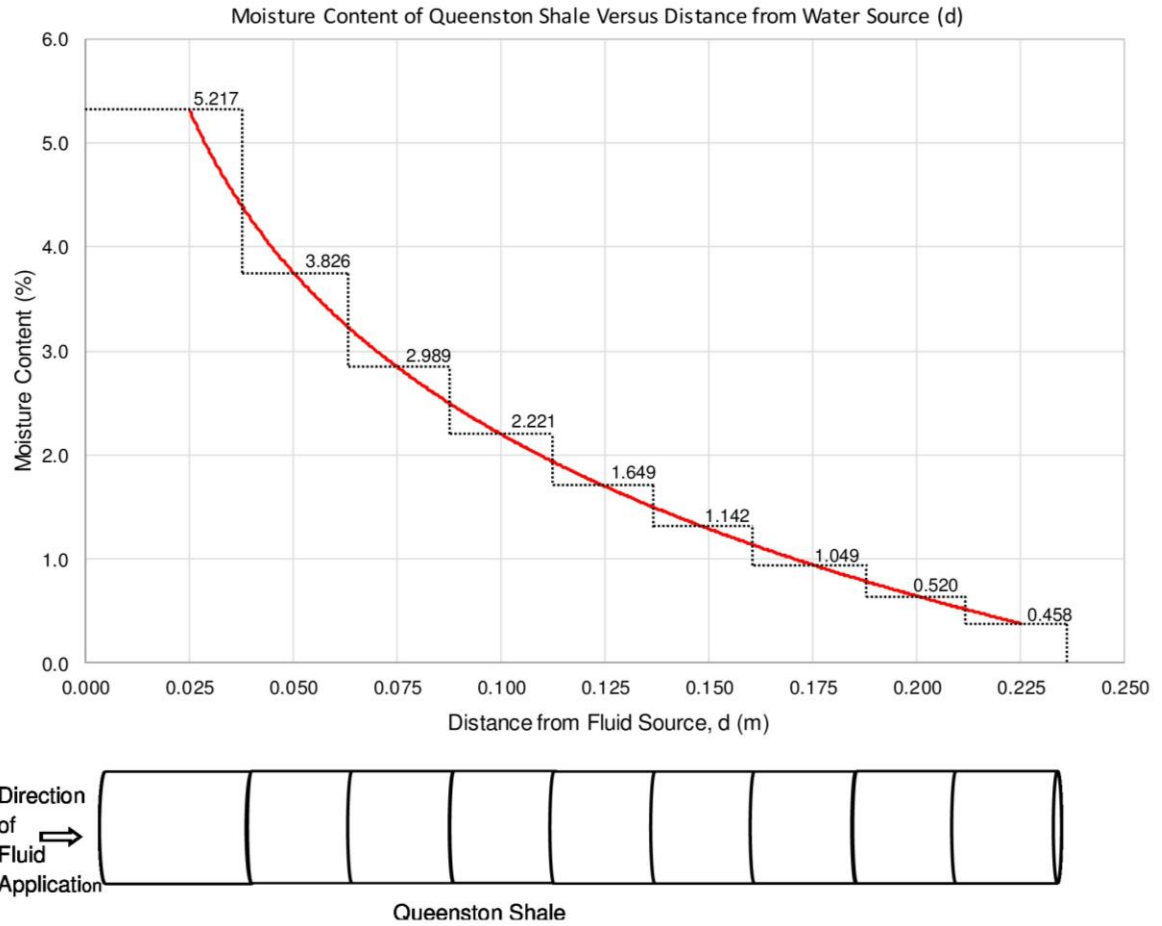


Figure 6.2. Schematic drawing for calculating the hydraulic conductivity of the Queenston shale.

was measured, and it is considered constant for the entire length of that piece. Figure 6.2 shows a schematic drawing of moisture content, considered in the calculations, along the length of Queenston shale specimen. The overall moisture content for each specimen was approximated by taking the weighted average of moisture contents of all pieces, according to their length contribution to the entire length of the specimen. Based on the weight of solids in each Queenston shale specimen measured earlier, the weight of penetrated fluid during the 100 days period was calculated using the weighted average values of moisture content. The discharged amount of water, bentonite solution, and polymer solution during the test period was calculated based on the measured mass density of each fluid. To calculate the hydraulic conductivity of the Queenston shale, Darcy's law that links the fluid's flow rate with the pressure gradient through the test specimen, as indicated in Equation [6.1] was used, i.e.

$$Q=KAi \quad [6.1]$$

Where Q represents the discharge in (m^3/s),

K represents the hydraulic conductivity in (m/s),

A represents the cross-sectional area of the medium where flow occurs in (m^2),
and

i represents the hydraulic gradient (the difference in hydraulic head per unit length), ($\Delta h/\Delta l$)

As indicated earlier, all fluids used were applied under pressure of 200 kPa, similar to that expected in micro-tunneling applications in the field. This pressure was used to define the hydraulic gradient and the final dimensions of each specimen were used in the calculations. Final dimensions of the rock specimens increased after 100 days. These dimensions were calculated based on time-dependent deformation parameters measure in another study (Al-Maamori et al., 2016) and presented in Table 6.2. The test period was 100 days, therefore one cycle of swelling potential was considered in calculating the final dimensions as follows:

$$D_f = D_i (1 + \text{HSP}) \quad [6.2], \text{ and}$$

$$L_f = L_i (1 + \text{VSP}) \quad [6.3]$$

Where D_i represents the diameter of specimen before starting the fluid penetration test in (m),

L_i represents the length of specimen before starting the fluid penetration test in (m),

D_f represents the diameter of specimen at the end of the fluid penetration test in (m),

L_f represents the length of specimen at the end of the fluid penetration test in (m), and

VSP and HSP represent the vertical and horizontal swelling potential, respectively in (% strain/log cycle of time). The VSP and HSP are defined as the rate of swelling strain of the rock specimen in the vertical and horizontal directions, respectively, in a log cycle of time when they are kept exposed to fresh water or 100% humidity (Lo et al. 1978).

In Equation [6.3], the length penetrated by each fluid at the end of test (as indicated in Table 6.1) was used.

6.5 RESULTS AND DISCUSSION

Table 6.1 summarizes the measurements recorded in the fluids penetration tests, and Figure 6.3 shows the change in the colour of the powder silica gel with time in each specimen. These results are discussed in details in the following sections:

6.5.1 Moisture Content

The results of moisture content tests measured along the Queenston shale specimens after the application of water, and lubricant fluids (i.e. bentonite solution, and polymer solution) for 100 days are summarized in Table 6.1, and they are illustrated in Figure 6.4. The fluids used were applied under a pressure similar to that used in the field in micro-tunneling applications, (i.e. 200 kPa). As indicated in Figure 6.4, the difference between water, bentonite solution, and polymer solution in their influence on the moisture content is evident. Water caused generally higher increase in the moisture contents than lubricant fluids. In contrast, lubricant fluids caused similar increase in the moisture content of Queenston shale. However, polymer solution caused the smallest moisture content change, compared to other two fluids used. Moreover, the increase in moisture content for specimens subjected to water extended deeper and reached the entire length of the Queenston shale specimen. On the other hand, bentonite solution and polymer solution caused an increase in the moisture content within 0.175 m, and 0.150 m depth of the tested specimens after 100 days.

Naturally, the influence of lubricant fluids on the moisture content would be maximum at the closest part to the applied fluid. At the closest part to water, the moisture content of the Queenston shale was 5.22 %, approaching full saturation of the shale. The moisture content of the Queenston shale in bentonite and polymer solutions was 3.00 %, and 2.97 %, respectively. These results are consistent with the swelling mechanism suggested by Lee and Lo (1993), and extended to include the swelling behaviour of Queenston shale in lubricant fluids used in micro-tunneling applications (Al-Maamori et

Table 6.1. Fluids Penetration and Queenston Shale Properties After Terminating Fluids Penetration Tests

Fluid	Penetration distance from fluid source, d (m)	Time (days)	Moisture content after terminating test (%)	Rock pore fluid salinity after terminating test (g/L)	Calcite content (%)
Water	0.025	1.0	5.217	7.8	20.6
	0.050	5.0	3.826	10.6	20.8
	0.075	10.0	2.989	40.4	20.2
	0.100	18.0	2.221	85.2	20.3
	0.125	25.0	1.649	139.7	20.8
	0.150	33.0	1.142	208.5	20.3
	0.175	41.0	1.049	311.5	20.2
	0.200	49.0	0.520	455.1	19.5
	0.225	60.0	0.458	565.5	19.9
Polymer solution	0.025	9.0	2.976	34.2	20.8
	0.050	22.0	2.288	54.3	20.5
	0.075	33.0	1.558	113.7	20.8
	0.100	46.0	1.405	281.7	21.0
	0.125	63.0	0.824	418.8	20.6
	0.150	94.0	0.623	480.8	20.5
	0.175	-	0.0	-	20.5
	0.200	-	0.0	-	20.5
	0.225	-	0.0	-	19.9
Bentonite solution	0.025	7.0	3.002	15.9	19.8
	0.050	15.0	2.554	25.3	20.9
	0.075	21.0	1.900	68.0	20.0
	0.100	33.0	1.600	178.5	21.1
	0.125	51.0	1.100	272.3	19.5
	0.150	71.0	0.626	346.7	20.0
	0.175	99.0	0.586	469.3	20.1
	0.200	-	0.0	-	20.8
	0.225	-	0.0	-	20.7

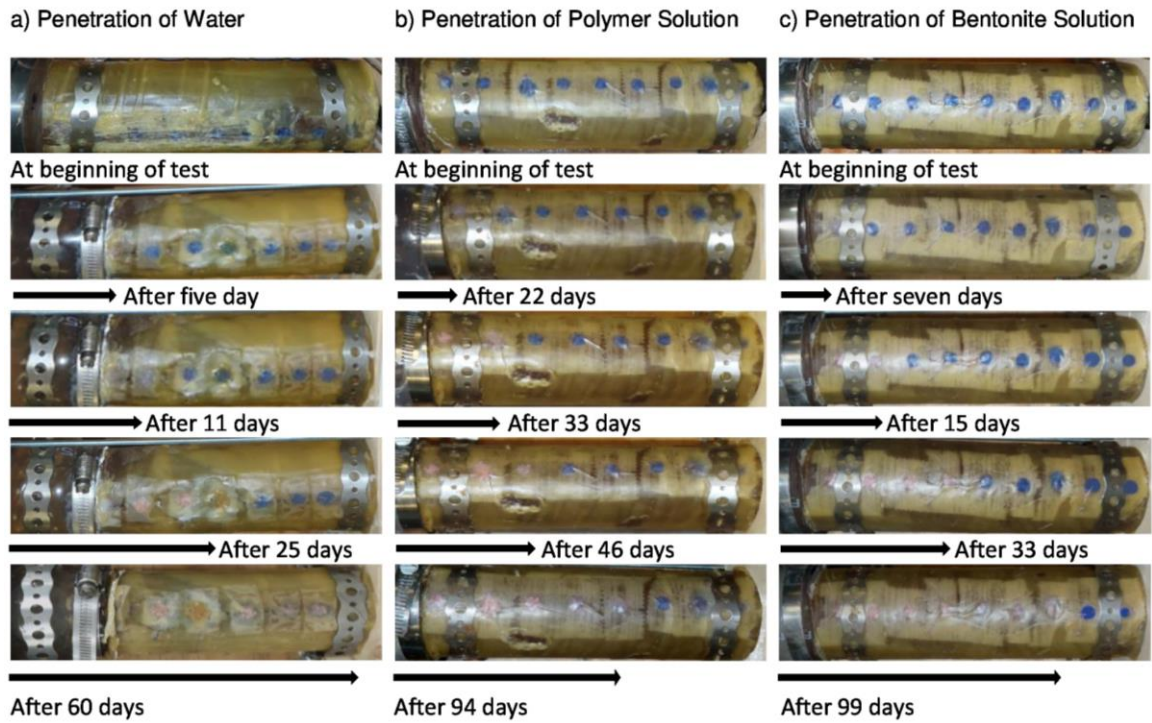


Figure 6.3. Fluid penetration in the Queenston shale: (a) water; (b) polymer solution and (c) bentonite solution.

al., 2016). It can be noted from Figure 6.4 that the influence of lubricant fluids on the moisture content of Queenston shale decreases gradually with increasing the distance from fluid application source. The differences in moisture content caused by various fluids used decreases with increasing the distance from the fluid source. The curves presented in Figure 6.4 demonstrate clearly that using lubricant fluids in micro-tunneling applications can considerably decrease the change in the moisture content within the depth of influence in Queenston shale. This, in turn, can decrease the time-dependent deformation in that depth and its related issues during construction of a pipeline or a tunnel in Queenston shale.

6.5.2 Rock Pore Fluid Salinity

The values of the measured pore fluid salinity of Queenston shale specimens and their corresponding depths are summarized in Table 6.1, and are plotted in Figure 6.5. Figure 6.5 shows the change in pore fluid salinity of the Queenston shale with the distance from source of fluid application. The plotted curves reflect a considerable decrease in the rock pore fluid salinity caused by various fluids used. On the one hand, the rock pore fluid salinity was changed differently in water and lubricant fluids, and the difference increases as the distance from applied fluid increases. On the other hand, water caused the highest decrease in the pore fluid salinity of Queenston shale after 100 days, while the polymer solution caused the least decrease. As indicated earlier, the pore fluid salinity is highly related to moisture content of the rock tested (Lee 1988). Therefore, as the moisture content of the Queenston shale specimen increases, its pore fluid salinity decreases.

Due to diffusion process, salinity free cations in the pore water of the Queenston shale move from higher concentration to lower concentration in the ambient fluid. This fact was concluded in earlier researches (Lee 1988, and Lee and Lo 1993). However, the cation exchange capacity of the Queenston shale in these fluids (i.e. water, bentonite solution, and polymer solution) was also found to be different (see Al-Maamori et al. 2016). This may explain the difference in the pore fluid salinity of Queenston shale when

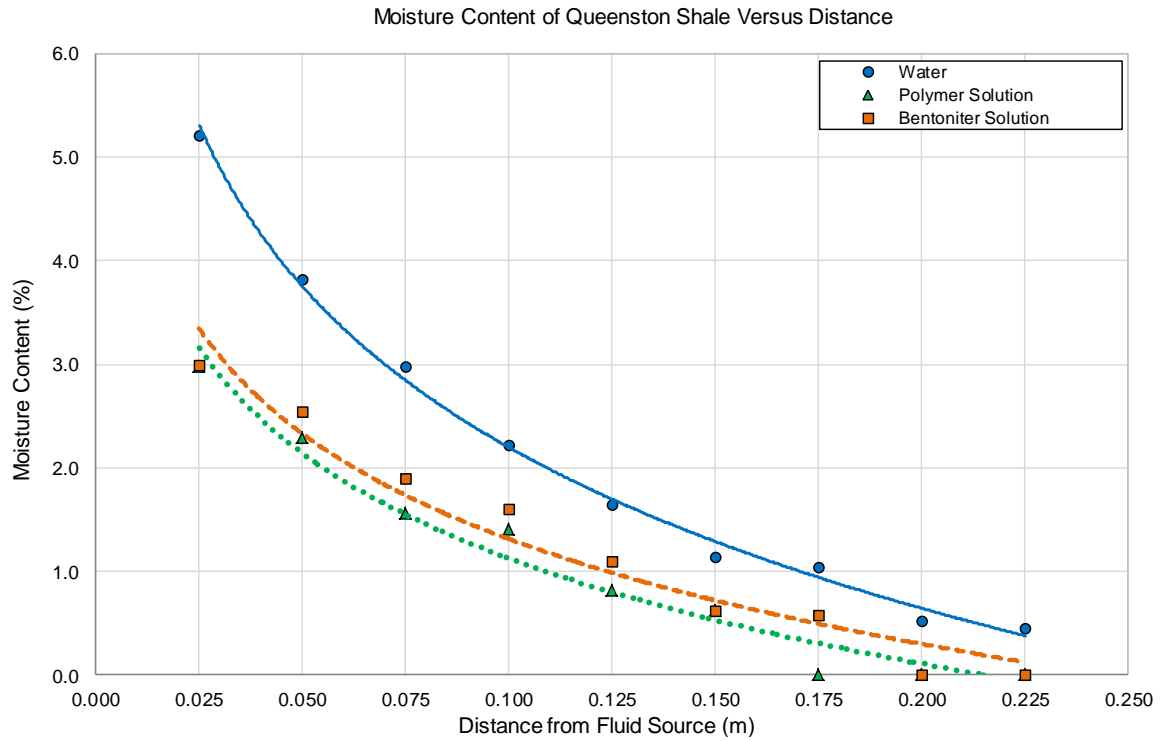


Figure 6.4. Change in moisture content of the Queenston shale with distance from source of fluid application.

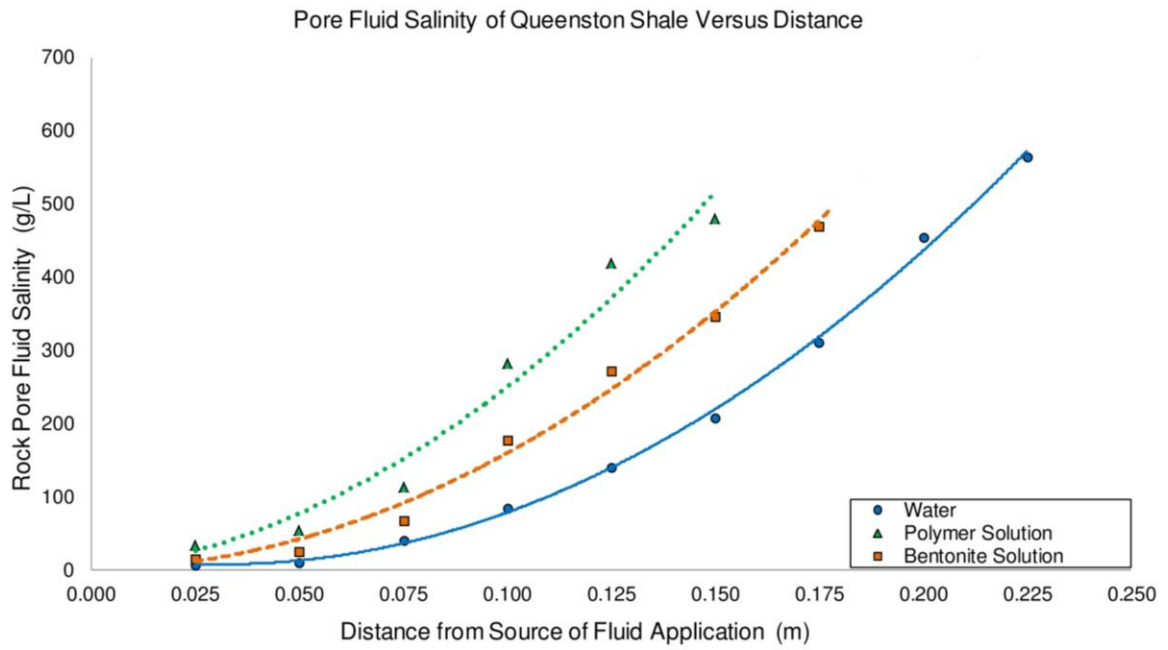


Figure 6.5. Change in pore fluid salinity of the Queenston shale with distance from source of fluid application.

exposed to different fluids. The rock pore fluid salinity was not calculated for the locus where moisture content was zero (i.e. beyond the penetrated depths). The change in the pore fluid salinity of the Queenston shale with depth indicates the occurrence of osmosis and diffusion processes. The combined osmosis and diffusion processes have caused these changes in the pore fluid salinity of Queenston shale with increasing distance from fluid source. This conclusion is based on the earlier researches mentioned above.

6.5.3 Calcite Content

The results of the calcite content are presented in Table 6.1. The purpose of measuring calcite content in the Queenston shale used in this research is to insure that the variation of calcite content in the fluid penetration test specimens is minimal. The calcite content test results presented in Table 6.1 indicate that the tested Queenston shale has calcite content between 19.5% and 21.1% with a difference of 0.6%. This difference of calcite content in the tested Queenston shale is relatively small, and its influence on the fluids penetration tests results can be neglected.

6.5.4 Fluids Penetration

The penetration depth of water, bentonite solution, and polymer solution in Queenston shale was monitored along the test period (i.e. 100 days). These results are presented in Table 6.1, and they are illustrated in Figure 6.3. When the colour of the powder silica gel turned from purple to pink as indicated in Figure 6.3, it is considered that the fluid has reached that distance from the source of fluid application. The results of penetration depth of water and lubricant fluids in Queenston shale summarized in Table 6.1 are plotted in Figure 6.6, which displays the depth of influence (d) in meters versus characteristic time (t) in days. The characteristic time is the time of penetration to the power 0.588. In this case, the best fitting straight line of each fluid penetration results can be produced. For the three fluids used, three best fitting straight lines were produced and their equations with the least square values are presented in Figure 6. The results show a

considerable difference in the depth of influence (d) of water and lubricant fluids. For sample subjected to water, penetration reached its full depth (i.e. 0.24 m) in 60 days; while bentonite solution penetrated only 0.175 m in 99 days and polymer solution reached 0.150 m depth in 94 days. The difference in penetration depth for different lubricant fluids, and the corresponding time required to reach that depth can be observed at the early stage of the test. This difference continued to increase with time up to the end of the test.

The results presented in Figure 6.6 are of high significance as they represent a reasonable tool to predict the influence zone of water, bentonite solution, and polymer solution in Queenston shale at longer time. The following correlation was derived from Figure 6.6:

$$d = C_{fl} \cdot t^{0.588} \quad [6.4]$$

Where d represents the depth of influence of applied fluid in Queenston shale in (m),

C_{fl} is a fluid constant in $(\text{m}/\text{day}^{0.588})$, and its value equals to:

0.0197 $(\text{m}/\text{day}^{0.588})$ for water,

0.0120 $(\text{m}/\text{day}^{0.588})$ for bentonite solution, and

0.0102 $(\text{m}/\text{day}^{0.588})$ for polymer solution,

and t represents the time in (days)

Using the presented approach, the following can be established:

If we consider a life time of 24 years of underground structures, (i.e. 8766 days), assuming fluids were applied under similar pressure of 200 kPa, and substitute this value for the time (t) in the above equation, the depth of the influenced zone in Queenston shale is: 4.1 m for water, 2.5 m for bentonite solution, and 2.1 m for polymer solution.

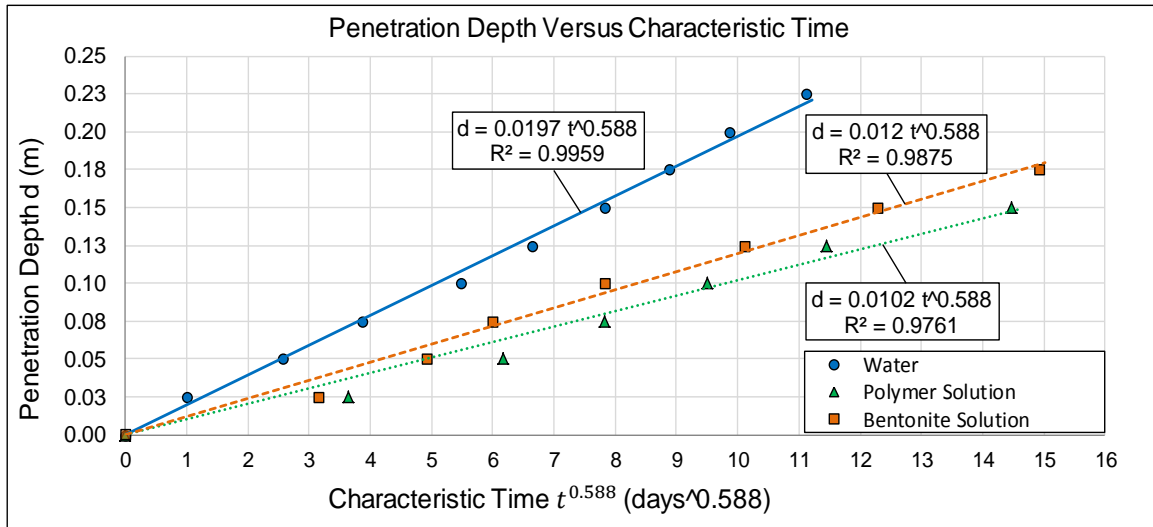


Figure 6.6. Penetration depth of fluids into the Queenston shale with time.

This calculated depth of water influence in Queenston shale is consistent with some field observations on relatively similar shales in southern Ontario (Lo, 2005). The uniaxial compressive strength of Georgian Bay shale samples collected from the Heart Lake tunnel at four meters depth approximately was found to be decreased from 24.4 MPa to 10.0 MPa and from 24.0 MPa to 6.5 MPa in the vertical and horizontal directions, respectively, after the passage of 24 years of the tunnel construction (Lo, 2005). This decrease in the strength was attributed to the time-dependent deformation associated with water absorption and the formation of micro-cracks in this shale (Lee and Lo 1993). Therefore, it can be concluded that water have reached a depth of four meters in the Georgian Bay shale after 24 years of continuous exposure to water in the tunnel (Lo, 2005), which is very consistent with our finding for the Queenston shale, with a difference of 2.5% between measured depth and predicted depth of water penetration, taking into account the different rock type in both cases . Lubricant fluids used in micro-tunneling applications were found to have physical and chemical influence on the Queenston shale. Detailed description of these influences on the development of micro cracks in the Queenston shale can be found in (Al-Maamori et al., 2016). In the absence of accurate long-term field measurements in Queenston shale, the derived correlation can be useful to some extent. It can be used as a preliminary prediction of the influence zone of water and lubricant fluids in Queenston shale. The predicted zone can be considered in calculating the time-dependent deformation of the Queenston shale. However, further investigation is required to examine the in-situ influence zone of fluids in different types of rocks in the region of southern Ontario, and elsewhere.

6.5.5 Hydraulic Conductivity

The calculated hydraulic conductivity of Queenston shale based on Darcy's law is presented in Table 6.3. Three values of the hydraulic conductivity were calculated based on the used fluid. It is clearly indicated that the hydraulic conductivity of the Queenston shale measured in bentonite solution and polymer solution was smaller than its value

Table 6.2. Properties of Queenston shale specimens and applied fluids

Specimen No.	Properties of Fluid			Properties of Queenston Shale Specimen								
	Fluid Used In Penetration Test	Fluid Mass Density (g/cm ³)	In-situ Moisture Content, w (%)	Weight of Solids in Specimen (g)	Initial Diameter Di (cm)	Initial Length Li (cm)	Initial Volume (cm ³)	Initial Dry Density (g/cm ³)	Vertical Swelling Potential, VSP (% vertical strain/log cycle of time)	Horizontal Swelling Potential, HSP (% horizontal strain/log cycle of time)	Final Diameter Df (cm)	Final Length Lf (cm)
1	Water	0.997	2.01	1918.005	6.2998	24.130	745.075	2.574	0.190	0.156	6.3096	24.1758
2	Bentonite Solution	1.046	2.00	1905.200	6.3002	23.998	741.055	2.571	0.235	0.170	6.3109	24.0421
3	Polymer Solution	0.998	2.10	1910.707	6.3001	24.091	743.931	2.568	0.065	0.027	6.3018	24.1016

measured in water. In comparison to water, using bentonite solution caused a decrease of 56% in the hydraulic conductivity of Queenston shale, while using polymer solution caused relatively higher decrease of 65%. This finding is consistent with the decrease in the swelling potential of Queenston shale caused by lubricant fluids (see Al-Maamori et al. 2016). Water penetration into the Queenston shale after completing the construction in micro-tunneling applications, where rock surface was in direct contact with lubricant fluids, needs to be investigated. In-situ instrumentation near tunnels is highly recommended where it is the only trusted means to investigate the penetration depth of water and its effects in the surrounding rock.

Table 6.3. Calculated hydraulic conductivity of the Queenston Shale

Fluid	Hydraulic Conductivity (cm/s)
Water	1.9×10^{-9}
Bentonite Solution	8.3×10^{-10}
Polymer Solution	6.6×10^{-10}

6.6 SUMMARY AND CONCLUSIONS

A new setup was developed to measure the influence depth of water, bentonite solution, and polymer solution into the Queenston shale from Milton, Ontario. The setup attempts to simulate the field conditions during micro tunneling construction in Queenston shale, where lubricant fluids are applied under a pressure of approximately 200 kPa. Water was used in this research as a control fluid. The penetration of these fluids was monitored visually through the changed colour of the silica gel powder from purple to pink upon increasing the moisture content. The depth of penetration of these fluids was plotted versus the penetration characteristic time, which is time in days to the power of 0.588. A correlation was derived to predict the depth of influence of water, bentonite solution, and polymer solutions in Queenston shale at longer time assuming similar fluid pressure. The hydraulic conductivity of the Queenston shale was calculated using Darcy's law. The following conclusions can be drawn from this research:

- 1) The suggested test method can be performed in the lab to measure depth of influence of water, bentonite solution, and polymer solution in Queenston shale in a limited time. Based on the test results, a correlation was derived to predict long-term penetration of these fluids in Queenston shale.
- 2) The primary hydraulic conductivity of Queenston shale from Milton, Ontario was calculated using the measured amounts of the penetrated fluids at the end of the fluid penetration tests, adopting Darcy's law. Different hydraulic conductivity of the Queenston shale was calculated for the different fluids used. The hydraulic conductivity measured in lubricant fluids was smaller compared to water.
- 3) Lubricant fluids used in micro tunneling applications can have a considerable influence in reducing the penetration of moisture into the Queenston shale, compared to water. Moreover, polymer solution was found to be more efficient in reducing the influenced zone of the Queenston shale compared to bentonite solution.

It is recommended to have field investigation on built water conveying tunnels to investigate the zone of water influence in the host rock. It is also recommended to extend this research to include other types of rocks from Southern Ontario.

6.7 REFERENCES

- ASTM 2010. Standard Test Methods for Laboratory Determination of Water (Moisture) Content of Soil and Rock by Mass. ASTM standard D2216-10. ASTM International, West Conshohocken, Pa.
- Al-Maamori, H.M.S., El Naggar, M.H., Micic, S., and Lo, K.Y. (2016). The Influence of Lubricant Fluids on Swelling Behaviour of Queenston Shale In Southern Ontario. *Canadian Geotechnical Journal*, **53** (7): 1059-1080.
- Daniel Fernàndez-Garcia, D., Gómez-Hernández, J. J., and Mayor, J.C. 2007. Estimating hydraulic conductivity of the Opalinus Clay at the regional scale: Combined effect of desaturation and EDZ. *Physics and Chemistry of Earth*, **32** (8-14), 639-645.
- Dreimanis, A. 1962. Quantitative Gasometric Determination of Calcite and Dolomite By Using Chittick Apparatus. *Journal of Sedimentary Petrology*, **32** (3): 520 - 529.
- Flint, G.R. 1992. Tunnelling Using Earth Pressure Balance Machines for the Boulac Spine Sewers of the Greater Cairo Wastewater Project. *Tunnelling and Underground Space Technology*, **7**(4): 415-424.
- Flint, G.R. and Foreman, W. 1992. Bentonite Tunnelling for the Greater Cairo Wastewater Project. *Tunnelling and Underground Spate Technology*, **7**(1): 45-53.

- Fritz, P. 2006. Additives for slurry shields in highly permeable ground. *Rock Mechanics and Rock Engineering*, 40 (1): 81-95.
- Gale, J. E., and Reardon, E. J. 1984. Effects of groundwater geochemistry on the permeability of grouted fractures. Canada. *Canadian Geotechnical Journal*, **21** (1): 8-20.
- Heystee, R., and Roegiers, J.-C. 1981. The effect of stress on the primary permeability of rock cores-a facet of hydraulic fracturing. *Canadian Geotechnical Journal*, **18** (2): 195-204.
- Hudson, J. A., and Harrison, J. P. *Engineering Rock Mechanics, An Introduction to the Principles*. First Edition, Gray Publishing, Tunbridge Wells, Kent, Redwood Books, Trowbridge, Great Britain, 1997, 444 p.
- Lawson, D. W. 1968. Groundwater flow systems in the crystalline rocks of the Okanagan Highland, British Columbia. *Canadian Journal of Earth Sciences*, **5**: 813-824.
- Lee, Y.N. 1988. Stress-strain-time relationship of Queenston shale. Ph.D. thesis, Civil and Environmental Engineering Department, The University of Western Ontario, London, ON.
- Lee, Y.N. and Lo, K.Y. 1993. The swelling mechanism of Queenston shale. *Canadian Tunnelling 1993*, The Tunnelling Association of Canada, pp. 75-97.
- Liu, Y., Gates, W.P., Bouazza, A., and Rowe, K. 2013. Fluid loss as a quick method to evaluate hydraulic conductivity of geosynthetic clay liners under acidic conditions. *Canadian Geotechnical Journal*, **51**: 158-163. [.doi.org/10.1139/cgj-2013-0241](https://doi.org/10.1139/cgj-2013-0241)

Lo, K. Y. From Soft Clay to Hard Rock in Geotechnical Engineering, First Edition, Western University Publications, London, Ontario, Canada, 2005, 1936 p.

Lo, K.Y. 1989. Recent Advances in Design and Evaluation of Performance of Underground Structures in Rocks. *Tunnelling and Underground Space Technology*, **4** (2): 171-183.

Lo, K.Y., Cooke, B.H., and Dunbar, D.D. 1987. Design of buried structures in squeezing rock in Toronto, Canada. *Canadian Geotechnical Journal*, **24** (2): 232-241.
Doi: 10.1139/t87-028.

Lo, K.Y., Wai, R.S.C., Palmer, J.H.L., and Quigley, R.M. 1978. Time-dependent deformation of shaly rocks in southern Ontario. *Canadian Geotechnical Journal*, **15** (4): 537–547. doi:10.1139/t78-057.

Marshall, P., Croisé, J., Schlickenrieder, J.-Y., Boisson, P., Vogel, P., Yamamoto, S., 2004. Synthesis of hydrogeological investigations at the mont terri site (phases 1 to 5). In: Heitzmann, P. (Ed.), *Mont Terri Project – Hydrogeological Synthesis, Osmotic Flow*. Reports of the Federal Office for Water and Geology (FOWG), Geology Series No. 6.

Nadon, R. L., and Gale, J. E., 1984. Impact of groundwater on mining and underground space development in the Niagara Escarpment area. *Canadian Geotechnical Journal*, **21**(1): 605-74.
Doi: 10.1139/t84-005.

Raven, K. G., Novakowski, K. S., Yager, R. M., and Heystee, R. J. 1992. Supernormal fluid pressures in sedimentary rocks of southern Ontario – western New York State.

Canadian Geotechnical Journal, **29**(1): 80-93.

Doi: 10.1139/t92-009.

Wang, E. Z., Yue, Z. Q., Tham, L. G., Tsui, Y., and Wang, H. T. 2002. A dual fracture model to simulate large-scale flow through fractured rocks. Canadian Geotechnical

Journal, **39**(6): 1302-1312.

Doi: 10.1139/t02-068.

Chapter 7

FINITE ELEMENT ANALYSES OF TIME-DEPENDENT DEFORMATION AND INDUCED STRESSES IN CONCRETE PIPES CONSTRUCTED IN QUEENSTON SHALE USING MICRO-TUNNELING TECHNIQUE⁶

7.1 INTRODUCTION

The time-dependent deformation behaviour of shales in southern Ontario was extensively investigated during the past few decades (e.g. Hawlader et al., 2003; Hefny et al., 1996; Lo and Hefny, 1996; Lee and Lo, 1993; Lo and Lee, 1990; Lo and Yuen, 1981; Yuen, 1981; and Lo et al., 1978 and 1975). These studies provided good insights of the swelling phenomenon of these shales, its measurements, its causes and its controlling mechanism. A closed form visco-elastic solution was developed by Lo and Yuen in 1981 to predict deformations and stresses in concrete lining of circular tunnels in swelling rocks. Hefny et al. (1996) extended this solution to account for long-term swelling and the critical stress, defined as minimum stress required to stop rock swelling. Both solutions were utilized to analyze many tunnels in southern Ontario (Lo and Hefny, 1996 and Lo and Yuen, 1981).

The strength of shales in southern Ontario was also investigated (Lee 1988; Lo et al. 1987; Wai et al. 1981; Lo and Yuen, 1981; Yuen, 1979; and Lo and Hori 1979). The strength was found to be anisotropic and decreases with increasing size of sample approaching the rock mass modulus. Investigations on other rocks showed that increasing their moisture content had significant impact on their strength (Wasantha and Ranjith, 2014; Dan et al. 2013; Liang et al. 2012; Gorski et al. 2007; Paterson and Wong, 2005; Claesson and Bohlooli 2002; Baud et al. 2000; Paterson 1978; and Colback and Wiid,

⁶ A version of this chapter has been submitted for publication in the Canadian Geotechnical Journal in July, 2016

1965). The investigated rocks showed strength degradation after increasing their moisture content.

Al-Maamori et al. (2016) investigated the impact of lubricant fluids used in micro-tunneling applications on both time-dependent deformation and strength of the Queenston shale. The swelling behaviour of Queenston shale in lubricant fluids was found to be different than its behaviour in water, and its strength was generally degraded with different percentages after soaking it in water and lubricant fluids. Given that time-dependent deformation behavior of Queenston shale and its strength degradation are different in lubricant fluids compared to water, it is necessary to evaluate the effects of lubricant fluids used in micro-tunneling construction on pipes and tunnel lining.

Finite element studies of swelling rock are limited. Hawlader et al., (2003) developed a plane strain finite element model to predict deformations and stresses induced at tunnel lining in swelling rock. Kramer and Moore (2005) used Lo and Hefny (1996) swelling model and developed plane strain finite element model to calculate stresses and time-dependent deformation of rock and lining interaction. Heidkamp and Katz (2002) proposed an implicit integration scheme using Grob's swelling law to predict volume increase of Gypsum and clay minerals and implemented it in FE program. Wittke and Wittke (2004) developed a constitutive elasto-plastic law describing swelling of non-leached Gypsum, considering the anisotropic behaviour and implement it in 3D FE program. Schädlich et al. (2012) extended the model into a general rock swelling model using Grob's swelling law. Schädlich et al. (2013) implemented the rock swelling model in PLAXIS computer program to back analyze in-situ measurements of the Pfaender railway tunnel in Austria.

7.2 RESEARCH OBJECTIVE

The main objective of this research is to investigate the time-dependant deformations and stresses induced in pipes or tunnels constructed using the micro-tunneling technique in Queenston shale. This objective is achieved through finite element analyses utilizing the computer program PLAXIS 2D (PLAXIS, 2016). The rock swelling

model developed and utilized in PLAXIS 2D environment is based on the Lo and Hefny swelling mathematical model (1996). The results are envisioned to aid owners and contractors to determine whether or not micro-tunneling technique is a feasible construction technique for pipelines / tunnels in Queenston shale of southern Ontario.

7.3 GEOLOGICAL BACKGROUND

The geological map of southern Ontario is shown in Figure 7.1, which demonstrates the bedrock stratification of this region. Most of southern Ontario region is located in the Appalachian sedimentary basin, where the sediments were eroded during the Taconic Appalachian orogeny. The Appalachian basin is bounded by the Precambrian basement highs in the west, Taconic Mountain Range in the east and south, and the Frontenac arch in the north (Perras, 2009). The Queenston shale layer is an argillaceous sedimentary rock formed in the upper Ordovician age in south-west region of Ontario. It forms most of south and west shores of Lake Ontario and extends to the north towards the Georgian Bay. Together with other rocks in the Appalachian basin, the Queenston shale layer dips 6 m/km to the south (Yuen, 1992), and it becomes thinner and overlain by other rocks from the Silurian and Devonian ages, such as Grimsby and Eramosa shales, Dolomite, and limestone of different formations. The Queenston shale layer in south-west Ontario forms the host ground for many important engineering projects (e.g. Niagara tunnel). The Queenston shale may also be the host ground of pipelines / tunnels that may be constructed using the micro-tunneling technique.

7.3.1 Locations of Investigated Queenston Shale

In this research, the investigation was performed on two Queenston shale samples collected from Milton and Niagara Falls regions in southern Ontario. Figure 7.1 shows the location of the two boreholes where the Queenston shale samples were collected. The rock quality designation (RQD) of Queenston shale layer from Milton varied from 50.0%

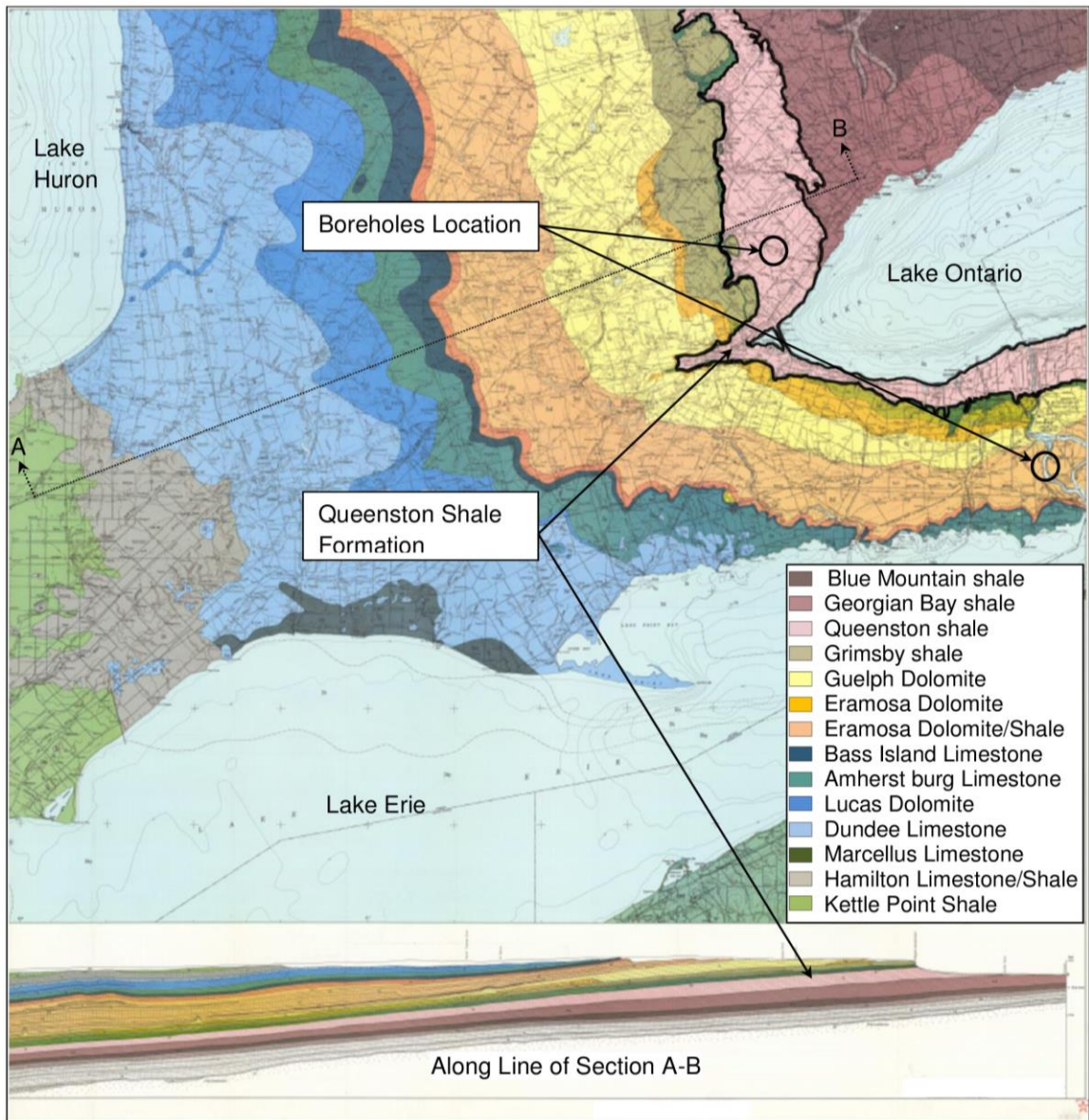


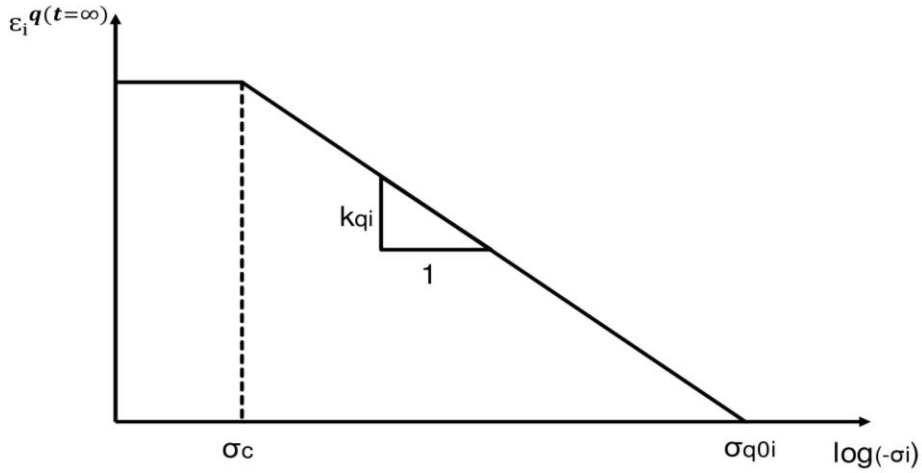
Figure 7.1. Geological map of southern Ontario.

to 99.2%, indicating fair to excellent rock condition with increasing depth. The bedrock in this region starts at a depth of 15.5 m below ground level. Based on the RQD value and the occurrence of joints, the Queenston shale layer of Milton can be divided into three sublayers: i) upper seven meters from 15.5 m to 22.5 m depth BGL, with an average RQD value of 68.9 %, and 2-5 mm of compacted clay joints that occurred at an average of 4 joints/m leading to geological strength index (GSI) of 42 (Hoek et al. 1995), ii) middle 4.0 m layer at 22.5-26.5 m depth BGL with an average RQD value of 89.9 %, and 2-5 mm joints of compacted clay that occurred at an average of 1 joint/m, leading to GSI of 54 and iii) lower 8.0 m layer at 26.5-34.52 m depth BGL with average RQD value of 96.8 %, and joints of compacted clay occurred at 1 joint/4m, and GSI value of 59. The Niagara Queenston shale was collected from the invert of Niagara tunnel at its lowest part at a depth of 125-137 m BGL. The recovered samples were approximately 12.0 m long. The suggested GSI value for this layer is 59.

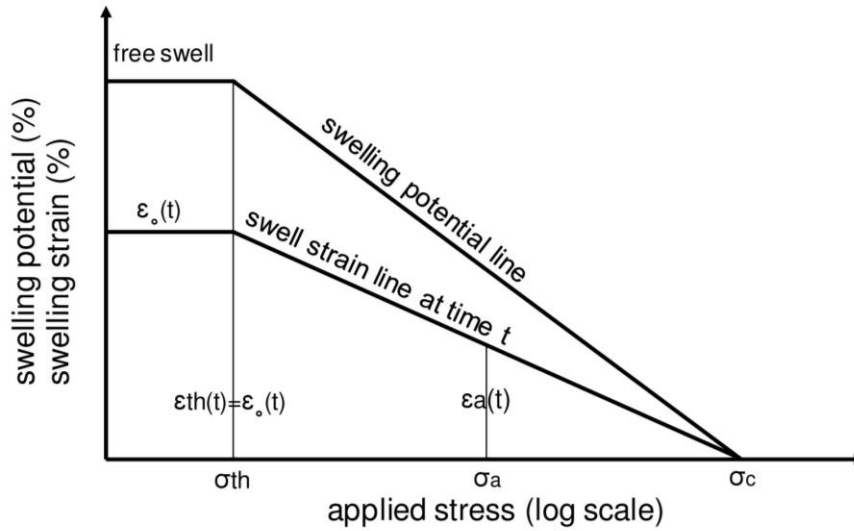
Based on GSI value of 59, the strength envelopes of the rock mass of Milton and Niagara Queenston shale were developed utilizing RocLab software from RocScience (www.rocscience.com). The rock mass modulus, cohesion and frictional angle of the rock mass of each layer were derived from the developed strength envelopes. The parameters were derived for intact rock (i.e. as collected from the site) and after soaking the Queenston shale in water and lubricant fluids for 100 days to account for the strength degradation of the shale near the excavation. This is done based on results of the experimental study performed in Chapter 4 and Chapter 5 to evaluate the strength degradation of Queenston shale exposed to water and lubricant fluids.

7.4 FINITE ELEMENT PLAXIS 2D ROCK SWELLING MODEL

The computer program PLAXIS 2D has a two dimensional, user-defined constitutive model that can simulate rock swelling behaviour (PLAXIS, 2016). This constitutive model simulates the time-dependent deformation behaviour of rocks based



a) Grob's swelling law (Grob, 1972)



b) Lo and Hefny swelling model (Lo and Hefny, 1996)

Figure 7.2. Rock swelling models: (a) Grob's swelling law; (b) Lo and Hefny swelling model.

on swelling clay minerals that exist in their micro-structure. The mathematical formulation of the time-dependent deformation behaviour of rocks in this constitutive model was developed essentially based on Grob's swelling law (Grob, 1972), which is shown in Figure 7.2 (a). In this model, the swelling mechanism of rocks is related to the osmotic swelling and the inner-crystalline swelling of clay minerals (Madsen and Müller-Vonmoss, 1989). The osmotic swelling is caused by the differences in cation concentration in the clay and in the free pore water, and it occurs after the completion of the inner-crystalline swelling. This swelling is caused by the increase in the repulsive forces between the negatively charged neighbouring clay layers which in turn increases the distance between these layers. The inner-crystalline swelling occurs first, and it can result in 100% of volume increase of clay particles in the case of montmorillonite. This swelling occurs due to the integration of water molecules into the clay mineral crystals when the existing cations hydrate in the presence of water. When the energy released in the process of cations hydration exceeds the anion-cation bond within the clay mineral, swelling occurs. The swelling pressure in this process depends on the nature of the existing cations, where Na^{2+} cations results in larger swelling pressure than Ca^{2+} cations (PLAXIS, 2014). The stress dependency of the time-dependent deformation of rock follows a semi-logarithmic relation, as indicated in Figure 7.2 (a). The time-dependent deformation decreases with increasing the applied stress in a log scale. The mathematical expression of the developed rock swelling model in PLAXIS is given by (PLAXIS, 2014) as follows:

$$\boldsymbol{\varepsilon}_i^{(t=\infty)} = -k_{qi} \cdot \log_{10}(\sigma_i / \sigma_{qoi}) \quad [7.1]$$

Where,

$\boldsymbol{\varepsilon}_i^{(t=\infty)}$ is final swelling strain

k_{qi} is axial swelling parameter (i.e. swelling potential in axial direction under the axial applied stress in Lo and Hefny (1996) model)

- σ_i is applied stress in that direction
- σ_c is minimum axial stress to limit excessive swelling (i.e. threshold stress in Lo and Hefny (1996) model)
- σ_{qoi} is maximum axial swelling stress where no swelling occurs beyond it (i.e. critical stress in Lo and Hefny (1996) model)

7.5 DEVELOPMENT OF MATHEMATICAL TIME-DEPENDENT DEFORMATION MODEL OF ROCKS IN SOUTHERN ONTARIO

The region of southern Ontario exhibits high in-situ horizontal stresses, which are believed to be due to the current movements of continental drift according to the plate tectonic theory (Lo, 1978). In fact, the ratio of horizontal to vertical in-situ stress of some rocks in this region is usually 5 and it could be higher (Al-Maamori, et al., 2014 and Lo, 1978). Thus, the time-dependent deformation of these rocks is anisotropic with respect to the rock beddings, and is highly dependent on the applied pressure (Lo and Lee, 1990). The mechanism of time-dependent deformation of Queenston shale is affected by three main factors: i) relief of initial in-situ stresses, which serves as initiation mechanism; ii) accessibility to fresh water, and iii) outward salt concentration gradient from rock pore water to the ambient fluid (Lee and Lo, 1993).

Three laboratory tests are usually employed to measure and quantify the time-dependent deformation of Queenston shale in southern Ontario. These tests are: i) the free swell test, where the rock sample is kept submerged in water for 100 days, while its deformation in three orthogonal directions is continuously measured (Lo et al., 1978); ii) the semi-confined swell test, where the rock sample is submerged in water and subjected to a specified pressure applied in one direction while the corresponding deformation in the same direction is continuously measured for 100 days (Lo et al., 1978) and iii) the null swell test, where the deformation of the rock sample is completely suppressed in one

direction when it is submerged in water, while the developed swelling pressure in the same direction is continuously measured until it is stabilized (Lo and Lee, 1990). Full description of these tests is given in Chapter 3.

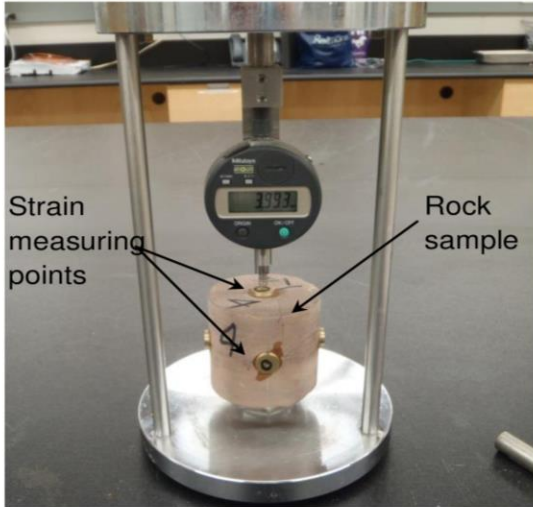
Lo and Yuen (1981) developed a mathematical model for time-dependent deformation of Queenston shale based on its swelling mechanism and the results of semi-confined swell test. However, this model may overestimate the deformations and the induced stresses in tunnels constructed in swelling rocks because it considers only semi-confined swell test results. Lo and Hefny (1996) developed a more accurate mathematical model, shown in Figure 7.2(b), which accounts for the results of the three types of swelling tests. It can be noted from Figure 7.2 that both Grob's swelling law (incorporated in PLAXIS 2D) and Lo and Hefny (1996) model are quite similar. Since both models use same mathematical formulation, the rock swelling incorporated in PLAXIS 2D is utilized in the current study to analyze time-dependent deformation and induced stress of pipe / tunnel segments constructed in Queenston shale.

7.6 VERIFICATION OF FE PLAXIS 2D ROCK SWELLING MODEL

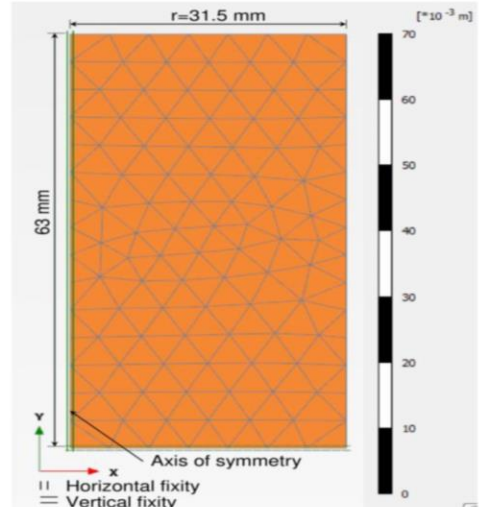
The rock swelling finite element (FE) model in PLAXIS 2D was first verified using the results of the swelling tests measurements: free swell test, semi-confined swell test, and null swell test that were performed on Milton and Niagara Queenston shale samples. The test setups for these tests are shown in Figure 7.3. In these tests, water and LFs (i.e. bentonite and polymer solutions used in micro-tunneling applications) were used as the ambient fluids (Al-Maamori et al., 2016). The time-dependent deformation parameters of the Queenston shale from Milton and Niagara regions, which were derived in Chapter 3, are summarized in Table 7.1. These parameters are utilized in the FE analyses.

Table 7.1. Time-dependent deformation parameters for (Lo and Hefny 1996 swelling model) from (Al-Maamori et al., 2016)

Direction	Milton Queenston shale		Niagara Queenston shale	
	vertical	horizontal	vertical	horizontal
In water				
Free swelling potential (% strain/log cycle of time)	0.190	0.156	0.525	0.210
Threshold stress, σ_{th} (MPa)	0.010	0.002	0.015	0.018
Critical stress, σ_c (MPa)	2.140	2.057	2.070	1.600
In polymer solution				
Free swelling potential (% strain/log cycle of time)	0.065	0.027	0.053	0.043
Threshold stress, σ_{th} (MPa)	0.022	0.002	0.010	0.013
Critical stress, σ_c (MPa)	1.505	1.497	1.495	0.780
In bentonite solution				
Free swelling potential (% strain/log cycle of time)	0.235	0.170	0.390	0.160
Threshold stress, σ_{th} (MPa)	0.006	0.002	0.002	0.008
Critical stress, σ_c (MPa)	2.353	2.233	1.800	1.130



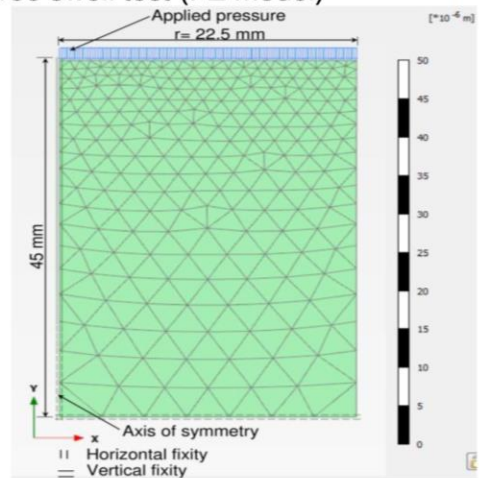
a) free swell test (experiment)



b) free swell test (FE model)



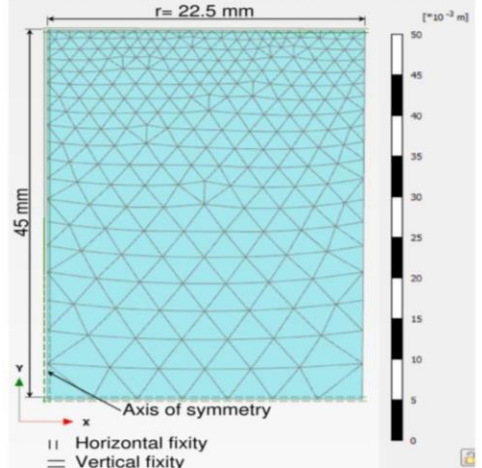
c) semi-confined swell test (experiment)



d) semi-confined swell test (FE model)



e) null swell test (experiment)



f) null swell test (FE model)

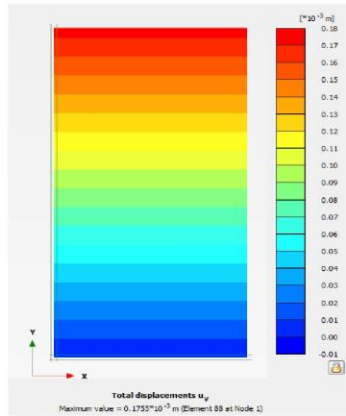
Figure 7.3. Rock swelling tests apparatus developed earlier at the University of Western Ontario and their finite element models.

7.6.1 FE Model of Free Swell Test

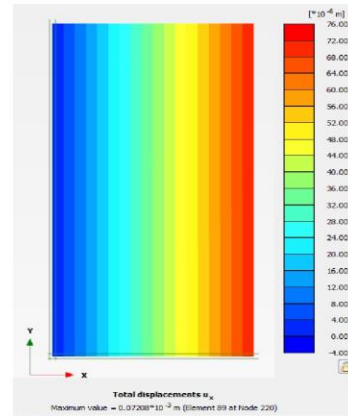
The free swell test was simulated using an axi-symmetry model that represents a cylindrical rock specimen. The initial dimensions of the FE model were the actual test specimen dimensions as indicated in Figure 7.3 (a) (i.e. cylinder 63 mm in diameter and 63 mm high). The FE model represented a specimen submerged in water or LFs for 100 days. The default medium refined FE mesh of PLAXIS 2D shown in Figure 7.3 (b) was used in the test model, which produced optimum balance between accuracy and computing efficiency. The developed mesh consisted of 126 triangular 15-noded elements. The deformations were monitored at top and at the mid-height of the free edge of the FE model, which simulate the actual measuring locations in the free swell test. The axis of symmetry was fixed in the horizontal direction (X-axis) and the bottom of the FE model was fixed in the vertical direction (Y-axis), while all other boundaries were free to move. In order to simulate time-dependent deformation behaviour of Queenston shale, the time and other time-dependent deformation parameters of the rock swelling model for Queenston shale were defined in the developed finite element model utilizing the coupled flow and deformation analysis. Water table was located on top of the model similar to the lab test. The average vertical and horizontal swelling potentials of Queenston shale that were established from swelling tests (Al-Maamori et al., 2016) are used in the FE rock swelling model. These values are given in Table 7.1. The anisotropy in the strength and in time-dependent deformation was defined in the model by using different values in the vertical and horizontal directions of the following: tensile strength, elastic modulus, Poisson's ratio, free swelling potential, threshold stress and critical stress. These values are listed in Table 7.6. The analysis was performed in one phase lasts for 100 days.

Figures 7.4 (a) and 7.4 (b) present the deformation contours obtained from the FE analysis of Milton Queenston shale after being submerged 100 days in water in the vertical and horizontal direction, respectively. The results presented in Figure 7.4 demonstrate that the time-dependent deformation occurred over the entire sample and its value is minimum (zero) at the fixed boundary and accumulated to a maximum at the model free boundary, similar to observed behaviour in the laboratory test. In addition, the maximum values were in excellent agreement with the experimental results, which

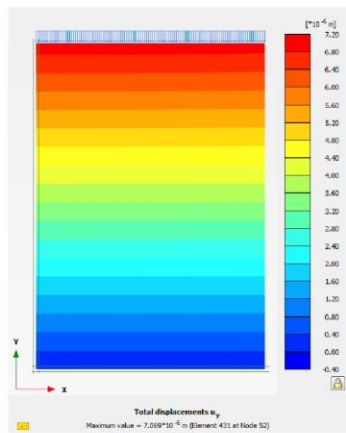
further confirmed the ability of the numerical model to simulate the time-dependent deformation behaviour of Queenston shale. Three cases of free swell test of Milton Queenston shale in water, polymer solution and bentonite solution were modeled. The computed time-dependent deformation from the FE models and the measured time-dependent deformation from free swell tests performed on Milton Queenston shale in water and LFs are plotted in Figure 7.5. The solid lines represent the computed time-dependent deformation from the FE model while individual points represent the measured time-dependent deformation from free swell tests. It is quite clear from Figure 7.5 that computed time-dependent deformation values agree well with the measured values for all cases analyzed.



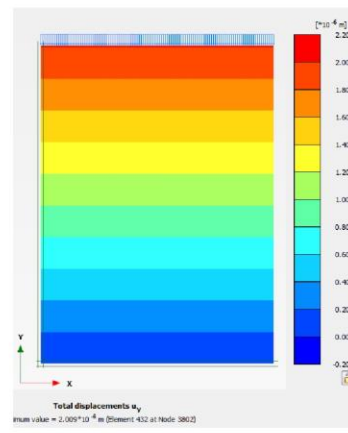
a) Vertical deformation contours



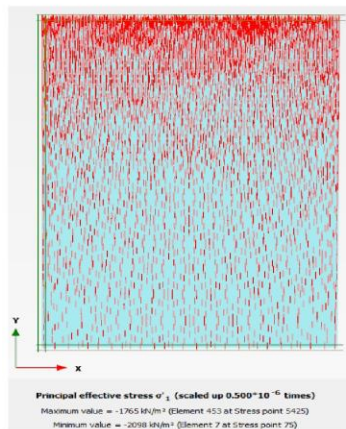
b) Horizontal deformation contours



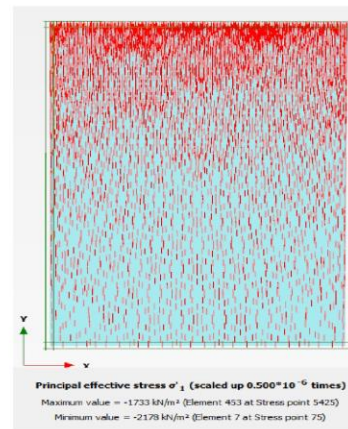
c) Vertical deformation contours under 1 MPa



d) Horizontal deformation contours under 0.7 MPa



e) Developed vertical swelling pressure



f) Developed horizontal swelling pressure

Figure 7.4. Graphical results of finite element models of swelling tests: (a, b) free swell test in water; (c, d) semi-confined swell tests in polymer solution in vertical and horizontal directions, respectively, (e, f) null swell test in bentonite solution in vertical and horizontal direction, respectively.

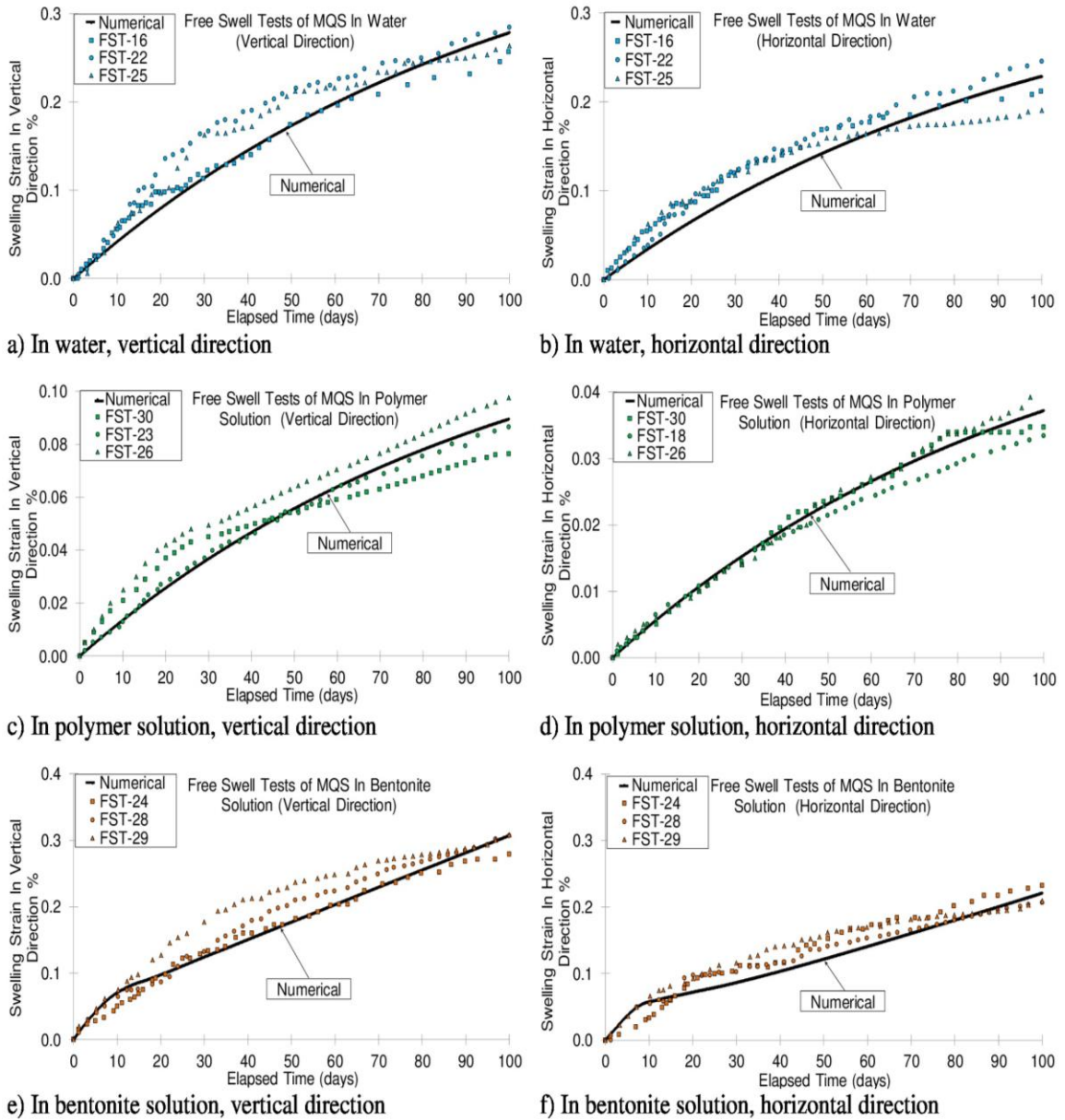


Figure 7.5. Computed finite element results and measured laboratory free swell tests results of Milton Queenston shale in water, polymer and bentonite solutions in vertical and horizontal directions.

7.6.2 FE Model of Semi-Confined Swell Test

The semi-confined swell test indicated in Figure 7.3 (c) was simulated using an axi-symmetry model with only half of the test cylinder was modeled as shown in Figure 7.3 (d). The FE model represented a sample submerged in water or lubricant fluids for 100 days. A vertical uniform pressure was applied to the test cylinder having same value of applied pressure used in the semi-confined swell test. The bottom boundary of the model was fixed along Y-axis and the axis of symmetry was fixed along X-axis, while all other boundaries were free to move. The height of the actual test specimen in the semi-confined swell test ranged from 35 mm to 50 mm and its diameter was 63 mm. In The FE model, the initial height of the specimen was taken as 45 mm and the initial diameter was taken 63mm. The default medium refined FE mesh was used producing 126 triangular 15-noded elements of the model. Three cases of Queenston shale specimen submerged in water, bentonite solution, or polymer solution were modeled using the average measured values of time-dependent deformation derived from laboratory tests listed in Table 7.1. The anisotropy in the strength and time-dependent deformation was modeled through defining different values in the vertical and horizontal directions for: tensile strength, elastic modulus, Poisson's ratio, swelling potential, threshold stress and the critical stress. The values used in the analyses are given in Table 7.6. The strength parameters of the rock mass were derived using GSI value of 59. Water was located on top of the model similar to the lab condition. The analysis was performed in one phase lasts for 100 days and the time-dependent deformation was calculated on the top of the model.

Figures 7.4 (c) and 7.4 (d) display the computed contours of swelling deformation of Queenston shale specimen submerged in polymer solution obtained from the finite element model under different applied pressure in the vertical and horizontal directions. It can be noted from Figures 7.4 (c) and 7.4 (d) that time-dependent deformation occurred in the same direction of the applied pressure and that the maximum deformation occurred at the free edge of the model where time-dependent deformation of the entire sample is accumulated. Figure 7.4 (d) shows a flipped horizontally cored specimen subjected to an applied pressure in the direction of rock bedding. It shows smaller time-dependent deformation at the free edge of the model compared to vertical specimen. These results

are consistent with the measured time-dependent deformation in the semi-confined swell tests.

The computed and measured time-dependent deformation of the specimen exposed to different fluids are displayed in Figure 7.6. It can be seen from Figure 7.6 that the computed deformations match the general trend of the measured values in all modeled cases. The measured time-dependent deformation curves in the semi-confined swell test usually follow a stepwise deformation pattern (Al-Maamori et al., 2016, and Hefny et al., 1996). However, the swelling potential under a specific applied pressure is the slope of the straight line of the swelling curve when the time is plotted in log scale (Lo et al., 1978). The computed swelling curves have generally matched the measured swelling curves indicating the ability of the FE model to simulate the stress-dependency of the time-dependent deformation behaviour of Queenston shale in the three fluids used.

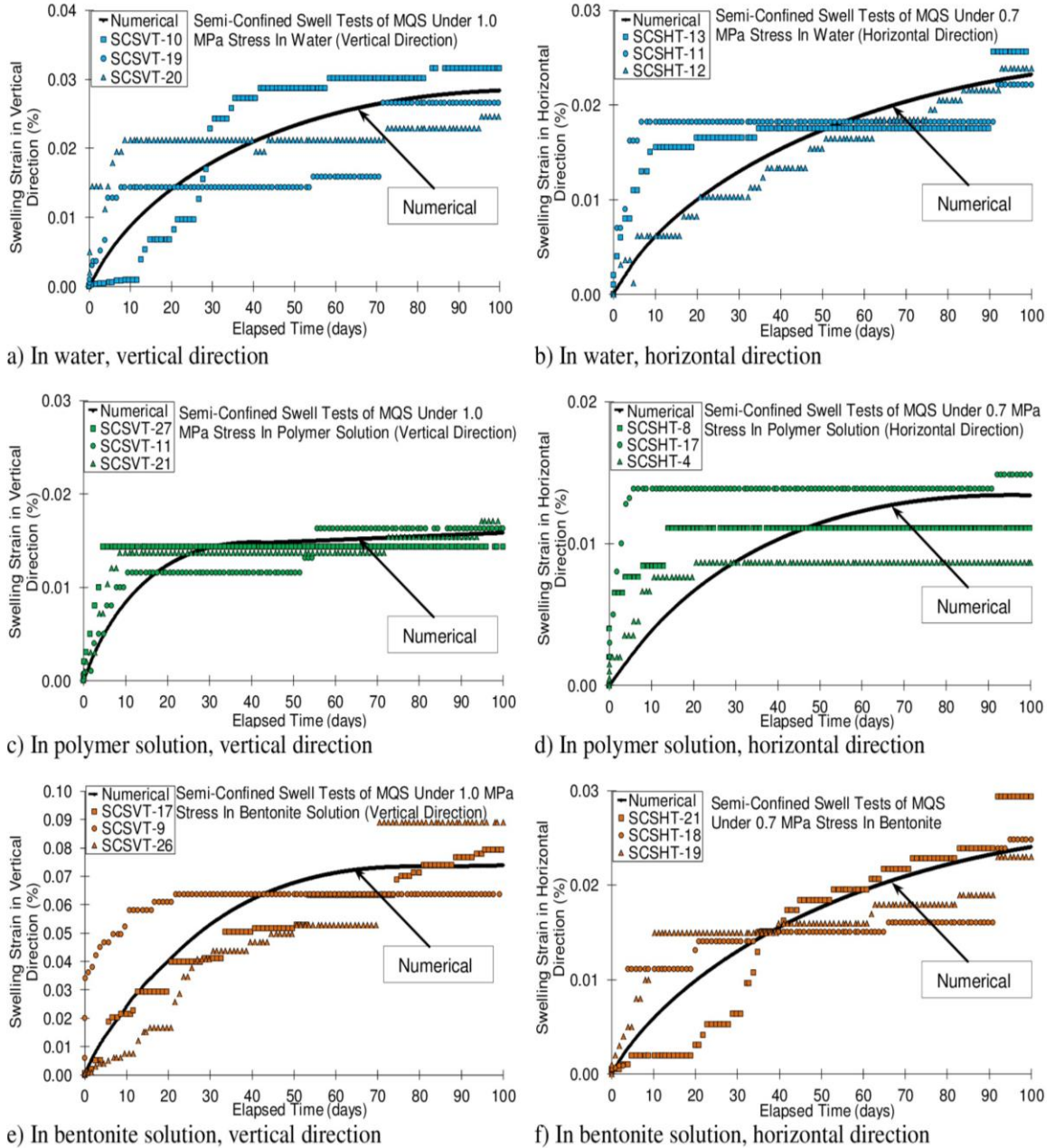


Figure 7.6. Computed finite element results and measured laboratory semi-confined swell tests results of Milton Queenston shale in water, polymer and bentonite solutions in vertical and horizontal directions.

7.6.3 FE Model of the Null Swell Test

The geometry of the null swell test specimen, shown in Figure 7.3 (e), was represented in the null swell test model. Exploiting symmetry, only half of the sample was simulated using an axi-symmetry model as indicated in Figure 7.3 (f). The numerical model mesh was prevented from vertical swelling (i.e. along Y-axis) by assigning fixed boundaries at top and bottom of the model, while the horizontal swelling of the model (i.e. along X-axis) was allowed by assigning free deformation to both sides. These deformation boundary conditions are same as those applied in the laboratory setup of null swell test. The maximum time required for the developed pressure in the null swell test of Queenston shale was found to be 45 days (Al-Maamori et al., 2016). Therefore, the FE analyses involved 45 phases, with one-day time interval for each phase. Three cases (with separate analyses for vertical and horizontal specimens) were modeled for Queenston shale in water, bentonite solution, and polymer solution. The parameters of the time-dependent deformation and the strength of the Queenston shale used in the previous models were also used here. The mesh produced 130 elements. The developed swelling pressure at the top of the model was calculated.

Figures 7.4 (e) and 7.4 (f) present the developed swelling pressure obtained from the finite element model after 45 days of swelling for Queenston shale specimen submerged in bentonite solution. The calculated swelling pressure at the end of each phase was plotted in Figure 7.7 together with the measured swelling pressure in the null swell test. The excellent match between computed results from FE model and measured pressure from the null swell test is evident from Figure 7.7. This means that the FE model is able to capture the behaviour of induced swelling pressure of Queenston shale with time.

The excellent agreement between the numerical and experimental results of the different swelling tests as discussed above verify the ability of developed FE models to simulate the observed behaviour of Queenston shale in laboratory swelling tests. It confirms that the model can accurately simulate the different aspects of the swelling behaviour of Queenston shale and can capture the time-dependent deformation behaviour of Queenston shale. The stress-dependency of the time-dependent deformation of

Queenston shale was also accurately simulated using the developed models of semi-confined swell and null swell tests. Thus, it is concluded that the FE model can be used to analyze different infrastructure projects constructed in Queenston shale of southern Ontario. In addition, the FE model will be further verified against some case studies that document observed behaviour of actual projects including excavations and tunnel segments in Queenston shale rocks as discussed in the following sections.

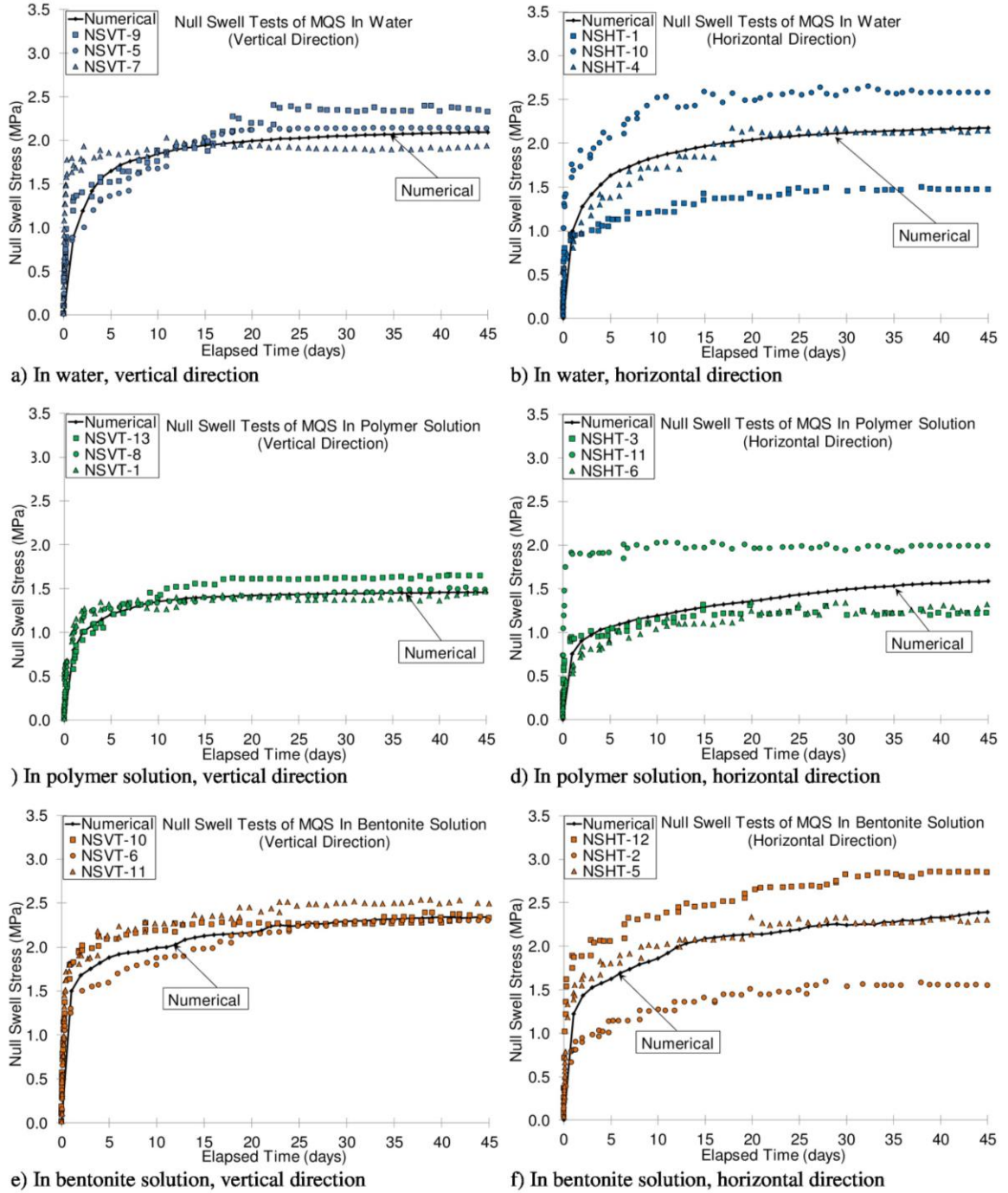


Figure 7.7. Computed finite element results and measured laboratory null swell tests of Milton Queenston shale in water, polymer and bentonite solutions in vertical and horizontal directions.

7.6.4 Modelling Excavations In Rocks

The reported cases of excavations in rocks with long term in-situ measurements are limited in the literature. Two well documented cases are studied herein: i) the Niagara wheel pit excavation and ii) the Scotia plaza foundation excavation.

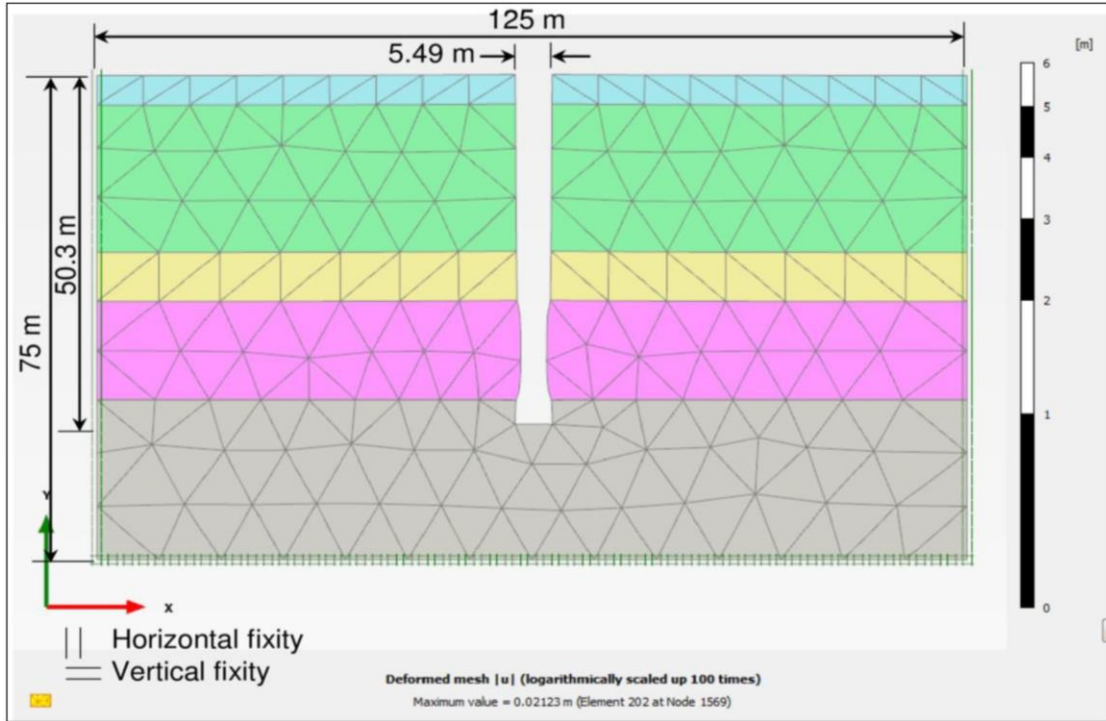
7.6.4.1 The Niagara Wheel Pit Excavation

The Niagara wheel pit excavation is an excellent reported case where the time-dependent deformation of excavated rock for 72 years was recorded. The Canadian Niagara Generation Station was constructed in 1902-1906 to generate clean energy utilizing the water head loss at the Niagara Falls on the Niagara River. As part of the construction requirements to host the penstocks and the turbines units, a deep and narrow slot was excavated in the rock between 1902 and 1903. The slot was 174 m long; 5.49 m wide and 50.3 m deep. The overburden soil layer was 4.6 m of gravel underlain by four types of rocks: 21.3 m of Lockport dolomite; 7.2 m of Gasport and Decew limestone; 17.1 m of Rochester shale and the lower 45 m layer of Grimsby limestone and Power Glen shale (Lee and Lo, 1976, Morison 1953). Inward movement of around 38 mm in the Rochester shale layer was noticed during the excavation period (Lee and Lo, 1976, Smith, 1905). This inward movement continued after the excavation was completed, and caused damage to some of the turbines and draft tubes (Lee and Lo, 1976). Extensometers were installed in 1905 at different elevations to measure the inward movement of the sides of the slot, especially at the Rochester shale layer where the maximum inward movement was reported. The in-situ horizontal stress of the Niagara Falls was 6.9 MPa (Lee and Lo, 1976).

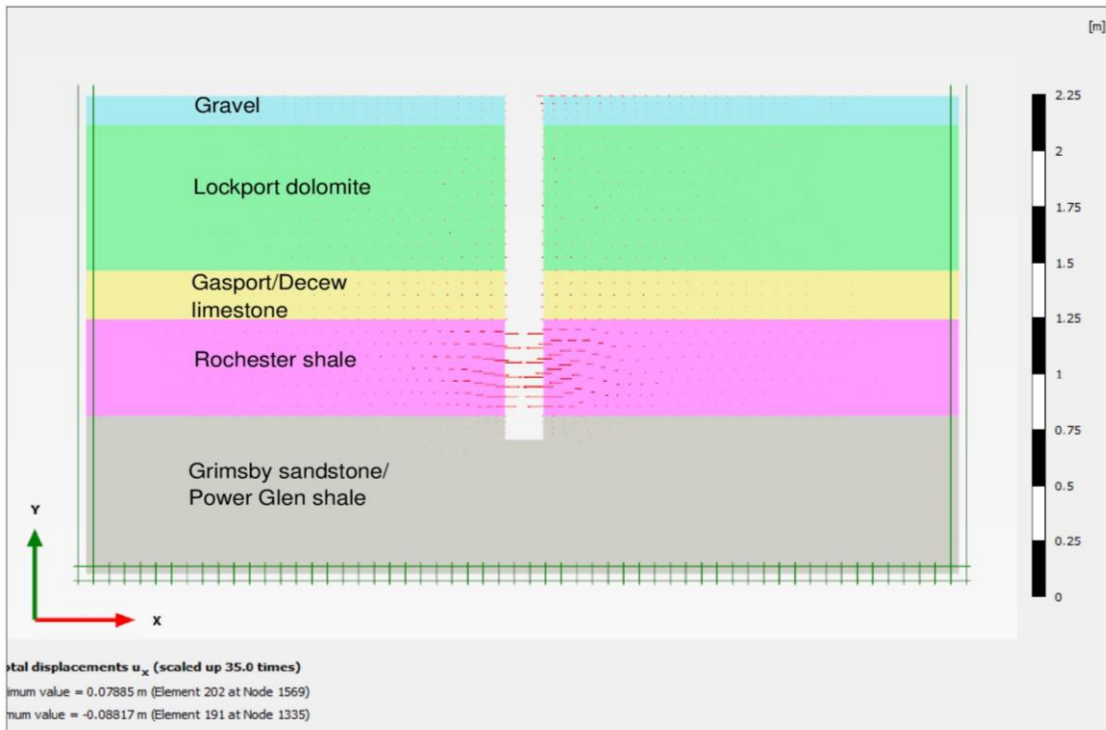
This case was modeled using the verified rock swelling model. The parameters used in this analysis are summarized in Table 7.2. As shown in Figure 7.8 (a), the slot was modeled in a rock block of 75 m height and 125 m width to account for the high horizontal in-situ stress effect. Both sides of the model were assigned horizontal fixity (i.e. along x-axis) and its bottom was assigned vertical and horizontal fixities while the

Table 7.2. Parameters used in the analysis of the Niagara Wheel Pit (Lee and Lo, 1976)

Overburden (gravel)	
Unit weight (kN/m ³)	20.0
Elastic modulus (MPa)	25000
Poisson's ratio, ν	0.3
Lockport dolomite	
Initial horizontal stress (MPa)	6.9
Free swelling potential in the horizontal direction (% strain/log cycle of time)	0.10
Threshold stress, σ_{th} (MPa)	0.01
Critical stress, σ_c (MPa)	1.0
Unit weight (kN/m ³)	26.7
Elastic modulus (MPa)	62.05*10 ³
Poisson's ratio, ν	0.3
Gasport and Decew limestone	
Initial horizontal stress (MPa)	6.9
Free swelling potential in the horizontal direction (% strain/log cycle of time)	0.10
Threshold stress, σ_{th} (MPa)	0.01
Critical stress, σ_c (MPa)	1.0
Unit weight (kN/m ³)	26.7
Elastic modulus (MPa)	34.47*10 ³
Poisson's ratio, ν	0.3
Rochester shale	
Initial horizontal stress (MPa)	6.9
Free swelling potential in the horizontal direction (% strain/log cycle of time)	0.17
Threshold stress, σ_{th} (MPa)	0.1
Critical stress, σ_c (MPa)	1.0
Unit weight (kN/m ³)	26.7
Elastic modulus (MPa)	10.34*10 ³
Poisson's ratio, ν	0.4
Grimsby sandstone and Power Glen shale	
Initial horizontal stress (MPa)	6.9
Free swelling potential in the horizontal direction (% strain/log cycle of time)	0.17
Threshold stress, σ_{th} (MPa)	0.01
Critical stress, σ_c (MPa)	1.0
Unit weight (kN/m ³)	26.7
Elastic modulus (MPa)	31.03*10 ³
Poisson's ratio, ν	0.2



a) finite element mesh



b) finite element inward horizontal deformation vectors

Figure 7.8. Finite element model of the Niagara wheel pit excavation.

top was free to deform. The water table was located at the top of the model. According to (Lee and Lo, 1976), there were some localized steel frames supports, which were found penetrated into the rock, and suffered from severe deflections. Accordingly, these limited supports were neglected in this analysis, and the slot was modeled as unsupported excavation. The default medium refined FE mesh was assigned, which produced 313 triangular 15-noded elements. The analysis was divided into 18 phases covering time from 1903 to 1972. Full excavation was modeled in phase 1, which lasted for 420 days. The deformation occurred in this phase represents the deformation prior to the installation of instruments. The next phase lasted for 720 days, and then next phase lasted for 1095 days, followed by 1826 days of time intervals up to year 1972. The results of FE model are illustrated in Figure 7.8 (b) with the computed maximum inward movement indicated in the Rochester shale layer. This behaviour is quite similar to what was reported based on in-situ measurements (Lee and Lo, 1976). The computed inward deformation from 1905 to 1972 is presented in Figure 7.9 along with the in-situ measured inward time-dependent deformation of the Rochester shale at the turbine deck level. Figure 7.9 demonstrates the excellent agreement of the computed deformation with the measured in-situ deformation from 1905 till 1952. The discrepancy between the two curves beyond 1952 is due to the excavation of a new tunnel, which started in 1952 at a distance of 152 m away from the pit (Lee and Lo, 1976). This example shows the capability of the rock swelling model developed in PLAXIS to capture the time-dependent deformation behaviour of rocks when an unsupported vertical excavation is created in the rock mass.

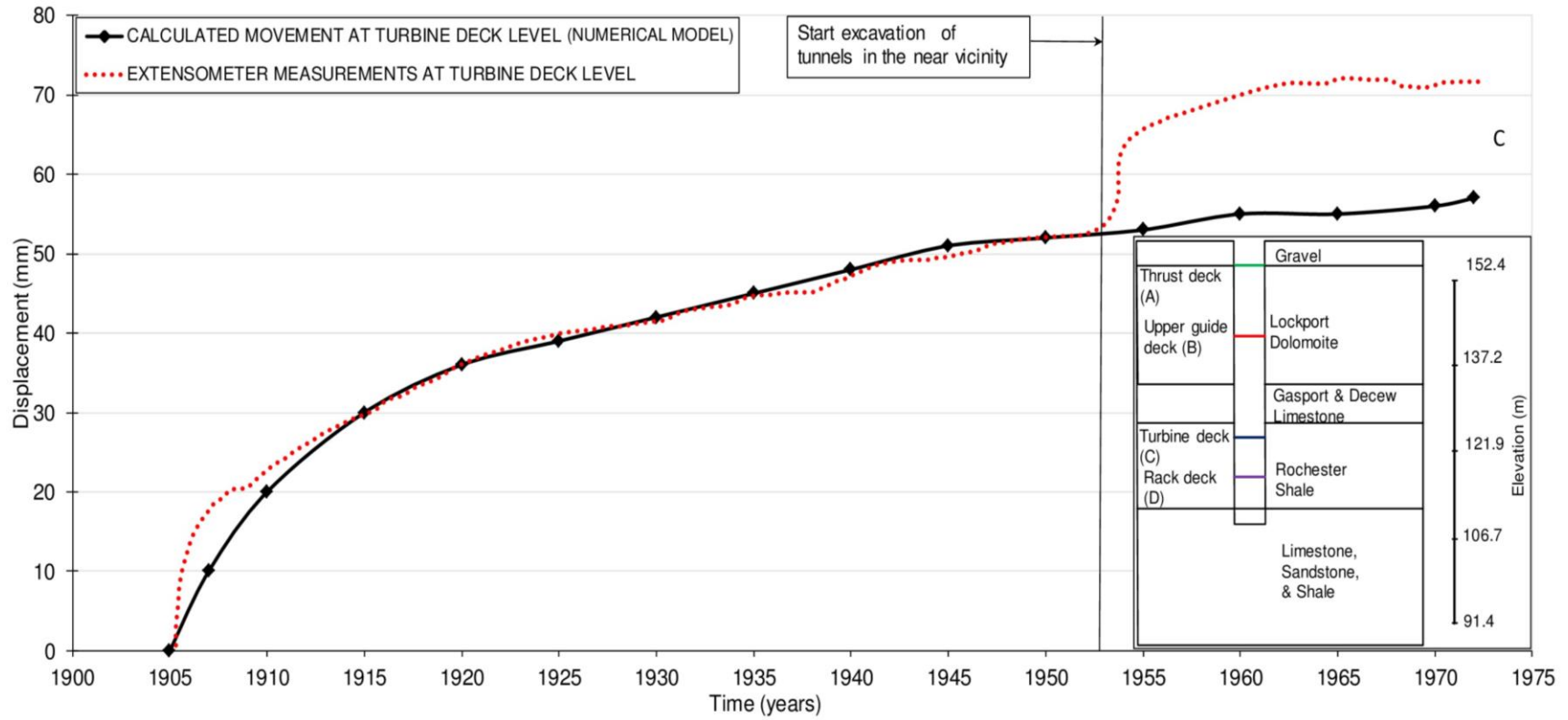


Figure 7.9. Time-dependent deformation of the Niagara wheel pit excavation at Rochester shale level.

7.6.4.2 The Scotia Plaza Foundation Excavation

This case illustrates a supported vertical excavation made in the rock with high initial horizontal in-situ stresses, and the associated inward deformations at different locations away from the excavation. When these high in-situ stresses are relieved due to an excavation, the elastic and time-dependent deformation of the rock commences, as it was the case of Scotia plaza foundation excavation.

The Scotia plaza is a 69-story-high rise complex in downtown Toronto, and is surrounded by existing tall buildings (Trow and Lo, 1989). The critical section of excavation was the east-west section, 40 m wide and 24 m deep, 14 m of which passed through rock. The upper two meters of rock was fractured and it had different parameters than the lower rock, as indicated in Table 7.3. The water table was at one meter below the rock top surface. Relative displacement that may occur on the rock surface due to the excavation of swelling rock can seriously impact the adjacent buildings. Therefore, monitoring devices were installed at the excavation face and at distances away from the excavation on the ground surface to measure the relative displacement of the ground during and after the excavation.

The adjacent building consisted of a bearing wall located on the face of the excavation, having line load of 820 kN/m. At 7.3 m away from the bearing wall, there were five rows of columns distributed at constant spacing of 5.5 m, and supporting 5650 kN of load on each column. The bottom of the excavation was subjected to 0.19 MPa of distributed load of equipment during construction. With progressing the excavation, a 0.4 MPa shoring support of uniformly distributed anchors was gradually applied on the side of the excavation.

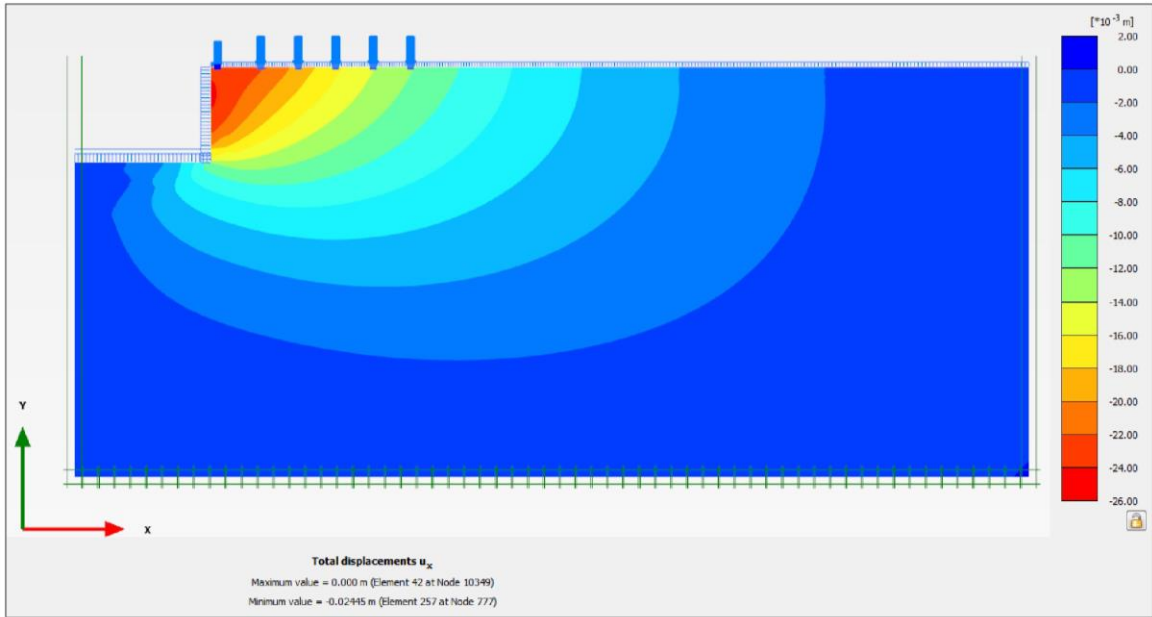
This excavation and the critical loads from the adjacent building on the east side were modeled in PLAXIS utilizing the rock swelling model. The numerical model was 60 m deep and 140 m wide starting from the centre line of the excavation towards the east. The default medium size FE mesh with 15-noded triangular elements was selected producing 1268 elements. The overburden was simulated as distributed load of 0.19 MPa. The columns loads were represented as line load to account for the other column loads in

Table 7.3. Parameters used in the analysis of the Scotia plaza excavation (Trow and Lo, 1989)

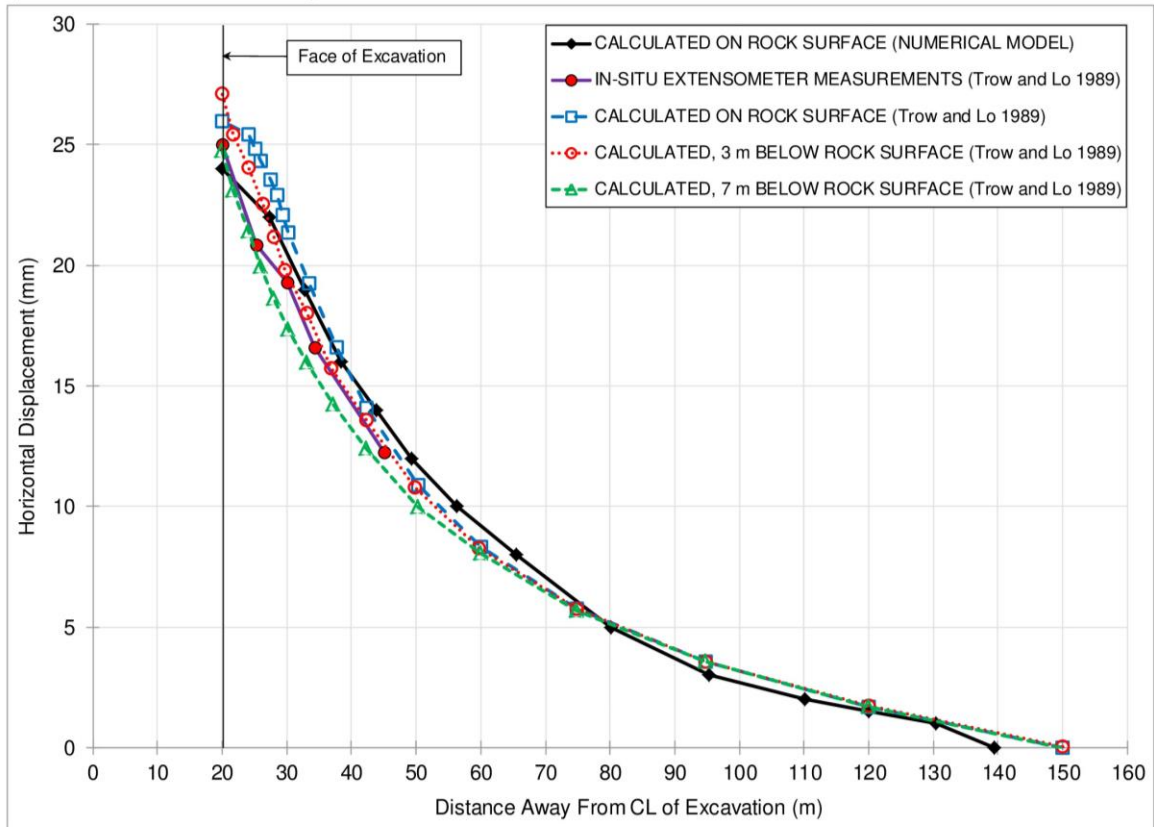
Overburden (clay till, York clay, and York till)	
Unit weight (kN/m ³)	19.0
Undrained shear strength (MPa)	0.1
Georgian Bay shale (upper 2m)	
RQD (%)	10-20
Initial horizontal stress (MPa)	4.0
Free swelling potential in the horizontal direction (% strain/log cycle of time)	0.08-0.16
Threshold stress, σ_{th} (MPa)	0.01
Critical stress, σ_c (MPa)	1.2
Unit weight (kN/m ³)	25.8
Elastic modulus (MPa)	2000
Poisson's ratio, ν	0.15
Georgian Bay shale (lower layer)	
RQD (%)	60
Initial horizontal stress (MPa)	4.0
Free swelling potential in the horizontal direction (% strain/log cycle of time)	0.08-0.16
Threshold stress, σ_{th} (MPa)	0.01
Critical stress, σ_c (MPa)	1.2
Unit weight (kN/m ³)	25.8
Elastic modulus (MPa)	4000
Poisson's ratio, ν	0.15
Anchor pressure (MPa)	0.4

the perpendicular direction to plane of the model. The rock was modeled in two layers: the upper two meters of weathered rock and the bottom layer. Each layer has different values of strength and swelling parameters as indicated in Table 7.3. The analysis was performed in seven phases up to 180 days after the excavation. The shoring pressure was applied gradually in these phases, similar to the actual case, until maximum pressure of 0.4 MPa was achieved. The boundaries of the model were fixed against movement in perpendicular direction, except the top of the model and the bottom of excavation were allowed to move freely. The excavation face was free to move in both vertical and horizontal directions. Two meters of excavation was modeled in each phase until full excavation was achieved in phase seven. The shoring load produced by the uniformly distributed anchors was applied in stages starting from 100 kPa in phase one and ending by 400 kPa in phase seven.

The maximum surface displacement measured at the face of the excavation was 25 mm (Trow and Lo, 1989), while the computed deformation from the developed FE model at the same location was 24 mm. The variation of deformation with time of the excavation face and at the columns and at different intervals along the rock surface were computed up to 1972 and the results are presented in Figure 7.10. The measured deformations obtained from the readings of the extensometers are also presented in Figure 7.10. It can be noted from Figure 7.10 that the computed deformations match well with the measured values, with some negligible differences. Figure 7.10 also shows the computed deformations based on FE analysis conducted by Trow and Lo (1989). Figure 7.10 shows that the results from both FE models have similar trends and their values are close. These results confirm the ability of the rock swelling model in PLAXIS to simulate the swelling behaviour of rocks in supported excavation.



a) Finite element analysis results, horizontal deformation contours



b) Calculated (finite element) and in-situ measured horizontal deformation of rock excavation

Figure 7.10. Scotia plaza excavation: (a) finite element model and (b) measured and calculated deformation of excavation face.

7.6.5 Modelling Circular Tunnel in Rock and Comparison with Closed Form Solutions

This case is presented to verify the FE model against the closed form solution proposed by Lo and Hefny (1996) for a circular tunnel in swelling rock. Full details of the adopted tunnel are given in Lo and Hefny (1996). The considered tunnel had radius of 6.8 m diameter in Queenston shale, and concrete lining 0.55 m thick, similar to the tunnel used in Sir Adam Beck Niagara Generation Station No. 3 project. The time-dependent deformation and strength parameters of the Queenston shale and concrete lining are given in Table 7.4.

The depth of the analyzed tunnel was 200 m. The in-situ horizontal stress measured from hydraulic fracture test at the location of the tunnel was 21 MPa in average. The vertical in-situ stress was 5.2 MPa, indicating horizontal to vertical stress ratio (K_v) of 4 (Lo and Hefny, 1996). Only a quarter of the tunnel is modeled in consistence with the studied example. The finite element model simulated two hundred m block of Queenston shale, discretized using 15-noded triangular element FE mesh. The FE mesh included 272 elements. The mesh was refined around the tunnel to minimize time required for the analysis while maintaining acceptable accuracy. The side boundaries were fixed horizontally and the bottom was fixed vertically while the top of the model was free to move. The water table was set in the model at the top of the Queenston shale layer. The rock parameters in Table 7.4 were assigned to the rock layer in the model. The concrete lining was modeled as a plate element with parameters of the concrete lining given in Table 7.4.

The waiting period prior to install the lining was 30 days (Lo and Hefny, 1996). Accordingly, the plate representing the concrete lining in the FE model was activated after phase 1, which lasts for 30 days. Phase two was assigned a period of 150 years, which corresponds to infinity in the closed form solution. The axial thrust acting in the concrete lining after 150 years (i.e. axial force divided by the cross-sectional area of concrete lining) was obtained from the FE analysis. Two cases of analysis were considered: i) full slip is allowed at the interface between the concrete lining and rock, and ii) no slip at the interface between the concrete lining and rock.

Table 7.4. Parameters used in the analyses of the Lo and Hefny 1996 model, (Lo and Hefny, 1996)

Queenston shale	
Initial horizontal stress (MPa)	21
Initial vertical stress (MPa)	5.2
Initial stress ratio (K_v)	4
Free swelling potential in the horizontal direction (% strain/log cycle of time)	0.3
Free swelling potential in the vertical direction (% strain/log cycle of time)	0.5
Threshold stress, σ_{th} (MPa)	0.04
Critical stress, σ_c (MPa)	3.93
Unit weight (kN/m^3)	26
Poisson's ratio in horizontal direction, ν_h	0.3
Poisson's ratio in vertical direction, ν_v	0.3
Concrete lining	
Elastic modulus E (MPa)	28000
Poisson's ratio ν	0.2
Tensile strength (MPa)	3.5
Compressive strength (MPa)	28-40

Figures 7.11 and 7.12 compare the axial thrust values calculated from the FE analysis with those obtained from the closed form solution for the full slip and no-slip conditions, respectively. Figure 7.11 shows that for the case of full slip at the interface, the computed bending moment is in reasonable agreement with the value calculated from the closed form solution. The bending moment is positive at the springline and it causes tension in the inner face fibers of the concrete lining. The bending moment decreases gradually and becomes zero close to the tunnel shoulder, and reaches its maximum negative value at the tunnel crown. This negative bending moment causes tension in the outer fibers of the concrete lining. The axial thrust is positive and it causes compression in the concrete lining along the tunnel. The thrust value obtained from the FE model is close to the thrust calculated from the closed form solution.

For case of no-slip at interface, the trends of both axial thrust and the bending moment computed from the FE analyses are similar to the full slip case, but with different magnitudes. Figure 7.12 shows that the FE prediction of axial thrust at the crown is very close to the value calculated from the closed form solution. However, the thrust at the springline obtained from FE analysis is higher than the prediction of the closed form solution. Similar observations can be made for the bending moment, where the FE prediction is higher than the value obtained from the closed form solution. These minor discrepancies between the FE computations and the closed form solution calculations may be attributed to the following reasons: i) the FE model has limited size of 200 m block of swelling rock while Lo and Hefny (1996) closed form solution considers an infinite rock medium and ii) the time in the FE analyses was taken as 150 years while in the closed form solution the swelling time is considered to be infinity.

The acceptable predictions of the FE model of time-dependent deformation behaviour and induced stresses of tunnel segments for the discussed cases confirm the suitability of the FE model for analyzing pipes / tunnel segments constructed in Queenston shale using the micro-tunneling technique. Thus, the verified numerical model can be used to conduct further analyses of reinforced concrete pipe / tunnel segments in Queenston shale.

Full Slip at Interface

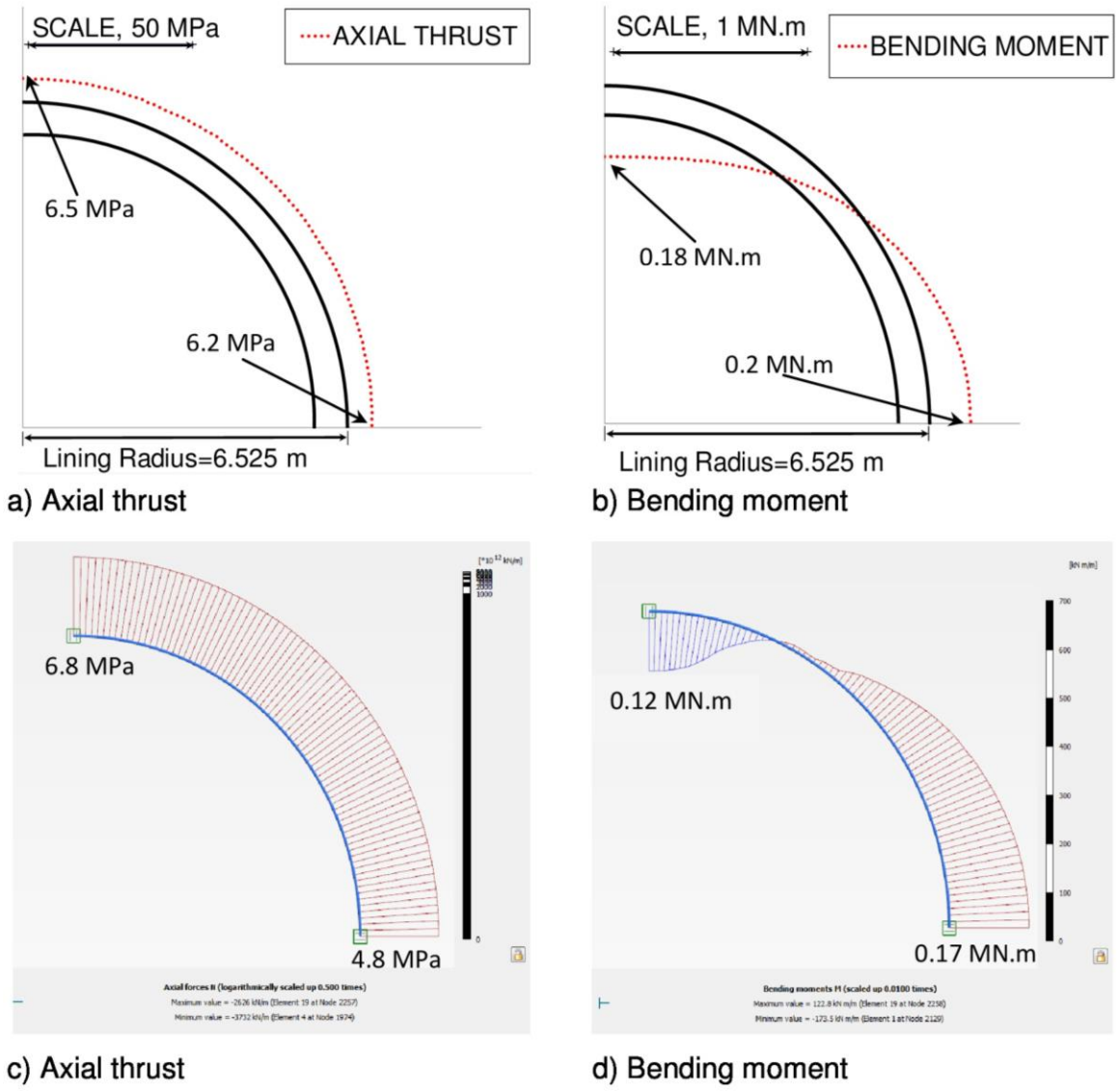


Figure 7.11. Calculated and computed axial thrust and bending moment in concrete lining with full slip interface: (a, b) Lo and Hefny (1996) closed form solution results; (c, d) Finite Element analyses results.

No Slip at Interface

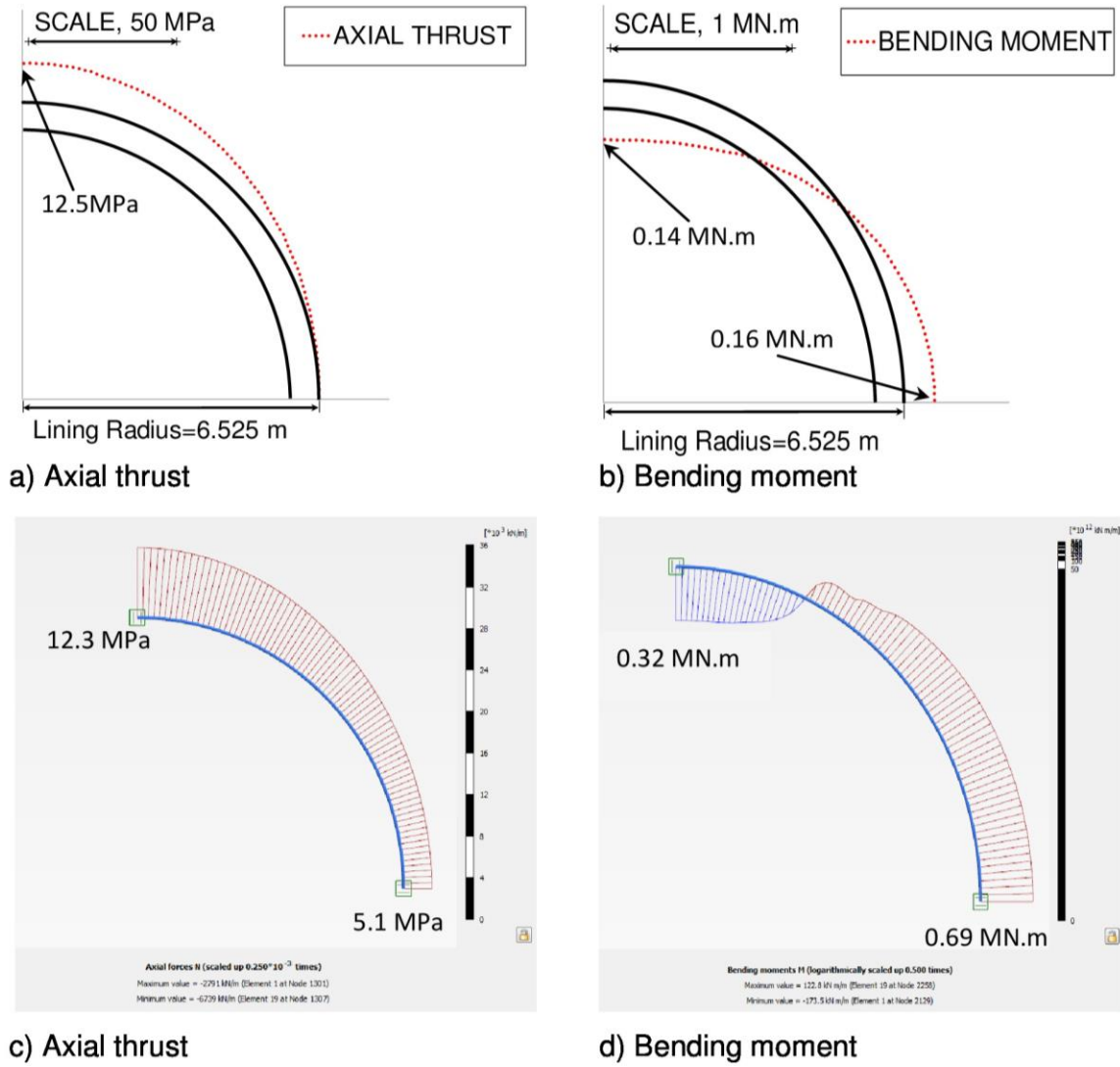


Figure 7.12. Calculated and computed axial thrust and bending moment in concrete lining with no slip at interface: (a, b) Lo and Hefny (1996) closed form solution results; (c, d) Finite Element analyses results.

7.7 TWO-DIMENSIONAL FINITE ELEMENT MODELLING OF TIME DEPENDENT DEFORMATION BEHAVIOUR AND INDUCED STRESSES IN TUNNELS CONSTRUCTED USING MICRO-TUNNELING IN QUEENSTON SHALE

The time-dependent deformation behaviour and induced stresses in tunnels constructed using micro-tunneling in Queenston shale are analyzed in this study. The pipes considered in this parametric study are reinforced concrete. The mechanical properties of the reinforced concrete pipes, obtained from actual test results as provided by the manufacturer, are summarized in Table 7.5. Eight pipe sizes are considered in this study: diameter $d = 0.6; 0.9; 1.2; 1.5; 1.8; 2.0; 2.5$ and 2.7 m. The tensile strength of the pipes concrete is considered to be 10% of its compressive strength (Nevile, 1996). The cellular cement grout to be used to replace the lubricant fluids at the end of the construction period has compressive strength of 0.5 MPa as indicated by the manufacturer.

The time-dependent deformation and strength properties of Milton and Niagara Queenston shales used in the analyses are summarized in Table 7.6. Three values of the stress ratio (i.e. horizontal in-situ stress / vertical overburden stress) were used in the analyses: $K_0 = 5; 10$ and 20 (Al-Maamori et al., 2014 and Lo and Yuen, 1981). The length of construction period of a pipeline or a tunnel segment using the micro-tunneling construction technique depends on the site condition and the hosting rock. This period is expected to be several days up to several weeks (Flint and Foreman, 1992 and Fritz, 2007; Bezuijen, 2009). Additional waiting time is suggested by Lo et al. (1987) to reduce the time-dependent deformation effects on the constructed pipeline / tunnel. In the following discussion the “construction period” refers to the actual time required to install the pipeline in addition to the waiting time prior to replace the lubricant fluid in the gap between the pipe and the excavated rock with the permanent cellular cement grout. Accordingly, the construction period considered in this study is $t = 15, 30, 60, 100, 150$ and 200 days.

Table 7.5. Properties of concrete pipes used in micro-tunnelling applications (Ward and Burke micro-tunneling Ltd.)

Pipe inner diameter (m)	Pipe outer diameter (m)	Pipe wall thickness (m)	Lubricant fluid Gap (m)	Pipe weight (kN/m)	Concrete compressive strength of the pipe (MPa)	Concrete tensile strength of the pipe (MPa)	Elastic modulus, E (MPa)
0.600	0.760	0.080	0.030	4.02	60.0	6.0	34.857
0.914	1.162	0.121	0.025	9.52	60.0	6.0	34.857
1.200	1.490	0.114	0.025	14.42	60.0	6.0	34.857
1.500	1.780	0.140	0.040	16.97	60.0	6.0	34.857
1.800	2.120	0.160	0.040	23.18	60.0	6.0	34.857
2.040	2.400	0.182	0.040	29.54	48.3	4.8	31.274
2.500	2.980	0.240	0.035	58.04	48.3	4.8	31.274
2.700	3.260	0.280	0.040	65.40	48.3	4.8	31.274

Table 7.6. Time-dependent deformation and strength parameters of the Queenston shale used in finite element analyses

Parameter	Milton Queenston shale	Niagara Queenston shale
Unit Weight (kN/m ³)	25.74	25.74
Stress Ratio (in-situ horizontal stress/overburden stress)	5; 10; 20	5; 10; 20
Friction angle of intact rock, ϕ (degrees)	23.8	20.6
Friction angle of rock soaked in polymer solution, ϕ (degrees)	18.7	11.2
Friction angle of rock soaked in bentonite solution, ϕ (degrees)	16.1	8.6
Cohesion of intact rock, C (kPa)	3013	2590
Cohesion of rock soaked in polymer solution, C (kPa)	2270	1924
Cohesion of rock soaked in bentonite solution, C (kPa)	1924	1449
Tensile strength of intact rock (kPa)	4500	4700
Tensile strength of rock soaked in polymer solution (kPa)	2600	680
Tensile strength of rock soaked in bentonite solution (kPa)	1800	570
Elastic Modulus of intact rock, vertical direction (kPa)	16.79*10 ⁶	14.21*10 ⁶
Elastic Modulus of intact rock, horizontal direction (kPa)	11.48*10 ⁶	11.48*10 ⁶
Elastic Modulus of rock soaked in polymer solution, vertical direction (kPa)	3.29*10 ⁶	6.18*10 ⁶
Elastic Modulus of rock soaked in polymer solution, horizontal direction (kPa)	9.28*10 ⁶	9.29*10 ⁶
Elastic Modulus of rock soaked in bentonite solution, vertical direction (kPa)	1.89*10 ⁶	3.27*10 ⁶
Elastic Modulus of rock soaked in bentonite solution, horizontal direction (kPa)	5.28*10 ⁶	5.28*10 ⁶
Poisson's ratio of intact rock, vertical direction	0.27	0.23
Poisson's ratio of intact rock, horizontal direction	0.25	0.25
Poisson's ratio of rock soaked in polymer solution, vertical direction	0.43	0.35
Poisson's ratio of rock soaked in polymer solution, horizontal direction	0.33	0.33
Poisson's ratio of rock soaked in bentonite solution, vertical direction	0.39	0.42
Poisson's ratio of rock soaked in bentonite solution, horizontal direction	0.33	0.33
Vertical swelling potential of intact rock (%)	0.190	0.525
Horizontal swelling potential of intact rock (%)	0.156	0.210
Critical stress of intact rock, vertical direction (kPa)	2140	2070
Critical stress of intact rock, horizontal direction (kPa)	2057	1600
Vertical swelling potential of rock soaked in polymer solution (%)	0.065	0.053
Horizontal swelling potential of rock soaked in polymer solution (%)	0.027	0.043
Critical stress of rock soaked in polymer solution, vertical direction (kPa)	1505	1495
Critical stress of rock soaked in polymer solution, horizontal direction (kPa)	1497	780
Vertical swelling potential of rock soaked in bentonite solution (%)	0.235	0.039
Horizontal swelling potential of rock soaked in bentonite solution (%)	0.170	0.016
Critical stress of rock soaked in bentonite solution, vertical direction (kPa)	2353	1800
Critical stress of rock soaked in bentonite solution, horizontal direction (kPa)	2233	1130

The unit weight of overburden soil is assumed to be 20.0 kN/m³. The following sign convention is followed: negative axial force acting along the pipe diameter causes compressive tangential stress while positive axial force causes tensile tangential stress; and positive bending moment causes tension at the inner fibers while negative bending moment causes compression at the inner concrete fibers of the pipe. As shown in Figure 7.13, exploiting symmetry the mesh size is 35 m x 35 m, which represents only half of the total rock medium that hosts the tunnel. The default medium size mesh refined at the pipe / tunnel with triangular 15-noded elements was used in the analyses.

In Chapter 6, the depth of percolation of water and lubricant fluids into the Queenston shale was investigated, and a correlation was derived to calculate this depth. In this study, the derived correlation is utilized to identify the depth upon which the lubricant fluid is percolated into the Queenston shale during the construction period. This correlation is given in equation 7.2 as follows:

$$d = C_{fl} * t^{0.588} \quad [7.2]$$

Where d = the depth of percolation of the applied fluid into the Queenston shale in (m),

C_{fl} = fluid constant in (m/day^{0.588}), and its value equals to:

0.0120 (m/day^{0.588}) for bentonite solution and 0.0102 (m/day^{0.588}) for polymer solution, and

t = time of fluid application (i.e. the construction period) in (days)

The time-dependent deformation properties and strength degradation of Queenston shale due to the penetration of lubricant fluids, which is a function of the construction period, are different than intact shale. Thus, the Queenston shale near the excavation, which has been percolated by lubricant fluid used in micro-tunneling process (i.e. bentonite solution or polymer solution) is assigned different parameters than intact shale. The default medium size FE mesh refined near the pipe was used producing 1750 of 15-noded elements of the model. This mesh size maintained accuracy of the analyses

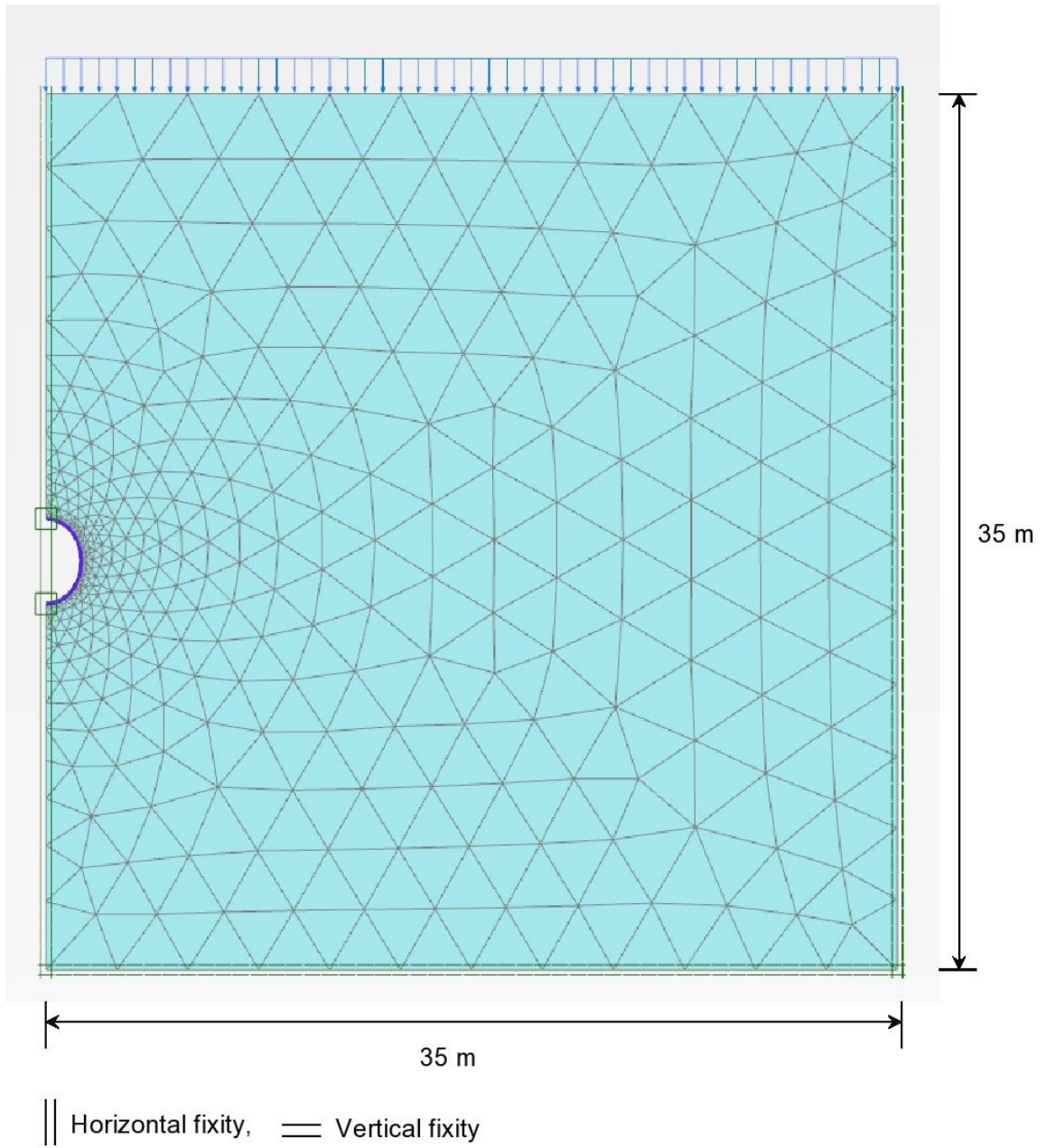


Figure 7.13. Finite element mesh used to model the Queenston shale and a pipeline / tunnel constructed using micro-tunneling technique.

as it was concluded from the sensitivity analysis. The water is located at top of the model. The analysis was performed in 17 phases with gradually increasing time intervals starting from 30 days of construction period in phase one, followed by 70, 100, 165, and 365 days up to 150 years. In phase one, the cement grout was not active. In the gap between the pipe and the Queenston shale, lubricant fluids are applied and they are activated in this stage. After phase one, the gap around the pipe is filled with cement grout which has compressive strength of 0.5 MPa and Poisson's ratio of 0.2. Both of the pipe and the cement grout are kept active for the rest of phases. The analysis was performed for 30 years. Parameters summarized in Table 7.6 were assigned to the soaked shale near the excavation, while the intact shale properties were assigned to the rest of the rock block.

The finite element analyses also accounted for the anisotropy in the strength and the time-dependent deformation properties of the Queenston shale. Different strength and time-dependent deformation parameters of the Queenston shale are assigned in vertical and horizontal directions with respect to the rock bedding, as indicated in Table 7.6. The analyses were performed for both Milton and Niagara Queenston shale. For each shale type, the analyses are performed using the relevant parameters for either polymer solution or bentonite solution during the construction period. The parametric study covers the variation in: i) in-situ stress ratio (K_0); ii) depth of construction below the top of Queenston shale layer; iii) diameter of pipe / tunnel and iv) the construction period. In this study, 30 years was considered as a lifetime for the constructed pipeline / tunnel.

7.7.1 SENSITIVITY ANALYSIS

In this section, the sensitivity of the FE model to the size of mesh elements was investigated. For the 1.8 m pipe, constructed in 30 days using bentonite solution at 1.7 m below top of the Queenston shale layer was investigated. Four sizes of the FE mesh were used: very coarse (218 elements), very fine (2297 elements), medium (860 elements) and medium with more refinement near the pipe (1750 elements). The analyses were performed for 30 years and the pipe inward movement at the springline is plotted in Figure 7.14 for these four models. It can be observed that changing the mesh element size

from very fine to very coarse causes a remarkable difference in the inward movement of the pipe. Using mesh with very fine elements produced the highest inward movements, as indicated in the figure. Comparing to the results of very fine FE mesh model, it also can be observed that using medium FE mesh refined near the pipe produced identical results. Therefore it was decided to use medium FE mesh refined near the pipe for the following analyses.

7.7.2 INFLUENCE OF STRESS RATIO (K_o)

Figure 7.15 shows the maximum developed tensile stress at the springline of the pipe / tunnel constructed in Milton Queenston shale using bentonite solution as lubricant fluid in micro-tunneling construction technique. The results are presented for three pipe sizes ($d = 0.6$ m; 1.2 m and 2.7 m) considering shallow; moderate and deep pipes along with stress ratio: $K_o = 5, 10$ and 20. From Figure 7.15, the following observations can be made:

- i) For the considered pipes / tunnel segments, the developed tensile stress at the springline decreases with increasing the stress ratio (K_o) for the same depth. The stress state at the springline changes from tension at low value of K_o to compression at high values of K_o .
- ii) At shallow depth, the developed stress at the springline of most used pipes / tunnels is tensile regardless of pipe diameter and the K_o value.
- iii) Increasing the pipe depth decreases the tensile stress at the springline and increases the compressive stress at the crown. The stress state at the springline changes from tension to compression with increasing the depth.
- iv) Increasing the diameter of the pipe / tunnel causes higher tensile stresses developed at their springline.
- v) The highest tensile stress at the springline of all pipes / tunnels used occurs at short construction period (i.e. 30 days).

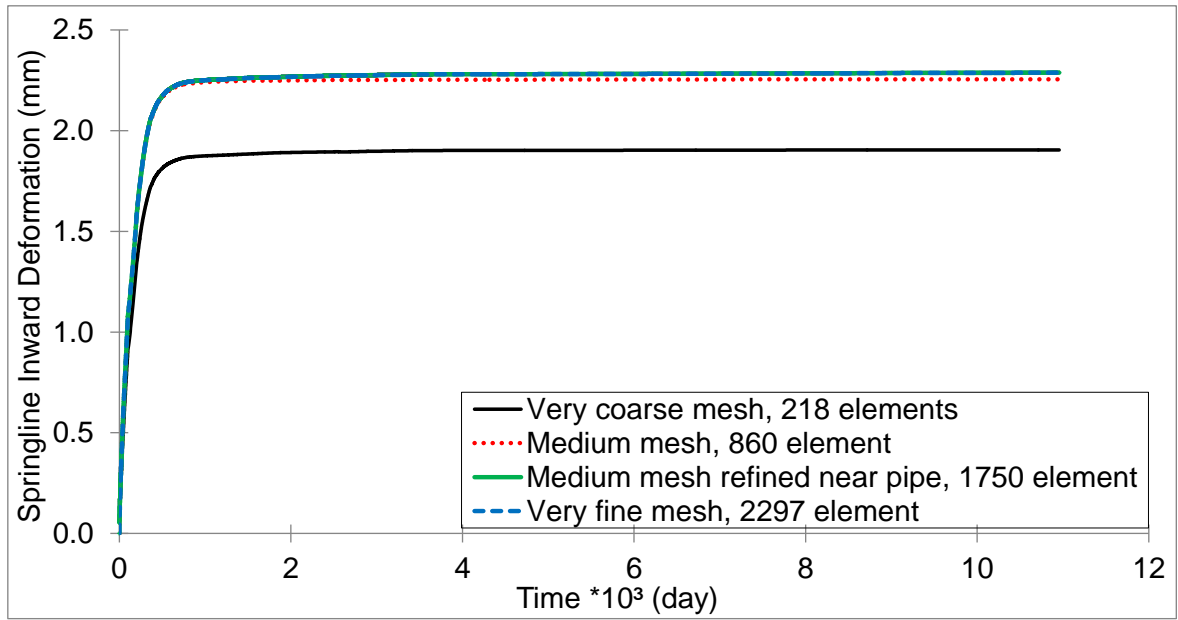


Figure 7.14. Variation of pipe convergence at springline with time for different sizes of FE mesh.

Based on these observations, it is concluded that the most critical state of concrete pipes / tunnels can be at shallow depths and short construction period (i.e. 30 days). At this state, the tensile stresses at the springline are at their higher value. Accordingly, the following analyses are performed on pipes constructed in Milton and Niagara Queenston shale using 30-day construction period and stress ratio, $K_o = 5$ as these two values are expected to produce highest tensile stress at the springline of the pipe.

7.7.3 INFLUENCE OF PIPE DIAMETER

The results of finite element analyses performed on pipes of different diameter constructed in Milton and Niagara Queenston shales are presented in Figure 7.16 and Figure 7.17, respectively. The analyses were performed using bentonite and polymer solutions as lubricant fluids during the construction period. The results are presented for shallow; moderate and deep pipes constructed in Queenston shale. It is noted from Figures 7.16 and 7.17 that the maximum stresses developed at the springline and at the crown of the pipe.

Figure 7.16 shows that for pipes constructed in Milton Queenston shale the tensile stress acting at the springline increases substantially as the pipe diameter increases. The tensile stress reaches its peak value at 1.8 m pipe diameter and then slightly decreases with increasing the diameters beyond 1.8 m. The compressive stress acting at the crown does not change at small pipe diameters. However, it remarkably increases for pipe diameter greater than 1.2 m and remains almost same value for larger diameters. The compressive stress at the crown is generally well below the concrete compressive strength. The concrete tensile strength for pipes with $d = 0.6$ m to 1.8 m, is 6.0 MPa while it is 4.8 MPa for pipes of diameter larger than 1.8 m. The calculated tensile stress acting at the springline of all pipes considered in the analysis does not exceed the tensile strength of the concrete when polymer solution is used. In other words, for pipes herein

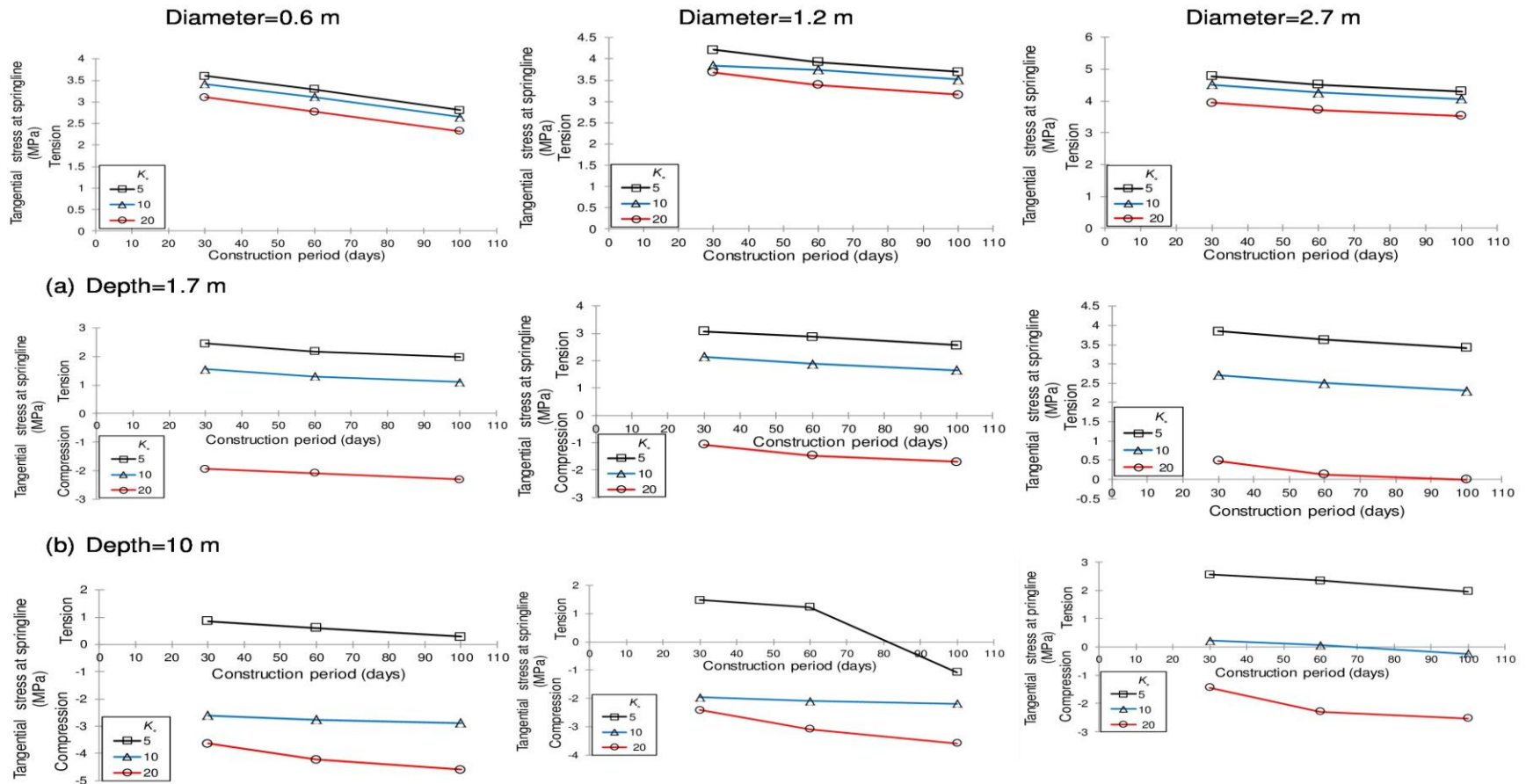


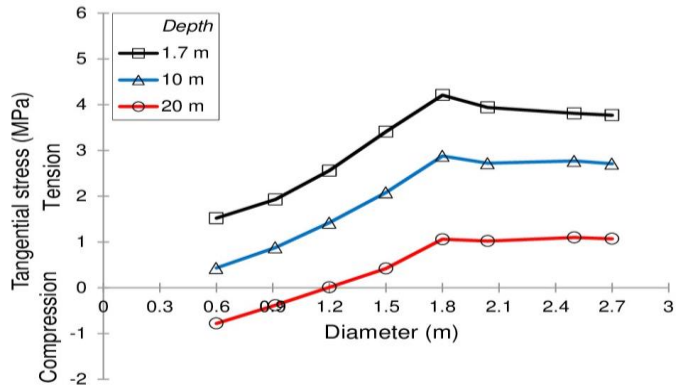
Figure 7.15. Variation of maximum tangential tensile stress at springline of concrete pipes constructed in Milton Queenston shale at different construction periods; different in-situ stress ratios (K_0) and different diameters: (a) at 1.7 m depth; (b) at 10 m depth and (c) at 20 m depth below top of the Queenston shale layer.

do not exert tension cracks during a lifetime of 30 years. However, the developed tensile stress at the springline of pipes of diameter greater than 1.8 m may exceed the tensile strength of its concrete when they are constructed at shallow depth (i.e. 1.7 m) and using bentonite solution as lubricant fluid during the construction period. This means that tension cracks may appear in these pipes only when they are constructed under these conditions. Deeper pipes did not experience stresses higher than their tensile strength, which indicates undamaged pipes throughout the lifetime of 30 years considered in this study.

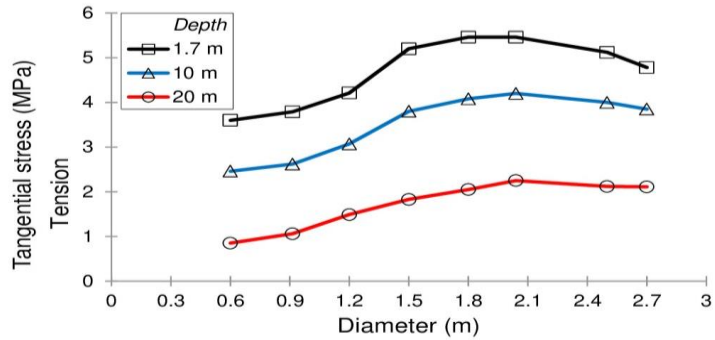
Due to the higher swelling potentials of Niagara Queenston shale, the tensile strength of the concrete pipe may be reached for pipes constructed at shallow and moderate depths below the top of the shale layer. The trends of behaviour of pipes constructed in Niagara Queenston shale presented in Figure 7.17 are similar to those noted for Milton Queenston shale. However, the curve shape is slightly different. For pipes of diameter greater than 1.8 m constructed at shallow depth using bentonite or polymer solution, the stresses at the springline have reached the concrete tensile strength. The stress at the springline of pipes constructed at moderate depths has also reached the tensile strength of concrete when bentonite solution is used. This indicates that the construction period of 30 days is not suitable for these pipes and has to be increased to a longer period or the pipes have to have higher compressive and tensile strength (i.e. compressive strength higher than 60.0 and 4.8 MPa). In general, the predicted compressive stress at the crown is well below the compressive strength of the concrete and its value ranges between 4.4 MPa and 10.3 MPa.

7.7.4 INFLUENCE OF PIPE DEPTH

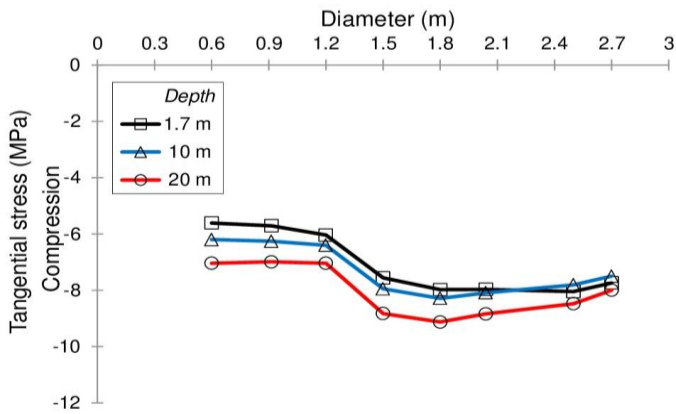
The influence of the pipe depth on the developed tensile stresses at springline and the developed compressive stresses at the crown of the pipe is also illustrated in Figures (7.16, 7.17). In general, increasing the pipe depth causes significant decrease in the developed tensile stress at the springline of the pipe and causes an increase in the



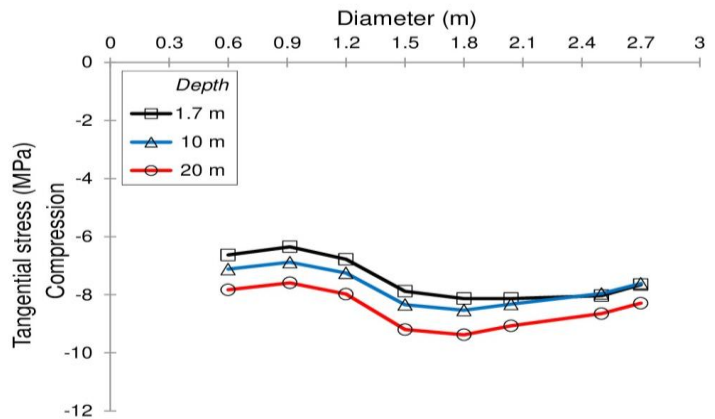
a) Tangential stress at springline / polymer solution



b) Tangential stress at springline / bentonite solution

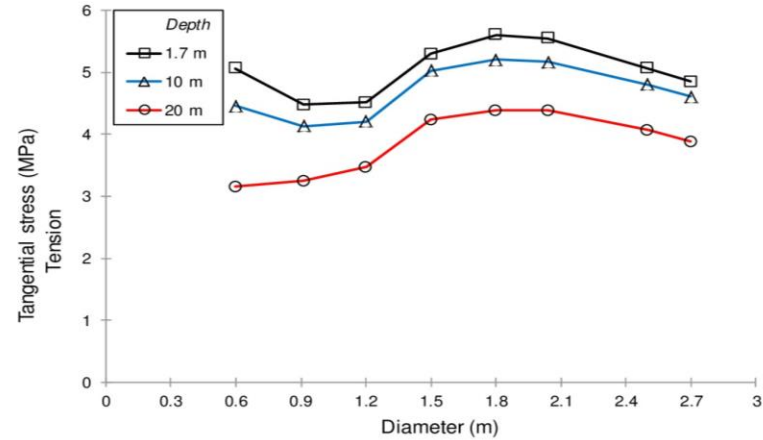
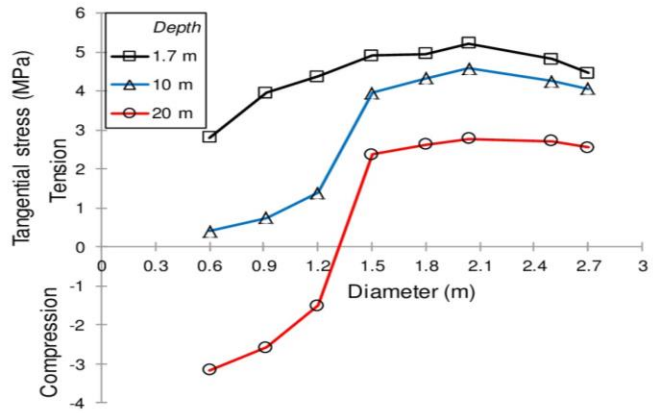


c) Tangential stress at crown / polymer solution



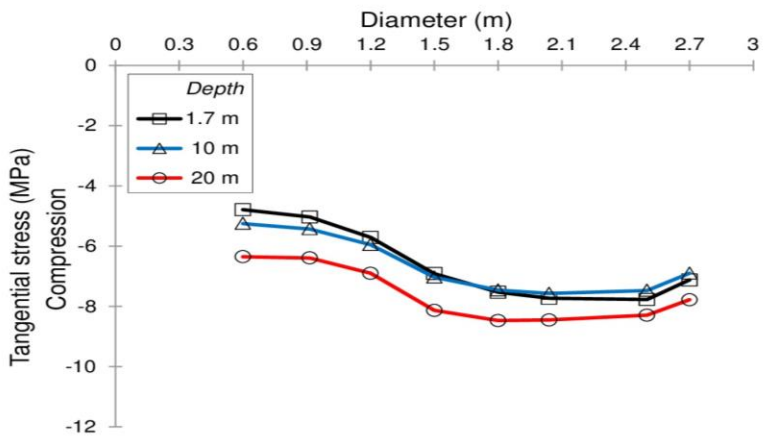
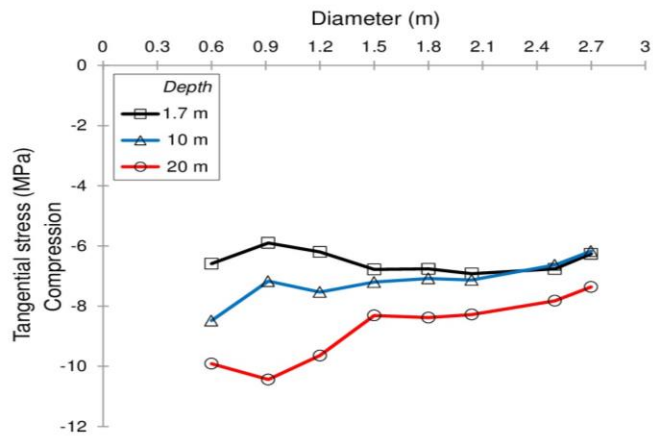
d) Tangential stress at crown / bentonite solution

Figure 7.16. Maximum tangential stresses at springline and crown of a concrete pipe constructed in Milton Queenston shale with in-situ stress ratio = 5: (a, c) using polymer solution and (b, d) using bentonite solution.



a) Tangential stress at springline / polymer solution

b) Tangential stress at springline / bentonite solution



c) Tangential stress at crown / polymer solution

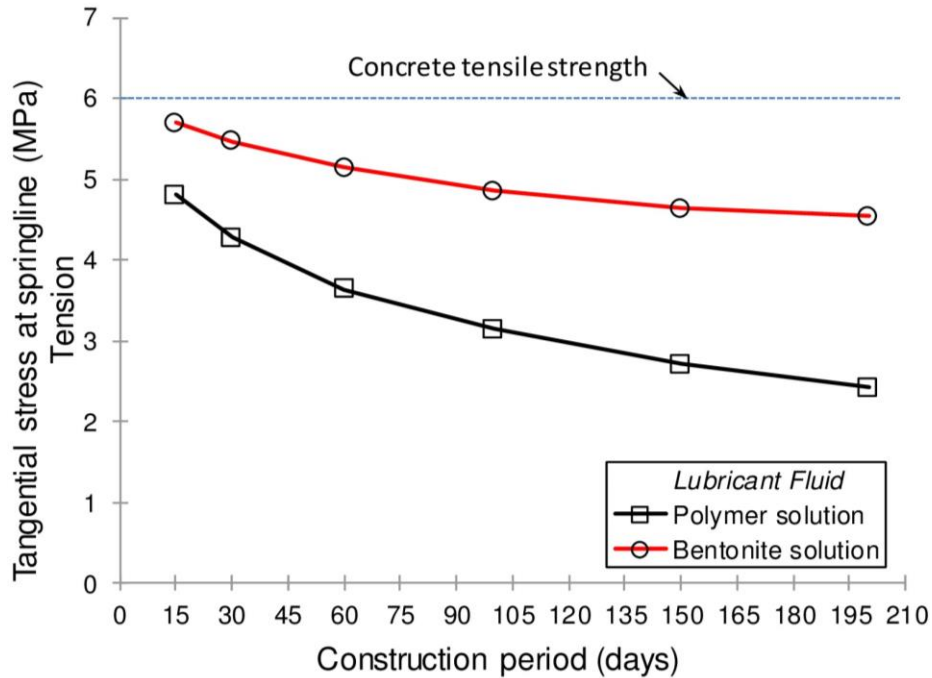
d) Tangential stress at crown / bentonite solution

Figure 7.17. Maximum tangential stresses at springline and crown of a concrete pipe constructed in Niagara Queenston shale with in-situ stress ratio = 5: (a, c) using polymer solution and (b, d) using bentonite solution.

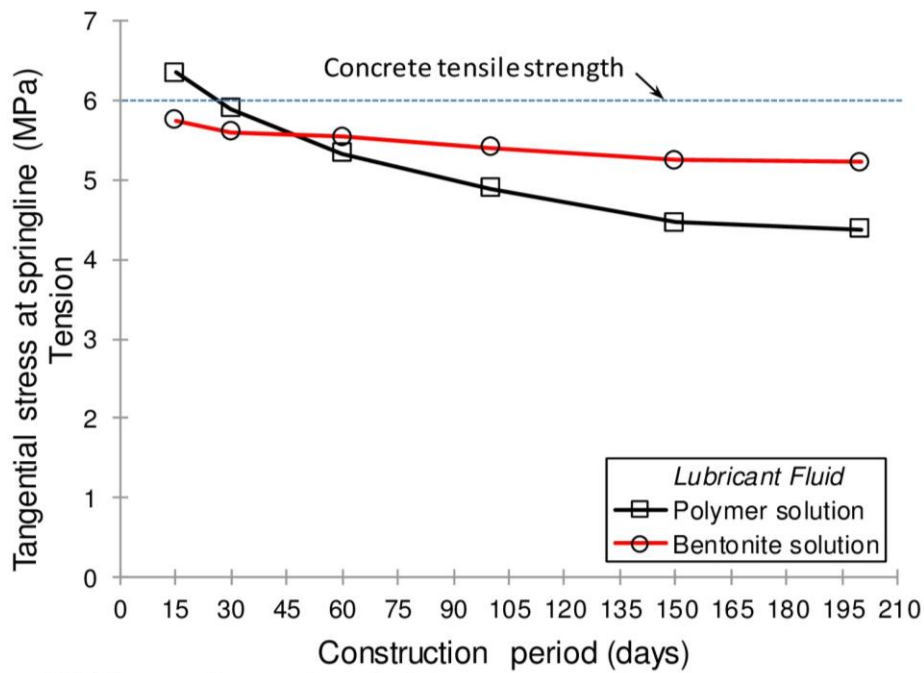
compressive stress developed at the crown for both Milton and Niagara Queenston shales using bentonite or polymer solution. The decrease in the tensile stress at the springline with increasing the diameter is more evident for pipes of small diameter constructed in Niagara Queenston shale and it becomes smaller for large pipe diameters. In Milton Queenston shale, the decrease in the tensile stress developed at the springline of the pipe is almost constant for all of pipe diameters. The decrease in the tensile stress at the pipe springline may be attributed to the confinement of the constructed pipe, where deeper pipes sustain more confinement in all directions compared to shallow pipes. Deep pipes overlain by thicker shale which produces more swelling pressure on the pipe in the vertical direction compared to shallow pipes. This may cause more uniform stress distribution around the pipe in all directions which may result in less tensile stress at the springline. The stress state at the springline changes from tension at shallow depth to compression at high depths in both Milton and Niagara Queenston shale. The developed compressive stress at the crown of the pipe increases with increasing the pipe depth for both Milton and Niagara Queenston shale using both lubricant fluids. This increase can also be attributed to the confinement effect of deep pipes compared to shallow pipes of the same diameter.

7.7.5 INFLUENCE OF CONSTRUCTION PERIOD

The “construction period” refers to the time required to install the pipeline / tunnel plus the waiting time before replacing lubricant fluid between the pipe / tunnel and the excavated rock with the permanent cement cellular grout. The variation in the tangential tensile stress developed at the springline of 1.8 m diameter concrete pipe constructed at 1.7 m depth below top of the Queenston shale layer with different construction periods is illustrated in Figure 7.18. Six construction periods were selected: $t = 15, 30, 60, 100, 150$ and 200 days. It can be noted from Figure 7.18 that increasing the construction period significantly decreases the developed tangential tensile stress at the springline of the pipe. This impact is more distinct when polymer solution is used in micro-tunneling



(a) Milton Queenston shale



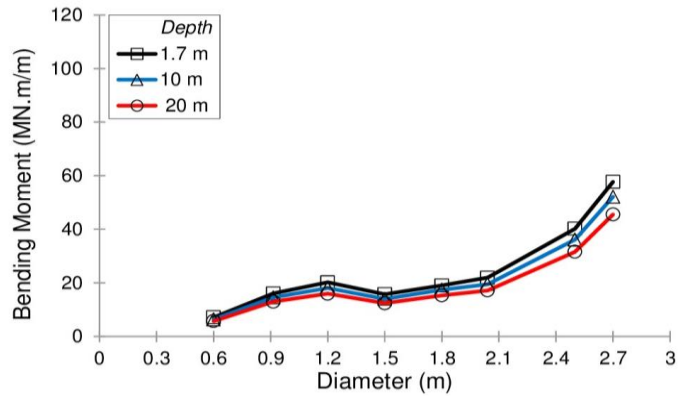
(b) Niagara Queenston shale

Figure 7.18. Variation of tangential tensile stress developed at the springline of 1.8 m diameter concrete pipe constructed at 1.7 m depth below top of the Queenston shale layer with different construction period.

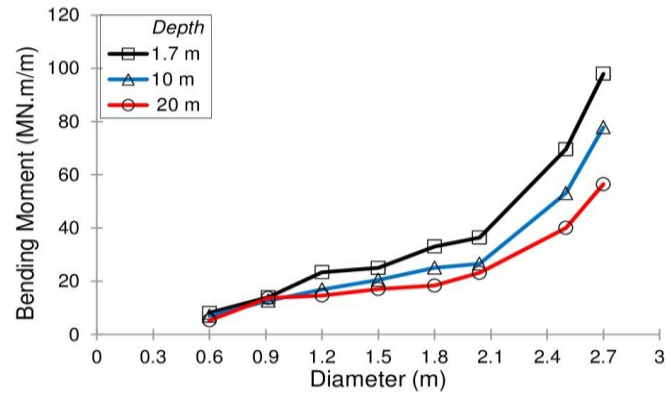
application compared to bentonite solution in Milton and Niagara Queenston shale. The impact of increasing the construction period when bentonite solution is used seems to be limited to 100 days for Milton Queenston shale and to 60 days for Niagara Queenston shale while this impact continues for longer construction periods for both shales when polymer solution is used. Longer construction period produces smaller tangential tensile stresses at the springline of the pipe for both shales. Increasing the construction period depends on the site condition and the construction schedule. Accordingly, the right construction period can be specified based on the shale type, pipe depth and pipe diameter.

7.7.6 VARIATION OF BENDING MOMENT AT SPRINGLINE AND CROWN

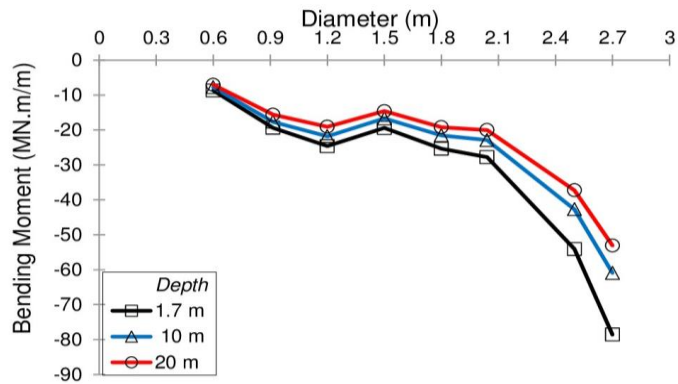
Figures 7.19 and 7.20 show the variation of the bending moment at the springline and the crown of pipes of different diameters constructed at different depths below the top surface of Milton and Niagara Queenston shale layer, respectively, using polymer and bentonite solution, for $K_s = 5$ and $t = 30$ days. Figures 7.19 and 7.20 show similar trends for time-dependent deformation behaviour in both shales. The positive bending moment developed at the springline and the negative bending moment developed at the crown of the pipe increase as the pipe diameter increases. The bentonite solution causes similar effects on the developed bending moments at the springline and at the crown of the pipe constructed in Milton and Niagara Queenston shale. For same pipe diameter, increasing pipe depth reduces the positive bending moment at the springline and reduces the negative bending moment at the crown. However, the decrease in bending moments is negligible for small pipe diameter and is significant for large diameter pipes, especially for Niagara Queenston shale.



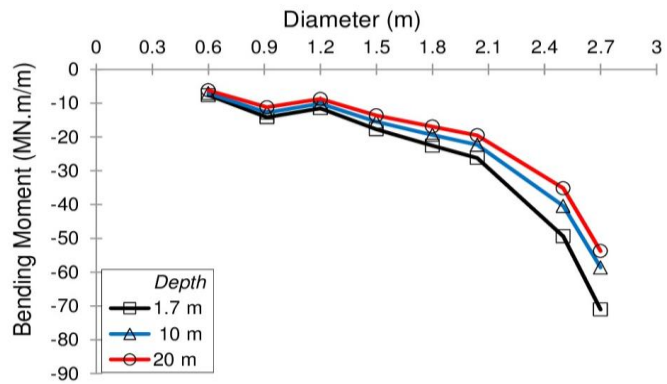
a) Bending moment at springline / polymer solution



b) Bending moment at springline / bentonite solution



c) Bending moment at crown / polymer solution



d) Bending moment at crown / bentonite solution

Figure 7.19. Bending moment at springline and crown of a concrete pipe after 30 years of construction in Milton Queenston shale with in-situ stress ratio = 5: (a, c) using polymer solution and (b, d) using bentonite solution.

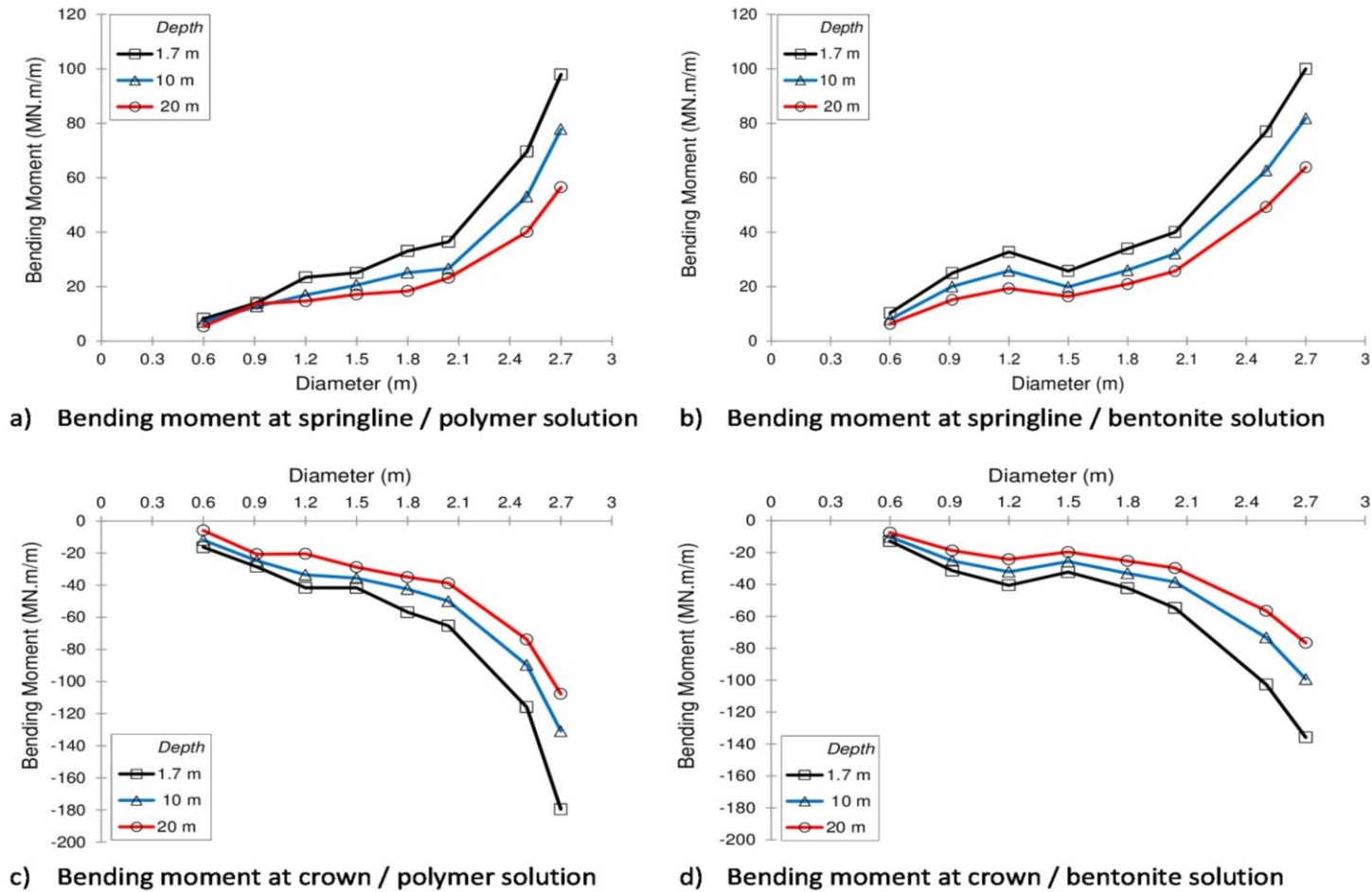


Figure 7.20. Bending moment at springline and crown of a concrete pipe after 30 years of construction in Niagara Queenston shale with in-situ stress ratio = 5: (a, c) using polymer solution and (b, d) using bentonite solution.

7.7.7 PIPE INWARD CONVERGENCE AT THE SPRINGLINE

Figure 7.21 shows typical results of horizontal deformations that occurred after 30 years of constructing concrete pipe in Niagara Queenston shale. Figure 7.22 shows the inward convergence of a concrete pipe with $d = 1.8$ m constructed at 1.7 m below the top surface of Milton and Niagara Queenston shale layer, respectively, at the springline. The stress ratio $K_o = 5$ and construction period, $t = 30$ days. Figure 7.22 shows that the majority of the inward convergence of the pipe wall at the springline occurs within the first 1000 days of the structure life. During this period, the inward convergence at the springline of the pipe is remarkably built in both shales when polymer and bentonite solutions are used. In both Milton and Niagara Queenston shales, using polymer solution as lubricant fluid during the construction period causes slightly smaller convergence in the springline compared to the bentonite solution. This difference between both fluids is more obvious in Niagara Queenston shale. The vertical dashed lines represent the time after construction where most of the inward convergence at the springline of the pipe has occurred. For pipes constructed in Milton Queenston shale, more than 98% of the inward convergence occurs at the first 500 days of the structure life. This period is slightly higher for pipes constructed in Niagara Queenston shale due to its higher swelling parameters.

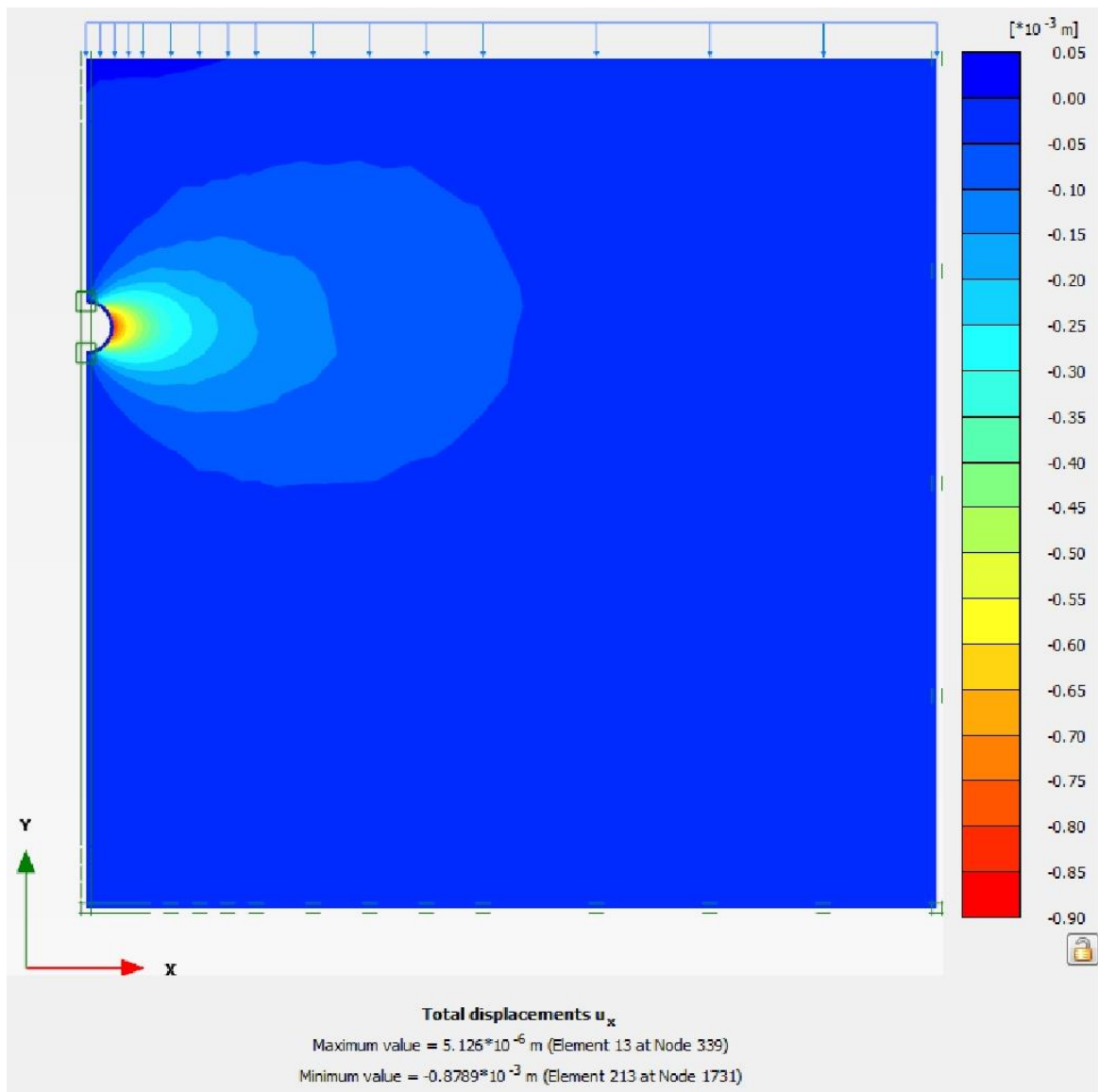
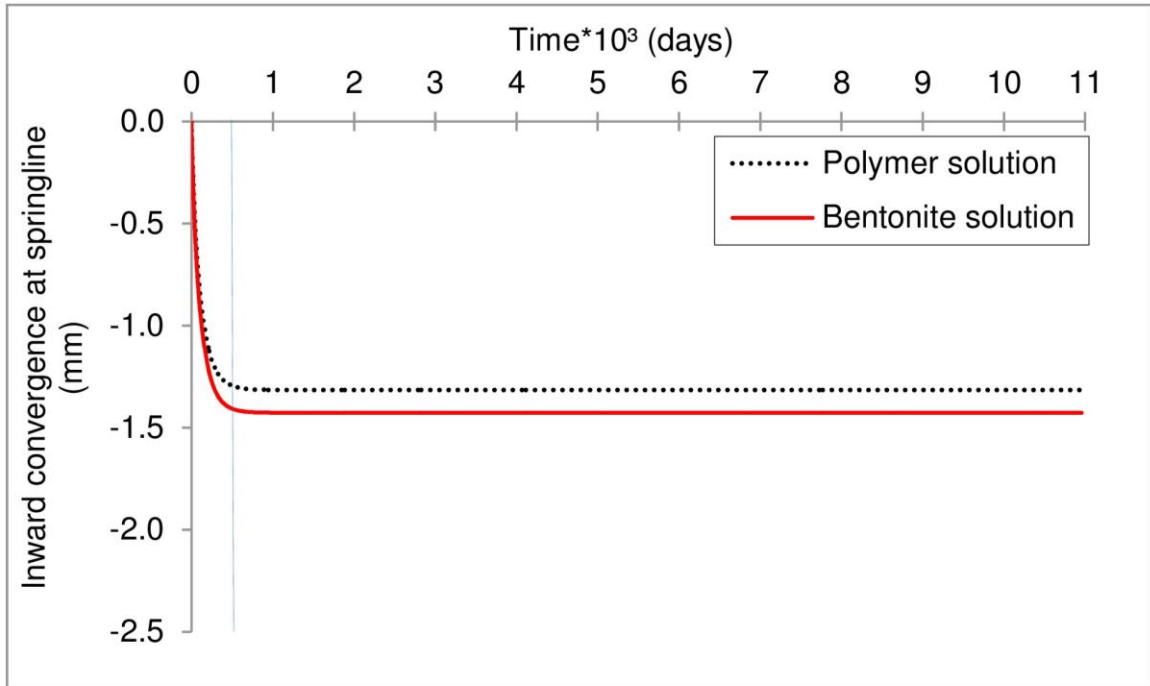
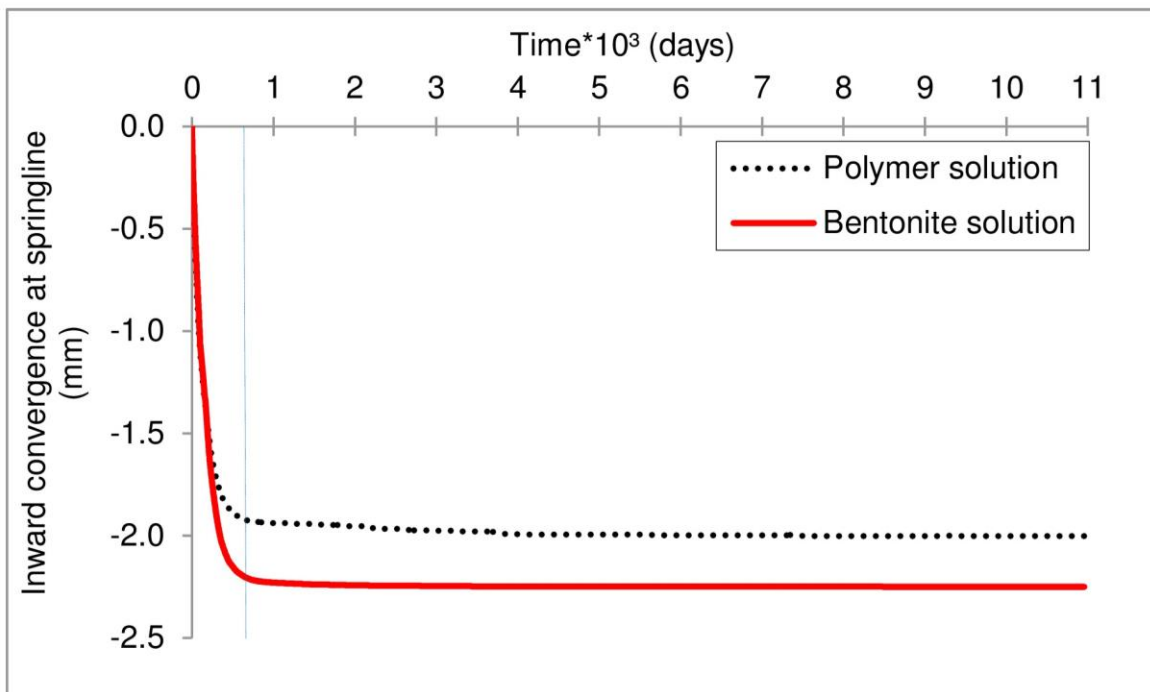


Figure 7.21. Contours of the horizontal deformation occurred after 30 years of the construction.



a) In Milton Queenston shale



b) In Niagara Queenston shale

Figure 7.22. Predicted inward convergence of 1.8 m diameter concrete pipe at the springline.

7.8 SUMMARY AND CONCLUSIONS

The rock swelling model incorporated in PLAXIS 2D environment was utilized to perform finite element analyses simulating time-dependent behaviour of pipes constructed using micro-tunneling technique in Queenston shale of southern Ontario. The rock swelling model was first verified against laboratory tests and published case studies.

The verified model was then used to conduct a parametric study of time-dependent behaviour of pipes constructed using micro-tunneling technique in Queenston shale considering: i) the in-situ stress ratio (K_0); ii) the pipe diameter; iii) the pipe depth and iv) the construction period. Based on the results of these analyses, the following conclusions can be drawn:

- 1) Increasing the construction period (i.e. pipe installation time plus waiting time before adding the permanent grout) plays a major role in reducing the developed tensile stress at the springline.
- 2) High stress ratio produces higher compressive stresses at the crown; it decreases the tensile stresses at the springline and changes the stress state from tension to compression at the springline.
- 3) For the considered concrete strength, pipes of diameter greater than 1.5 m constructed at 1.7 m in Niagara Queenston shale may experience tension cracks at their springline.
- 4) The tensile stress developed at the springline is higher for shallow pipes than deep pipes.

A general conclusion can be drawn from this study: micro-tunneling as a construction technique to install pipelines or tunnels can be considered workable and feasible in Queenston shale of southern Ontario. However, the following recommendations must be addressed:

- 1) The concrete strength of large pipes must be greater than 48 MPa to ensure acceptable performance. For pipes used at shallow depths, the concrete strength has to be upgraded.
- 2) The waiting period before applying the final cement grout has to be wisely selected. Periods less than one month are not recommended.

7.9 REFERENCES

- Al-Maamori, H.M.S, El Naggar, M.H, Micic, Silvana and Lo, K.Y. 2016. Influence of lubricant fluids on swelling behaviour of Queenston shale in southern Ontario. *Canadian Geotechnical Journal*, **53** (7): 1059-1080. doi.org/10.1139/cgj-2015-0300
- Baud, P., Zhu, W., Wong, T., 2000. Failure Mode and Weakening Effect of Water on Sandstone. *Journal of Geophysical Research*, **105**: 16371–16389.
- Bert Schädlich, Schweiger, H.F. and Mrcher, T. 2013. Modelling Swelling Rock Behaviour in Tunnelling. *Plaxis Bulletin*, spring issue 2013, pp. 1-9. www.plaxis.nl.
- Bert Schädlich, Marcher, T. and Schweiger, H.F. 2012. Application of a constitutive model for swelling rock to tunnelling. *Geotechnical Engineering Journal of the SEAGS & AGSSEA*, **43** (4): 4-27.
- Bezuijen, A. 2009. The influence of grout and bentonite slurry on the process of TBM tunnelling. *Geomechanics and Tunnelling*, **3**: 294-303. doi: 10.1002/geot.200900025
- Claesson, J., and Bohlooli, B. 2002. Brazilian test: stress field and tensile strength of anisotropic rocks using an analytical solution. *International Journal of Rock Mechanics and Mining Sciences*, **39**: 991-1004.

- Colback, P.S.B., Wiid, B.L., 1965. The Influence of Moisture Content on the Compressive Strength of Rock. Rock Mechanics Symposium, Ottawa 1965. University of Toronto, Department of Mines and Technical Surveys, pp. 65–84.
- Dan, D.Q., Konietzky, H., and Herbst, M. 2013. Brazilian tensile strength tests on some anisotropic rocks. *International Journal of Rock Mechanics and Mining Sciences*, **58**: 1-7.
- Flint, G. R. and Foreman, W. 1992. Bentonite tunnelling for the greater Cairo wastewater project. *Tunnelling and Underground Space Technology*, **7**(1): 45-53.
- Fritz, P. 2007. Additives for slurry shields in highly permeable ground. *Rock Mechanics and Rock Engineering*, **40** (1), 81-95. doi 10.1007/s00603-006-0090-y
- Gorski, B., Conlon, B., Ljunggren, B., and AB, T. 2007. Determination of the direct and indirect tensile strength on cores from borehole KFM01D. Forsmark Site Investigation Report ISSN 1651-4416, SKB P-07-76, AP PF 400-06-067. CANMET-MMSL, Mining and Mineral Sciences Laboratories, Natural Resources Canada, Svensk Kärnbränslehantering AB, Swedish Nuclear Fuel and Waste Management Co, Stockholm, Sweden.
- Grob, H. 1972. Schwelldruck im Belchentunnel. *Proceedings of International Symposium für Untertagebau*, Luyern, pp. 99-119.
- Hawlder, B.C., Lee, Y.N. and Lo, K.Y., 2003. Three-dimensional stress effects on time-dependent swelling behaviour of shaly rocks. *Canadian Geotechnical Journal*, **40** (3): 501-511.

- Hefny, A., Lo, K.Y., and Huang, J.A. 1996. Modelling of long-term time-dependent deformation and stress-dependency of Queenston shale. *Canadian Tunnelling 1996*, pp. 115-146.
- Heidkamp, H., and Katz, C. 2002. Soils with swelling potential- Proposal of a final state formulation within an implicit integration scheme and illustrative FE-calculations. *Fifth World Congress on Computational Mechanics, July 7-12, 2002, Vienna, Austria*, pp. 1-10.
- Hoek, E., Kaiser, P.K. and Bawden. W.F. 1995. *Support of underground excavations in hard rock*. Rotterdam: Balkema.
- Kramer, G.J.E., and Moore, I.D., 2005. Finite element modelling of tunnels in swelling rock. *K.Y.Lo Symposium, The University of Western Ontario, Technical Session d, July 7-8, 2005*.
- Lee, Y.N. 1988. *Stress-strain-time relationship of Queenston shale*. Ph.D. thesis, Civil and Environmental Engineering Department, The University of Western Ontario, London, ON.
- Lee, C.F., and Lo, K.Y. 1976. Rock squeeze study of two deep excavations at Niagara Falls. *Proceedings of the specialty conference on rock engineering for foundations and slopes, Geotechnical Engineering Division ASCE, University of Colorado, Boulder, Colorado, August 15-18, 1976, Vol. 1, pp 116-140*.
- Lee, Y.N., and Lo, K.Y. 1993. The swelling mechanism of Queenston shale. *Tunnelling Association of Canada Annual Publication. Canadian Tunnelling*, pp. 75-97.

- Liang, W., Yang, X., Gao, H., Zhang, C., and Zhao, Y. 2012. Experimental study of mechanical properties of gypsum soaked in brine. *International Journal of Rock Mechanics and Mining Sciences*, **53**: 42-50. doi:10.1016/j.ijrmms.2012.05.015.
- Lo, K.Y. and Hefny, A., 1996. Design of tunnels in rock with long-term time-dependent and nonlinearly stress-dependent deformation. *Canadian Tunnelling 11996*, pp. 179-214.
- Lo, K.Y., and Hori, M. 1979. Deformation and strength properties of some rocks in Southern Ontario. *Canadian Geotechnical Journal*, **16** (1): 108-120. doi: 10.1139/t79-010.
- Lo, K.Y., Cooke, B.H., and Dunbar, D.D. 1987. Design of buried structures in squeezing rock in Toronto, Canada. *Canadian Geotechnical Journal*, **24** (2): 232-241. doi: 10.1139/t87-028
- Lo, K.Y. and Lee, Y.N. 1990. Time-dependent deformation behaviour of Queenston shale. *Canadian Geotechnical Journal*, **27**(4): 461-471. doi: 10.1139/t90-061.
- Lo, K.Y. and Yuen, C.M.K. 1981. Design of tunnel lining in rock for long term time effects. *Canadian Geotechnical Journal*, **18**(1): 24-39. doi: 10.1139/t81-004.
- Lo, K.Y., Lee, C.F., Palmer, J.H.L. and Quigley, R.M., 1975. Stress relief and time-dependent deformation of rocks. Final Report, National Research Council of Canada Special Project No. 7303, Faculty of Engineering Science, The University of Western Ontario, London, ON.
- Lo, K.Y., Wai, R.S.C., Palmer, J.H.L. and Quigley, R.M., 1978. Time-dependent deformation of shaly rocks in Southern Ontario. *Canadian Geotechnical Journal*, **15** (4): 537-547. doi: 10.1139/t78-057

- Madsen, F.T & Müller-Vonmoss, M. 1989. The swelling behaviour of clay. *Applied Clay Science* **4**: 143-156.
- Morison, W.G., Rock stability in the Niagara region, Ontario Hydro Research Division, report No. 57-13, 1957.
- Neville, A.M. 1996. *Properties of Concrete*. 4th edition, Pearson Education Limited, Harlow, England.
- Paterson, M.S. 1978. *Experimental Rock Deformation: The Brittle Field*. Springer-Verlag, Berlin.
- Paterson, M.S., and Wong, T.F. 2005. *Experimental Rock Deformation - The Brittle Field*, 2nd Edition. Springer-Verlag, Berlin, Heidelberg, New York.
doi:10.1017/S0016756806242973.
- Perras, M.A., 2009. *Tunnelling in horizontally laminated ground: The influence of lamination thickness on anisotropic behaviour and practical observations from the Niagara tunnel project*. MSE thesis, Queen's University, Kingston, Ontario, Canada.
- PLAXIS, 2016. *PLAXIS 2D 2016- material models manual* [online]. Available:
<http://www.plaxis.nl/plaxis2d/manuals/>
- PLAXIS, 2014. Swelling rock model. *Plaxis bulletin*, spring issue, 2014, pp 4-27.
- RocLab, 2016. Rocscience: www.rocscience.com.
- Smith, C.B. 1905. Construction of Canadian Niagara company's 100,000 H.P. hydroelectric plant at Niagara Falls, Ontario, *Transactions, Canadian Society of Civil Engineers*, Vol. 19.

Trow, W.A. and Lo, K.Y. 1989. Horizontal displacements induced by rock excavation: Scotia Plaza, Toronto, Ontario. *Canadian Geotechnical Journal*, **26** (1): 114-121.

doi: 10.1139/t89-012

Wai, R.S.C., Lo, K.Y. and Rowe, R.K., 1981, Thermal stresses in rocks with nonlinear properties. Research report, Faculty of Engineering Science, The University of Western Ontario, GEOT-8-81.

Wasantha, P.L.P. and Ranjith, P.G. 2014. Water-weakening behavior of Hawkesbury sandstone in brittle regime. *Engineering Geology*, **178**: 91-1.

doi:10.1016/j.enggeo.2014.05.015.

Wittke-Gattermann, P. and Wittke, M. 2004. Computation of strains and pressures for tunnels in swelling rocks. *Tunnellind and Underground Space Technology, Underground Space for Sustainable Urban Development. Proceedings of the 30 th ITA-AITES World Tunnel Congress Singapore, 22-27 May 2004.* **19** (4-5). URL: <http://worldcat.org/issn/08867798>.

Yuen, C.M., 1979. Rock-Structure Time Interaction in Lined Circular Tunnels in High Horizontal Stress Field. PhD Thesis, Civil and Environmental Engineering Department, The University of Western Ontario, London, ON.

Yuen, Clement M.K. et al 1992. Design of diversion tunnels Niagara River Hydroelectric Development. 45th CJC. Paper 106A.

Chapter 8

SUMMARY, CONCLUSIONS AND RECOMMENDATIONS

8.1 SUMMARY

The Queenston shale was formed in southern Ontario during the upper Ordovician age. It outcrops at the south west shores of Lake Ontario and extends up to the North. Moving to the South-West, the Queenston shale layer dips slightly down, becomes thinner and overlain by other rock formation. According to its location, the Queenston shale forms the hosting ground for many constructed and anticipated engineering projects in major cities in southern Ontario. The Queenston shale is characterized with its time-dependent deformation behaviour which can cause severe damage to the hosted underground structures. However the demand to expand existing infrastructure and build new one in major cities in southern Ontario has postulated the need to involve construction technique, such as micro-tunnelling to fulfill this requirement. Micro-tunnelling technique is being considered to construct pipelines / tunnels in Queenston shale of southern Ontario. Implementing this technique involves the use of lubricant fluids (i.e. bentonite and polymer solutions) during the construction period, which may influence the properties of the Queenston shale. This thesis investigates the time-dependent deformation of the shale and stresses induced in the pipelines and tunnel segments constructed in Queenston shale using the micro-tunneling technique.

A comprehensive literature review of the geo-mechanical properties of different rocks in southern Ontario and the neighbouring regions was performed and the collected data were presented in Chapter 2. This data includes the measured in-situ stresses, strength and stiffness properties, time-dependent deformation properties and dynamic properties of different rocks at different depths below the ground level. These data can serve as a preliminary source of information for any prospective study of the geo-mechanical properties of rocks in southern Ontario.

An extensive testing program was undertaken in order to investigate the time-dependent deformation behavior of the Queenston shale in lubricant fluids used in micro-tunneling applications and the results are presented in Chapter 3. The test program included: free swell tests, semi-confined swell tests under different applied pressure and null swell tests. These tests were performed on vertically and horizontally cored samples of Queenston shale collected from Milton and Niagara in Ontario. Additional tests, such as: x-ray diffraction, cation exchange capacity, rate of water absorption, calcite content, moisture content and the rock pore water salinity in addition to the scanning electron microscopy were also performed on these shales. Results were extensively discussed and the mechanism of the influence of lubricant fluids on the time-dependent deformation of the Queenston shale was suggested. The time-dependent deformation behavior of the Queenston shale in bentonite solution and polymer solutions was found to be different than the behavior in water. The results were utilized to develop the swelling envelopes of Milton and Niagara Queenston shale in lubricant fluids and water in the vertical and horizontal directions with respect to the rock bedding. The developed swelling envelopes are essentials in predicting swelling stresses in pipelines / tunnels constructed in Queenston shale using micro-tunneling technique.

A series of strength tests were performed on Milton Queenston shale before and after soaking for 100 days in water; bentonite solution and polymer solution and the tests results are presented in Chapter 4. The goal of this study was to investigate the degradation that may occur in Milton Queenston shale after the continuous exposure to water and lubricant fluids used in micro-tunneling applications. Tests were performed on vertically and horizontally cored samples with respect to the rock bedding to study the strength anisotropy of this shale before and after soaking. Four tests were performed on Milton Queenston shale: Brazilian split test; direct tension test; unconfined compression test and triaxial compression test under different confining pressure up to 20 MPa. Full description of the triaxial cell used in this study as well as its modifications in order to accommodate rock samples of different sizes, to apply high confining pressure and to reduce time required to perform the test was given. Additional tests, such as calcite content; moisture content and rock pore water salinity were also performed on each sample. Results of these tests were presented with an explanation of the expected

mechanism of strength degradation due to soaking in water and lubricant fluids. Finally, the measured strength in these tests was utilized to develop the full strength envelope of Milton Queenston shale before and after soaking in water and lubricant fluids. Strength envelopes of non-soaked Queenston shale were much higher than strength envelopes of soaked shales and the degradation was discussed.

The strength degradation of Niagara Queenston shale due to soaking in water; bentonite solution and polymer solution was investigated in Chapter 5. Strength tests were performed on Niagara Queenston shale before and after soaking in different fluids for 100 days. The Brazilian split test, direct tension test, unconfined compression test and multistage triaxial compression test were performed in this study. Additional tests such as the calcite content; the moisture content and the rock pore water salinity were also performed on each sample before and after soaking. The procedure followed to perform the multistage triaxial compression test on both non soaked and soaked samples was indicated. Results of multistage triaxial compression tests together with other strength tests results were utilized to develop strength envelopes of Niagara Queenston shale before and after soaking in water and lubricant fluids. The developed strength envelopes demonstrated the strength degradation of Niagara Queenston shale when is is exposed to water and lubricant fluids for long time.

A new setup was developed to measure the depth of penetration of water; bentonite solution and polymer solution into the Queenston shale from southern Ontario and was presented in Chapter 6. The developed test setup attempts to simulate field conditions in micro-tunneling applications in Queenston shale where lubricant fluids are applied to the excavated rock under pressure of approximately 200 kPa. In the proposed test method, the depth of percolation of water, bentonite solution and polymer solution was visually monitored with time up to 100 days. Based on the observations of this test, a correlation was derived to predict the depth of percolation of water, bentonite solution, and polymer solutions into the Queenston shale. Utilizing the moisture content results along the entire sample at the end of percolation tests, a procedure was suggested to calculate the hydraulic conductivity of the Queenston shale in these fluids. The obtained results were used to evaluate the hydraulic conductivity of Queenston shale and its value was found to be consistent with values reported in the literature.

The experimental results obtained from the previous studies were utilized to calibrate and verify a finite element model simulating the time dependent deformation and stresses induced in pipelines constructed in Queenston shale using the micro-tunneling technique. The finite element model was developed utilizing Lo and Hefny (1996) swelling model in Plaxis 2D computer program as it was presented in Chapter 7. The model was also verified against two documented cases of vertical excavations in swelling rocks with in-situ deformation measurements. These two cases are the Niagara wheel pit excavation and the Scotia plaza foundation excavation in Toronto. This was followed by modelling large tunnel in the Queenston shale and comparing the finite element model results with Lo and Hefny (1996) closed form solutions of the time-dependent deformations and stresses developed at the tunnel lining. The validation process indicated that the developed finite element models were adequate and capable to capture the time-dependent deformation behavior of the swelling rocks. Accordingly, a finite element model of the time-dependent deformations and induced stresses on a tunnel / pipeline constructed in the Queenston shale using micro-tunneling technique and the rock swelling model suggested by Lo and Hefny (1996) was developed. The developed model was used to perform analytical study considering: i) the in-situ stress ratio (K_0); ii) the pipe diameter; iii) the pipe depth below the top surface of the Queenston shale and iv) the length of the construction period prior to add the permanent cement cellular grout in the gap between the excavated shale and the pipe / tunnel. The performed analytical study provided an insight of the influence of the considered parameters on the developed deformations and stresses in the pipeline / tunnel during its life.

8.2 CONCLUSIONS

From the results of studies performed in this research, the following conclusions can be drawn:

- 1) Some rocks in southern Ontario exhibit initial in-situ horizontal stress that may reach up to 38 MPa at shallow depths (i.e. less than 30 m) where most of engineering

projects are located, while at greater depths up to 1000 m where mining projects are located, it may reach up to 86 MPa. At very high depths greater than 1000 m, where hydrocarbons projects are located, the in-situ horizontal stress in these rocks may reach 135 MPa. The in-situ stress ratio (K_h) in the Queenston shale is found to be between 5 and 20.

- 2) The time-dependent deformation behavior of Milton and Niagara Queenston shales in the lubricant fluids, as in the case of water, is anisotropic with respect to the rock bedding, and it is stress-dependent with the swelling strain in the vertical direction is generally higher than in the horizontal direction. This behavior can be represented by Lo and Hefny (1996) model.
- 3) Compared to water, both of bentonite and polymer solutions used in micro-tunneling applications can cause a considerable influence on the time-dependent deformation of the Queenston shale. Polymer solution can effectively reduce the swelling strains of Milton and Niagara Queenston shales in both vertical and horizontal directions. This reduction can be as high as 90% while bentonite solution can reduce the swelling strains of Niagara Queenston shale by 24%-26% and it may slightly increase the swelling strains of Milton Queenston shale.
- 4) The reverse influence of bentonite solution on the swelling strain of the Milton and Niagara Queenston shales may be attributed to the movement of cations from the shale to the bentonite solution and vice versa.
- 5) Both Milton and Niagara Queenston shale experienced significant decrease in their strength after being soaked for 100 days in water, bentonite solution and polymer solution. The polymer solution caused the least impact on strength.
- 6) The Poisson's ratio of Milton and Niagara Queenston shale increased approaching 0.5 and the elastic modulus decreased after soaking these shales for 100 days in water; bentonite solution and polymer solution.

- 7) The strength of the Queenston shale is anisotropic with respect to the rock bedding and this behavior was maintained for Milton Queenston shale after being soaked for 100 days in water; bentonite solution and polymer solution.
- 8) The multistage triaxial compression test was found doable for Niagara Queenston shale using the modified triaxial cell, and it has almost a negligible influence on the measured strength compared to the single stage triaxial test.
- 9) Strength envelopes were generated for both Milton and Niagara Queenston shales before and after being soaked for 100 days in water and bentonite and polymer solutions. These envelopes demonstrate the remarkable decrease in the strength of these shales due to soaking in these fluids.
- 10) A laboratory test method was developed to measure the depth of percolation of water; bentonite solution and polymer solution into the Queenston shale in 100 days and a correlation was derived to predict the long-term penetration of these fluids. Using results of the suggested test method and Darcy's law, a method was suggested to calculate the primary hydraulic conductivity of the Queenston shale. Different fluids caused different depth of percolation and different hydraulic conductivity of the Queenston shale. The calculated hydraulic conductivity of the Queenston shale is consistent with the reported in the literature, indicating the adequacy of the proposed calculation procedure.
- 11) Based on the performed finite element analyses, delaying the final cement cellular grout significantly decreases the tensile stress at the springline of the pipeline / tunnel.
- 12) Increasing the pipe / tunnel diameter increases the tensile stress at the springline, while increasing the depth of the same diameter decreases the tensile stress at springline. Increasing the in-situ stress ratio changes the stress state at the springline from tension to compression.

- 13) As an overall conclusion of this research, the micro-tunneling construction technique is doable; workable and feasible in the Queenston shale of southern Ontario provided that selecting suitable construction period and using adequate strength of the concrete mix for the pipes / tunnels.

8.3 RECOMMENDATIONS AND FUTURE RESEARCH

This research illustrates that micro-tunneling construction technique can be considered workable and feasible in Queenston shales of southern Ontario. The application of this construction technique may also be applicable to other shales in southern Ontario depending on the location of the project. Other shales, such as Georgian Bay shale may have different time-dependent deformation behavior than the Queenston shale in lubricant fluids used in micro-tunneling applications. Therefore, the following recommendations are made for future research studies:

- 1) Study the time-dependent deformation behavior of Georgian Bay Shale, and other rocks in southern Ontario in lubricant fluids used in micro-tunneling applications.
- 2) Study the strength degradation of Georgian Bay shale and other rocks from southern Ontario caused by continuous exposure to water and lubricant fluids.
- 3) Extend the finite element modelling to study the influence of the time-dependent deformations of the Queenston shale on vertical shafts constructed in this shale.

Appendix A

STANDARD DEVIATION OF TIME-DEPENDENT DEFORMATION AND STRENGTH MEASUREMENTS

Table A.1. Standard deviation of free swell test of Milton Queenston shale

Specimen No.	Ambient Fluid	Horizontal Swelling Potential (% strain/ log cycle of time)	Standard Deviation	Vertical Swelling Potential (% strain/ log cycle of time)	Standard Deviation
M-FST 16	Water	0.16	0.032	0.2	0.049
M-FST 21	Water	0.145		0.18	
M-FST 22	Water	0.21		0.24	
M-FST 25	Water	0.155		0.21	
M-FST 27	Water	0.11		0.12	
M-FST 24	8% Bentonite Solution	0.2	0.029	0.226	0.007
M-FST 28	8% Bentonite Solution	0.13		0.24	
M-FST 29	8% Bentonite Solution	0.18		0.24	
M-FST 14	0.8 % Polymers Solution	0.06	0.025	0.1	0.033
M-FST 18	0.8 % Polymers Solution	0.01		0.08	
M-FST 23	0.8% Polymers Solution	0.053		0.095	
M-FST 26	0.8% Polymers Solution	0.01		0.02	
M-FST 30	0.8% Polymers Solution	0		0.03	

Table A.2. Standard deviation of free swell test of Niagara Queenston shale

Specimen No.	Ambient Fluid	Horizontal Swelling Potential (% strain/ log cycle of time)	Standard deviation	Vertical Swelling Potential (% strain/ log cycle of time)	Standard deviation
N-FST 11	Water	0.21	0.041	0.6	0.089
N-FST 15	Water	0.26		0.575	
N-FST 16	Water	0.16		0.4	
N-FST 13	8% Bentonite Solution	0.16	0.000	0.38	0.008
N-FST 17	8% Bentonite Solution	0.16		0.4	
N-FST 18	8% Bentonite Solution	0.16		0.39	
N-FST 10	0.8 % Polymers Solution	0.01	0.024	0.05	0.012
N-FST 12	0.8 % Polymers Solution	0.06		0.07	
N-FST 14	0.8 % Polymers Solution	0.06		0.04	

Table A.3. Standard deviation of vertical semi-confined swell test of Milton Queenston shale

Specimen No.	Ambient Fluid	Applied Pressure (MPa)	Vertical Swelling Potential (% strain/ log cycle of time)	Standard deviation
M-SCSVT 2	Water	0.05	0.14	0.216
M-SCSVT 13	Water	0.05	0.14	
M-SCSVT 14	Water	0.05	0.16	0.204
M-SCSVT 1	Water	0.1	0.125	
M-SCSVT 7	Water	0.1	0.075	
M-SCSVT 25	Water	0.1	0.1	0.115
M-SCSVT 10	Water	1	0.04	
M-SCSVT 19	Water	1	0.01	
M-SCSVT 20	Water	1	0.01	
M-SCSVT 5	8% Bentonite Solution	0.05	0.215	0.268
M-SCSVT 6	8% Bentonite Solution	0.05	0.15	
M-SCSVT 23	8% Bentonite Solution	0.05	0.115	0.183
M-SCSVT 12	8% Bentonite Solution	0.1	0.1	
M-SCSVT 18	8% Bentonite Solution	0.1	0.11	
M-SCSVT 24	8% Bentonite Solution	0.1	0.08	0.058
M-SCSVT 9	8% Bentonite Solution	1	0.01	
M-SCSVT 17	8% Bentonite Solution	1	0.06	
M-SCSVT 26	8% Bentonite Solution	1	0.065	
M-SCSVT 3	0.8 % Polymers Solution	0.05	0.06	0.141
M-SCSVT 8	0.8 % Polymers Solution	0.05	0.07	
M-SCSVT 16	0.8 % Polymers Solution	0.05	0.07	0.115
M-SCSVT 4	0.8 % Polymers Solution	0.1	0.04	
M-SCSVT 15	0.8 % Polymers Solution	0.1	0.035	
M-SCSVT 22	0.8 % Polymers Solution	0.1	0.045	0.071
M-SCSVT 11	0.8 % Polymers Solution	1	0.015	
M-SCSVT 21	0.8 % Polymers Solution	1	0.03	
M-SCSVT 27	0.8% Polymers Solution	1	0	

Table A.4. Standard deviation of horizontal semi-confined swell test of Milton Queenston shale

Specimen No.	Ambient Fluid	Applied Pressure (MPa)	Horizontal Swelling Potential (% strain/ log cycle of time)	Standard deviation
M-SCSHT 1	Water	0.1	0.075	0.183
M-SCSHT 2	Water	0.1	0.065	
M-SCSHT 7	Water	0.1	0.06	
M-SCSHT 10	Water	0.2	0.03	0.258
M-SCSHT 22	Water	0.2	0.02	
M-SCSHT 23	Water	0.2	0.04	
M-SCSHT 11	Water	0.7	0.01	0.483
M-SCSHT 12	Water	0.7	0.03	
M-SCSHT 13	Water	0.7	0.01	
M-SCSHT 9	8% Bentonite Solution	0.1	0.065	0.183
M-SCSHT 5	8% Bentonite Solution	0.1	0.075	
M-SCSHT 6	8% Bentonite Solution	0.1	0.07	
M-SCSHT 20	8% Bentonite Solution	0.2	0.055	0.258
M-SCSHT 26	8% Bentonite Solution	0.2	0.06	
M-SCSHT 27	8% Bentonite Solution	0.2	0.05	
M-SCSHT 18	8% Bentonite Solution	0.7	0.015	0.483
M-SCSHT 19	8% Bentonite Solution	0.7	0.01	
M-SCSHT 21	8% Bentonite Solution	0.7	0.03	
M-SCSHT 3	0.8 % Polymers Solution	0.1	0.008	0.183
M-SCSHT 14	0.8 % Polymers Solution	0.1	0.01	
M-SCSHT 15	0.8 % Polymers Solution	0.1	0.01	
M-SCSHT 16	0.8 % Polymers Solution	0.2	0.003	0.258
M-SCSHT 24	0.8 % Polymers Solution	0.2	0.002	
M-SCSHT 25	0.8 % Polymers Solution	0.2	0.004	
M-SCSHT 4	0.8 % Polymers Solution	0.7	0	0
M-SCSHT 8	0.8 % Polymers Solution	0.7	0	
M-SCSHT 17	0.8 % Polymers Solution	0.7	0	

Table A.5. Standard deviation of null swell pressure of Milton Queenston shale in vertical and horizontal direction

Specimen No.	Ambient Fluid	Null-Swell Pressure (MPa)	Standard deviation
M-NSVT 5	Water	2.14	0.180
M-NSVT 7	Water	1.92	
M-NSVT 9	Water	2.36	
M-NSVT 6	8% Bentonite Solution	2.3	0.105
M-NSVT 10	8% Bentonite Solution	2.26	
M-NSVT 11	8% Bentonite Solution	2.5	
M-NSVT 1	0.8 % Polymers Solution	1.485	0.095
M-NSVT 8	0.8 % Polymers Solution	1.4	
M-NSVT 13	0.8 % Polymers Solution	1.63	
M-NSHT 1	Water	1.46	0.819
M-NSHT 4	Water	2.14	
M-NSHT 10	Water	2.57	
M-NSHT 2	8% Bentonite Solution	1.55	0.533
M-NSHT 5	8% Bentonite Solution	2.3	
M-NSHT 12	8% Bentonite Solution	2.85	
M-NSHT 3	0.8 % Polymers Solution	1.22	0.732
M-NSHT 6	0.8 % Polymers Solution	1.28	
M-NSHT 11	0.8 % Polymers Solution	1.99	

Table A.6. Standard deviation of the Brazilian Split test of Milton Queenston shale in vertical direction

Specimen No.	Ambient Fluid	Brazilian Splitting Strength (MPa)	Standard deviation
BZVT 1	Air	8.189	0.652
BZVT 2	Air	9.783	
BZVT 3	Air	9.056	
BZVT 4	Air	8.739	
BZVT 5	Air	7.942	
BZVT 6	Water	6.523	0.263
BZVT 7	Water	5.516	
BZVT 8	Water	5.462	
BZVT 9	Water	7.854	
BZVT 10	Water	6.024	
BZVT 11	Water	5.682	
BZVT 12	0.8 % Polymers Solution	7.399	0.143
BZVT 13	0.8 % Polymers Solution	7.587	
BZVT 14	0.8 % Polymers Solution	7.464	
BZVT 15	0.8 % Polymers Solution	7.7	
BZVT 16	0.8 % Polymers Solution	8.749	
BZVT 17	0.8 % Polymers Solution	7.786	
BZVT 18	8% Bentonite Solution	5.094	0.133
BZVT 19	8% Bentonite Solution	5.021	
BZVT 20	8% Bentonite Solution	5.199	
BZVT 21	8% Bentonite Solution	6.218	
BZVT 22	8% Bentonite Solution	5.364	
BZVT 23	8% Bentonite Solution	5.004	

Table A.7. Standard deviation of the Brazilian split strength of Milton Queenston shale in horizontal direction

Specimen No.	Ambient Fluid	Brazilian Splitting Strength (MPa)	Standard deviation
BZHT 1	Air	8.948	1.019
BZHT 2	Air	7.499	
BZHT 3	Air	6.463	
BZHT 4	Water	3.277	0.128
BZHT 5	Water	3.439	
BZHT 6	Water	3.126	
BZHT 7	0.8 % Polymers Solution	4.871	0.523
BZHT 8	0.8 % Polymers Solution	5.711	
BZHT 9	0.8 % Polymers Solution	4.452	
BZHT 10	8% Bentonite Solution	3.658	0.189
BZHT 11	8% Bentonite Solution	3.242	
BZHT 12	8% Bentonite Solution	3.274	

Table A.8. Standard deviation of unconfined compression strength of Milton Queenston shale in vertical direction

Specimen No.	Ambient Fluid	Unconfined Compression Strength (MPa)	Standard deviation
UCVT 1	Air	53.1	8.746
UCVT 2	Air	43.751	
UCVT 3	Air	31.732	
UCVT 4	Water	24.769	5.954
UCVT 5	Water	11.881	
UCVT 6	Water	12.443	
UCVT 7	0.8 % Polymers Solution	25.433	4.629
UCVT 8	0.8 % Polymers Solution	15.689	
UCVT 9	0.8 % Polymers Solution	15.63	
UCVT 10	8% Bentonite Solution	25.61	5.071
UCVT 11	8% Bentonite Solution	15.1	
UCVT 12	8% Bentonite Solution	14.702	

Table A.9. Standard deviation of unconfined compression strength of Milton Queenston shale in horizontal direction

Specimen NO.	Ambient Fluid	Unconfined Compression Strength (MPa)	Standard deviation
UCHT 1	Air	44.956	9.209
UCHT 2	Air	23.171	
UCHT 3	Air	22.161	
UCHT 4	Air	33.251	
UCHT 5	Water	27.144	4.489
UCHT 6	Water	17.131	
UCHT 7	Water	18.2	
UCHT 8	0.8 % Polymers Solution	18.44	3.684
UCHT 9	0.8 % Polymers Solution	25.21	
UCHT 10	0.8 % Polymers Solution	28.685	
UCHT 11	8% Bentonite Solution	13.303	1.544
UCHT 12	8% Bentonite Solution	14.794	
UCHT 13	8% Bentonite Solution	17.058	

Curriculum Vitae

Name: Hayder Al-Maamori

Post-secondary Education and Degrees: University of Technology-Iraq
Baghda, Iraq
1992-1994 M.E.Sc. Geotechnical Engineering.

University of Technology-Iraq
Baghda, Iraq
1986-1990 B.Sc. Civil Engineering.

The University of Western Ontario
London, Ontario, Canada
2011-2016 Ph.D. Geotechnical Engineering.

Related Work Experience Teaching Assistant/ Research Assistant
The University of Western Ontario
2012-2016

Sr. Civil Engineer
Dar Alhandasah Consultants,
Dubai Intl. Airport Expansion Projects
2002-2011

Laboratory Manager
Impregilo s.p.a.
Libya
1996-2001

University Lecturer
Libya
1995-1996

Publications:

Al-Maamori, H.M.S, El Naggar, M.H, Micic, Silvana and Lo, K.Y. 2016. Influence of lubricant fluids on swelling behaviour of Queenston shale in southern Ontario. Canadian Geotechnical Journal, **53** (7): 1059-1080.

Al-Maamori, H.M.S., El Nagggar, M.H., and Micic, Silvana 2014. A compilation of the geo-mechanical properties of rocks in Southern Ontario and the neighbouring regions. *Open Journal Of Geology*. **4**: 210-227.

Al-Maamori, H.M.S, El Nagggar, M.H, Micic, Silvana and Lo, K.Y., 2015. Swelling Potential of Queenston Shale in Lubricant Fluids. *Proceedings of GeoQuebec 2015, Challenges from North to South, Quebec City, September, 2015.*